DATA TRANSMISSION THROUGH CHANNELS PERTURBED BY IMPULSIVE NOISE

BY

NELSON LEMOS ESTEVES

APRIL, 1975

A Thesis submitted for the
Degree of Doctor of Philosophy
of the University of London

Department of Electrical Engineering,
Imperial College of Science and Technology,
London, S.W.7.

AOS MEUS PAIS

Every fulfilment is slavery.

It drives us to a higher fulfilment.

Albert Camus, "The Rebel".

ABSTRACT

This thesis is concerned with two methods of improving the reliability of binary data transmission over linear channels in situations where the error-rate is essentially determined by impulsive noise.

The first proposed method utilizes a new class of signal waveforms which allows the designer to choose at will the duration of the transmitted waveforms and to achieve, for a given channel bandwidth, the same transmission rate as in the conventional systems. The transmitted waveforms overlap in the channel but, owing to their autocorrelation and crosscorrelation properties, intersymbol interference can be prevented from arising at the detector output. This method turns out to be useful only in the high signal-to-noise ratio (SNR) region.

The second method, which is more effective in the low SNR region, involves the use of several identical pulses for each binary symbol to be transmitted. The proposed decision device first detects which pulses are more likely to have been strongly corrupted by impulsive noise and then uses this knowledge to choose the decision rule. A procedure for calculating the optimum number of pulse repetitions when the system includes a binary linear forward-acting error-correcting coding scheme is also presented.

The error-rate analysis for the two methods is carried out in the presence of Poisson impulse noise and one example of non-Poisson impulse noise. In the latter case the results were obtained by means of a Monte-Carlo simulation and the exercise is intended to provide an indication of the effect of long bursts of impulsive noise on the performance of the proposed systems.

ACKNOWLEDGEMENTS

I wish to express my gratitude to all members of the Communication Section from whom, in one way or another, I received help during my stay of over three years at Imperial College.

In particular, I should like to express my gratitude to Dr. L.F. Turner, my Supervisor, for his guidance, encouragement and helpful criticism which have greatly influenced the work of this thesis.

Thanks are also due to all my colleagues; they have been a permanent source of advice and encouragement. Among these colleagues are Dr. Theodore Koubanitsas who first directed my attention to the problem of impulsive noise in data transmission and communicated to me his knowledge of the subject and Michael Buckley whose knowledge of communication systems design was of great help in understanding the practical viability of some ideas presented in this thesis. The advice and encouragement of Dr. Victor Lawrence, Dr. Dalip Sud, Dr. Abdullah Hashim, Michael Lai, Jide Olaniyan and Musa Adongo are also very much appreciated.

I am grateful to Dr. D.J. Goodman of the Bell Laboratories, U.S.A., for his valuable comments on some parts of the thesis. The time and effort spent by Dr. D.C. Newton and my colleagues Michael Buckley, Dr. Peter Beevor, Stuart Lawson and David Haigh should also be acknowledged.

I am indebted to Professors M.A. Faro, F.R. Simões and A.F. dos Santos of Instituto Superior Técnico, Lisbon, for their interest in my research.

The financial support provided by Instituto de Alta Cultura, Ministry of Education, Portugal, is also gratefully acknowledged.

Finally, thanks are due to Mrs Shelagh Murdock for the conscientious and careful way in which she approached the typing of this thesis.

CONTENTS

LIST OF DIAGRAMS

LIST OF TABLES

CHAPTER I

INTRODUCTION

Dimidium facti qui coepit habet: sapere aude.

Horace, "Epistles".

1.1 THE PROBLEM AND BASIC ASSUMPTIONS

This thesis contains the results of an investigation into the problem of transmitting binary data through a channel perturbed by impulsive noise. Impulsive noise consists of transient disturbances of random energies separated in time by random intervals, during which the background Gaussian noise is the dominant noise process. In practice the fraction of time for which these transient disturbances show significant amplitudes is usually small. However, the amplitudes of the impulsive disturbances are generally quite large compared with the peaks of Gaussian noise having the same average power as the observed noise. This explains why the observed noise usually has a first-order probability density function (PDF) with much longer tails than a Gaussian PDF of the same variance, and why most of the errors are caused by the impulsive component of the noise.

Fig. 1.1 is the functional diagram of the communication systems considered in this thesis. The encoder-decoder is assumed to be that part of the system in which a binary linear error-correcting code is implemented [1-1]. Let the encoded binary symbols be presented at a constant rate of one every T_1 seconds to the waveform generator which is assumed to transmit a group of L symbols at a time by sending through the channel every LT_1 seconds (signalling interval) one of 2^L signal waveforms $s_i(t-kLT_1)$ ($i = 0,1,\ldots, 2^L-1$; $k = 0,1,2\ldots$), selected in some way depending on the corresponding group of L binary symbols.* It is further assumed that the channel is linear and perturbed by an additive noise n(t) of the type defined above. It follows from this channel model that if $s_i(t-kLT_1)$ is transmitted, the received waveform is given by $Z_{ik}(t-kLT_1)+n(t)$

---

* Throughout the thesis, any information-bearing entity is termed signal. Signal waveform, waveform or, more often, pulse, are names given to analog (continuous-time, continuous-amplitude) signals.

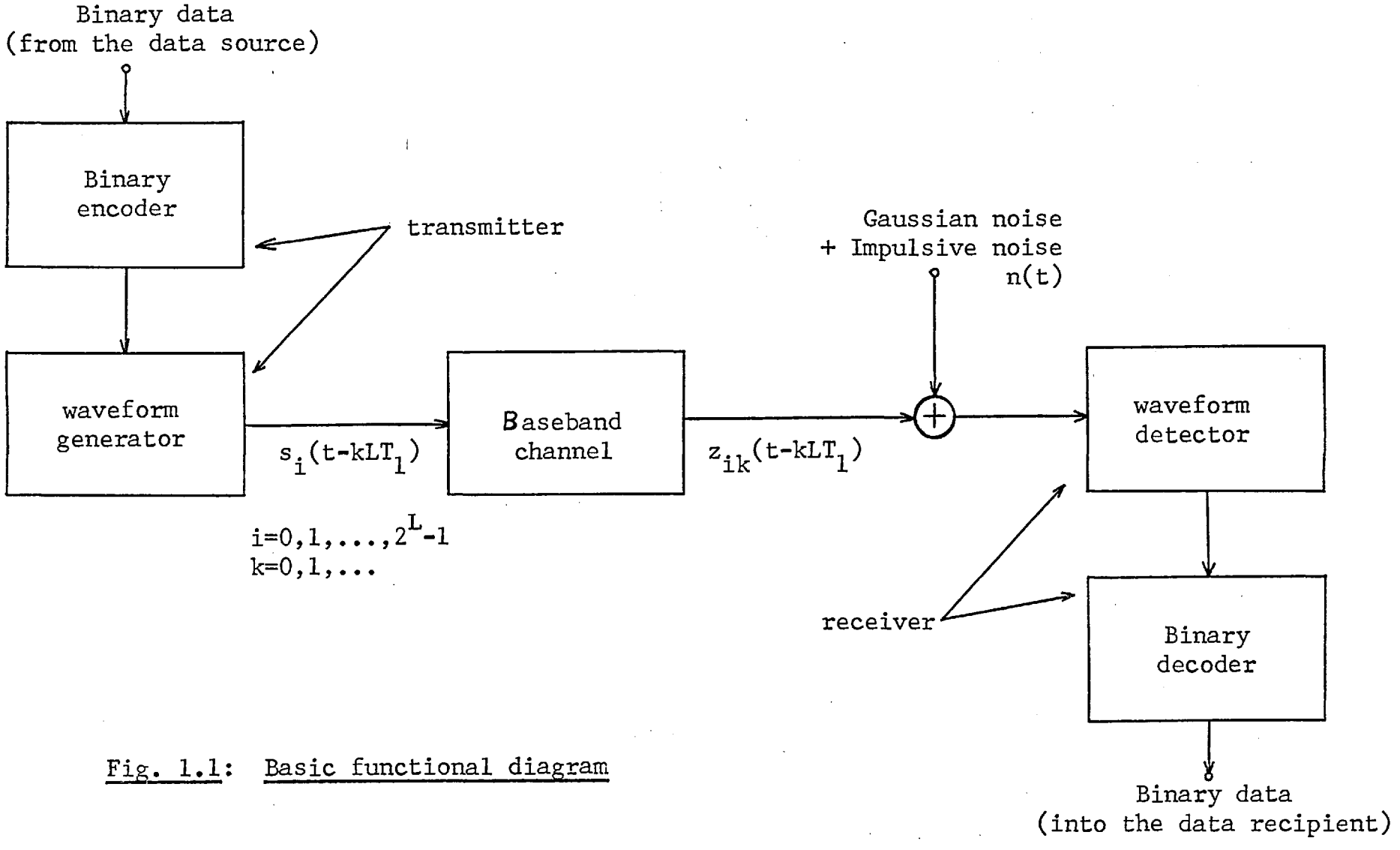

Fig. 1.1: Basic functional diagram

where $Z_{ik}(t-kLT_1)$ is the result of a linear operation* performed on $s_i(t-kLT_1)$. The waveform detector, which is assumed to operate in synchronism with the waveform generator, will have to decide on the basis of the received waveform $Z_{ik}(t-kLT_1)+n(t)$, and its knowledge of the channel and the transmitter, which group of L symbols was transmitted. The waveform $Z_{ik}(t-kLT_1)$ may be a highly distorted version of $s_i(t-kLT_1)$ and the overlap** of consecutive waveforms may prevent the waveform detector from always reaching a correct decision, even in the absence of noise. In general it is not possible to distinguish between the errors caused by the noise and the errors caused by the overlap of the received waveforms. Therefore, in searching for a method for combatting one cause of errors one tends to lose insight into the problem if the other inpairment is also present. For this reason the channel is assumed throughout this thesis to be distortionless, that is,

$$Z_{ik}(t-kLT_1) = \alpha s_i(t-kLT_1-\delta)$$

where α is a constant attenuation and δ is a constant delay. For simplicity, it will often be assumed that $\alpha = 1$ and $\delta = 0$. Other values of α and δ are readily accommodated into the theory. The techniques described and examined in this thesis are therefore only applicable to those cases where either the effect of the distortion introduced by the channel is known to be negligible or this distortion has been effectively removed by equalization***. In the latter situation the equalizer is considered in this thesis as part of the analog channel.

---

* The subscript k in Z_{ik} accounts for the possibility of the channel response depending on the epoch in which the transmitted pulse was sent (time-varying channel).

** This overlap accounts for what is usually known as intersymbol interference [1-2].

*** Equalization is the name given to the technique in which any device capable of compensating for the distortion introduced by the actual channel is used.

The operation of the system depicted in Fig. 1.1 can be summarized as follows. The waveform generator should use the set of 2^L signal waveforms which best counteract the detrimental features of the channel in the sense of easing the task of the waveform detector. Whenever waveform design and detection fails to yield an acceptably low error probability the encoder-decoder pair is included in the system. The encoder is intended to add extra symbols to the data stream so as to enable the decoder to correct most of the errors which occur at the output of the waveform detector.

The generation of the transmitted waveforms generally includes the modulation of a single-frequency carrier by a baseband waveform. In this thesis it is always assumed that a demodulation procedure exists for which the whole modulation-demodulation operation is linear. For convenience, the modulator and the demodulator will be considered parts of the analog channel so that the waveform generator and the waveform detector can be assumed to operate in the baseband region*. The channel in Fig. 1.1 can thus be described as a distortionless baseband channel.

In the systems proposed in this thesis the waveform generator has the form presented in Fig. 1.2(a). For each group of L binary symbols coming from the encoder the serial-to-parallel convertor applies simultaneously one of two antipodal pulses to each filter (e.g. +e for a symbol 0 and -e for a 1). For convenience it is assumed henceforth that $e(t) = \delta(t)$ (Dirac impulse). The waveform generator will thus transmit one of the 2^L baseband pulses of the following form:

$$s_i(t-kLT_1) = \sum_{j=1}^{L} \alpha_{ij} f_j(t-kLT_1), \quad \alpha_{ij} = \pm 1.$$

---

* The assumption of constant channel attenuation implies that the demodulator must be phase-locked to the modulator.

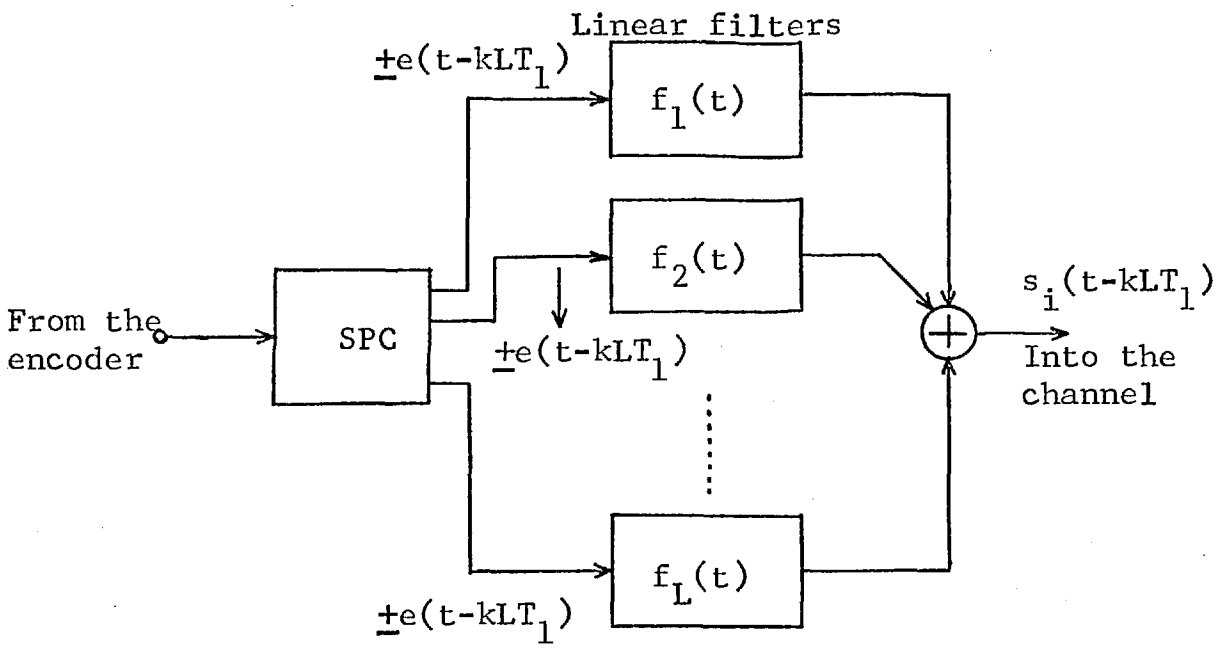

SPC : serial-to-parallel converter

Fig. 1.2(a): Waveform generator

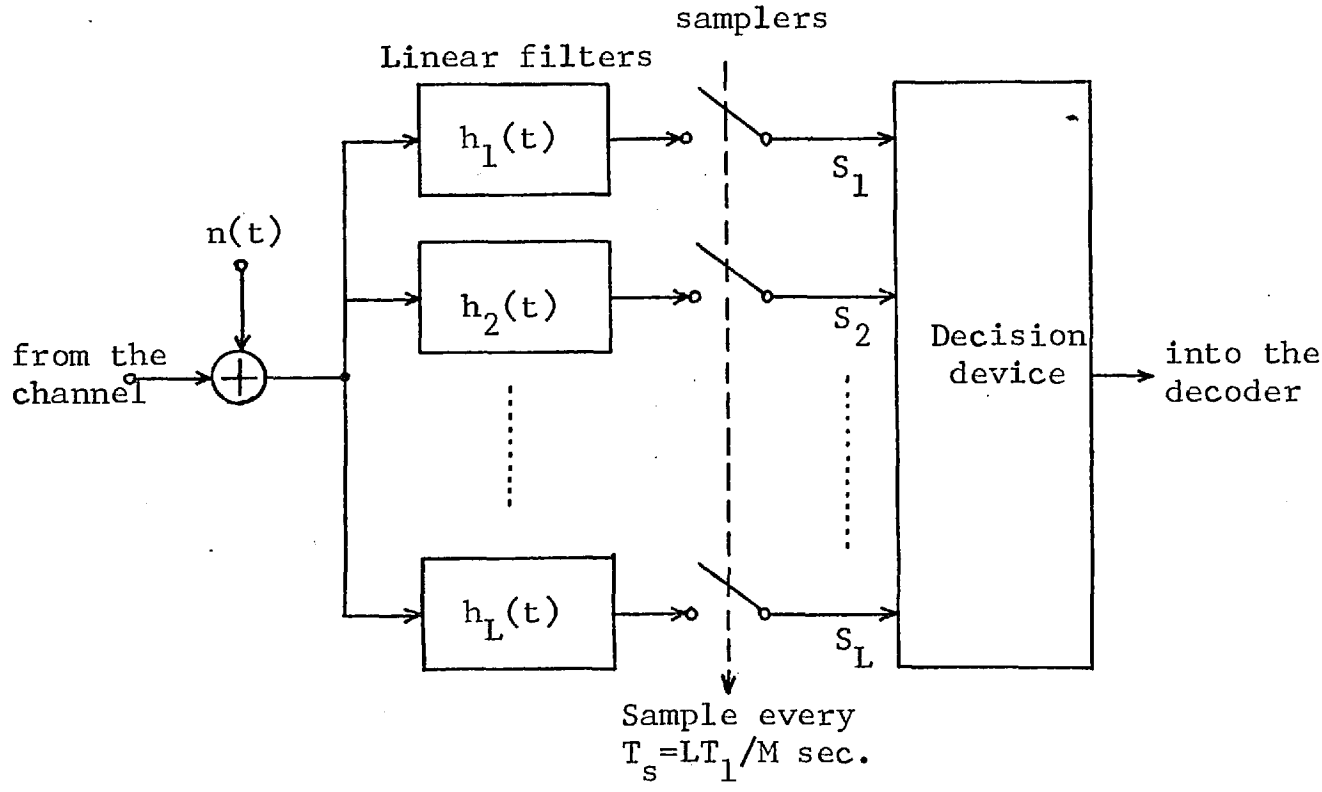

Fig. 1.2(b): Waveform detector

The waveform detector which will be used has the structure shown in Fig. 1.2(b). The samplers shown in this figure are assumed to operate simultaneously every $T_s = LT_1/M$ seconds and the decision device bases the decision about each group of L transmitted symbols on the LM samples obtained within each interval of LT_1 seconds. The integer M is thus the average number of samples the decision device uses per transmitted symbol.

In the presence of white Gaussian noise alone it is always possible to design the transmitting and receiving filters to achieve, with M=1, the minimum error probability corresponding to the system constraints (transmission rate, channel bandwidth and average transmitted power) [1-3]. Furthermore, the above-mentioned filters can be chosen so that each sample S_i in Fig. 1.2(b) depends only on one transmitted symbol*. In this case it is said that the samples S_i exhibit no artificial** intersymbol interference and the decision device consists simply of a parallel-to-serial converter presenting samples S_i sequentially to a zero-threshold detector.

On the other hand, it is not known whether the system structure presented in Fig. 1.2 can achieve the minimum error probability in the presence of any type of non-Gaussian noise. Nevertheless, most of the systems proposed in the literature are essentially based on the structure of Fig. 1.2. The cases studied in the literature suggest that in general an attempt to optimize the system against a given type of non-Gaussian noise necessitates an $M > 1$ and the use of a nonlinear decision device. In this case, the decision device processes the samples S_i nonlinearly in order to obtain the decision statistics. These

---

* The waveforms $f_i(t)$ (i=1,2,...,L) are in this case orthogonal to one another. The optimum performance is obtained if the receiving filter described by $h_i(t)$ is matched to $f_i(t)$ (for all i) [1-3].

** Called artificial because it results from waveform design and not from channel imperfections.

are then compared with a set of thresholds according to some decision rule. The fact that all the nonlinear operations are performed on discrete-time signals makes it easier to avoid intersymbol and interchannel interference than in some cases studied in the literature*.

In a conventional data transmission system both L and M have unit values and both $f_1(t)$ and $h_1(t)$ usually have a duration of about T_1 seconds. This is not the best solution for providing immunity against impulsive noise because it is very likely that the response of the receiving filter to an impulsive disturbance may have a duration in the order of T_1 seconds or longer and a peak amplitude which exceeds the response to a received data pulse. The use of receiving filters having impulse responses $h_i(t)$ much longer than 1/W (W being the channel bandwidth) has long been recognized as a means of combatting impulsive noise [1-4]. By increasing the duration of the $h_i(t)$ most peaks of impulsive noise will eventually be rendered too weak to cause error provided that the majority of the impulsive disturbances at the receiver input are sufficiently short and spaced apart. If this is not the case, one should transmit long waveforms and let the decision device neglect the samples that show the highest a posteriori probability of being affected by impulsive noise [1-5].

In this thesis the results of a theoretical investigation into the use of long waveforms for providing immunity against impulsive noise are reported. The transmitting and receiving filters are assumed to have impulse responses of the following form:

$$\sum_{i=0}^{N-1} a_i \, y(t-iT)$$

---

* See Chapter III for a further discussion of the detector structure.

where y(t) is a baseband pulse essentially time-limited to T seconds and frequency-limited to the channel bandwidth W. This type of filter was chosen for three reasons: (i) ease of implementation, (ii) mathematical tractability, and (iii) the possibility of realizing a large class of impulse responses, for which an at least nearly optimal solution can be expected to exist. In the cases where $NT > LT_1$, consecutively transmitted waveforms will overlap in the channel and thus further care must be taken to prevent artificial intersymbol interference from arising at the output of the waveform detector. Moreover, the overlap of the transmitted waveforms increases the peak transmitted power and thus the length N of these waveforms is limited to a value determined by the maximum peak power the system can handle.

Before considering the organization of this thesis a few words are in order about the noise models used in the error-rate analysis of the proposed techniques. It is always assumed that the impulsive noise component, as viewed by the decision device, can be considered to result from a series of short-duration spikes (elementary impulsive disturbances) applied at the input of the waveform detector*. In some cases it is further assumed that the elementary impulsive disturbances occur independently in time (Poisson impulse noise). In other cases these disturbances are assumed to cluster according to some convenient time distribution (non-Poisson impulse noise). All these assumptions will be justified in Chapter II.

1.2 LAYOUT OF THE THESIS

In the previous section the subject-matter of the thesis was defined in general terms. In this section the contents of the rest of this thesis will be described briefly.

---

* The duration of the spikes is assumed to be much shorter than T seconds.

Chapter II is devoted to a concise review of the literature on impulsive noise characterization and a mathematical description of the noise models is presented for use in later chapters.

Chapter III provides a critical survey of the techniques that have been suggested in the literature for combatting impulsive noise.

The work described in the next four chapters is believed to be original, unless it is specifically ascribed to others by the quoting of an appropriate reference.

In Chapter IV a new class of signal waveforms is presented which allows the designer to choose at will the length N of the transmitted waveforms without introducing any artificial intersymbol interference at the output of the waveform detector and to achieve, for a given channel bandwidth, the same transmission rate as is achieved with a conventional data transmission system. In a frequency division multiplexed (FDM) system interchannel interference can also be avoided. The error-rate analysis of this technique in the presence of a Poisson impulse noise is carried out in this chapter. The case in which the elementary impulsive disturbances tend to occur in bursts (non-Poisson impulse noise) is postponed until Chapter VI. As the title of Chapter IV suggests, the proposed method can only be advantageous under conditions of high signal-to-noise ratio (SNR).

In Chapter V the low SNR case is considered. The decision device is assumed to process several samples per transmitted symbol ($M > 1$) and the possibility of improving its performance by first detecting the samples which are more likely to have been affected by impulsive noise is investigated. The performance of the resulting waveform detector in the presence of Poisson impulse noise is evaluated.

Chapter VI is devoted to a Monte-Carlo simulation of the proposed techniques in the presence of impulsive noise. The numerical results obtained in the two previous chapters are checked and new results are obtained for one type of non-Poisson impulse noise. These new results are intended to show the effect of long bursts of impulsive noise on the data transmission systems.

Since the improvement recorded in Chapter V is obtained at the expense of either a reduction in transmission rate or an increase in channel bandwidth, the use of an encoder-decoder in the system was next considered. This possibility is investigated in Chapter VII where a method of maximizing the overall transmission rate while keeping the overall error probability below a given level is presented.

Finally, Chapter VIII summarizes the general conclusions arising out of the study and examines those questions remaining open at the end of the research project. The reader interested only in the results of the investigation should turn directly to Chapter VIII.

CHAPTER II

CHARACTERIZATION OF IMPULSIVE NOISE

'When I use a word', Humpty Dumpty said in rather a scornful tone, 'it means just what I choose it to mean - neither more nor less'.

Lewis Carroll, "Through the Looking Glass".

2.1 INTRODUCTION

The nondeterministic impairments present in data transmission systems can be divided into three categories:

(a) Background noise:

This noise component is due to ever-present causes, most of which are located at the receiver or in the adjacent equipment. It includes thermal noise, noise from electronic components, "hum" from power supplies, etc. Experience shows that in most situations this noise can be successfully treated as if it were an additive stationary Gaussian process. Moreover, its level is usually too low to seriously affect the error-rate in a data system*.

(b) Impulsive noise:

This noise component is due to causes that act intermittently and that are generally located outside the channel under consideration. Impulsive noise, which can generally be considered as additive, is troublesome because its time of occurrence is unpredictable and the noise pulses observed at the input of the decision device generally have a peak amplitude which is quite large compared with the peaks of background noise.

(c) Multiplicative noise:

As mentioned above, both the background noise and the impulsive noise are additive impairments. A third class of disturbances, which is due to erratic variations of the transmission system, gives rise to the so-called "multiplicative" noise. It includes sudden level fades, momentary equipment failure, or circuit interruptions, changes in the phase response of the channel, translations of frequency occurring in some single-sideband carrier systems, etc.

---

* The signal-to-background-noise ratio is typically 20 to 50 dB.

This thesis is mainly concerned with waveform design. Experience shows that waveform design techniques are quite ineffective against multiplicative noise because in this case most errors are due to signal "dropouts". Under these catastrophic (and fortunately exceptional) conditions, recourse to coding seems to be the only hope [2-1, 40]. As stated in Chapter I, only distortionless time-invariant data systems will be considered in this thesis and consequently the question of multiplicative noise will not arise.

The rest of this chapter deals with the detailed description of the impulsive noise component which, under the above conditions, is the major cause of errors.

2.2 OBSERVED CHARACTERISTICS OF IMPULSIVE NOISE

The vast majority of noise pulses observed at the input of the decision device are the response of the receiving filter(s) to transient disturbances arising from sources which are independent from the message-circuit noise sources. For this reason it will always be assumed that the impulsive noise is statistically independent of the background noise.

Sometimes the source of impulsive noise generates a wideband disturbance composed of a sequence of very short and nonoverlapping pulses. In this case the exciting disturbance will produce approximately the same effect on a narrow band receiving filter as a sequence of Dirac impulses. However, the original noise pulses may be so close to each other that considerable overlap will occur at the output of the receiving filter. Situations also arise in which the original disturbance is narrowband (e.g. noise due to intermodulation distortion or crosstalk) and, under these circumstances, the noise waveform observed at the output of the receiving filter looks very different from a sequence of identically shaped pulses. It

should be noticed that the shape of an observed noise pulse may strongly depend on the point where the exciting pulse has entered the message-circuit. Moreover, the number of possible noise sources and types of data system is usually very large and, in some cases, the noise source or the data system are not precisely defined. This is often the case with the telephone network. In view of the above, it is clear that any classification or identification of the observed shapes of the noise bursts, in relation to their causes and the type of transmission system, is a very difficult task which is bound to produce rather imprecise results [2-2,3].

Possible causes of impulsive noise are switching transients in the telephone plant, lightning storms, ignition discharges, crosstalk from adjacent circuits in a telephone cable, radio interference in a radio link, power line interference, intermodulation products, accidental hits during maintenance work, and a multitude of other causes. Because much of this noise is man-made, experience shows a close correlation between impulsive noise activity and the busy hours of the day. This dependence on human activity and the sporadic nature of some natural causes make impulsive noise a strongly nonstationary process over long periods of observation. Nevertheless the assumption can often be made that the process is stationary on a short-term basis, i.e. over periods of about an hour. Periods of this order of magnitude are usually taken as measurement intervals. Whether impulsive noise may be considered an ergodic process over these short intervals is still an open question. In some instances time-averaging measurements of impulsive noise have been found rather inconclusive [2-4].

By definition, impulsive noise is a noncontinual type of disturbance, that is to say, its sources are not permanently active. It thus seems that the simplest way of mathematically defining this noise is to give the statistical distribution of the time intervals during which the noise sources are active,

the distribution of the quiet intervals and the amplitude distribution of the noise.

The measurements of impulsive noise reported in the literature are of two types: analog measurements and measurements of error statistics. In an analog measurement the noise observed at the output of a receiving filter is recorded on magnetic tape, usually in the absence of any transmitted signal. Normally the only noise recorded is that above a fixed threshold that has a very low probability of being exceeded by the background noise and is somewhat lower than the normal signal levels. Analog measurements make it possible to study both the amplitude distribution and the time distributions of the noise. In a measurement of error statistics, two identical data generators are used, one at the transmitting end of the channel under test and the other at the receiving end. As both generators are synchronized to each other and produce the same pseudo-random sequence of data, it is possible to compare the received and the original messages and record the errors that occur at the detector output. Most noise measurements reported in the literature are of this type mainly because the aim is in most cases to devise efficient coding techniques and because the error measurements are easier to carry out. As far as the time distributions are concerned, a close correlation is to be expected between the results of both types of measurement. In other words, one could expect to find a burst of errors when a burst of impulsive noise is recorded and vice versa. However, when multiplicative noise is present errors may occur which do not correspond to any impulsive noise. For this reason, methods of measuring the multiplicative noise have also been proposed in the literature [2-2,5].

During each period of activity a source of impulsive noise generates a noise burst which, as already stated, may or may not look like a sequence of individual pulses. The peak amplitudes and the effective durations of the noise bursts at the output of a receiving filter vary over wide ranges. The

peak amplitudes may be much higher than the normal signal level and, on the other hand, they may be so small as to be confused with the background noise. Nevertheless, the average peak amplitude is usually much larger than that of the background noise. The burst durations may be of the order of magnitude of the signalling interval and, on the other hand, they may be hundreds of times longer. However, the average quiet (inter-burst) interval is usually much longer than the average burst duration. Experience shows that the average noise power is generally determined by the background noise whereas the impulsive noise determines the error rate [2-27].

Measured cumulative distribution functions of the burst durations, quiet intervals and burst amplitudes have been presented in several papers [2-6 to 26]. Empirical statistical laws have been proposed which seem to fit the experimental data with sufficient accuracy for common engineering purposes. These empirical laws will be considered briefly in the rest of this section.

A study of analog recordings of impulsive noise is best formulated in terms of a formal definition of a burst of noise. The following definition is taken from Ref. [2-23] and is illustrated by Fig. 2.1. All portions of the noise waveform that

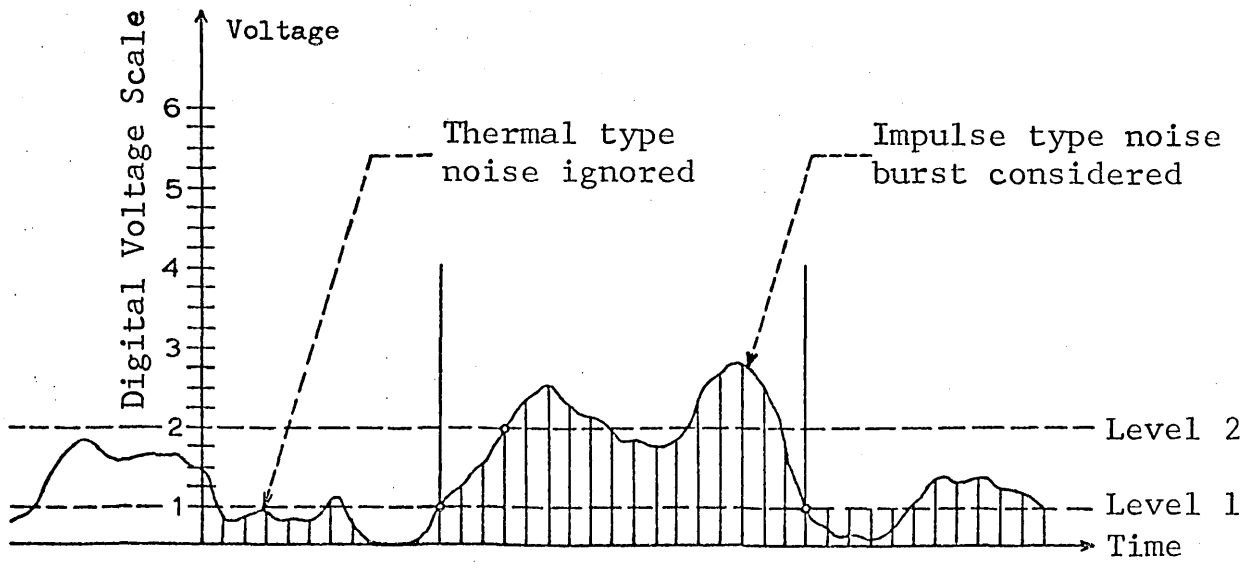

Fig. 2.1 Ideally rectified noise waveform illustrating definition of pulse length.

remain below a specified observation threshold, designated level 2, are considered as part of the background noise until level 2 is exceeded. Once level 2 is exceeded, the noise pulse is measured starting at the point where level 1 was exceeded (as indicated in the figure) and continuing until it returns below level 1 and remains below this level for a specified amount of time referred to as guard interval. The function of the guard interval is to provide a distinction between nodes of a single burst and two bursts which occur close together in time. A value twice the inverse of the baseband channel bandwidth has been found in practice to be a convenient guard interval [2-23]. The function of level 1 is to allow the study of the leading and trailing edges of the noise burst. Level 1 is set typically 10 dB above the r.m.s. value of the background noise*. The observation threshold (level 2) is typically between 13 and 16 dB above the r.m.s. value of the background noise and thus the probability of it being exceeded by the background noise is very low.

The amplitude distribution of impulsive noise can be defined in two different ways: as the probability distribution of the instantaneous amplitudes of the noise and as the probability distribution of the peak amplitudes of individual noise bursts**. As the decision device takes in noise samples that do not always coincide with the peak amplitudes of the noise bursts, the distribution of the instantaneous amplitudes appears to have greater meaning***. In fact, the peak amplitude is really only

---

* As already stated, this r.m.s. value is practically the same as the r.m.s. of the entire additive noise.

** In the case of bandpass noise the noise envelope is used for the measurement.

*** This distribution can be obtained by measuring the fraction of time for which the rectified noise exceeds an adjustable threshold or by studying the noise samples obtained at a sufficiently high rate.

suitable for specifying short noise bursts, i.e. bursts whose duration is in the order of the duration of a data pulse. When the burst duration increases the peak amplitude becomes less and less meaningful due to the increasing variety of possible burst shapes.

The above definition of noise burst implies that the measured amplitude distributions are only the tails of the actual distributions. In fact the noise is examined only when it has a value above level 1 in Fig. 2.1, i.e. at values which have probabilities of 10^{-2}, or less, of being exceeded. In practice this limitation is of little importance since only the high-amplitude disturbances are potentially destructive to data signals. On the other hand, the noise bursts of lower amplitude tend to be confused with the continual background noise and are thus difficult to measure.

Mertz [2-11, 20] suggested the use of an empirical hyperbolic distribution to describe the observed amplitudes of impulsive noise. This means that the probability density function (PDF) of the noise amplitude is given by

$$p(|v|) = \frac{n}{h}\left(1 + \frac{|v|}{h}\right)^{-n-1} \qquad (1)$$

where: v = noise amplitude
n = order of the distribution
h = bias of the distribution

The result of the noise measurement is normally the "exceedence" probability function (EPF), that is,

$$E(x) = \text{Prob}[|v| > x] = \left(1 + \frac{x}{h}\right)^{-n} \qquad (2)$$

In Ref. [2-6] a slightly different expression is proposed for the EPF of atmospheric impulsive noise at very low frequencies (VLF), which is,

$$E(x) = \left[1 + (x/h)^n\right]^{-1} \qquad (3)$$

The value of the parameter h in both expressions is normally such that it has practically no influence on the tail of the EPF, which is represented on a log-log paper by a straight line of slope -n. Since the measured values are on this tail, the expressions (2) and (3) are equivalent from a practical point of view. Values of n ranging from a little over 2 to 20 have been measured [2-18]. It can readily be shown that a finite r.m.s. value of the noise implies $n > 2$.

Other amplitude distributions have been used to describe the impulsive noise observed in telephone lines and radio channels [2-27 to 29]. Among them are the log-normal distribution* and the distribution whose EPF is

$$E(x) = \exp\left[-(x/x_o)^{\alpha}\right] \qquad (4)$$

where $0 < \alpha \leq 2$ [2-27].

It seems that any of the laws mentioned above can be made to fit measured values sufficiently well, provided that the distribution parameters are suitably chosen [2-27]. Experimental data for much higher and lower probabilities of occurrence would be necessary to determine which law (if any) is closest to nature.

As pointed out previously, most measured time statistics concern the errors rather than the noise itself. The errors caused by impulsive noise, unlike those due to the background noise, are strongly correlated and tend to occur in bursts. When analog measurements are not available, a definition is necessary to identify a burst of errors. Several definitions have been proposed in the literature [2-31]. In Ref. [2-21] a burst of length B and weight W is defined as a sequence of B digits, of which W are in error, such that:

---

* In Ref. [2-30] a log-normal law is used instead of the hyperboic law for reasons of mathematical tractability. The log-normal law is also used in Ref. [2-8].

(a) The first and the last digits of the sequence are in error;

(b) the error density W/B is higher than a specified minimum density Δ;

(c) the burst length B is the maximum number under the previous conditions.

Those sequences of bits which lie between bursts are called "intervals". If Δ is somewhat higher than the error probability due to the background noise*, the bursts of errors will coincide approximately with those regions of the data stream affected by bursts of impulsive noise, provided that the effect of the multiplicative noise is negligible.

The measured cumulative distributions published in Refs. [2-21, 22] show that long burst and interval lengths have a much higher probability of occurrence than a purely random distribution of errors would imply. Moreover, in all the channels considered in Refs. [2-21, 22] the occurrence of a long sequence of consecutive errors or the occurrence of an interval shorter than the adjacent bursts are rare events.

The problem of finding the statistical laws that govern the burst durations, the error occurrence within a burst and the interval durations has been considered by several authors [2-32]. Mertz [2-13, 14, 20] uses hyperbolic laws to fit the experimental data concerning the length of the error burst and the length of the inter-burst intervals. He also points out, without attempting to justify it, that the short-period and the long-period distributions often exhibit different parameters**. As in the case of the amplitude distribution, other empirical laws

---

* In Ref. [2-22] meaningful results were obtained for $\Delta = 0.05$.

** The same effect was pointed out in Ref. [2-7].

have been proposed in the literature. In Ref. [2-33] the log-normal distribution is chosen to describe the burst and interval durations whereas in Ref. [2-15] the error occurrence is described in terms of the Pareto distribution*.

A study of the literature on impulsive noise measurements suggests strongly that it is impossible to describe by a single mathematical theory the experimental facts. This is almost certainly due to the great variety of situations encountered in practice and to the fact that in most situations the noise is strongly non-stationary over periods of several hours.

2.3 THEORETICAL MODELS OF IMPULSIVE NOISE

In a search for methods of combatting impulsive noise it is obviously advantageous to have a mathematical description of the noise. This description will make it possible to obtain the PDF's of the noise samples at the input of the decision device, or at least to generate these samples in a computer. If possible, the noise model should exhibit those characteristics of the observed noise which are believed to determine the performance of the data system and, at the same time, it should be simple enough to be mathematically tractable. Usually a compromise between these requirements is necessary.

If $n_w(t)$ is the part of the impulsive noise at the input of a baseband receiving filter which is within the bandwidth W of the receiving filter, then, according to the sampling theorem,

$$n_w(t) = 2W \sum_{i=-\infty}^{\infty} a_i \frac{\sin 2\pi W(t-t_i)}{2\pi W(t-t_i)} \qquad (5)$$

where $$t_i = t_o + \frac{i}{2W} \qquad (6)$$

---

* The Pareto distribution is in fact a hyperbolic-type law with zero bias.

and $$2Wa_i = n_w(t_i) \tag{7}$$

Let h(t) be the impulse response of the receiving filter. It can readily be shown that the impulsive noise at the output of this filter is given with good approximation by

$$r_I(t) \approx \sum_{i=-\infty}^{\infty} a_i \, h(t - t_i) \tag{8}$$

The noise n(t) at the input of the receiving filter can thus be assumed to be given by

$$n(t) = n_G(t) + \sum_{i=-\infty}^{\infty} a_i \quad \delta(t - t_i) \tag{9}$$

where $n_G(t)$ represents the background noise.

The impulsive noise often originates in the bandpass section of the channel. If the impulse response of the front-end filter of the receiver is $r(t)\cos(2\pi f_c t + \varphi_o)$, f_c being the carrier frequency, it is possible to show that the impulsive noise at the demodulator input can be written in the following form (see Ref. [2-34], Sec. 2.3):

$$n_B(t) = \sum_{k=-\infty}^{\infty} A_K \, r(t - t_K)\cos(2\pi f_c t - \psi_K) \tag{10}$$

This relation is the bandpass equivalent to relation (8) and can be derived following a similar procedure. This bandpass noise can be split into two components in phase quadrature, that is,

$$n_B(t) = n_C(t)\cos(\omega_c t + \alpha_o) + n_S(t)\sin(\omega_c t + \alpha_o) \tag{11}$$

where $$n_C(t) = \sum_{K=-\infty}^{\infty} A_K \cos(\psi_K + \alpha_o) r(t - t_K) \tag{12}$$

and $$n_S(t) = \sum_{K=-\infty}^{\infty} A_K \sin(\psi_K + \alpha_o) r(t - t_K) \tag{13}$$

If α_o is suitably chosen, the noise at the demodulation output will be $n_c(t)$ and will thus have the form in Equation (8). This completes the proof that the impulsive noise at the output of an equivalent baseband receiving filter of impulse response h(t) can always be expressed as in Equation (8). In many cases the receiving filter has an impulse response whose amplitude is very small outside an interval in the order of 1/W seconds duration. It thus follows that each noise sample delivered to the decision device can be approximated by a linear function of a small number of amplitudes a_i [see Equation (7)]. To complete this model, it is reasonable to assume that the amplitudes a_i have zero value outside the time intervals corresponding to the noise bursts. An alternative approach used later in this thesis is to assume that the samples of impulsive noise at the input of the decision device have negligible amplitude when outside the noise bursts. The noise can thus be defined by the distribution of the samples within the noise bursts, the distribution of the burst lengths and the distribution of the gaps between bursts.

Other models of impulsive noise have been proposed in which the elementary noise pulses do not occur periodically [2-12,35,36]. The simplest and most important example is the so-called Poisson impulse noise. In this case the amplitudes a_i in Equation (8) are statistically independent of one another and also of the instants t_i and these instants form a Poisson sequence of rate ν per second [2-37]. If the amplitudes a_i are identically distributed, and their characteristic function (CHF) is $F_a(u)$, it can be shown [2-35] that the CHF of the noise samples at the output of the receiving filter is

$$F_r(u) = \exp\left\{\nu\int_{-\infty}^{\infty}[F_a(uh(t))-1]\,dt\right\} \qquad (14)$$

In most cases it is not possible to find a closed-form expression for $F_r(u)$ [2-38]. The situation is even more complicated when the times t_i are distributed according to a non-Poisson law.

The mean and autocorrelation of the process defined by Equation (8) can be readily obtained under the following assumptions:

(a) The amplitudes a_i are uncorrelated random variables with zero mean and variance α^2;

(b) The amplitudes a_i are statistically independent of the instants t_i and the elementary noise pulses $a_i h(t-t_i)$ occur at a uniform average rate of ν per second.

It is shown in Ref. [2-39] that under these assumptions

$$E[r_I(t)] = 0 \tag{15}$$

and

$$E[r_I(t).r_I(t+\tau)] = \nu\alpha^2 \int_{-\infty}^{\infty} h(t)h(t+\tau)dt \tag{16}$$

It thus follows that the power spectral density of $r_I(t)$ is given by

$$R_I(f) = \nu\alpha^2 |H(f)|^2$$

where H(f) denotes the transfer function of the receiving filter. The impulsive noise at the input of this filter thus has a uniform power spectral density (white noise). In the case of a Poisson impulse noise Equations (15) and (16) can be derived directly from Equation (14) and the highest-order characteristic functions, as shown in Ref. [2-37].

CHAPTER III

A SURVEY OF EXISTING TECHNIQUES FOR COMBATTING IMPULSIVE NOISE

A man must see, do and think things for himself, in the face of those who are sure that they have already been over all that ground. In science, there is no substitute for independence.

J. Bronowski, "Science and Human Values".

3.1 INTRODUCTION

Since impulsive noise can often be described by a large-variance amplitude distribution*, to increase the transmitted energy per symbol is a very inefficient method (from a power standpoint) of improving the system performance. Another alternative is the use of signal waveforms with a long duration relative to the average effective duration of the noise bursts [3-1]. There are three mechanisms by which this method may provide an improvement. Firstly, if the impulse responses of the receiving filters have long duration, a single elementary disturbance will be spread out and therefore the noise peaks will be reduced. Secondly, if a burst of elementary disturbances occurs, the smeared responses of each filter will overlap and, according to the central limit theorem, the PDF of the resulting noise will have shorter tails. Thirdly, if the transmitted waveforms have long duration the receiver can weight the samples of the received waveform in accordance with the a posteriori probability of them being corrupted by impulsive noise. Since in practice the noise bursts usually have a low density**, the receiver can generally obtain a sufficiently large number of reliable samples on which to base the decision.

If it is decided to maintain the data-rate while increasing the duration of the data pulses, then obviously the pulses must overlap in the channel. There are cases in which the overlap prevents the receiver from achieving any improvement and in these cases, in order to obtain some improvement, it is necessary to reduce the data-rate.

The remainder of this chapter is a brief and critical survey of the waveform design and detection techniques that have

---

* This means that the ratio of the standard deviation to the median of the absolute value of the noise is much higher than for a Gaussian distribution.

** Here "density" means "fraction of time in which the signal is strongly affected by impulsive noise".

been proposed in the literature for use in one-way communication systems perturbed by impulsive noise.

3.2 ORTHONORMAL FUNCTION CODING

In this case N mutually orthogonal waveforms, essentially time-limited to NT seconds, are sent simultaneously through the channel every NT seconds. Each group of K binary digits produced by the data source will thus be transmitted by means of a waveform of the following type:

$$s_i(t) = \sum_{j=1}^{N} a_{ij}\, \varphi_j(t) \qquad (1)$$

($i = 1,2,\ldots,2^K$), where the $\varphi_j(t)$ belong to an orthonormal set of functions and are essentially time-limited to NT seconds. The choice of the orthonormal set $\{\varphi_j(t)\}$ and the way of assigning the coefficients a_{ij} to a given group of K binary digits define the coding scheme. In this section, as in Refs. [3-3,4], it will be assumed that K=N and that each term in Equation (1) represents one of K binary digits. The corresponding optimum receiver for use in the presence of white Gaussian noise alone contains a set of filters matched to the waveforms $\varphi_j(t)$, the outputs of which are sampled every NT seconds [3-2]. The samples obtained in this way are the estimates of the coefficients a_{ij}, and the decision about each transmitted binary digit is then made by comparing the corresponding sample with a known threshold value. All the threshold values will be zero if $|a_{ij}| = a$, for all i and j, in which case Equation (1) becomes

$$s_i(t) = a \sum_{j=1}^{N} \varepsilon_{ij}\, \varphi_j(t) \qquad (2)$$

with $\varepsilon_{ij} = \pm 1$ and $i = 1,2,\ldots 2^N$.

It is shown in Ref. [3-2] that in the presence of white Gaussian noise the error probability achieved with the previous technique does not depend on the particular set $\{\varphi_j(t)\}$ chosen.

However, in the presence of impulsive noise the error probability is in general dependent on the orthonormal set of functions used but the exact form of this dependence is not usually known. It will be shown in Chapter IV that in the case of Poisson impulse noise a good design strategy is to choose each function $\varphi_j(t)$ so that the N subintervals of T seconds duration contain nearly the same fraction of the total unit energy. In the presence of non-Poisson types of noise it is also shown in Chapter IV that this may not be the best distribution of energy for the functions $\varphi_j(t)$.

The error-rate analysis of this technique in the presence of Poisson impulse noise was carried out in Refs. [3-3,4] for the following orthonormal set of functions:

$$\varphi_j(t) = \begin{cases} \sqrt{\frac{2}{NT}} \cos \frac{2\pi(n_o + j)t}{NT}, & 0 \leq t \leq NT \\ 0, \text{ otherwise, } j = 1,2,\ldots,N. \end{cases} \qquad (3)$$

This signalling scheme is equivalent to having N binary PSK adjacent subchannels, each one having a bandwidth N times smaller than the overall channel bandwidth. For a fixed average transmitted power the energy per symbol in each subchannel conserves its value as N increases, but the amplitude of the impulse response of each subchannel decreases proportionally as $1/\sqrt{N}$. Moreover, as N increases the data-rate and the required bandwidth maintain their values and no intersymbol interference is introduced.

By analysing the results presented in Refs. [3-3,4] it can be concluded that an increase in N will only lead to an error-rate reduction if the SNR exceeds a critical threshold which decreases as N increases. This is readily understood if one notes that:

(a) for sufficiently low SNR's, a given isolated noise pulse will cause more errors if $N>1$ than if $N = 1$;

(b) as N increases, the noise at the input of the decision device tends to become Gaussian because many long impulsive disturbances overlap at a given instant. Therefore, a reduction in the probability of a high noise magnitude is obtained at the expense of an increase in the probability of a low noise magnitude. It should therefore be expected that, as the amplitude distribution of the impulsive disturbances at the receiver input deviates from a Gaussian distribution, the improvement obtained for a given N and an SNR above the critical threshold will be reduced.

A disadvantage of this technique is that the peak amplitude of the transmitted signal is proportional to $\sqrt{N}$. For large N this transmitted signal will exhibit a nearly Gaussian amplitude distribution.

Another method of designing a set of orthonormal functions overlapping not only in time but also in frequency will be used in Chapter IV. It consists of designing the functions $\varphi_j(t)$ as sequences of similar pulses, i.e.

$$\varphi_j(t) = \sum_{i=0}^{N-1} r_{ji} y(t - iT) \qquad (4)$$

where y(t) is a pulse essentially time-limited to T seconds and frequency-limited to the channel bandwidth W.

3.3 NOISE-SMEARING TECHNIQUE

The structure of the data system in this case is shown in Fig. 3.1.

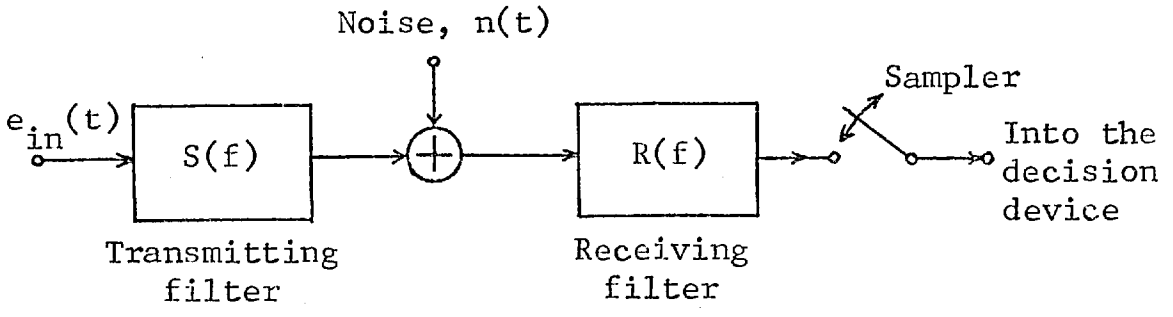

Fig. 3.1:

For convenience, $e_{in}(t)$ is a signalling sequence of positive and negative unit impulses which recur at intervals of T seconds duration. The receiving filter is designed so as to spread out the impulsive noise energy and thus reduce the noise peak amplitude at the input of the decision device. In order to avoid intersymbol interference the transmitting filter is designed so that the overall transfer function S(f).R(f) is the Fourier spectrum of a pulse whose samples obtained at intervals of T seconds duration are all zero but one.

This technique was first proposed in Refs. [3-5,6] but no procedure was given there for optimally designing the filters. In Ref. [3-7] an amplitude-response $|R(f)|$ was derived which minimizes an upper-bound on the impulse response r(t) of the filter. This upper-bound is given by

$$\int_{-\infty}^{\infty} |R(f)|\, df \geq |r(t)| \qquad (5)$$

where the equality holds if the filter has a linear phase-response. Since this optimization technique is obviously insensitive to phase, no optimum phase-response could be obtained in Ref. [3-7]. In Ref. [3-8] another amplitude-response R(f) was obtained by minimizing the error probability of a system using an approximate PDF for the impulsive noise. This technique is also insensitive to the phase of R(f) and the results are approximately the same as in Ref. [3-7]. The beneficial effect a nonlinear phase-response may have on the performance of the system is analysed in Ref. [3-8] for some special cases.

The best optimization procedure presented in the literature is the one in Ref. [3-9] because it takes into account both the amplitude-response and the phase-response of the receiving filter. The approach followed in this reference can be regarded as an extension of that in Ref. [3-7] and consists in minimizing the functional

$$F[\underline{r}(t)] = \int_{-\infty}^{\infty} r^{2n}(t)dt \qquad (6)$$

If n is sufficiently large only the largest peaks in r(t) will make an appreciable contribution to the integral and if, furthermore, one peak is slightly higher than the others it will predominate. The value of the largest peaks of r(t) will therefore be minimized, regardless of their location. No general solution of this problem was presented in Ref. [3-9] and the particular impulse response presented there does not lead to a better performance than the class of waveforms given in Chapter IV, which have the form in Equation (4). Since no constraint is placed on the effective duration of r(t) (or on the peak transmitted power) no unique optimum solution should be expected from the optimization procedure used in Ref. [3-9].

It is important to point out that a reduction in the highest peak of r(t) does not necessarily minimize the number of errors produced by several noise impulses. The general problem of minimizing the error probability under the constraints of average and peak transmitted powers still remains unsolved. Until its solution is found it seems that the best one can do is to try families of waveforms optimizing their parameters for minimum error probability under the channel constraints. This is the approach followed in Chapter IV.

3.4 NONLINEAR AND NOISE-CONTROLLED RECEIVERS

In this section some attempts to optimize the receiver in the presence of impulsive noise are considered. The transmitter will be assumed to send through the channel nonoverlapping waveforms somewhat longer than the average impulsive disturbance at the output of the receiver front-end filter.

It is well known that the optimum receiver for use in the presence of Gaussian noise alone is linear. On the other hand, in the presence of impulsive noise, the most efficient receivers are in general nonlinear. Two intuitive approaches to the design of these nonlinear receivers have been proposed

in the literature [3-10 to 16]:

(a) The inclusion of nonlinear saturating elements (noise clippers) in the receiver;

(b) disturbance-triggered, gating-out schemes, whereby the receiver signal path is interrupted at some suitable stage when a noise pulse is recognized.

In both cases the receiver can be described by means of the diagram shown in Fig. 3.2, where the block B contains the nonlinear elements. In a typical noise-clipping scheme the nonlinear block consists of a clipper arranged to clip off as much of the noise as possible without running into the danger of clipping the signal between the noise pulses. The smoothing filter (block C) then suppresses the frequency components out of the frequency-band of the desired signal [3-11].

In a typical noise-gating-out scheme the nonlinear block B comprises two signal paths with a common input, one of which is essentially a noise-detecting circuit and the other a circuit whose operation is controlled by the first one. The noise-detecting branch gates out completely the controlled branch whenever the amplitude of the received signal-plus-noise exceeds a threshold set somewhere above the expected level of the signal. The desired signal emerges from the controlled branch with "holes" which are then smoothed out by filter C [3-10]. Since these "holes" will have a duration in the order of W^{-1} seconds, or longer, (W Hertz being the bandwidth of the front-end filter A) it can be concluded that the previous techniques can only be effective if W^{-1} is somewhat smaller than the signalling interval (T_1 seconds), that is, the bandwidth W must be somewhat greater than the bandwidth of the data pulses [3-12,16].

When the nonlinear block B is a zero-memory device its ideal transfer characteristic is as shown in Fig. 3.3. If the

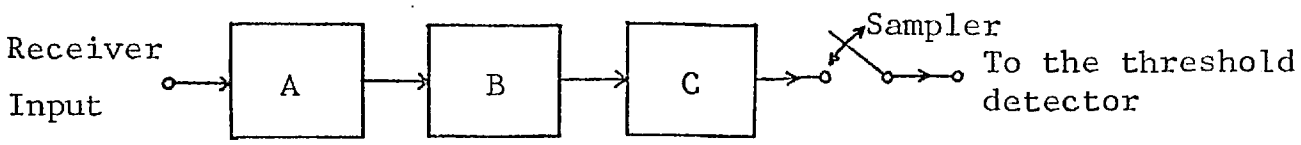

A - Front-end filter
B - Clipping or gating-out stage
C - Smoothing filter

Fig. 3.2

—/—

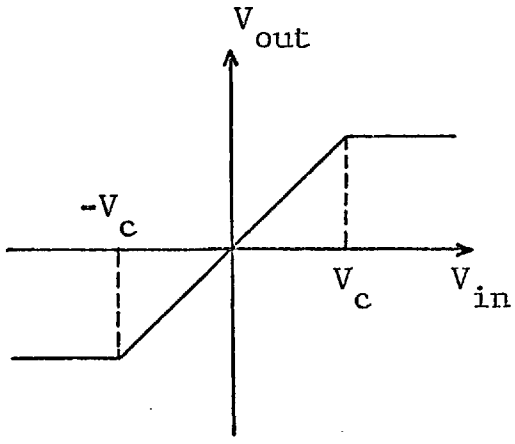

(a) Clipping

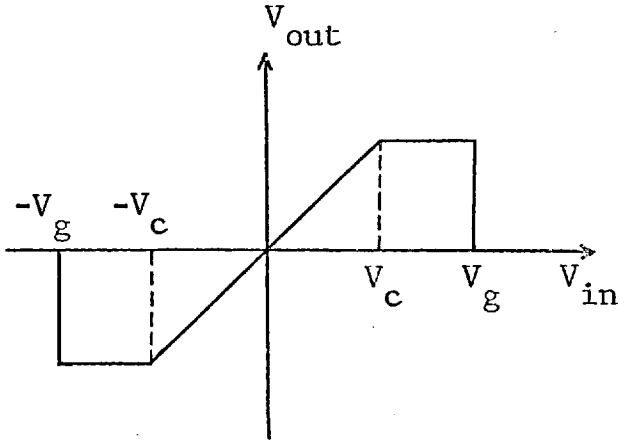

(b) Gating-out

Fig. 3.3

V_c : clipping threshold

V_g : Gating-out threshold

—/—

Fig. 3.4

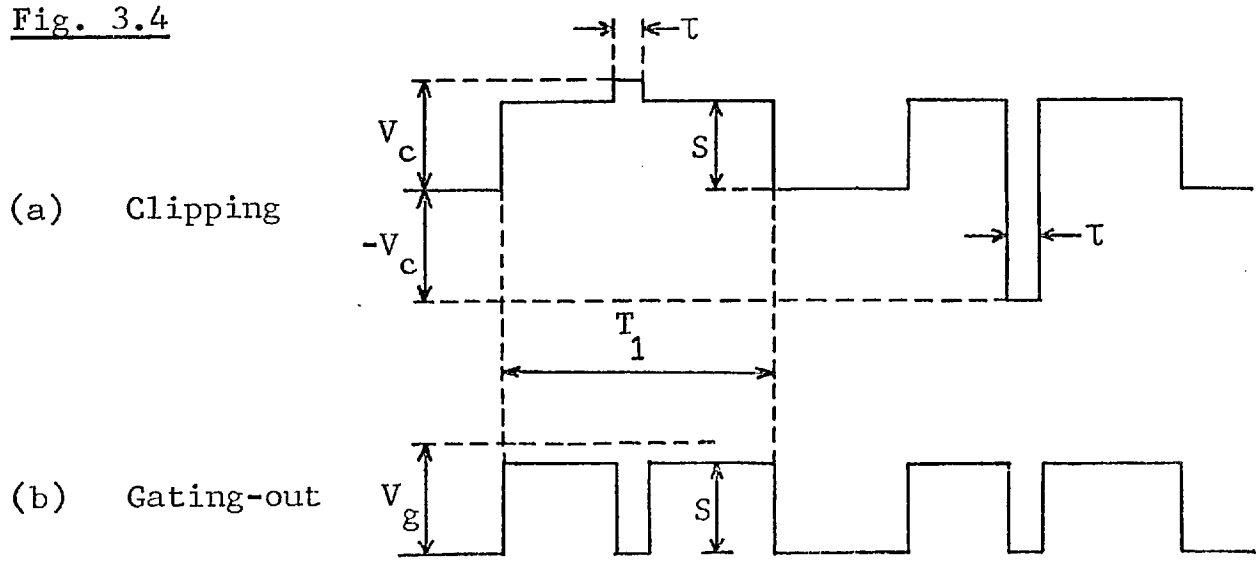

(a) Clipping

(b) Gating-out

data pulses have an approximately rectangular shape and $W^{-1} \ll T_1$ then the waveform obtained at the output of block B will display shapes like those in Fig. 3.4, where the noise pulses were assumed to have peak amplitudes much greater than the signal amplitude S. If further the smoothing filter is matched to the data pulses* it can readily be concluded from Fig. 3.4 that an error may only occur if $T_1 < 2\tau$. Therefore the previous schemes can only be efficient when the fraction of the signalling interval occupied by the noise pulses at the output of the front-end filter is sufficiently small.

In the previously quoted references no attempt was made to optimize the receiver in a decision theoretic sense. This was done in Refs. [3-17 to 24] where optimum and suboptimum nonlinear receivers for use against non-Gaussian noise were derived. In Ref. [3-20] it is assumed that the input bandwidth W of the receiver is several times as large as the bandwidth of the data pulses. In data transmission it is more convenient to shorten the elementary pulses to about W^{-1} seconds duration and to transmit each data symbol by means of M consecutive pulses [3-17]. The waveform received for each data symbol will thus be:

$$v(t) = \pm \sum_{k=0}^{M-1} f(t - Kt) + n(t) \qquad (7)$$

where f(t) stands for the elementary pulse shape and n(t) for the noise process. The corresponding receiver is shown in Fig. 3.5(a) and, apart from the zero-memory nonlinearity (ZNL) and the storage device, is assumed to operate in the conventional manner [3-7]. The receiving filter is designed so that the samples delivered to the zero-memory nonlinear device exhibit no interpulse interference. When n(t) is a continual non-Gaussian noise the zero-memory nonlinearity is designed optimally

---

* Under the previous assumptions this means that the smoothing filter performs an integration operation.

Fig. 3.5(a)

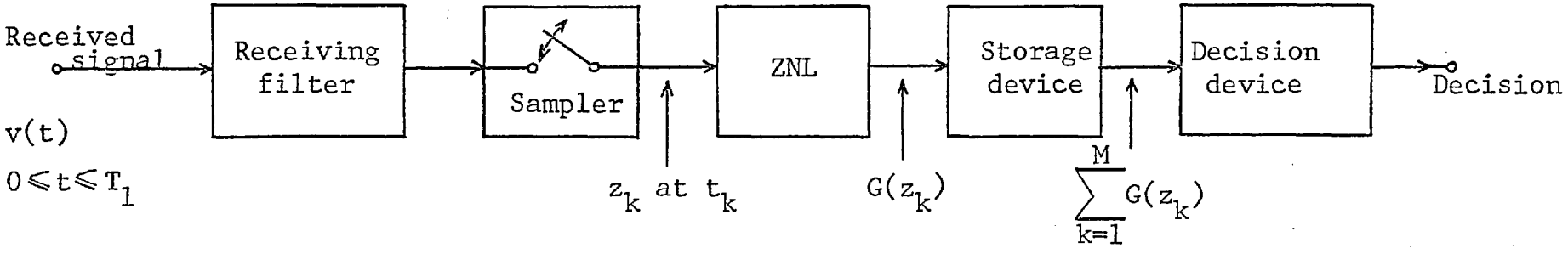

ZNL : zero-memory nonlinear device

$t_k = kT$: sampling instants; $t_M = MT = T_1$

Fig. 3.5(b)

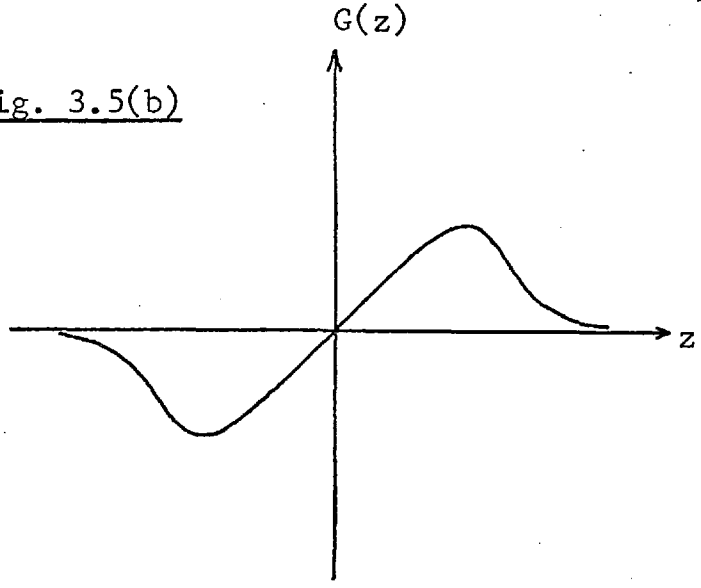

as follows [3-20]. Let Z_K (K = 1,2,...,M) be the samples corresponding to a given data symbol. In the absence of noise either $Z_K = +S$ or $Z_K = -S$. The log-likelihood ratio is thus

$$\log\Lambda = \sum_{K=1}^{M} \log \frac{p(Z_K - S)}{p(Z_K + S)} \qquad (8)$$

where $p(\cdot)$ is the PDF of the noise samples at the output of the receiving filter. Therefore if the shape of the nonlinearity is

$$G(Z) = \log \frac{p(Z - S)}{p(Z + S)} \qquad (9)$$

it follows that the output of the storage device immediately after the M^{th} sampling instant is the value of $\log\Lambda$. The threshold device will decide in favour of one symbol if $\log\Lambda \geq 0$ and in favour of the other symbol if $\log\Lambda < 0$.

A typical shape of G(Z) for a large-variance noise amplitude PDF is shown in Fig. 3.5(b). There is a striking similarity between this and the characteristic given in Fig. 3.3(b), but in the case of Fig. 3.5(b) the suppression of the contributions to the decision statistic that are much larger than the signal amplitude is carried out in an optimal manner.

The optimization of the receiver shown in Fig. 3.5(a) against an additive combination of Gaussian and impulsive noise was attempted in Ref. [3-17]. It was shown there that an optimum number of pulse repetitions can be found which depends on the relative proportion of the two noise components, and on the amplitude and time distributions of the impulsive noise.

In Ref. [3-18] the possibility was considered of the the detector producing an erasure symbol when the decision statistic falls into certain regions of ambiguity (null-zone detection). A special encoding operation must thus be performed at the transmitter which will enable the receiver to replace the erasure symbols.

3.5 NOISE-CANCELLING RECEIVERS

In these receivers a cancelling device is connected in parallel with part of the main signal path and the outputs of the two parallel blocks are subtracted from each other to obtain a substantial reduction in the overall response to an impulsive disturbance. Two schemes have been proposed in the literature. In the first scheme the branches in parallel are bandpass amplifiers with the same centre frequency but the cancelling amplifier has a bandwidth somewhat larger than the other one [3-10]. This scheme is nothing but a special case of the noise-smearing techniques considered in Section 3.3.

In the second scheme the cancelling device accepts the noise from a channel through which no signal is transmitted and performs a frequency-shifting operation which transfers the noise spectrum to the frequency-band of the signal before subtraction takes place [3-25,26].

In both cases a significant improvement is only possible if the responses of the two branches in parallel to almost every impulsive disturbance have nearly equal phases and nearly identical envelopes. In practice, the set of possible impulsive disturbances is generally too large for these conditions to be satisfied.

3.6 CONCLUDING REMARKS

All the systems analysed above have an equivalent structure to that in Fig. 1.2 except those in which a nonlinear analog operation is performed on the received signal (Fig. 3.2). In these cases the elimination of intersymbol interference entails the use of a signalling rate below that which the bandwidth usually permits. This is not so in Fig. 1.2 because there the analog waveforms are sampled before being nonlinearly processed.

The techniques described previously can be subdivided into two main categories: those in which the system attempts to make the non-Gaussian noise appear Gaussian and then uses the optimum receiver for Gaussian noise, and those in which the receiver directly exploits the specific characteristics of the non-Gaussian noise. The first category includes the systems considered in Sections 3.2 and 3.3 in which the receiving filters have long impulse responses and are thus capable of averaging out the contributions of several noise impulses. As stated before, these systems are only advantageous for sufficiently high SNR's. The second category includes the systems considered in Section 3.4 in which the receiver front-end filter has a short impulse response and the long transmitted waveforms are nonoverlapping to avoid intersymbol interference. These systems provide a lower data-rate than the previous ones but, on the other hand, they are particularly efficient in the low SNR region. The reason is that in this region the receiver will find it easier to recognize the impulsive noise in the background formed by the signal and the Gaussian noise.

CHAPTER IV

PROPOSED SIGNAL DESIGN: I - HIGH SNR

The weak have one weapon:
the mistakes of those who
think they are strong.

Georges Bidault.

4.1 INTRODUCTION

In the previous chapter three methods of combatting impulsive noise were described which employed data signals much longer than the average duration of the noise pulses. These methods were described as the smear-desmear technique (Section 3.3), the orthonormal function coding (Section 3.2) and the long non-overlapping signal technique (Section 3.4). It was pointed out in Chapter III that both the smear-desmear technique and the orthonormal function coding (OFC) can yield a significant improvement in the presence of impulsive noise provided that its amplitude PDF has reasonably short tails and the SNR exceeds a certain critical threshold. Below this threshold the conventional system performs better and the required improvement can only be achieved by using long non-overlapping signals, with a consequent reduction in signalling rate. An improvement of this long non-overlapping signal technique, which is particularly efficient in the case of a noise amplitude PDF with long tails, will be presented in Chapter V.

In this chapter a modification of the smear-desmear concept, which turns out to be more efficient than the procedures described in the literature, is studied. Before beginning this study it is helpful to show that the OFC method, the proposed method and the conventional smear-desmear technique can be viewed as aspects of a more general signal design scheme.

In the conventional binary data system one of two antipodal pulses $\pm s(t)$ is transmitted every T seconds. The signal s(t) can be written as

$$s(t) = \sqrt{E_s}\, y(t) \qquad (1)$$

where E_s is the energy of s(t) and y(t) is a pulse with unit energy, essentially time-limited to T seconds. If it is assumed that the transmission channel is distortionless then,

as is well known, the probability of detecting a single transmitted pulse in error in the presence of white Gaussian noise is minimized when the receiving filter is matched to the waveform s(t). In this case the receiving filter will thus have an impulse response h(t) given by, say,

$$h(t) = y(\ell T - t) \tag{2}$$

for some integer ℓ, and consequently a transfer function H(f) given by

$$H(f) = Y^{*}(f) \exp(-j2\pi \ell T f) \tag{3}$$

When a sequence of data pulses is transmitted, it is possible to show that, under the assumed conditions, the error probability is minimized if the pulse y(t) is designed so as to avoid any intersymbol interference [4-1]. The overall impulse response of the system depicted in Fig. 4.1, whose frequency spectrum is given by

$$S(f)\, H(f) = \sqrt{E_s}\, |Y(f)|^2 \exp(-j2\pi \ell T f) \tag{4}$$

should thus have a non-zero sample at the instant $t_\ell = \ell T$ and zero samples at all instants $t_n = nT$, $n \neq \ell$. This property will be expressed by saying that y(t) is a Nyquist pulse. One case where this complete elimination of the intersymbol interference is achieved is that where $|Y(f)|^2$ belongs to the family of raised-cosine frequency characteristics [4-1]. It is obvious that the same result is obtained when $|Y(f)|^2$ is the spectrum of a waveform which is exactly time-limited to the interval [-T,T] and is continuous at the extremes of this interval. It will be shown in Section 4.2 that a transmission free from intersymbol interference is also possible when y(t) belongs to a class of pulses which will be called perfect Nyquist pulses. These pulses have the additional property of allowing the transmission of a maximum number of channels within a given bandwidth without any interchannel interference.

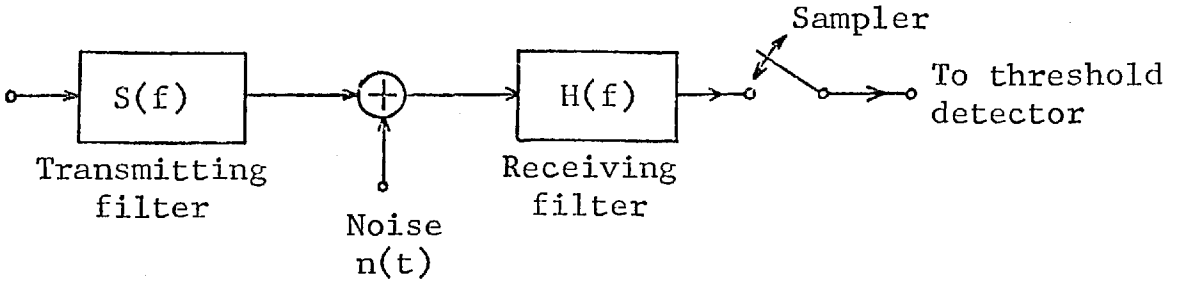

Fig. 4.1: Conventional data transmission system.

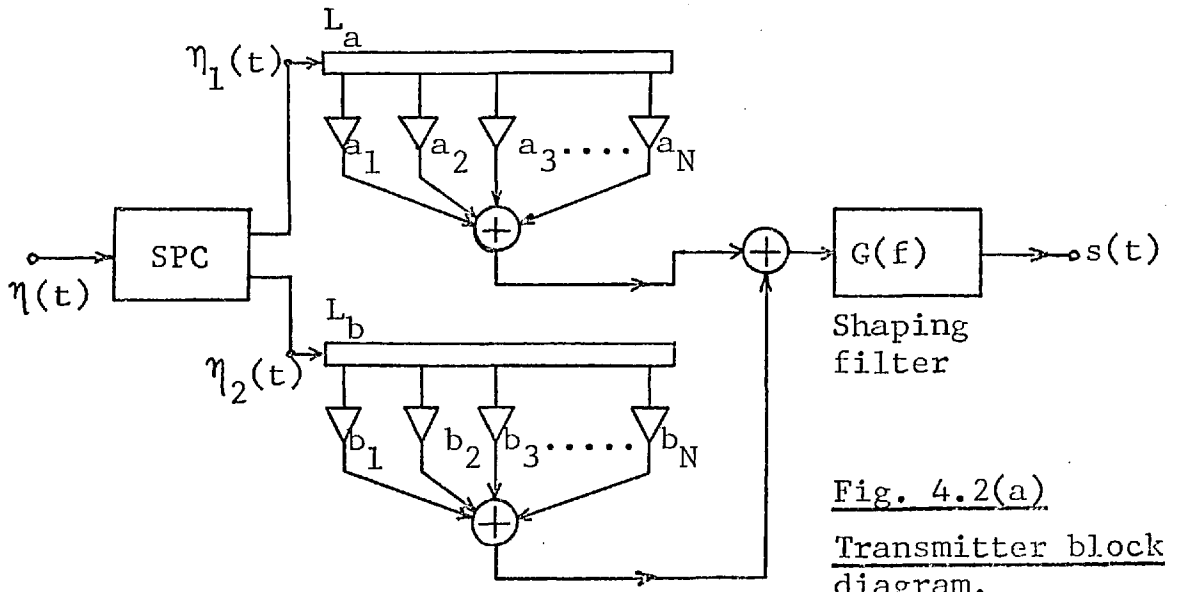

Fig. 4.2(a)
Transmitter block diagram.

L_a, L_b, L_r, L_s - tapped delay lines
SPC - serial-to-parallel converter

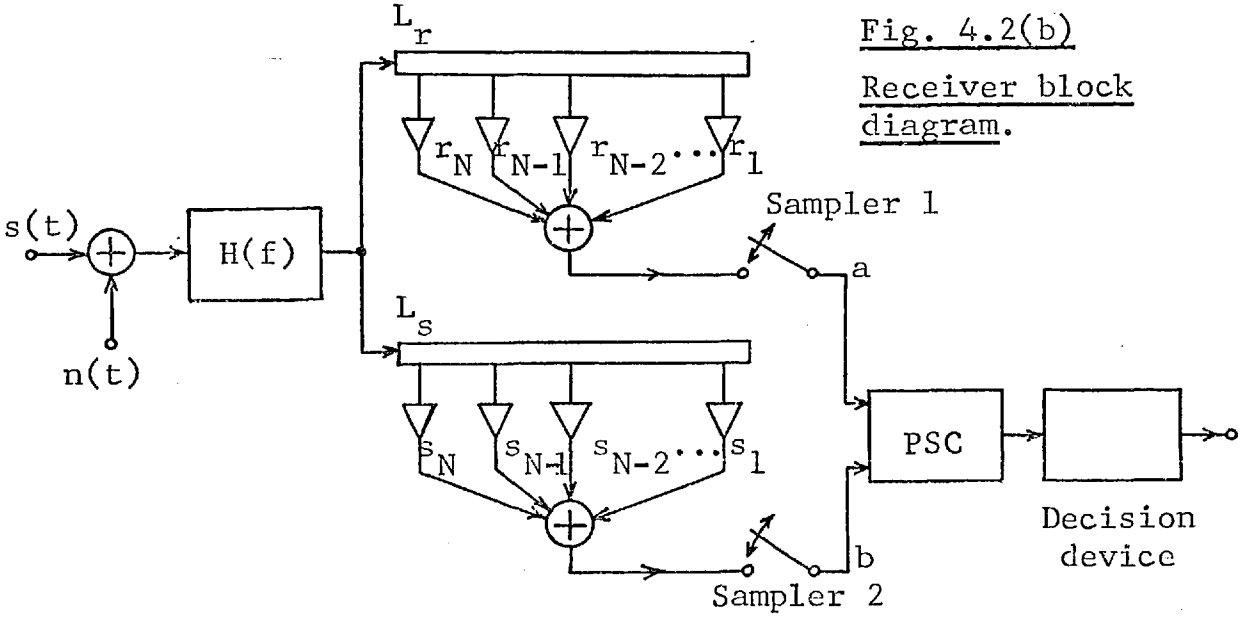

Fig. 4.2(b)
Receiver block diagram.

PSC - parallel-to-serial converter

In the orthonormal function coding scheme N mutually orthogonal signals $s_K(t)$, K = 1, 2, ..., N, are sent simultaneously every NT seconds, with either polarity. If the signals $s_K(t)$ have the same energy E_s then $s_K(t)$ can be written as

$$s_K(t) = \sqrt{E_s}\, y_K(t) \tag{5}$$

where the $y_K(t)$, K = 1,2,...,N, form an orthonormal set of functions. Thus, the possible transmitted waveforms in an interval of duration NT seconds are

$$g_i(t) = \sqrt{E_s} \sum_{K=1}^{N} \varepsilon_{iK}\, y_K(t) \tag{6}$$

i = 1,2,...,M, where $\varepsilon_{iK} = \pm 1$ and $M \leq 2^N$. The choice of the signals $g_i(t)$ to be transmitted determines the coding scheme. Henceforth it will be assumed that no redundancy is introduced into the signals $g_i(t)$, i.e. $M = 2^N$, and further that the coefficients ε_{iK} stand for the N binary digits to be transmitted every NT seconds. In data transmission, a natural way of choosing the orthonormal set $\{y_K(t)\}$ is to take some Nyquist pulse y(t), essentially time-limited to T seconds, and design $y_K(t)$ so as to occupy the whole interval $[0,nT]$ in the following way:

$$y_K(t) = \sum_{j=1}^{N} a_{Kj}\, y(t + T - jT) \tag{7}$$

The choice of the elementary pulse y(t) is usually governed by bandwidth requirements and ease of generation. It should be noted that if $N = 2^n$ then the OFC technique is a special case of a more general method where $L = 2^K$ signals $(0 < K \leq n)$ are transmitted simultaneously, their transmission being initiated every LT seconds. When $K < n$ the coefficients a_{Kj} must fulfil additional conditions in order to avoid any intersymbol interference. The case in which L = 2 is in fact the signalling method proposed later in this chapter, with the choice of L = 2 being adopted on account of its associated ease of implementation.

The structures of the transmitter and receiver corresponding to this case are identical to those shown in Fig. 4.2 where G(f) and H(f) represent a conventional filter set. These structures are easy to generalize for any $L > 2$. The performance of the optimum receiver in the presence of white Gaussian noise does not depend on the coefficients a_{Kj} provided that they are chosen so as to prevent any intersymbol interference. Such performance is in fact the same as that of the conventional system shown in Fig. 4.1. Therefore the signal design method described previously may only be useful in the presence of non-Gaussian types of noise. All these points will become more obvious after studying the case in which L = 2 in Section 4.2.

If it is desired to transmit a single long signal every T seconds then the so-called smear-desmear technique results. This scheme, which has already been studied in detail in Chapter III, can be viewed from a slightly different viewpoint. The block diagram shown in Fig. 3.1 can be modified by breaking the transmitting filter S(f) and the receiving filter R(f) into two elements as follows:

$$S(f) = M(f).G(f) \qquad (8)$$

and

$$R(f) = H(f).N(f) \qquad (9)$$

where G(f), H(f) represent the matched filters of a conventional system and M(f), N(f) represent a smear-desmear filter set (see Fig. 4.3).

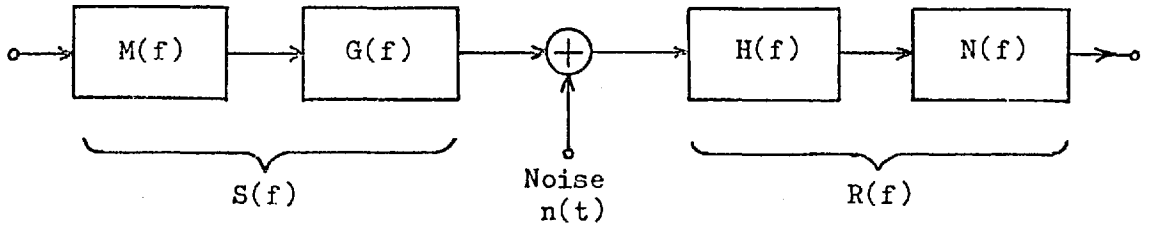

Fig. 4.3 Smear-desmear technique.

If, in order to avoid intersymbol interference, the condition

$$S(f).R(f) = G(f).H(f)\exp(-j\omega\delta) \qquad (10)$$

is satisfied, then

$$M(f).N(f) = \exp(-j\omega\delta) \qquad (11)$$

that is, the overall effect of M(f) and N(f) is simply a time delay. If, further, the system is to be optimized against white Gaussian noise, the filters M(f) and N(f), as G(f) and H(f), should be matched to each other, i.e.

$$N(f) = M^{*}(f)\exp(-j\omega\delta) \qquad (12)$$

and thus, according to Equations (11) and (12),

$$|M(f)| = |N(f)| = 1 \qquad (13)$$

within the frequency band of interest. The filters M(f), N(f) should thus be designed as complementary delay filters [4-11]. In general a criterion of optimization against impulsive noise will lead to amplitude characteristics $|M(f)|$ and $|N(f)|$ which are not uniform over the frequency band of interest and thus the resulting system will not be optimum in the face of white Gaussian noise. This implies that the optimization criterion should take into account the relative importance of the Gaussian and impulsive noise components. If, as suggested in Ref. [4-2], the filters M(f), N(f) are designed on the basis of tapped delay lines and thus signals of the form in Equation (7) are transmitted at intervals of T seconds, it is obvious that the intersymbol interference cannot be eliminated. It follows that in this case the optimization procedure should take into account the three system impairments: white Gaussian noise, impulsive noise and intersymbol interference*. The task is

---

* It has been recognized in Ref. [4-3] although in a different context, that an optimum receiving system may give rise to a certain amount of intersymbol interference.

much simpler when using the method proposed later in this chapter, whereby the intersymbol interference can be eliminated and at the same time the system can be optimized against the impulsive noise component without increasing the error probability due to the background Gaussian noise.

4.2 ANALYSIS OF THE PROPOSED TECHNIQUE

4.2.1 Major Assumptions

In this section a new signal design technique to be used in the presence of impulsive noise is developed. Throughout the study it is assumed that the modulation scheme is linear, which makes it possible to analyze any channel in terms of its equivalent baseband response [4.1]. Binary data are assumed to be transmitted by means of antipodal waveforms which give rise to no intersymbol interference when the transmission channel is assumed distortionless. In the case of a frequency division multiplexed (FDM) system it is further assumed that no interchannel interference occurs. For these reasons Nyquist pulses play an important part in the signal design and thus deserve detailed consideration.

4.2.2 Some properties of Nyquist pulses

A Nyquist pulse of signalling period δ is defined here as any waveform s(t) for which

$$A_K = \int_{-\infty}^{\infty} s(t)\, s^*(t + K\delta)dt$$

$$= \int_{-\infty}^{\infty} S(f)\, S^*(f)\, \varepsilon^{-j2\pi K\delta f}\, df$$

$$= \begin{cases} E_s & \text{if } K = 0 \\ 0 & \text{otherwise,} \end{cases} \qquad (14)$$

where K is an integer and δ is some real number. Furthermore, s(t) is defined to be a perfect Nyquist pulse of parameters (ρ, δ) if

$$A_{Kn} = \int_{-\infty}^{\infty} s(t)\, s^*(t+K\delta)\, \mathcal{E}^{j4\pi n\beta t}\, dt$$

$$= \int_{-\infty}^{\infty} S(f - 2n\beta)\, S^*(f)\, \mathcal{E}^{-j2\pi K\delta f}\, df$$

$$= \begin{cases} E_s & \text{if } n = K = 0 \\ 0 & \text{otherwise} \end{cases} \qquad (15)$$

where n, K are integers and

$$\beta = \frac{1}{\rho\delta}\,, \quad \rho = 2,\ 1 \text{ or } \tfrac{1}{2} \qquad (16)$$

Two perfect Nyquist pulses, s(t) and r(t), of parameters (ρ, δ) will be said to be associated with each other if

$$B_{Kn} = \int_{-\infty}^{\infty} s(t)\, r^*(t + K\delta)\, \mathcal{E}^{j4\pi n\beta t}\, dt$$

$$= \int_{-\infty}^{\infty} S(f - 2n\beta)\, R^*(f)\, \mathcal{E}^{-j2\pi K\delta f}\, df = 0 \qquad (17)$$

for any pair of integers (n,K) and $\beta = 1/\rho\delta$.

In the previous definitions s(t) and r(t) are not necessarily real signals. In fact if s(t) is a real Nyquist pulse it is obvious that s(t) exp(j4πℓβt) is also a Nyquist pulse for any integer ℓ. Moreover, it follows immediately from Equation (15) that if s(t) is a Nyquist pulse of parameters (ρ, δ) then its spectrum S(f) is a Nyquist pulse of parameters $(\rho, 2\beta)$. Therefore

$$s_1(t) = \frac{1}{\delta}\sqrt{\frac{2}{\rho}}\; S\left(\frac{2t}{\rho\delta^2}\right) \qquad (18)$$

is a Nyquist pulse of parameters (ρ,δ) with the same energy as s(t). The pulse $s_1(t)$ given by Equation (18) will be called the dual of s(t). The spectrum of $s_1(t)$ is thus given by

$$S_1(f) = \delta\sqrt{\rho/2}\; s^*\left(\frac{\rho\delta^2}{2}f\right) \qquad (19)$$

Furthermore, it is very easy to show that if s(t) and r(t) are perfect Nyquist pulses associated with each other, then As(t)+ Br(t) is a perfect Nyquist pulse for any complex constants A

and B. Henceforth, unless otherwise stated, use will be made only of real perfect Nyquist pulses. By making $n = 0$ the analysis can easily be extended to any real Nyquist pulse since Equation (14) is the special form of Equation (15) for $n = 0$.

The construction of an FDM data system on the basis of some perfect Nyquist pulse is an easy matter in view of Theorem 1 stated below. In presenting it here it is intended mainly to make clear the meaning of the parameters ρ and β used in the above definitions.

Theorem 1 Given the real baseband perfect Nyquist pulse $s(t)$, of parameters (ρ, δ), it is possible to transmit the pulses $\pm G_o s(t - K\delta)$, $\pm g_n(t - K\delta)$ and $\pm h_i(t - K\delta)$, where

$$g_n(t) = G_n s(t) \cos(4\pi n\beta t + \alpha_n) \qquad (20)$$

$$h_i(t) = H_i s(t) \sin(4\pi i\beta t + \alpha_i) \qquad (21)$$

$$n, i = 1, 2, 3, \ldots$$

$$K = 0, \pm 1, \pm 2, \ldots, \quad \beta = \frac{1}{\rho\delta},$$

and detect them without any interpulse interference.

Therefore, by sending the pulses at a rate of $1/\delta$ per second, it is possible to transmit $\rho(2L+1)\beta$ Baud in the bandwidth $[0, (2L+1)\beta]$ Hertz, for any integer $L \geq 0$, thereby achieving a transmission rate of ρ Baud/Hertz.

The following two theorems are the basis of the signal design method introduced later in this section. Their proofs are presented in Appendix 1.1 together with the proof of Theorem 1.

Theorem 2 Two real baseband perfect Nyquist pulses, $s_1(t)$ and $s_2(t)$, of parameters (ρ, δ), which are associated with each other, can be used simultaneously as in Theorem 1 without giving rise to any mutual interference.

It can be concluded as a corollary that no pair of associated Nyquist pulses can be found for which $\rho = 2$ Baud/

Hertz, otherwise it would be possible to exceed the Nyquist rate.

Consider now the sequences of N real Nyquist pulses

$$s_a(t) = \sqrt{\frac{E_s}{N}} \sum_{i=0}^{N-1} a_{i+1}\, y(t - iT) \tag{22}$$

and

$$s_b(t) = \sqrt{\frac{E_s}{N}} \sum_{i=0}^{N-1} b_{i+1}\, y(t - iT) \tag{23}$$

The elementary waveform y(t) is assumed to be a perfect Nyquist pulse of parameters (ρ, T) having unit energy. Thus if

$$\sum_{i=1}^{N} a_i^2 = \sum_{i=1}^{N} b_i^2 = N, \tag{24}$$

the parameter E_s is the energy of both $s_a(t)$ and $s_b(t)$. By introducing two infinite sequences $\{a_i\}$ and $\{b_i\}$, N can be defined, with no loss of generality, as the smallest even integer such that $a_i = b_i = 0$ when $i<1$ or $i>N$.

Theorem 3 The real waveforms $s_a(t)$ and $s_b(t)$ given by Equations (22) and (23), y(t) being a Nyquist pulse of parameters (ρ, T), are Nyquist pulses of parameters $(\rho/2, 2T)$ if and only if

$$\sum_i a_i\, a_{i+2K} = 0, \quad \text{any } K \neq 0 \tag{25}$$

and

$$\sum_i b_i\, b_{i+2K} = 0, \quad \text{any } K \neq 0. \tag{26}$$

The same waveforms $s_a(t)$ and $s_b(t)$ are associated Nyquist pulses if and only if

$$\sum_i b_i\, a_{i+2K} = 0, \text{ any } K. \tag{27}$$

Thus, according to Theorems 2 and 3, the pulses defined by Equations (22) and (23) make it possible to transmit

at the rate achieved when using the Nyquist pulse y(t) and the signalling method of Theorem 1.

The following two theorems, whose proofs are presented in Appendix 1.1, provide a method of finding pairs of associated Nyquist pulses.

Theorem 4 If s(t) is a symmetric or antisymmetric real waveform, time-limited to $[-T/2, T/2]$, then s(t) is a perfect Nyquist pulse of parameters (1,T) if and only if*

$$s^2(t) \neq \frac{E_s}{T} G_a(\frac{t}{T}) \tag{28}$$

and

$$s^2(t) + s^2(t-T/2) = \frac{2E_s}{T}, \qquad 0 \leqslant t \leqslant T/2 \tag{29}$$

where E_s is the energy of s(t).

Theorem 5 If s(t) is a real symmetric Nyquist pulse of parameters (1,T), time-limited to $[-T/2, T/2]$, then the antisymmetric pulse

$$r(t) = s(\frac{T}{2} - |t|)\, G_a(t/T)\, sgn\, t \tag{30}$$

is a perfect Nyquist pulse associated to s(t).

At this point it may be helpful to give a few examples of Nyquist pulses, some of which will be used later in this chapter. The simplest form of Nyquist pulse known is the rectangular pulse of duration T:

$$s_1(t) = \frac{1}{\sqrt{T}} G_a(\frac{t}{T}) = \begin{cases} 1/\sqrt{T}, & |t| < T/2 \\ 0\ , & |t| > T/2 \end{cases} \tag{31}$$

In order to prove that $s_1(t)$ is a perfect Nyquist pulse of parameters (2,T) it is sufficient to note that

$$A_{on} = \frac{1}{T} \int_{-\infty}^{\infty} G_a(t/T) \exp(j2\pi n \frac{t}{T}) dt$$

$$= \begin{cases} \frac{\sin(\pi n)}{\pi n} = 0, & n \neq 0 \\ 1\ , & n = 0 \end{cases} \tag{32}$$

---

* $G_a(x) = 1$, if $|x| < 0.5$; $G_a(x) = 0$, if $|x| > 0.5$.

The spectrum of $s_1(t)$ is given by

$$S_1(f) = \sqrt{T}\ \frac{\sin(\pi Tf)}{\pi Tf} \tag{33}$$

and thus

$$\begin{aligned} s_2(t) &= \frac{1}{T}\, S_1\left(\frac{t}{T^2}\right) \\ &= \frac{1}{\sqrt{T}}\ \frac{\sin(\pi t/T)}{\pi t/T} \\ &= \frac{1}{\sqrt{T}}\ \mathrm{sinc}(t/T) \end{aligned} \tag{34}$$

is another Nyquist pulse of parameters (2,T). As a second example, consider the unit energy pulse

$$s_3(t) = \sqrt{\frac{2}{T}}\, G_a(t/T)\, \cos(\pi t/T) \tag{35}$$

Since

$$s_3^2(t) = \frac{1}{T}\left(1 + \cos\frac{2\pi t}{T}\right)$$

it follows, according to Theorem 4, that $s_3(t)$ is a Nyquist pulse of parameters (1,T). Its spectrum is given by

$$S_3(f) = \frac{2}{\pi}\sqrt{2T}\ \frac{\cos\pi Tf}{1 - (2fT)^2} \tag{36}$$

from which another Nyquist pulse of parameters (1,T) can be derived:

$$\begin{aligned} s_4(t) &= \frac{\sqrt{2}}{T}\, S_3\left(\frac{2t}{T^2}\right) \\ &= \frac{4}{\pi\sqrt{T}}\ \frac{\cos(2\pi t\,/\,T)}{1 - (4t/T)^2} \end{aligned} \tag{37}$$

As a further example, consider the following antisymmetric pulse:

$$s_5(t) = \sqrt{\frac{2}{T}}\, G_a(t/T)\sin(\pi t/T) \tag{38}$$

Since

$$s_5(T/2 - |t|)\, G_a(t/T)\ \mathrm{sgn}\ t = s_3(t)$$

it follows, according to Theorem 5, that the pulses $s_3(t)$ and $s_5(t)$ are associated perfect Nyquist pulses of parameters (1,T).

Therefore, according to Theorems 1 and 2 it is possible to transmit both orthogonal pulses $s_3(t)$ and $s_5(t)$ in the baseband and modulate by the same pulses two carriers in quadrature at each of the frequencies $\frac{2n}{T}$Hz, n = 1,2,..., thereby achieving the maximum possible rate of 2 Baud/Hz overall. The spectrum of the pulse $s_5(t)$ is given by

$$S_5(f) = -jB_5(f) \tag{39}$$

where

$$B_5(f) = \sqrt{2T}\,\frac{\cos(\pi Tf)}{\pi Tf}\cdot\frac{(2fT)^2}{1-(2fT)^2}$$

This result makes it possible to add another Nyquist pulse to the list, namely:

$$\begin{aligned} s_6(t) &= \frac{\sqrt{2}}{T}\,B_5\left(\frac{2t}{T^2}\right) \\ &= \frac{2}{\sqrt{T}}\cdot\frac{\cos(2\pi t/T)}{2\pi t/T}\cdot\frac{(4t/T)^2}{1-(4t/T)^2} \end{aligned} \tag{40}$$

It is not difficult to show that the duals of two associated Nyquist pulses are also associated with each other. Therefore $s_4(t)$ and $s_6(t)$ form a pair of associated Nyquist pulses. In view of Theorem 4 the symmetric pulse

$$s_7(t) = \sqrt{\frac{2}{T}}\sqrt{1-2\left|\frac{t}{T}\right|}\;G_a(t/T) \tag{41}$$

is another perfect Nyquist pulse of parameters (1,T). Therefore, according to Theorem 5, the antisymmetric pulse

$$s_8(t) = \frac{2}{T}\sqrt{|t|}\;G_a\left(\frac{t}{T}\right)\operatorname{sgn} t \tag{42}$$

is also a perfect Nyquist pulse of parameters (1,T) which in addition is associated with $s_7(t)$. The duals of $s_7(t)$ and $s_8(t)$ form another pair of associated pulses but, since their mathematical expressions are quite complicated, they will not be dealt with here.

4.2.3 Proposed signal design

As stated above, the signal design proposed in this chapter consists of sending every 2T seconds the associated Nyquist pulses defined by Equations (22) and (23), the waveform y(t) being a Nyquist pulse essentially time-limited to T seconds. As expressed by Theorem 3, in order to avoid any artificial intersymbol interference resulting from the overlap of the transmitted waveforms, the sequences $A = \{a_i\}$ and $B = \{b_i\}$ should satisfy the conditions (25), (26) and (27). Sequences satisfying Equations (25) and (26) are termed self-orthogonal sequences and those satisfying Equation (27) are called associated sequences.

The diagram shown in Fig. 4.2(a) makes it possible to satisfy these conditions. In this figure it is assumed that a train of Dirac impulses

$$\eta(t) = \sum_{i=-\infty}^{\infty} \alpha_i \, \delta(t - iT), \qquad \alpha_i = \pm 1 \tag{43}$$

representing the binary symbols, is applied at the input. The serial-to-parallel converter (SPC) is assumed to generate the impulse trains

$$\eta_1(t) = \sum_{K=-\infty}^{\infty} \alpha_{2K} \, \delta(t - 2KT) \tag{44}$$

and

$$\eta_2(t) = \sum_{K=-\infty}^{\infty} \alpha_{2K-1} \delta(t - 2KT), \tag{45}$$

which are applied to the inputs of the tapped delay lines L_a and L_b respectively. The output of the shaping filter, whose transfer function is

$$G(f) = \sqrt{\frac{E_s}{N}} \, Y(f), \tag{46}$$

is signal

$$s(t) = \sum_{K=-\infty}^{\infty} [\alpha_{2K} s_a(t-2KT) + \alpha_{2K-1} s_b(t-2KT)] \qquad (47)$$

where $s_a(t)$ and $s_b(t)$ are given by Equations (22) and (23). This signal s(t) is transmitted through a channel which is assumed to be distortionless and, after being corrupted by the noise n(t), it is applied to the receiver, whose block diagram is shown in Fig. 4.2(b). The front-end filter is assumed to have the transfer function

$$H(f) = \frac{1}{\sqrt{N}} Y^*(f) \exp(-j2\pi \ell Tf) \qquad (48)$$

for some integer ℓ, and is thus matched to the transmitter shaping filter. It is shown in Appendix 1.2 that if the artificial intersymbol interference is to be avoided, the tap gains of the transmitter and receiver delay lines must satisfy the following relations:

$$\sum_i b_i \, r_{i+2K} = \sum_i a_i \, s_{i+2K} = 0, \text{ any } K \qquad (49)$$

$$\sum_i a_i \, r_{i+2K} = \sum_i b_i \, s_{i+2K} = 0, \; K \neq 0. \qquad (50)$$

It is shown in Appendix 1.3 that if $\{a_i\}$ is a self-orthogonal sequence then the relations (27) and (49) are satisfied if and only if

$$b_i = b(-1)^i a_{N-i+1} \qquad (51)$$

$$r_i = r(-1)^i b_{N-i+1} \qquad (52)$$

$$s_i = s(-1)^i a_{N-i+1} \qquad (53)$$

for some constants b, r and s. It can thus be concluded that

$$r_i = G \, a_i \qquad (54)$$

and

$$s_i = H \, b_i, \qquad (55)$$

for some constants G and H, and that the relations (50) are

automatically satisfied. The two samplers in Fig. 4.2(b) are assumed to operate at the instants 2KT, for any integer K, and the resulting samples are presented serially to the decision device by means of a parallel-to-serial converter (PSC).

The general solution to the problem of finding the sequences $A = \{a_i\}$, $B = \{b_i\}$, $R = \{r_i\}$ and $S = \{s_i\}$ so as to minimize the error probability due to a non-continual noise could not be found. It is shown in Appendix 1.2 that in the case of a white Gaussian noise the error probability attains its minimum value, for a given transmitted power, if and only if the relations (54) and (55) are satisfied for any subscript i, that is, if and only if the delay lines L_r and L_s are matched to L_a and L_b respectively. Since the filters G(f) and H(f) are matched to each other the whole system is then optimum with respect to white Gaussian noise. The magnitudes of the signal samples produced by the samplers 1 and 2 in Fig. 4.2(b) are given respectively by

$$A_1 = \frac{\sqrt{E_s}}{N} \sum_i a_i r_i = |G| \sqrt{E_s} \qquad (56)$$

and

$$A_2 = \frac{\sqrt{E_s}}{N} \sum_i b_i s_i = |H| \sqrt{E_s}, \qquad (57)$$

provided that y(t) has unit energy and the relations (24) are satisfied. Without any loss of generality it is possible to set $|G| = |H| = 1$ so as to obtain the simple result

$$A_1 = A_2 = A_s = \sqrt{E_s} \qquad (58)$$

From the results in Appendix 1.2 it can further be concluded that the error probability due to white Gaussian noise does not depend on the pair of associated self-orthogonal sequences $A = \{a_i\}$ and $B = \{b_i\}$ chosen. This is certainly not the case in the presence of impulsive noise. An attempt at optimization against impulsive noise is made later in this chapter.

To conclude this section a method of constructing pairs of associated self-orthogonal sequences is presented. The method is based on the following theorems whose proofs are given in Appendix 1.3.

Theorem 6 If $A = \{a_i\}$ is a self-orthogonal sequence, the sequence $B = \{b_i\}$ determined by

$$b_i = (-1)^i a_{N-i+1}, \tag{59}$$

$i = 1, 2, \ldots, N$, is also self-orthogonal and the two sequences are associated with each other.

Theorem 7 If A and B are associated self-orthogonal sequences, $C = \{A,B\}$ and $D = \{-A,B\}$ are also associated self-orthogonal sequences*.

According to these theorems, it is possible to start with the sequences $X_o = Y_o = \{1\}$ and construct two associated self-orthogonal sequences of length $N = 2^n$, $n \geqslant 1$, by means of the recurrence relations:

$$X_K = \{\cos\mu_K \cdot X_{K-1},\ \sin\mu_K \cdot Y_{K-1}\} \tag{60}$$

$$Y_K = \{-\sin\mu_K \cdot X_{K-1},\ \cos\mu_K \cdot Y_{K-1}\} \tag{61}$$

where the μ_K, $K = 1, 2, \ldots, n$, are arbitrary real numbers. It is obvious that the sequences $A_n = \sqrt{N}\, X_n$ and $B_n = \sqrt{N}\, Y_n$ satisfy the relations (24). In general a self-orthogonal sequence which satisfies the conditions (24) has N/2 degrees of freedom for it is subjected to a total of N/2 conditions. Therefore, if $n > 2$ the previous rule cannot produce all the self-orthogonal sequences of length $N = 2^n$. The associated self-orthogonal sequences

$$A = \{2, -1, -5/3, 1/3, 3/2, 2, 1, 2\} \tag{62}$$

and

$$B = \{2, -1, 2, -3/2, 1/3, 5/3, -1, -2\} \tag{63}$$

---

* Here $-A = \{-a_1, -a_2, \ldots, -a_N\}$ and
$C = \{a_1, a_2, \ldots, a_N, b_1, b_2, \ldots, b_N\}$.

are an example of sequences that cannot be constructed by using the previous rule. So far it has not been possible to find a systematic rule* for generating sequences like those given in (62) and (63). However, the class of sequences generated by relations (60) and (61) will be found later to be large enough for the purposes of this chapter.

The class of uniform self-orthogonal sequences plays an important role in the remainder of this chapter. A sequence will be called uniform if all its elements have the same magnitude. If the set of parameters $\{\mu_i\}$ in the relation (60) are given the $N = 2^n$ possible combinations of values $\mu_i = \frac{\pi}{4}\alpha_i$ with $\alpha_i = \pm 1$, $i = 1, 2, \ldots, n$, then a set of N mutually orthogonal vectors are obtained which can be grouped in N/2 pairs of associated uniform sequences. In this way the examples presented in Table 4.1 can be obtained quite easily. In Appendix 1.3 a group of permutation operations is defined, by means of which a total of $(n-1)! - 1$ other sets of uniform self-orthogonal sequences can be derived from the basic set obtained by using the rule just described. By using a direct search procedure it has been possible to show that the previous rules generate all the possible uniform self-orthogonal sequences of length $N = 2^n$, $n \leqslant 4$. The method is possibly exhaustive for any value of n but no formal proof has been found for this conjecture.

The possibility of constructing uniform self-orthogonal sequences whose length N is not a power of 2 has also been investigated. This investigation has led to the following theorem, the proof of which is given in Appendix 1.4

Theorem 8 The length N of a uniform self-orthogonal sequence must either be 2 or a multiple of 4.

---

* By systematic rule is meant one in which the sequence elements are given in terms of a set of parameters $\{\mu_i\}$ corresponding to the degrees of freedom of the generator sequence (60).

Table 4.1

Some basic sets of uniform self-orthogonal sequences

N = 2:

α_1	a_1	a_2
1	1	1
-1	1	-1

N = 4:

α_1	α_2	a_1	a_2	a_3	a_4
1	1	1	1	-1	1
1	-1	1	1	1	-1
-1	1	1	-1	1	1
-1	-1	1	-1	-1	-1

N = 8:

α_1	α_2	α_3	a_1	a_2	a_3	a_4	a_5	a_6	a_7	a_8
1	1	1	1	1	-1	1	-1	-1	-1	1
1	1	-1	1	1	-1	1	1	1	1	-1
1	-1	1	1	1	1	-1	1	1	-1	1
1	-1	-1	1	1	1	-1	-1	-1	1	-1
-1	1	1	1	-1	1	1	-1	1	1	1
-1	1	-1	1	-1	1	1	1	-1	-1	-1
-1	-1	1	1	-1	-1	-1	1	-1	1	1
-1	-1	-1	1	-1	-1	-1	-1	1	-1	-1

In Appendix 1.4 the relationship between the self-orthogonal sequences and Golay's complementary series [4-4] is established. The N-long sequences $A = \{a_i\}$ and $B = \{b_i\}$ are complementary if and only if [4-4]:

$$\sum_{i=1}^{N-j} (a_i\, a_{i+j} + b_i\, b_{i+j}) = \begin{cases} 0, & j \neq 0 \\ 2N, & j = 0 \end{cases} \qquad (64)$$

It has been possible to prove that the pairs of associated uniform self-orthogonal sequences form a subclass of the complementary binary sequences studied by Golay. Let P and Q designate the numbers of -1's in two associated self-orthogonal sequences. Without any loss of generality it can be assumed that* Q, $P \leqslant N/2$ and that $P \geqslant Q$. It is proved in Ref. [4-4] that the length of the sequences must be expressible as a sum of at most two squares, that is

$$N = R^2 + S^2, \qquad R \geqslant S$$

and that,

$$P = \frac{N - R + S}{2}$$

$$Q = \frac{N - R - S}{2}$$

If N = 2 then R = S = 1 and thus P = 1, Q = 0. If $N > 2$ it is easy to show that N cannot be a multiple of 4 unless both R and S are even numbers. If R and S are chosen such that R = 2K and S = 2L, then

$$N = 4(K^2 + L^2) \qquad (65)$$

$$P = \frac{N}{2} - K + L \qquad (66)$$

and

$$Q = \frac{N}{2} - K - L, \qquad (67)$$

where K and L are any integers such that $K \geqslant L$. It should be noted, however, that the previous necessary conditions are not

---

* If P (or Q) $> N/2$ the sequence should be multiplied by -1.

sufficient for the existence of associated self-orthogonal sequences. Up to the length 128 the only values of N that satisfy the above conditions are the powers of 2 and the values in the following list, where the corresponding K and L are within brackets:

20(2,1), 36(3,0), 40(3,1), 52(3,2),
68(4,1), 72(3,3), 80(4,2), 100(5,0
or 4,3), 104(5,1), 116(5,2).

When N is not a power of 2, self-orthogonal sequences have only been discovered for those cases where $N = 10.2^n$, $n \geqslant 1$. It is easy to see that if two complementary sequences are interleaved, a self-orthogonal sequence is obtained. In this way sequences of length $N = 10.2^n$, $n \geqslant 1$, may be derived by starting with the complementary sequences* of length 10 which can be generated as explained in Ref. [4-4]. By using the two basic pairs of complementary sequences of length 10 given in Ref. [4-4] the following self-orthogonal sequences of length 20 are readily obtained:

{- - + + + + - + + + - + + + + - + - - +}
{+ + - + + + - + + - + + + + + - - - - +}

(+ stands for +1 and - stands for -1). A list of all the self-orthogonal sequences of length 20 is given in Appendix 1.4. It is easy to see that given a self-orthogonal sequence A of length N = 4M, the two sequences of length 2M which by interleaving reproduce A, are complementary sequences. Since complementary sequences do not exist for 2M = 18, as shown in Ref. [4-4], it is obvious that uniform self-orthogonal sequences of length N = 36 cannot exist. This fact proves the non-sufficiency of condition (65).

It is important to point out at this stage that non-binary self-orthogonal sequences can be constructed for any even

---

* Complementary sequences have only been discovered with lengths 10 or a power of 2 [4-4].

length. For example, in the case N = 6 there exist two basic pairs of associated ternary self-orthogonal sequences with a single zero element, from which all others may be derived by reversing them or altering the signs of their nonzero elements. These two pairs of sequences are:

$$+\ +\ 0\ +\ +\ -\qquad\qquad +\ +\ 0\ -\ +\ -$$

and

$$+\ +\ -\ 0\ -\ +\qquad\qquad +\ +\ +\ 0\ -\ +.$$

If in either of these pairs one of the zeros is replaced by +1 and the other by -1, then two sequences are obtained which, together with those given by Equations (52) and (53), satisfy the relations (49) and (50) and can thus be used as transmitted sequences. However, since they are not associated self-orthogonal sequences, it follows that Equations (54) and (55) are not satisfied in this case. Moreover, according to Equations (56) and (57),

$$A_1 = A_2 = A_s = \frac{4}{6}\sqrt{E_s}$$

instead of Equation (58)*.

4.2.4 Performance evaluation

The expression for calculating the error probability of the system described before, in the presence of Poisson impulse noise, is derived next. This noise model is used here since it is by far the simplest of the very few models for which the computation of the error probability can be carried out without recourse to noise simulation. Although the Poisson noise model represents reasonably well certain types of noise encountered in practice (e.g. VLF atmospheric noise, FDM cable systems disturbed by Corona "pops", etc.), there are many important circumstances in which this is not the case (e.g. non-Poisson HF atmospheric noise, impulsive noise in telephone

---

* It is assumed that $|a_i| = |b_i| = |r_i| = |s_i| = 1$ if $1 \leqslant i \leqslant N$.

facilities, etc.). However, it is felt that the qualitative conclusions drawn below will hold in any real situation. The performance in the presence of non-Poisson impulse noise is considered in Chapter VI by means of a Monte Carlo-type of simulation. It is important to point out here that the assumption of a purely random (Poisson) time structure of the noise can be made more realistic if the samples of the transmitted signal are scrambled before transmission and then descrambled at the receiver. The scrambler would be placed immediately before the shaping filter G(f) and the descrambler would be placed immediately after the receiving filter H(f) (see Fig. 4.2). It has been reported [4-5, 6, 7] that the use of scrambling in conjunction with error-control coding techniques is often useful in making the error performance less sensitive to changes in bit-error structure. In fact, since the existing burst-error-correcting codes are very sensitive to these changes, it is often advisable to choose an error-correcting code designed for random errors and use it in conjunction with a scrambling-descrambling system. However, in the case of the system under study the situation is not the same in that the detection is made on a bit-by-bit basis and thus the average error rate is the parameter that defines the system performance. The question thus arises as to whether the Poisson impulse noise is more or less harmful than a non-Poisson-type of noise, for the same fraction of signal samples corrupted by impulsive noise. Some examples studied in Chapter VI are intended to give insight into the problem of deciding whether scrambling should be used at both the coding and/or modulation levels rather than at the coding level only. In Chapter VII the use of scrambling at the coding level is considered.

It is shown in Appendix 1.2 that if the coefficients α_i in Equation (43) are statistically uncorrelated[1a] and equally likely to take on the value +1 or -1, then the average transmitted power P_s in Fig. 4.2(a) is given by

$$P_s = \frac{E_s}{2NT} \sum_{i=1}^{N} (a_i^2 + b_i^2) \int_{-\infty}^{\infty} y^2(t)dt \qquad (68)$$

If y(t) has unit energy and the relations (24) are satisfied, then

$$P_s = \frac{E_s}{T} \qquad (69)$$

If y(0) is the peak value of y(t) it is easy to conclude from Equations (22), (23) and (47) that the peak transmitted power P_M is given by*

$$P_M \cong \frac{E_s}{N} Z^2 y^2(0) \qquad (70)$$

where Z is the largest of

$$Z_1 = \sum_{K=1}^{N/2} (|a_{2K}| + |b_{2K}|) \qquad (71)$$

and

$$Z_2 = \sum_{K=1}^{N/2} (|a_{2K-1}| + |b_{2K-1}|) \qquad (72)$$

If $\{a_i\}$ and $\{b_i\}$ are uniform sequences then

$$P_M \cong E_s N y^2(0) = P_S N T y^2(0) \qquad (73)$$

Henceforth it will be assumed that

$$\sum_{i=1}^{N} r_i^2 = \sum_{i=1}^{N} s_i^2 = N \qquad (74)$$

and thus $|r| = |s| = 1$ in Equations (52) and (53). Therefore, according to Equations (56), (57) and (69), the signal samples magnitude at the input of the decision device is given by

$$A_1 = A_2 = A_s = \gamma\sqrt{E_s} = \gamma\sqrt{P_S T} \qquad (75)$$

where the parameter γ is such that

---

* If y(t) is limited to the interval $[-T/2, T/2]$ the relation (70) is valid with equality sign.

$$\sum_{j=1}^{N} a_j(-1)^j \, b_{N-j+1} = \pm\gamma N \qquad (76)$$

and thus $0 < \gamma \leq 1$. The parameter γ will take its maximum value 1 if and only if the sequences $\{a_i\}$ and $\{b_i\}$ are associated self-orthogonal sequences. In this case, as shown previously,

$$r_i = a_i, \qquad s_i = b_i \qquad (77)$$

It is necessary at this point to consider in a little more detail the description of the noise. As stated previously, a Poisson impulse noise is assumed present at the input of the receiver [Fig. 4.2(b)], that is,

$$n(t) = \sum_{i=-\infty}^{\infty} r_i \, \delta(t - \tau_i) \qquad (78)$$

where the τ_i form a sequence of purely random instants to which corresponds a fixed average impulse repetition rate of ν impulses per second. The impulse intensities (areas) r_i are assumed to be statistically independent and are assumed to obey a symmetric unimodal PDF $p_r(x)$ with zero mean and finite variance σ_r^2. The characteristic functions (CHF's) of the noise samples obtained at the points a and b in Fig. 4.2(b) are given respectively by*:

$$F_a(\omega) = \exp\left\{\nu\int_{-\infty}^{\infty}\left[F_r(\omega s_a(t)) - 1\right]dt\right\} \qquad (79)$$

and

$$F_b(\omega) = \exp\left\{\nu\int_{-\infty}^{\infty}\left[F_r(\omega s_b(t)) - 1\right]dt\right\} \qquad (80)$$

where ν is the average impulse repetition rate, $F_r(\omega)$ is the CHF corresponding to $p_r(x)$ and $s_a(t)$, $s_b(t)$ are given by Equations (22) and (23) with $E_s = 1$, that is,

$$s_a(t) = \frac{1}{\sqrt{N}} \sum_{i=0}^{N-1} a_{i+1} \, y(t - iT) \qquad (81)$$

---

* See Chapter II, Equation (14).

$$s_b(t) = \frac{1}{\sqrt{N}} \sum_{i=0}^{N-1} b_{i+1}\, y(t - iT) \tag{82}$$

Given the variance σ_r^2 of $p_r(x)$, the variances of both $F_a(\omega)$ and $F_b(\omega)$ have the value*

$$\sigma_a^2 = \nu \sigma_r^2 \tag{83}$$

since $s_a(t)$ and $s_b(t)$ are unit energy waveforms. In order to make the expressions of $F_a(\omega)$ and $F_b(\omega)$ more suitable for computation they can be written in terms of

$$\nu_1 = \nu T \tag{84}$$

and

$$y_1(t) = \sqrt{T}\, y(xT) \tag{85}$$

Note that ν_1 is the average number of noise impulses occurring within a signalling period T and that $y_1(x)$ is a unit-energy Nyquist pulse essentially time-limited to 1 second. It is very easy to show that

$$F_a(\omega) = \exp\left\{\nu_1 \int_{-\infty}^{\infty} \left[F_r\left(\frac{\omega}{\sqrt{T}}\, s_{a1}(x)\right) - 1\right] dx\right. \tag{86}$$

$$F_a(\omega) = \exp\left\{\nu_1 \int_{-\infty}^{\infty} \left[F_r\left(\frac{\omega}{\sqrt{T}}\, s_{b1}(x)\right) - 1\right] dx\right. \tag{87}$$

where

$$s_{a1}(x) = \sqrt{T}\, s_a(xT) = \frac{1}{\sqrt{N}} \sum_{i=0}^{N-1} a_{i+1}\, y_1(x-i) \tag{88}$$

$$s_{b1}(x) = \sqrt{T}\, s_b(xT) = \frac{1}{\sqrt{N}} \sum_{i=0}^{N-1} b_{i+1}\, y_1(x-i) \tag{89}$$

If $p_a(Z)$ and $p_b(Z)$ are the PDF's corresponding to $F_a(\omega)$ and $F_b(\omega)$ respectively, then the error probabilities corresponding to the transmission paths of the system under study are:

$$P_a = \int_{A_s}^{\infty} p_a(Z)\, dZ \tag{90}$$

---

* See Chapter II, Equation (16).

and $$P_b = \int_{A_s}^{\infty} p_b(Z)dZ \tag{91}$$

The overall error probability is then

$$P_e = \frac{1}{2}(P_a + P_b) \tag{92}$$

It is often convenient to work with probability distributions having unit variance, which, in this case, have CHF's

$$F_{r_1}(\omega) = F_r(\omega/\sigma_r) \tag{93}$$

$$F_{a_1}(\omega) = F_a(\omega/\sigma_a) \tag{94}$$

and $$F_{b_1}(\omega) = F_b(\omega/\sigma_a), \tag{95}$$

with PDF's $p_{r_1}(x)$, $p_{a_1}(x)$ and $p_{b_1}(x)$ respectively. The new expressions resulting in this case are

$$F_{a_1}(\omega) = \exp\left\{\nu \int_{-\infty}^{\infty} \left[F_{r_1}\left(\frac{\omega}{\sqrt{\nu}} s_a(t)\right)-1\right] dt\right\}$$

$$= \exp\left\{\nu_1 \int_{-\infty}^{\infty} \left[F_{r_1}\left(\frac{\omega}{\sqrt{\nu_1}} s_{a_1}(x)\right)-1\right] dx\right\} \tag{96}$$

$$F_{b_1}(\omega) = \exp\left\{\nu \int_{-\infty}^{\infty} \left[F_{r_1}\left(\frac{\omega}{\sqrt{\nu}} s_b(t)\right)- 1\right] dt\right\}$$

$$= \exp\left\{\nu_1 \int_{-\infty}^{\infty} \left[F_{r_1}\left(\frac{\omega}{\sqrt{\nu_1}} s_{b_1}(x)\right)-1\right] dx\right\} \tag{97}$$

$$P_a = \int_{B_s}^{\infty} p_{a_1}(x)dx \tag{98}$$

and

$$P_b = \int_{B_s}^{\infty} p_{b_1}(x)dx \tag{99}$$

where

$$\psi = \frac{A_s}{\sigma_r\sqrt{\nu}} = \gamma\sqrt{\frac{P_s T}{\nu\sigma_r^2}} \tag{100}$$

The parameter ψ is the magnitude of the signal samples at a point where the noise samples have unit variance and is referred to henceforth as signal-to-noise ratio.

In view of equations (96) and (97), it is obvious that if $y_1(t)$ is used instead of $y(t)$, at a transmission rate of 1 Baud, then the error probability P_e is not altered, provided that the average impulse repetition rate is given the value ν_1 instead of ν and the variance σ_r^2 is kept unchanged. In fact, if the pulse $y_1(t)$ given by Equation (85) is used the signal sample magnitudes become

$$A_{s_1} = A_s \sqrt{T}$$

and the SNR is given by

$$\psi_1 = \frac{A_{s_1}}{\sigma_r \sqrt{\nu_1}} = \frac{A_s}{\sigma_r \sqrt{\nu}} = \psi$$

The error rates given in Section 4.3 were calculated directly from the CHF's $F_{a_1}(\omega)$ and $F_{b_1}(\omega)$ using the method presented in Ref. [4-8]. A brief description of the method is given in Appendix 1.5 and the method used to compute the expressions (96) and (97) is described in the same appendix. It is important to point out that if the Nyquist pulse $y_1(x)$ is limited to the interval $[-1/2, 1/2]$ then the noise samples obtained at intervals of T sec at the output of the receiver front-end filter H(f) are statistically independent. This agrees with the fact that if* $y_1(x) = y_1(x)G_a(x)$ then Equations (96) and (97) can be rewritten in the following form

$$F_{a_1}(\omega) = \prod_{i=1}^{N} \phi_1(a_i\omega) \tag{101}$$

$$F_{b_1}(\omega) = \prod_{i=1}^{N} \phi_1(b_i\omega) \tag{102}$$

where, as shown in Appendix 1.5,

$$\phi_1(\omega) = \exp\left\{\nu_1 \int_{-\frac{1}{2}}^{\frac{1}{2}} \left[F_{r_1}\left(\frac{\omega}{\sqrt{\nu_1 N}}\, y_1(x)\right) - 1\right] dx\right\} \tag{103}$$

Thus, if $\{a_i\}$ and $\{b_i\}$ are associated sequences, then

---

* See footnote on page 59

$$F_{a_1}(\omega) = F_{b_1}(\omega) \tag{104}$$

and if further they are uniform sequences, then

$$F_{a_1}(\omega) = F_{b_1}(\omega) = [\phi_1(\omega)]^N \tag{105}$$

which, in view of Equation (103), depends only on V_1 and N through the product $V_1 N$.

In all the error rate calculations described in Section 4.3 uniform self-orthogonal sequences were used. For reasons explained in Appendix 1.5, it is conjectured that these sequences are optimal or nearly optimal in the presence of Poisson impulse noise, provided that the signal-to-noise ratio exceeds a certain critical value which decreases for increasing N. It is shown in the same appendix that in the case of non-Poisson types of noise the minimization of the error probability can lead to sequences $\{a_i\}$ and $\{b_i\}$ which are not uniform.

4.3 DISCUSSION OF NUMERICAL RESULTS

The computations were carried out with three different Nyquist pulses of parameters (1,T) used for y(t) in Equations (81) and (82). These are the pulses $s_3(t)$, $s_4(t)$ and $s_6(t)$ given by Equations (35), (37) and (40). In view of Theorem 5 (subsection 4.2.2) and Equation (103) it is obvious that the pulse $s_5(t)$ given by Equation (38) will give rise to the same performance as its associated pulse $s_3(t)$. In the case of $s_4(t)$ the data system has the same overall impulse response as in Ref. [4-9].

Four types of PDF were assumed for the intensities (areas) of the noise impulses:

(a) Gauss PDF:

$$p_r(x) = \frac{1}{\sigma_r\sqrt{2\pi}} \exp\left(-\frac{x^2}{2\sigma_r^2}\right) \tag{106}$$

(b) Laplace PDF:

$$p_r(x) = \frac{1}{\sigma_r\sqrt{2}} \exp(-\frac{|x|\sqrt{2}}{\sigma_r}) \tag{107}$$

(c) Generalized Cauchy PDF:

$$p_r(x) = \frac{n}{\pi b} \sin(\frac{\pi}{2n}) \frac{1}{1 + (x/b)^{2n}} \tag{108}$$

(n integral; $b > 0$).

(d) Cauchy-type PDF:

$$p_r(x) = \frac{\Gamma(v + \frac{1}{2})}{a\sqrt{\pi}\,\Gamma(v)} (1 + \frac{x^2}{a^2})^{-v-\frac{1}{2}} \tag{109}$$

($v > 0$; $a > 0$).

The Gauss and Laplace PDF's have also been used in Ref. [4-9]. Their CHF's are respectively

$$F_r(\omega) = \exp(-\frac{\sigma_r^2}{2}\omega^2) \tag{110}$$

and

$$F_r(\omega) = (1 + \frac{\sigma_r^2}{2}\omega^2)^{-1} \tag{111}$$

As their names indicate the third and the fourth distributions are modifications of the so-called Cauchy distribution which corresponds to the values n = 1 and v = ½. The CHF corresponding to the PDF (108) is

$$F_r(\omega) = \sin(\frac{\pi}{2n}) \cdot \sum_{s=0}^{n-1} \exp(-b|\omega| \sin\frac{2s+1}{2n}\pi) \cdot$$

$$\cdot \sin(\frac{2s+1}{2n}\pi + b|\omega| \cos\frac{2s+1}{2n}\pi) \tag{112}$$

If $n > 1$ the variance is given by

$$\sigma_r^2 = \frac{b^2}{1 + 2\cos(\pi/n)} \tag{113}$$

In the case of PDF (109) the CHF is given by

$$F_r(\omega) = \frac{2}{\Gamma(v)} (\frac{a|\omega|}{2})^v K_v(a|\omega|) \tag{114}$$

where $K_v(\cdot)$ is the modified Bessel function of the second kind. It should be noted that the variance of the Cauchy-type distribution is not finite, unless $v>1$. In this case it can easily be shown that the variance is given by,

$$\sigma_r^2 = \frac{a^2}{2(v-1)}, \qquad v>1 \tag{115}$$

It can also be shown that if

$$v = n + \tfrac{1}{2}, \tag{116}$$

for any integer $n \geq 1$, then $F_r(\omega)$ can be written in the following form:

$$F_r(\omega) = \varepsilon^{-a|\omega|}\left(1 + \frac{n!}{(2n)!}\sum_{K=1}^{n}\frac{(2n-K)!}{(n-K)!K!}(2a|\omega|)^K\right) \tag{117}$$

We notice that the important hyperbolic PDF discussed in Section 2.2 and the PDF's (108) and (109) have identical variations in the regions where the noise magnitude is large. These are the regions of particular interest in the present study. This fact, and the simple form of the CHF's (112) and (117), were the reasons for choosing the corresponding distributions. It should be noted, however, that for large n these distributions show completely different behaviour, since in the case of the generalized Cauchy PDF,

$$\lim_{n\to\infty} p_r(x) = \frac{1}{2\sigma_r\sqrt{3}}\, G_a\left(\frac{x}{2\sigma_r\sqrt{3}}\right) \tag{118}$$

and, in the case of the Cauchy-type distribution,

$$\lim_{v\to\infty} p_r(x) = \frac{1}{\sigma_r\sqrt{2\pi}}\exp\left(-\frac{x^2}{2\sigma_r^2}\right) \tag{119}$$

where, in both cases, σ_r^2 is the fixed value of the variance. The CHF corresponding to the rectangular PDF is given by,

$$F_r(\omega) = \frac{\sin\omega\sigma_r\sqrt{3}}{\omega\sigma_r\sqrt{3}} \tag{120}$$

It can readily be concluded from Equation (105) that the probability of error for a given SNR does not depend on the

particular sequences $\{a_i\}$ and $\{b_i\}$ used provided that they are associated uniform self-orthogonal sequences and, in addition, y(t) is time-limited to $[-T/2, T/2]$. It has been assumed in the computations that these conditions exist. In those cases where y(t) is not time-limited to $[-T/2, T/2]$ the numerical results have shown that the error probability P_e depends only slightly on the assumed pair of sequences and that the differences are too small to be indicated on the performance curves (Figs. 4.4 to 4.20). Moreover, the probabilities P_a and P_b defined by (90) and (91) are slightly different when y(t) is not limited to $[-T/2, T/2]$ but the numerical results have shown that both tend rapidly to P_e as N increases. The graphs of the error probability P_e versus the signal-to-noise ratio ψ [see Equation (100)] are presented in Figs. 4.4 to 4.20 for different values of ν_1 and N (or $\nu_1 N$)*. On account of the fact that when dealing with the modified Cauchy distributions and the pulses $s_4(t)$ and $s_6(t)$ the computation time is prohibitive, the graphs corresponding to these conditions were not obtained. By analysing Figs. 4.4 to 4.13 it can be concluded that the effect of the shape of the elementary pulse y(t) on the error probability is not important from a practical standpoint, at least in those cases where y(t) is essentially limited to the signalling period T and the system bandwidth W, which are both assumed fixed.

By comparing the graphs presented below, it can be seen that the performance of the smearing technique is strongly dependent on the shape of the PDF $P_r(x)$. This point can be illustrated by finding the smallest value of $N = 2^n$ capable of giving $P_e < 10^{-4}$ for each $p_r(x)$ referred to above, under the conditions:

$$y(t) = s_3(t),$$
$$\nu_1 = 1/32, \qquad \psi_{dB} = 20 \text{ dB}$$

---

* See end of Section.

The following values are obtained from the performance curves:

(a) Gauss PDF (see Fig. 4.4):

$$\nu_1 N = \tfrac{1}{4} \quad \therefore \quad N = 8$$

(b) Laplace PDF (see Fig. 4.9):

$$\nu_1 N = \tfrac{1}{2} \quad \therefore \quad N = 16$$

(c) Generalized Cauchy PDF (see Fig. 4.14):

$$\nu_1 N = 4 \quad \therefore \quad N = 128$$

(d) Cauchy-type PDF (see Fig. 4.18):

$$\nu_1 N = 8 \quad \therefore \quad N = 256$$

It should be noticed that the value of P_e for N = 1 is, in all cases, approximately 10^{-3}. It thus follows from the above example that the value of N necessary to achieve a required performance at a given SNR can vary widely with the change in $p_r(x)$. In Table 4.2 the values of N obtained above, together with the values corresponding to another two SNR's, are given. As can be seen, the minimum value of N for a required performance and a given PDF $p_r(x)$ can also vary over a wide range as a result of a change in SNR. If the SNR is too small the reduction in the error probability, obtained by increasing N up to an acceptable limit, may be too small to be of any practical interest (see Table 4.3). In this table the values of the error probability P_e corresponding to a SNR of 14 dB are presented for several values of N.

These facts indicate that the designer of a smear-desmear system should start by choosing the maximum acceptable value of N on the basis of factors like peak transmitted power or system complexity. Then the improvement in the SNR necessary to achieve a certain error probability P_e, with respect to the conventional system (N = 1), should be evaluated. Table 4.4 gives some values of the SNR improvement for $P_e = 10^{-4}$ and $\nu_1 = 1/32$. It can be seen that the SNR improvements for the

Table 4.2

Minimum values of $N = 2^n$ for $P_e < 10^{-4}$

$[y(t) = s_3(t), \quad \nu_1 = 1/32]$

$p_r(x)$ \ ψ_{dB}	14 dB	20 dB	26 dB
Gauss	128	8	1
Laplace	256	16	2
Gen. Cauchy (n=2)	16384	128	2
Cauchy-type (n=1)	32768	256	4

Table 4.3

Variation of P_e with N

$[y(t) = s_3(t), \quad \nu_1 = 1/32, \quad \psi_{dB} = 14 \text{ dB}]$

$p_r(x)$ \ N	1	8	32	128	512
Gauss	4.8×10^{-3}	3.8×10^{-3}	6.0×10^{-4}	7.0×10^{-5}	5.5×10^{-6}
Laplace	3.8×10^{-3}	4.8×10^{-3}	1.7×10^{-3}	2.7×10^{-4}	2.0×10^{-5}
Gen. Cauchy (n=2)	3.8×10^{-3}	3.0×10^{-3}	1.8×10^{-3}	9.7×10^{-4}	4.8×10^{-4}
Cauchy-type (n=1)	3.1×10^{-3}	3.3×10^{-3}	2.2×10^{-3}	1.3×10^{-3}	6.6×10^{-4}

Table 4.4*

SNR improvement in dB

$[y(t) = s_3(t), \quad \nu_1 = 1/32, \quad P_e = 10^{-4}]$

$p_r(x)$ \ N	32	64	128	256
Gauss	9.4	10.6	11.8	12.4
Laplace	9.0	10.8	12.2	13.5
Gen. Cauchy (n=2)	4.8	5.8	6.7	7.6
Cauchy-type (n=1)	4.2	5.1	6.0	7.0

* If ψ_N is the SNR necessary to achieve $P_e = 10^{-4}$ with signals of length N, this table gives the improvement $\psi_{1,dB} - \psi_{N,dB}$.

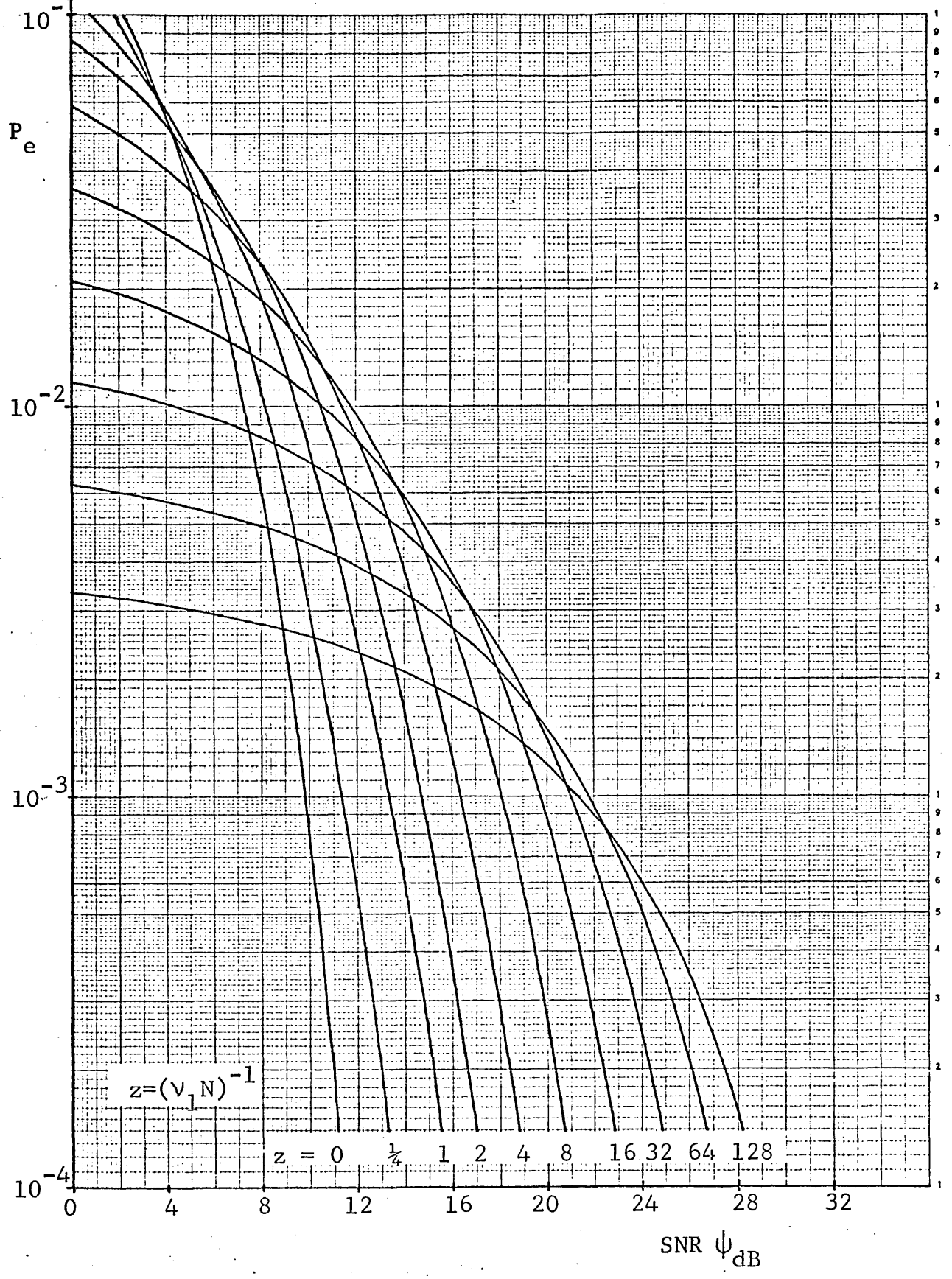

Fig. 4.4 $y(t) = s_3(t)$, Gauss PDF.

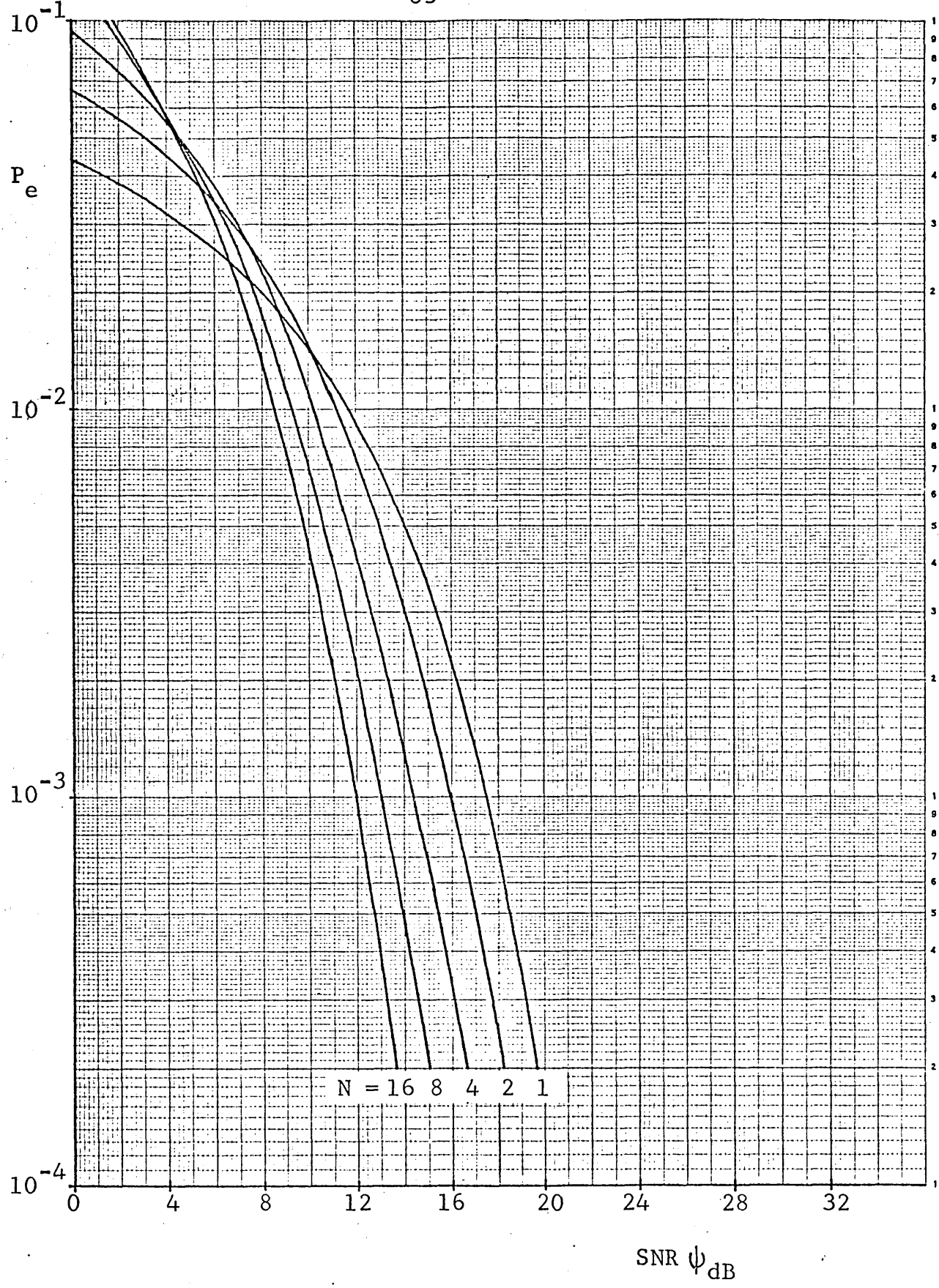

Fig. 4.5: $y(t)=s_4(t)$, $\nu_1=\frac{1}{8}$, Gauss PDF.

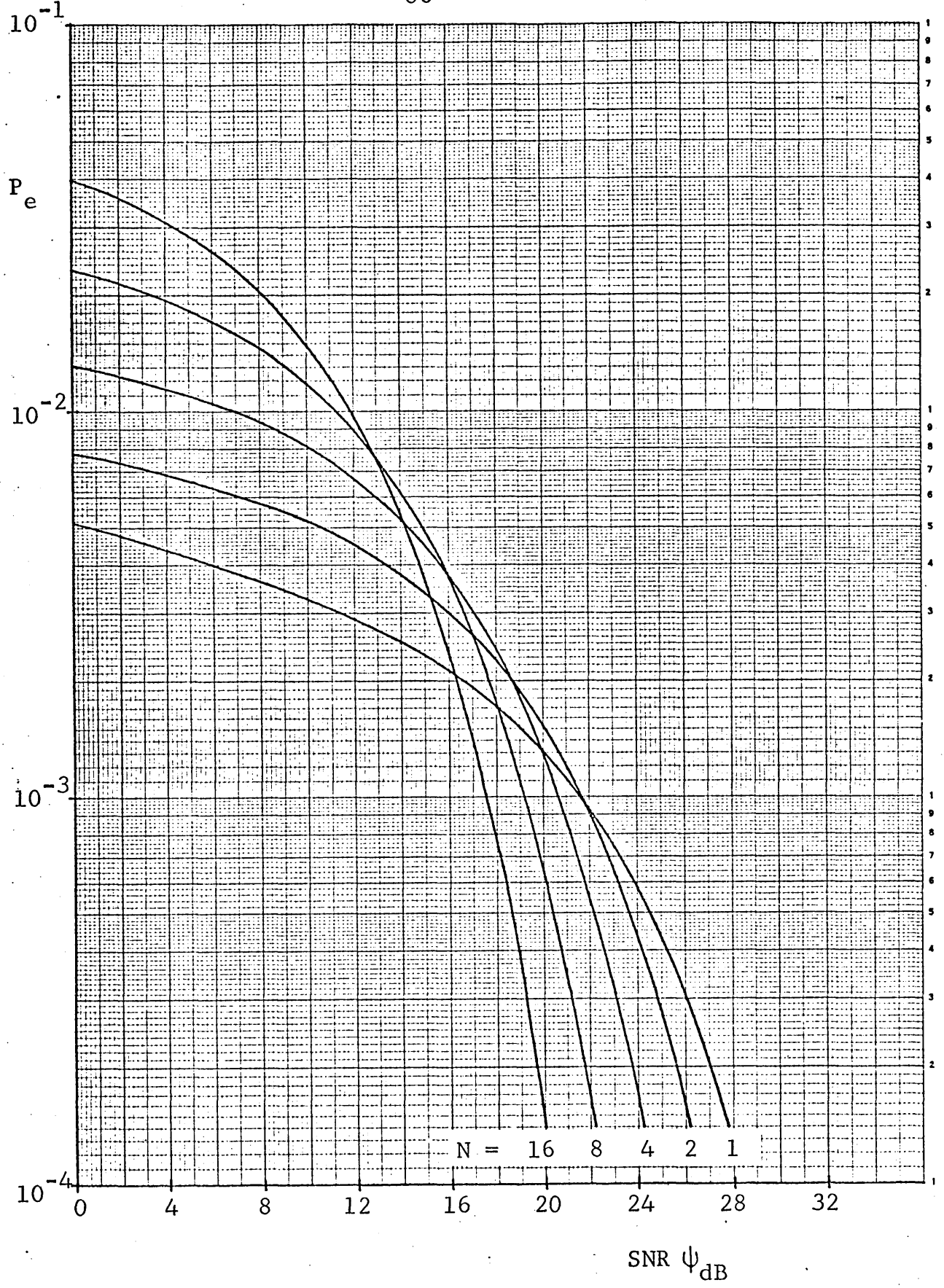

Fig. 4.6: $y(t)=s_4(t)$, $\nu_1=1/128$, Gauss PDF.

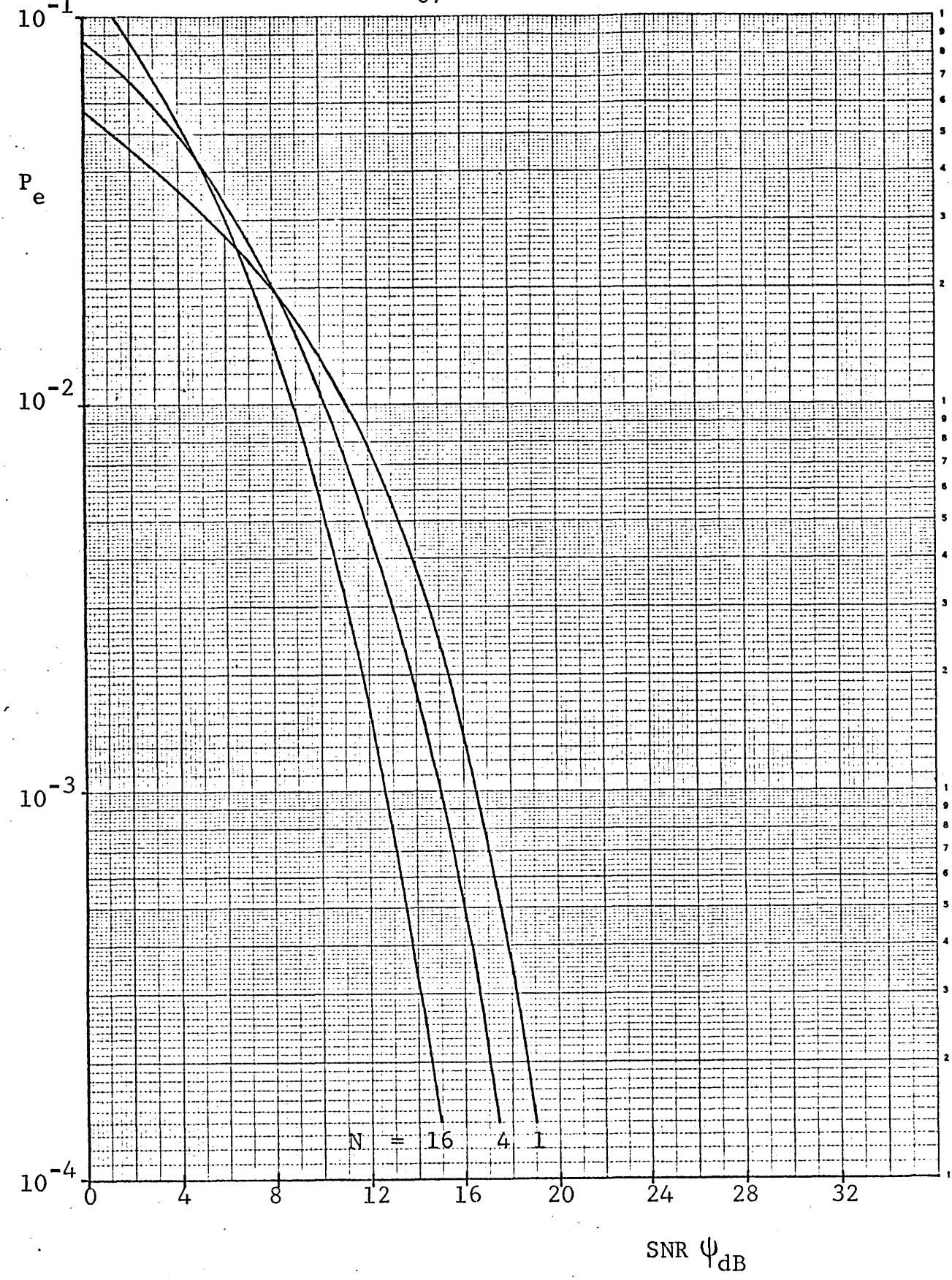

Fig. 4.7: $y(t)=s_6(t)$, $\nu_1=\frac{1}{8}$, Gauss PDF.

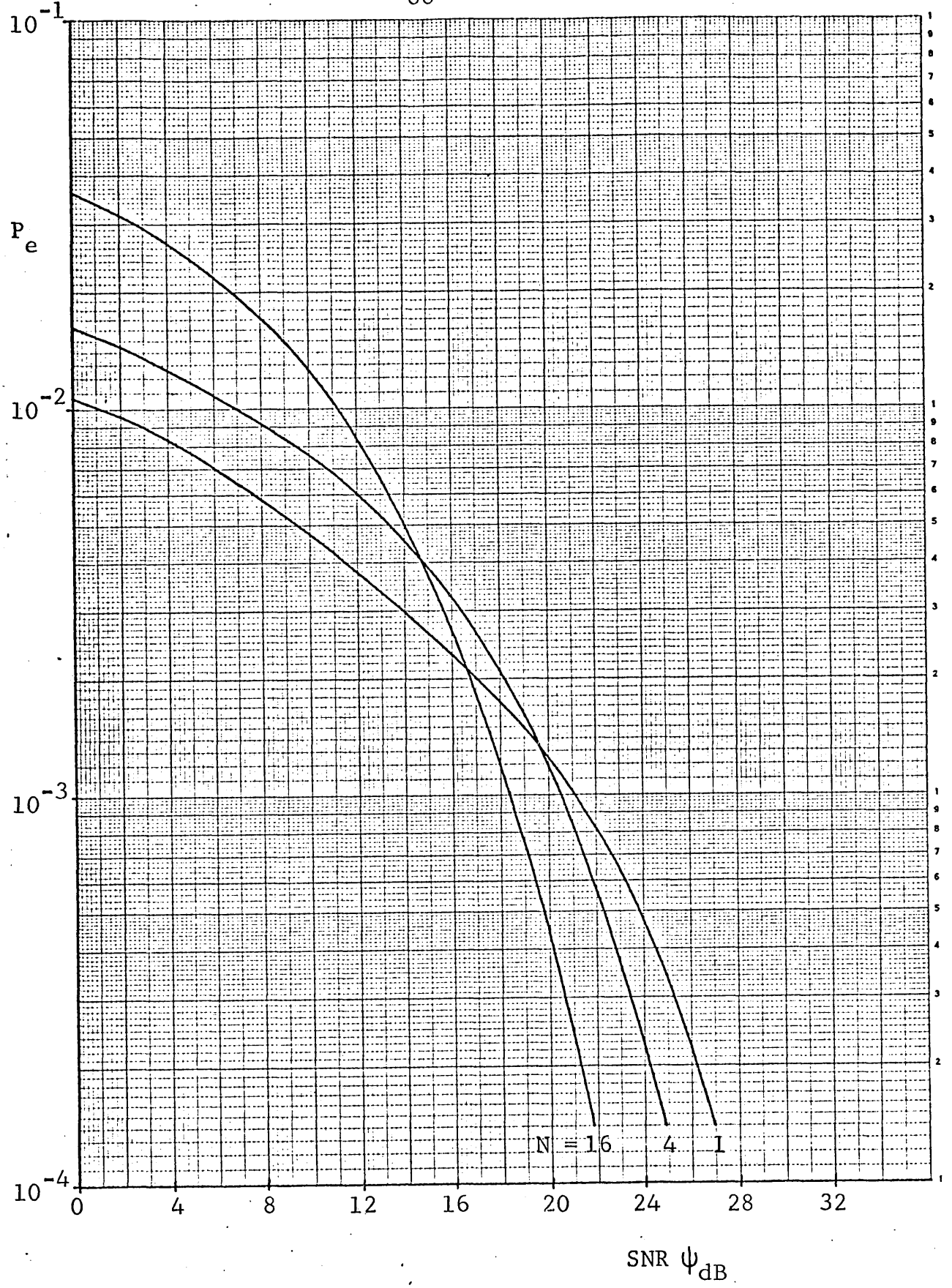

Fig. 4.8: $y(t)=s_6(t)$, $\nu_1=1/128$, Gauss PDF.

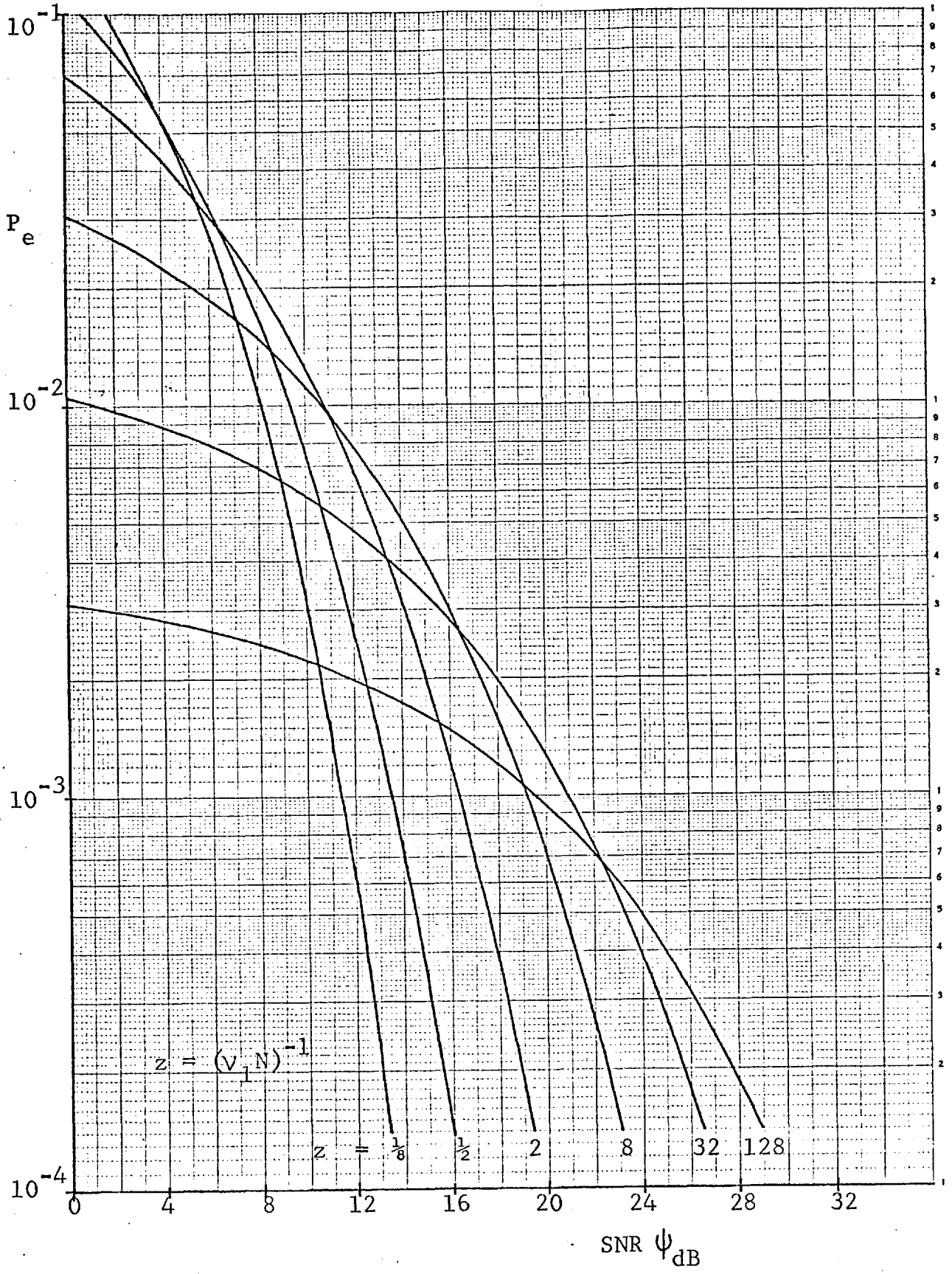

Fig. 4.9: $y(t)=s_3(t)$, Laplace PDF.

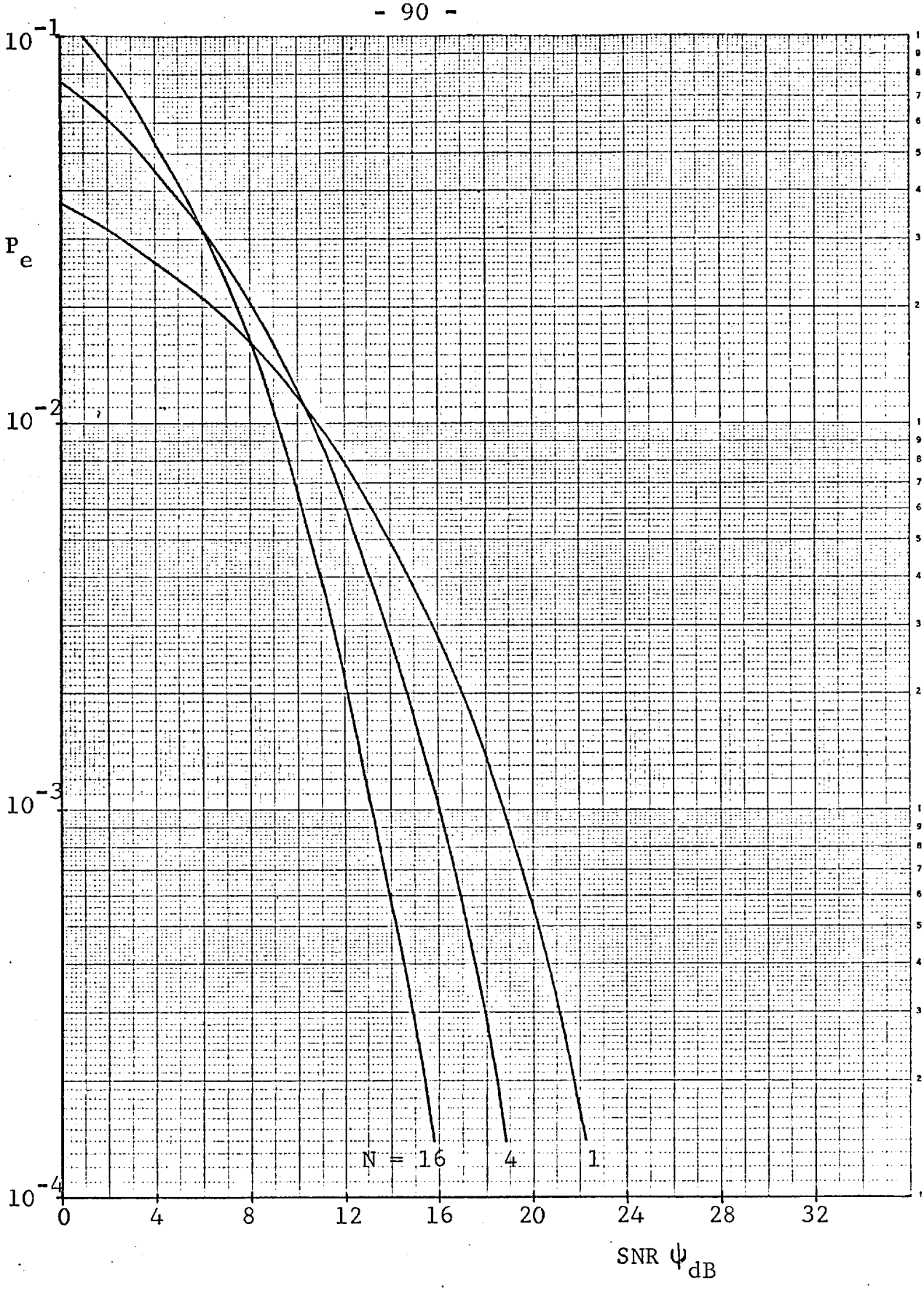

Fig. 4.10: $y(t)=s_4(t), \nu_1=\frac{1}{8}$, Laplace PDF.

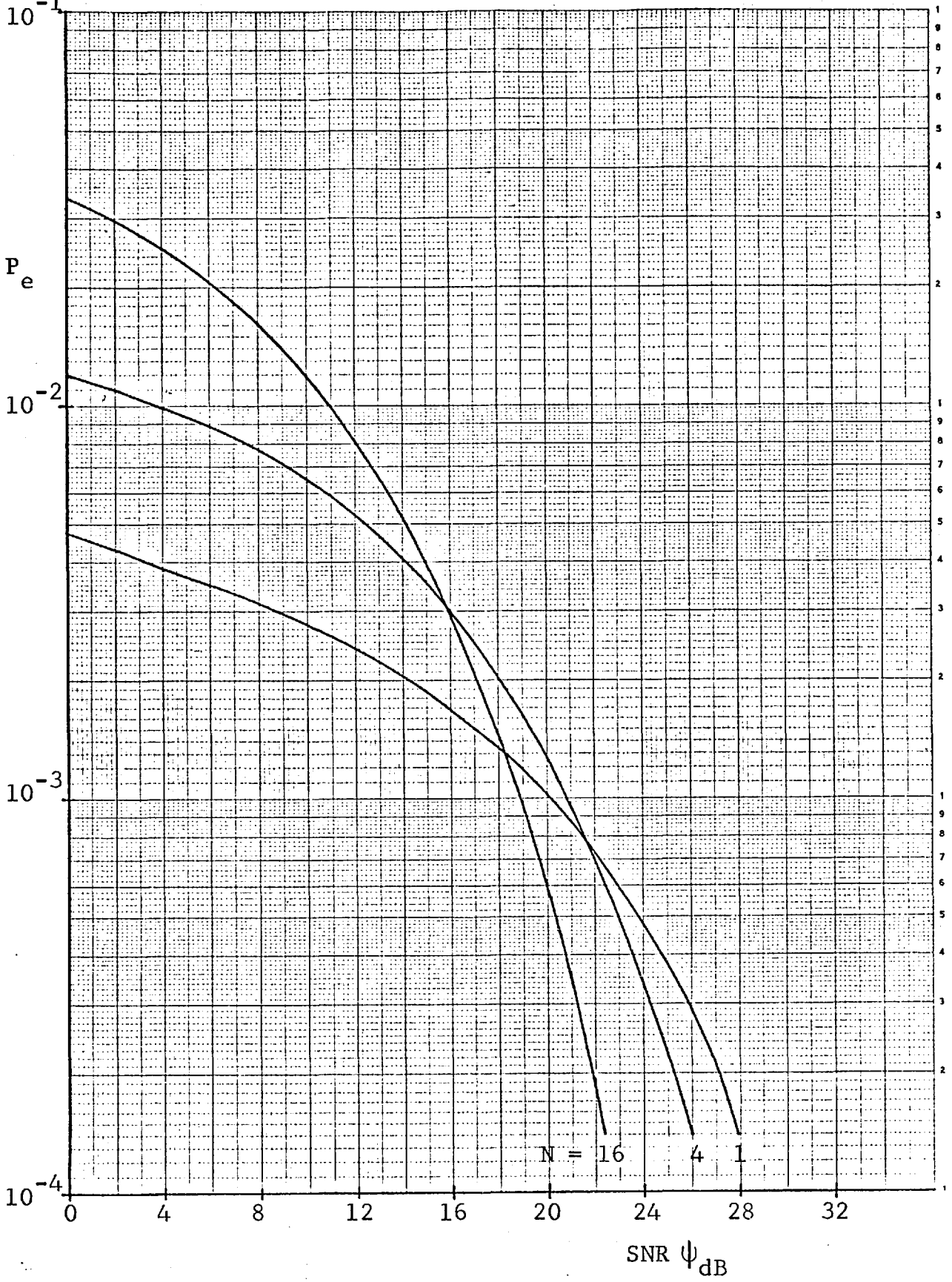

Fig. 4.11: $y(t)=s_4(t), \nu_1=1/128$, Laplace PDF.

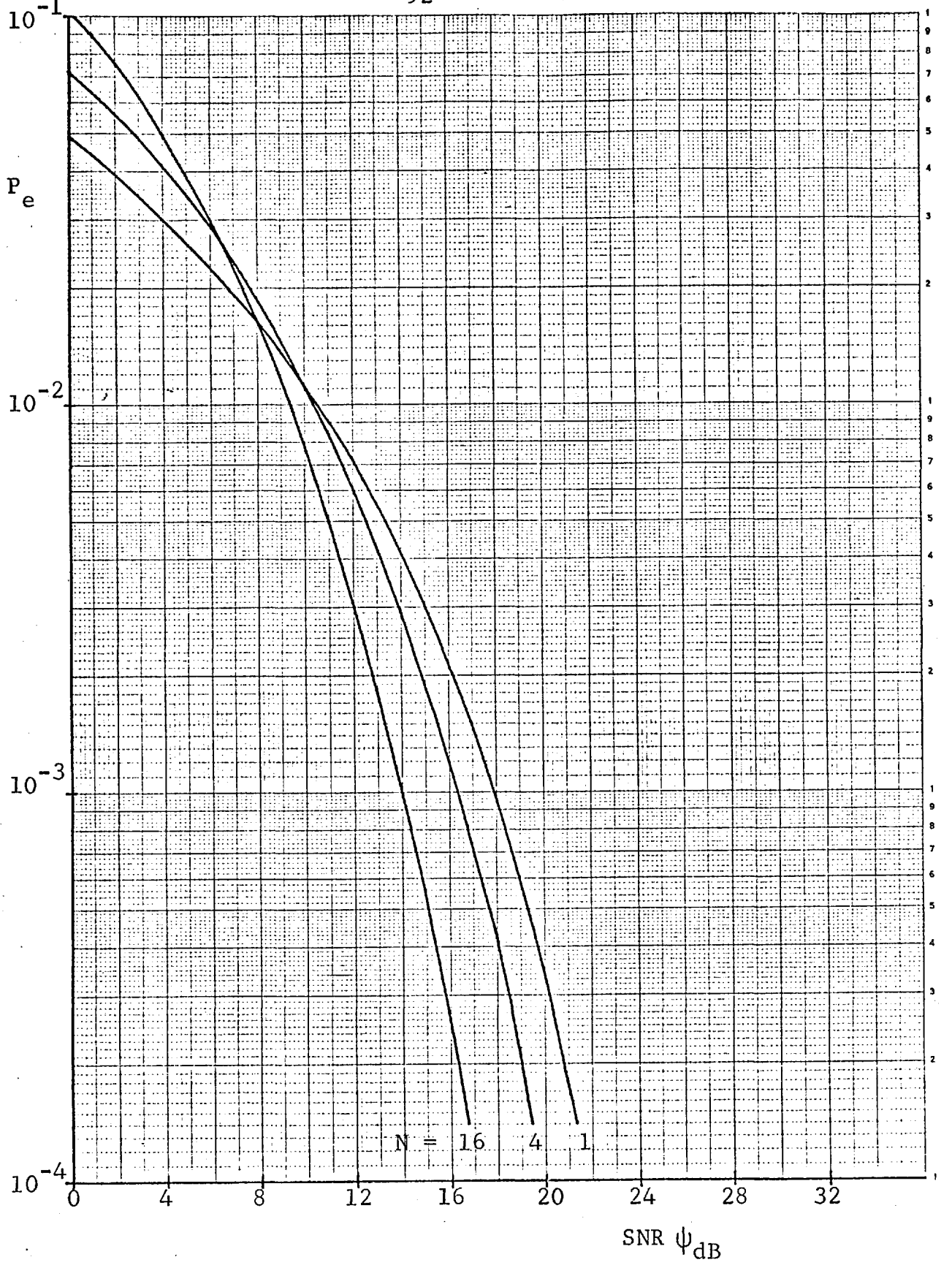

Fig. 4.12: $y(t)=s_6(t), \nu_1=\frac{1}{8}$, Laplace PDF.

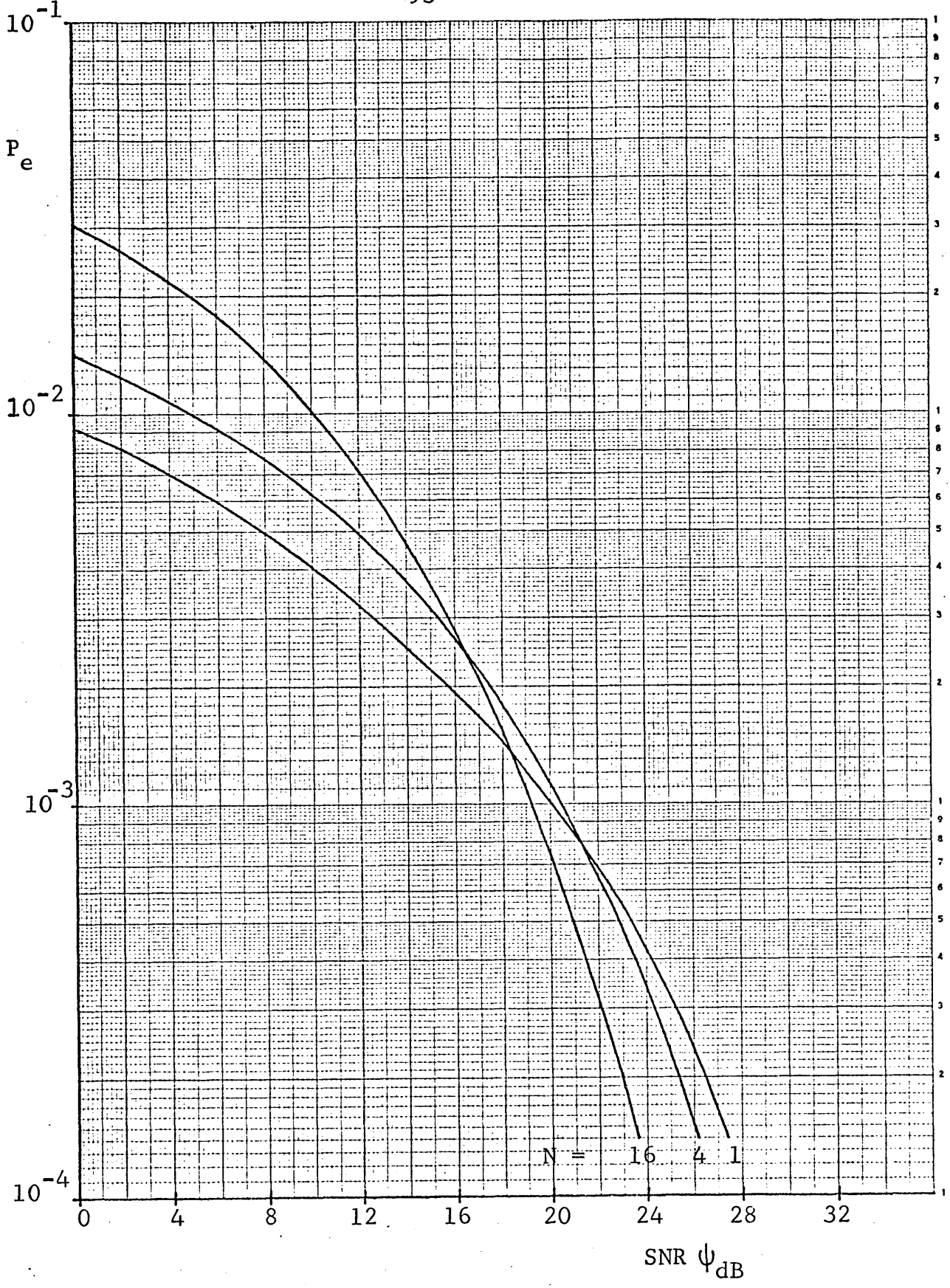

Fig. 4.13: $y(t)=s_6(t)$, $V_1=1/128$, Laplace PDF.

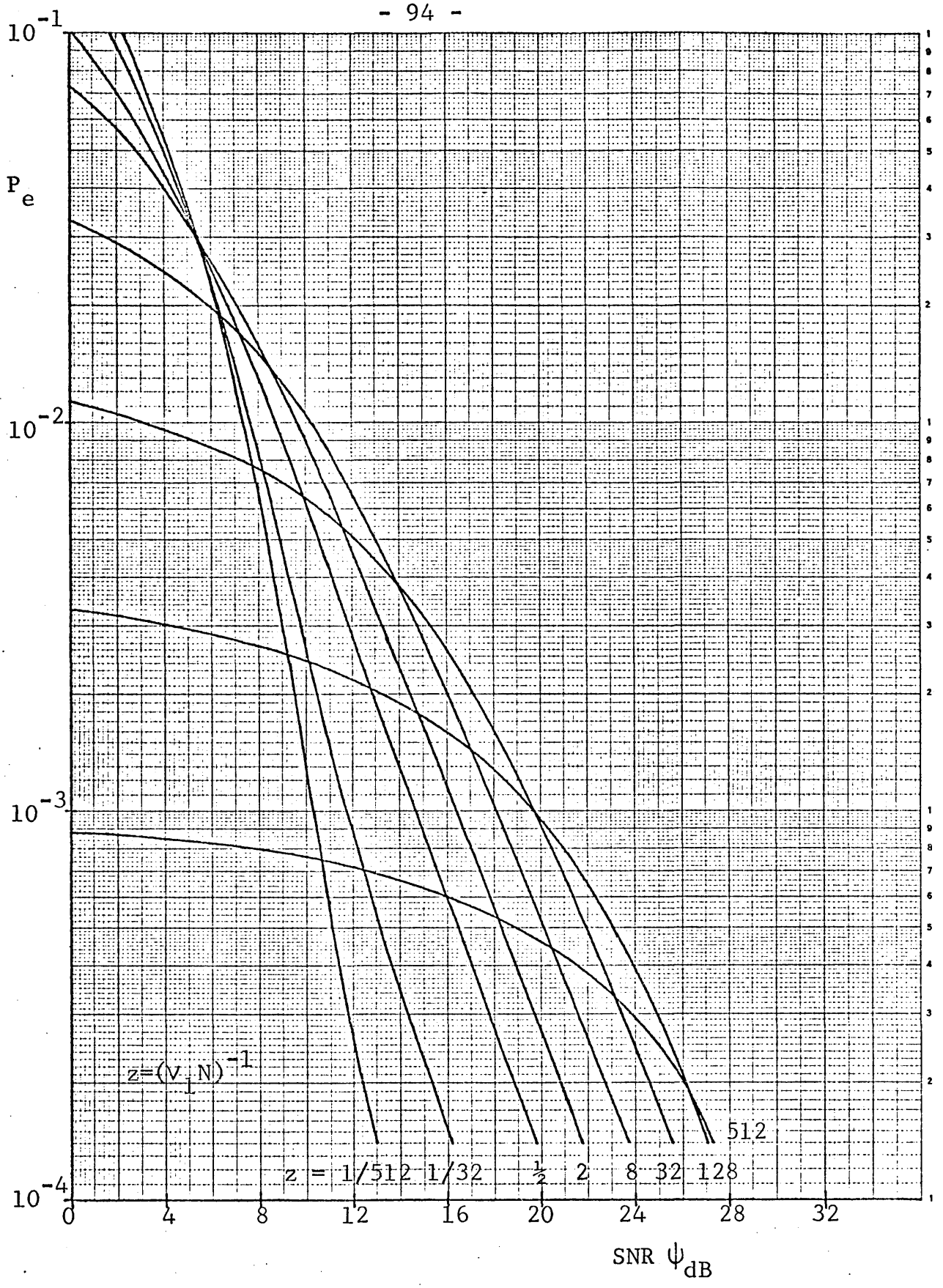

Fig. 4.14: $y(t)=s_3(t)$, Gen. Cauchy PDF (n=2).

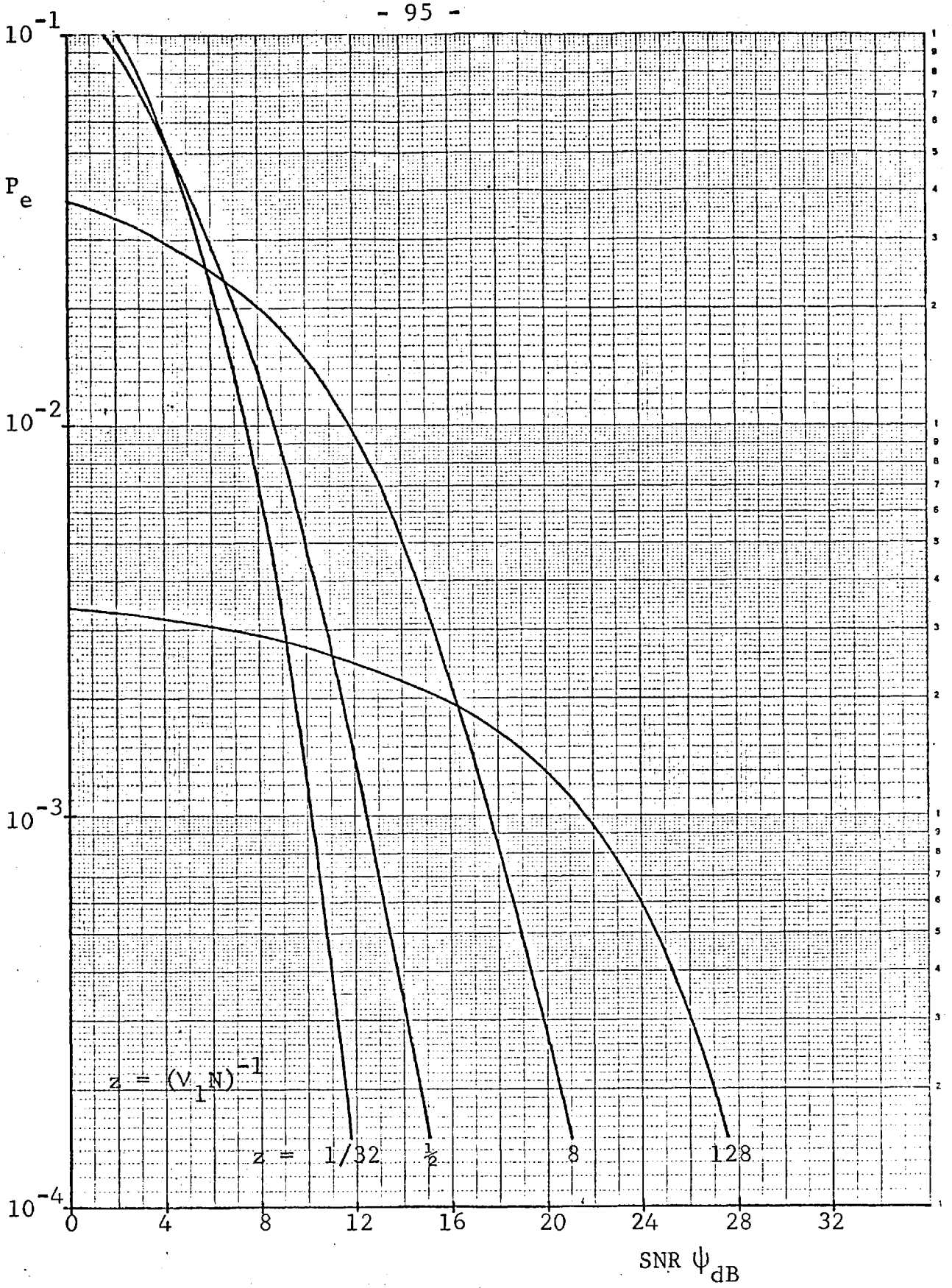

Fig. 4.15: $y(t)=s_3(t)$, Gen. Cauchy PDF (n=3).

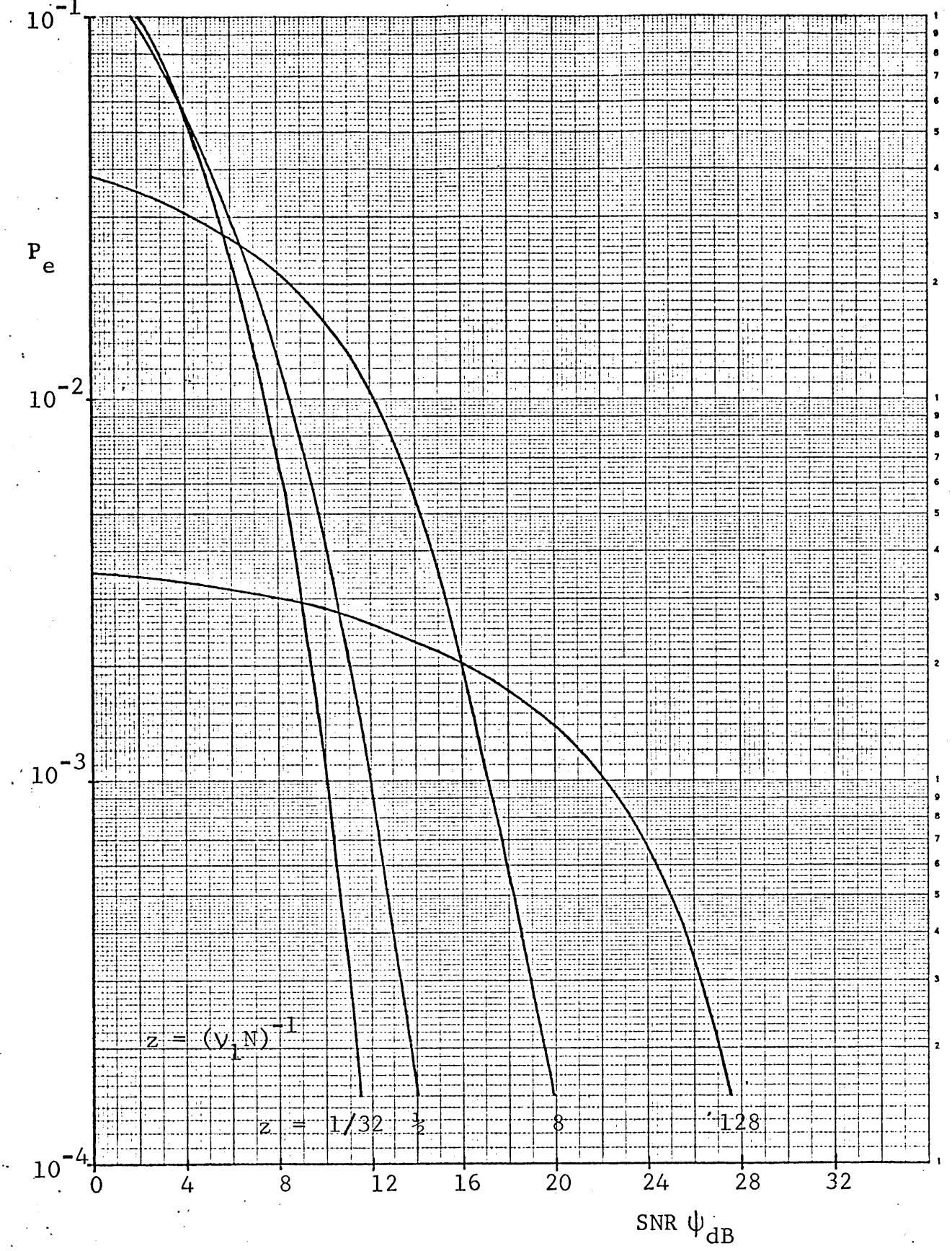

Fig. 4.16: $y(t)=s_3(t)$, Gen. Cauchy PDF (n=4).

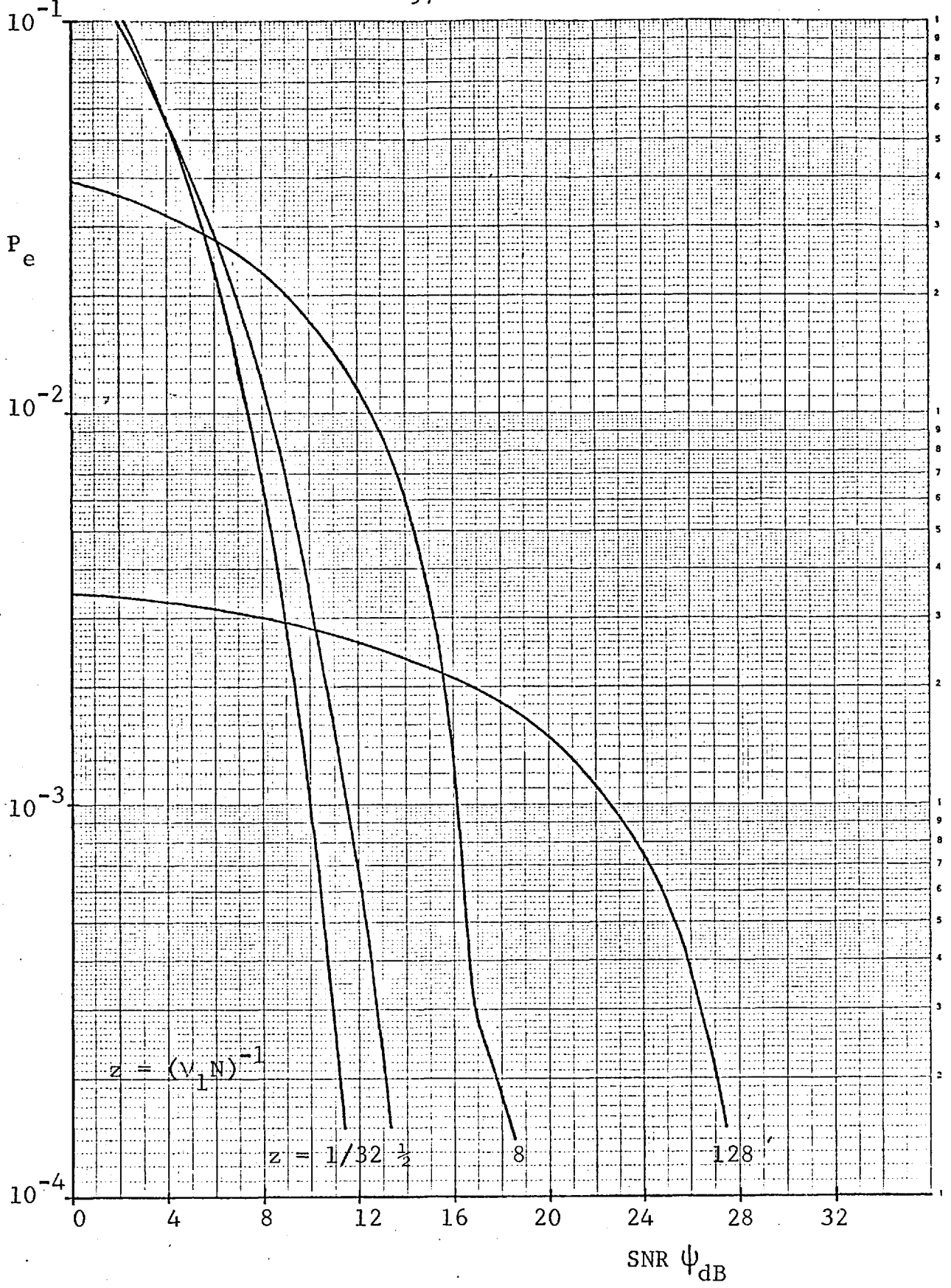

Fig. 4.17: $y(t)=s_3(t)$, Rectangular PDF, Equation (118).

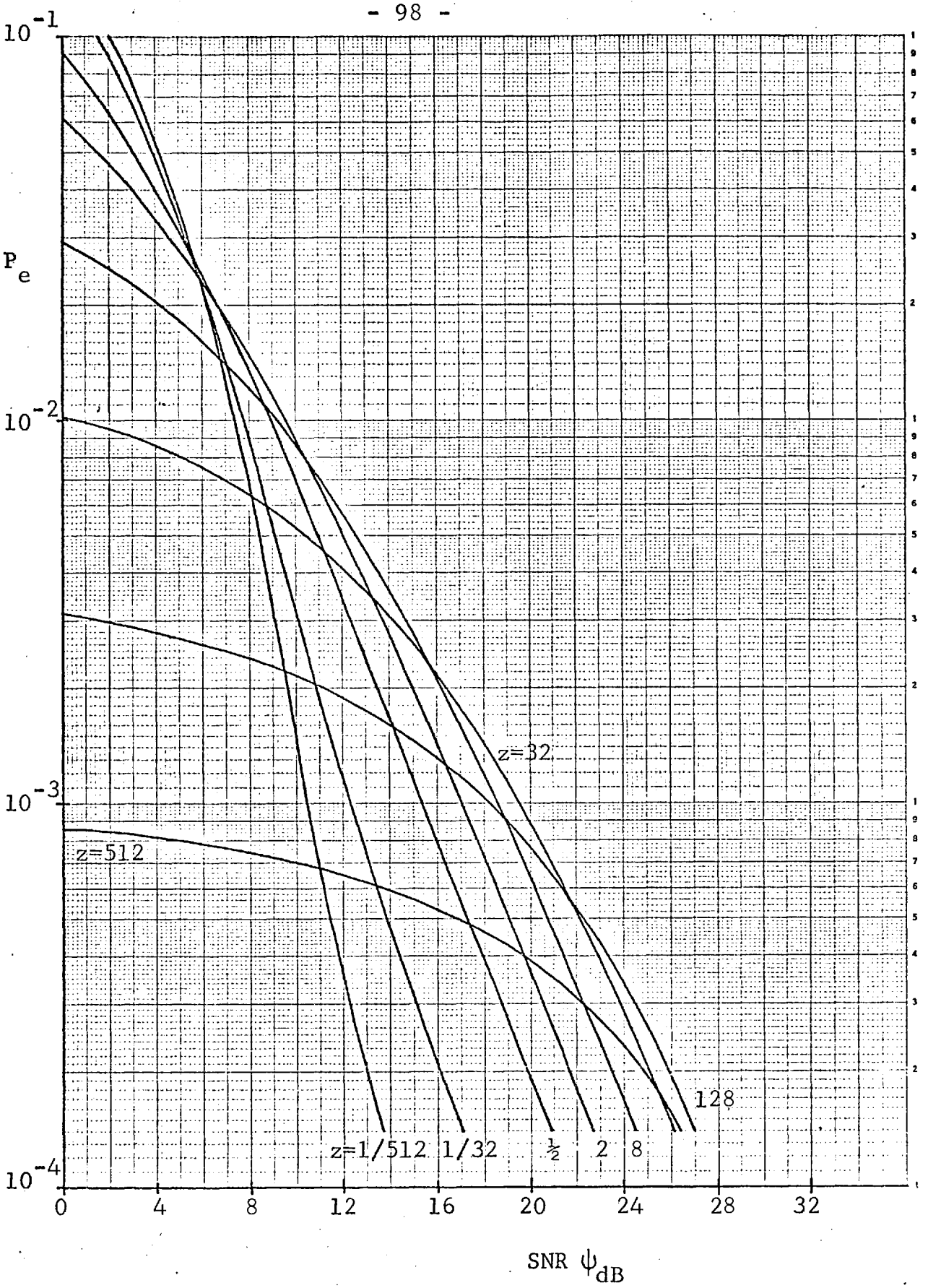

Fig. 4.18: $y(t)=s_3(t)$, Cauchy-type PDF (n=1).

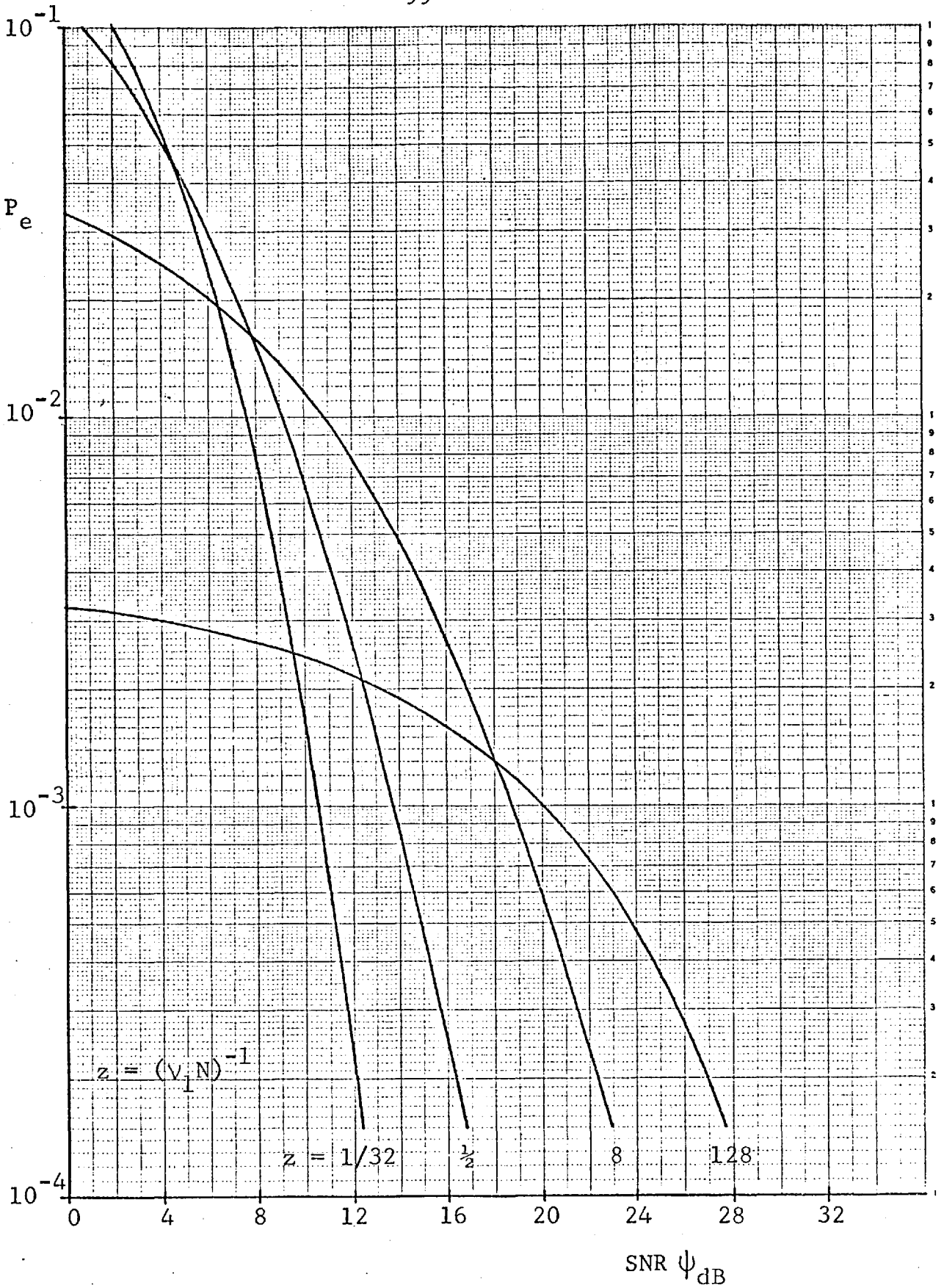

Fig. 4.19: $y(t)=s_3(t)$, Cauchy-type PDF (n=2).

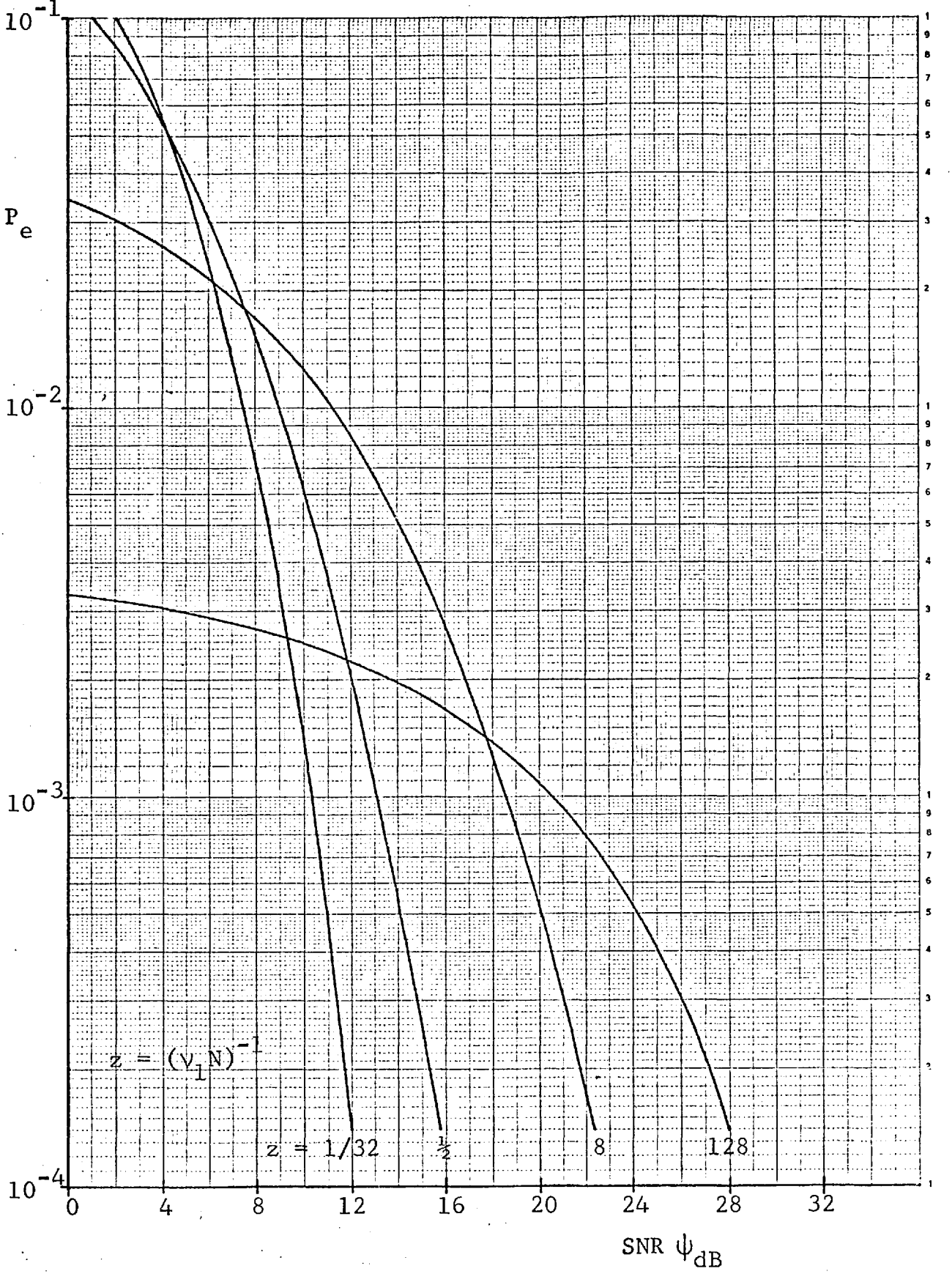

Fig. 4.20: $y(t)=s_3(t)$, Cauchy-type PDF (n=3).

Gaussian and Laplace PDF's are approximately twice those obtained for the other two distributions.

In view of the previous considerations, it can be concluded that a somewhat precise knowledge of the properties of the noise amplitude distribution must be obtained before any conclusion can be drawn about the efficiency of the proposed signal design technique. The longer the tails of the PDF $p_r(x)$ the lower the SNR improvement corresponding to a given value of N. In fact, since the improvement stems from the fact that the combination of several noise samples tends to become Gaussian, the farther $p_r(x)$ is from being Gaussian the larger the value of N necessary to achieve a certain SNR improvement.

4.4 CONCLUSIONS

From the results presented previously the following conclusions can be drawn concerning the performance of the proposed signalling method in the face of Poisson impulse noise:

(a) The method is only efficient if the signal-to-noise ratio exceeds a certain threshold which decreases for increasing signal length N. For lower SNR's the conventional system, obtained by removing the smearing delay-lines (case N = 1 in the error probability graphs), performs better. This stems from the fact that in a strongly non-Gaussian noise the high amplitudes normally have a greater probability, with respect to a Gaussian noise with the same variance, but the reverse is true for the low amplitudes. The receiver delay-lines tend to render the noise Gaussian and thus its effect can be harmful for low SNR's. In coding theory the same kind of SNR threshold arises below which the coded system has a higher probability of error than does the uncoded system.

(b) The error probability depends on the elementary pulse y(t) but, on account of the results, it is believed that the

effect is not important from a practical viewpoint, provided that y(t) is essentially limited to the fixed signalling period T and a fixed bandwidth W corresponding to the system bandwidth.

(c) There are grounds for conjecturing that, given the elementary pulse shape and the signal length N, then, provided that the SNR exceeds the threshold referred to in (a), the minimization of the error probability will lead to a pair of self-orthogonal sequences which are uniform, or nearly uniform. Below that SNR threshold the conventional system (N = 1) gives a better performance than the proposed signal design. The variation in P_e due to changing the pair of uniform sequences has been found negligible to the extent that it is not possible to show the difference on Figs. 4.4 to 4.20. The analysis in Appendix 1.5 suggests that in the presence of strongly non-Poisson noise the optimization will lead to strongly non-uniform sequences. In this appendix, a noise with a non-Poisson distribution of impulse arrival times is defined for which the uniform sequences can be proved not to minimize the error probability.

(d) The system performance was found to depend strongly on the amplitude distribution of the impulsive noise. This is due to the fact that the degree to which the noise becomes Gaussian, for a given signal length N, depends on how far the probability distribution of the accumulated noise samples is from the Gaussian distribution.

(e) By comparing the graphs presented in Figs. 4.5 and 4.6 with the graphs published in Ref. [4-9], which are reproduced in Fig. 4.21, it can be concluded that for $N \geq 8$ the signals proposed here perform better than the signal used in this reference. It should be noted also that the proposed system is much easier to implement than the one suggested in Ref. [4-9].

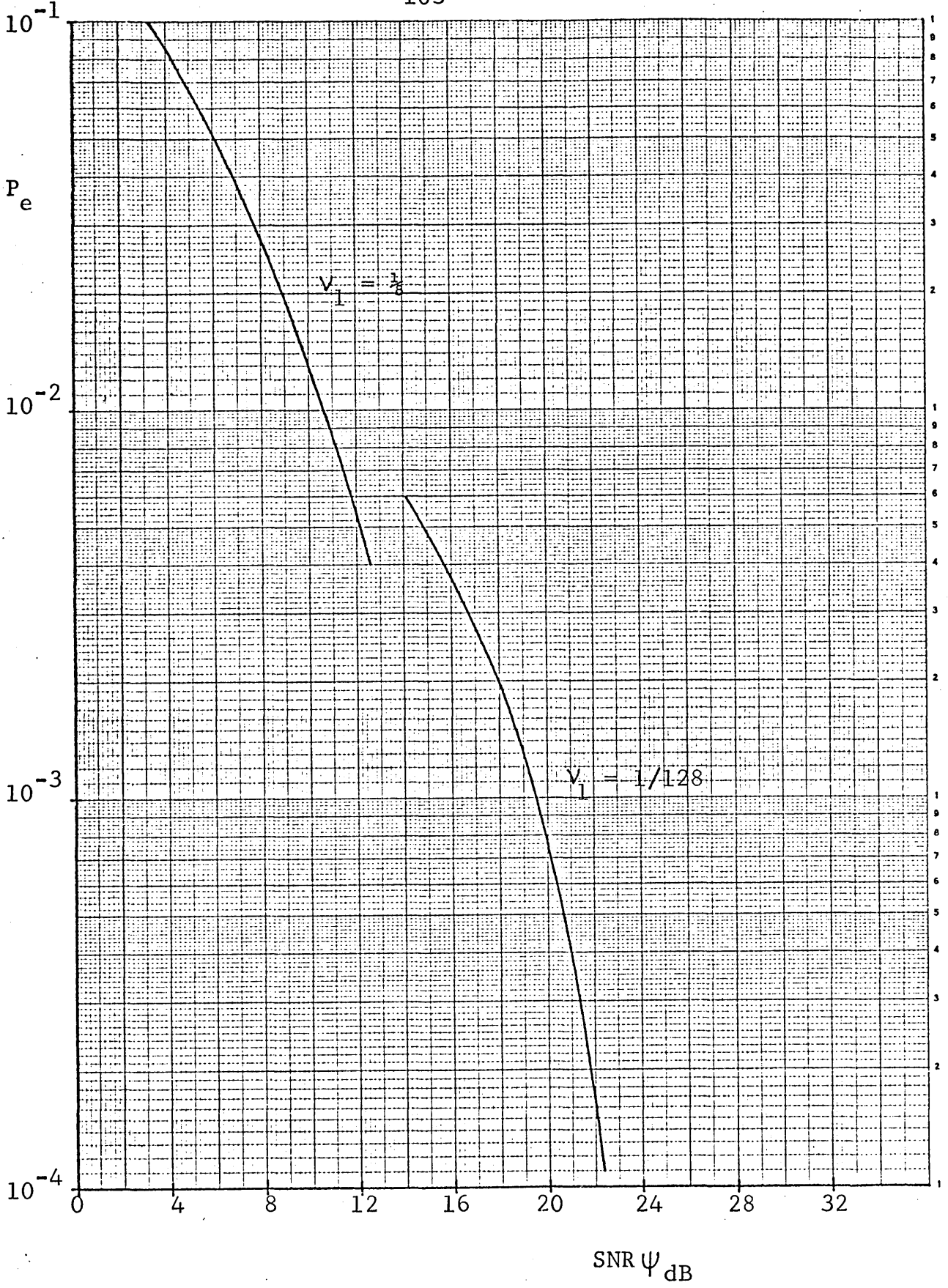

Fig. 4.21: Performance curves obtained in Ref. [4-9].

CHAPTER V

PROPOSED SIGNAL DESIGN: II - LOW SNR

Do not put all your
eggs in one basket.

Proverb, 18th Century.

5.1 INTRODUCTION

In the previous chapter the transmission rate was maintained at the value which can normally be achieved, for a given channel bandwidth, in the presence of background Gaussian noise alone. It was concluded that for this transmission rate, and in the presence of impulsive noise, the smear-desmearing technique results in an improvement in system performance when the signal-to-impulsive-noise ratio (SINR) is greater than a critical threshold, but that below this threshold the method gives rise to a deterioration of performance.

In this chapter attention is focused on the low SINR case. The technique proposed consists in transmitting a number of pulses per data element and trying to optimize the detection operation performed at the receiver. Although this idea is not new (see Section 3.4) an attempt will be made in this chapter to improve the detection operation in the presence of impulsive noise. The technique will obviously lead to a reduction in transmission rate or, if the transmission rate is to be maintained, an increase in necessary bandwidth.

In this chapter it is assumed that the noise possesses the following main characteristics:

(a) It is a non-continual noise (see Section 2.3) in the sense that each one of its samples can be drawn from one of several amplitude distributions, according to some time distribution which gives the amplitude distribution to be used at each sampling instant;

(b) A fraction of the noise samples is due to the background Gaussian noise alone and the other samples include, in addition, the contribution from the intermittent (impulsive) causes of noise;

(c) The level of the background Gaussian component is usually much lower than that of the impulsive components of the

noise*.

In view of these characteristics, it seems reasonable to try and detect first the presence of the impulsive noise and then to use this knowledge to improve the signal detection. This concept is depicted in Fig. 5.1. Depending on whether the noise detector decides that the incoming sample has been corrupted by impulsive noise or not, that sample will follow either the lower or upper branch of the receiver, respectively. These two branches should be designed in much the same way as the receiver shown in Fig. 3.5. That is, the sample values within each interval MT seconds long are accumulated after being optimally processed by a memoryless device** (S and T in Fig. 5.1) and the resulting value is fed into a decision device. The decision device in the upper branch is best designed as a null-zone detector because, if the accepted samples nearly cancel one another after accumulation, it is very likely that the noise detector has made a wrong decision in a large number of samples. For this reason, the decision device in the upper branch will produce an erasure symbol x at its output whenever its input is close enough to zero. In this instance the switch at the receiver output will choose the symbol coming from the lower branch, whose decision device is the usual single threshold detector.

The difference between the present approach and that described in Section 3.4 can be summarized as follows. The single-path detector of Section 3.4 (Fig. 3.5) is optimum under the assumption that the noise samples are independently drawn from the same statistical distribution (white continual noise). On the other hand, the detector now being proposed aims at exploiting the non-continual nature which is characteristic of impulsive noise. In order to achieve this, the detector cannot

---

* In this chapter it is assumed that the impulsive noise samples are drawn from a single statistical distribution which represents the effect of all intermittent causes of noise.

** Usually a nonlinear device.

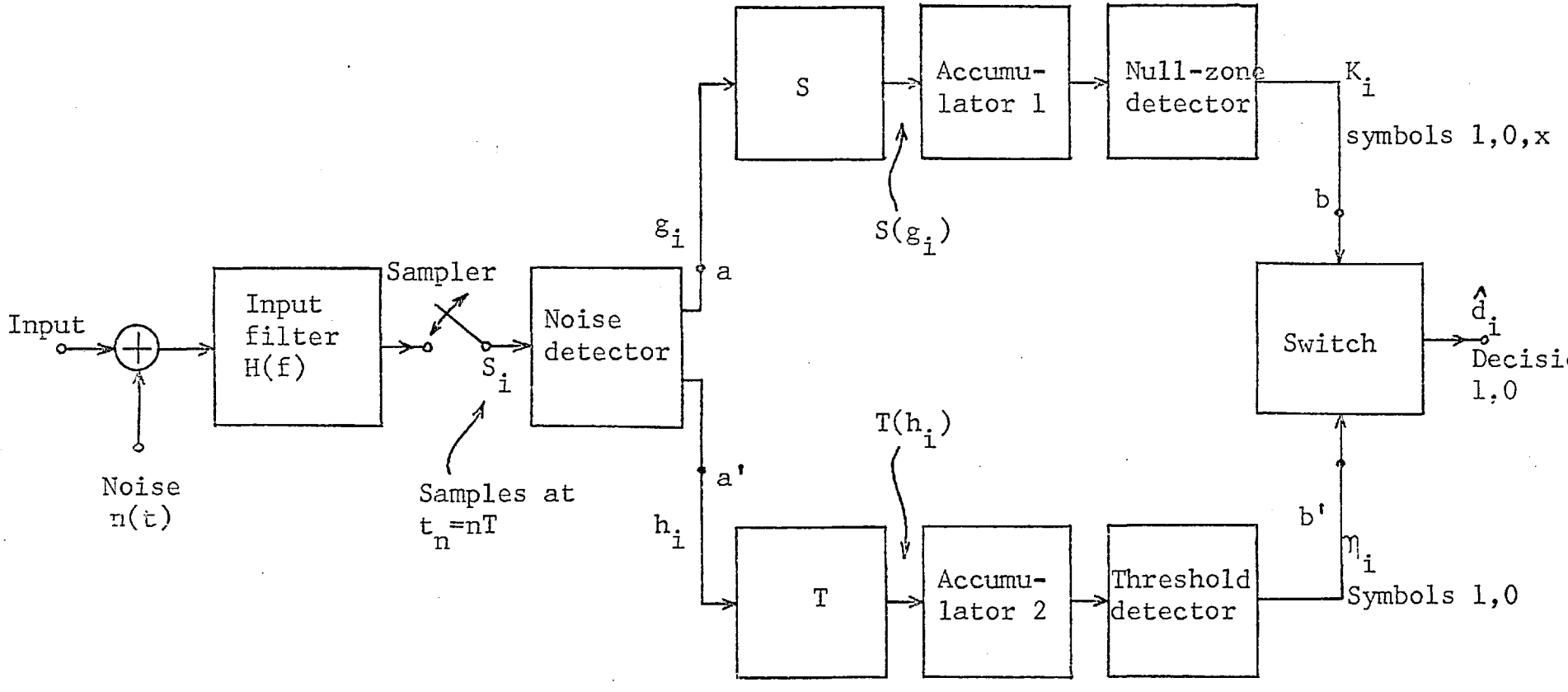

Fig. 5.1: Basic receiver structure.

treat identically all the noise samples and therefore it must incorporate some criterion for distinguishing between the Gaussian and the impulsive noise components. The criterion to be used in the following sections is the difference between the levels of these noise components*.

5.2 ANALYSIS OF THE PROPOSED TECHNIQUE

5.2.1 Major assumptions

As mentioned before, each binary digit is to be transmitted by means of a sequence of M pulses which will be assumed identically shaped. The transmitted signal corresponding to the i^{th} digit thus has the following form:

$$s_i(t) = \phi_i \sqrt{E_s} \sum_{K=0}^{M-1} a_K y(t-KT), \qquad \phi_i = \pm 1 \qquad (1)$$

where y(t) is assumed to be a Nyquist waveform (see Section 4.2.2) thus avoiding interference between pulses. It is further assumed that y(t) has unit energy and that

$$\sum_{K=0}^{M-1} a_K^2 = M \qquad (2)$$

Therefore, as in Section 4.2.4, the average transmitted power is given by

$$P_s = \frac{E_s}{T} \qquad (3)$$

The information is transmitted at a rate of 1/MT bit/sec since the pulse sequences are assumed non-overlapping.

As in the previous chapters the channel is assumed to be ideal (distortionless). At the receiver input the signal is additively corrupted by a combination of white Gaussian noise, $n_1(t)$, and Poisson impulse noise, $n_2(t)$; that is,

---

* It may be possible to devise more efficient noise detectors which exploit other distinguishing features of the impulsive noise bursts.

$$n(t) = n_1(t) + n_2(t) \tag{4}$$

where*

$$n_2(t) = \sum_{i=-\infty}^{\infty} r_i \, \delta(t-\tau_i) \tag{5}$$

In order to simplify the problem, it is assumed throughout this chapter that the receiver input filter has an impulse response

$$h(t) = y(\ell T - t) \tag{6}$$

(for some integer ℓ) which is precisely time-limited to an interval of duration T. This assumption implies that the samples of impulsive noise produced by the sampler in Fig. 5.1, at the instants $t_n = nT$ (n integer), are statistically independent. Since y(t) is a Nyquist pulse, the samples of Gaussian noise are also statistically independent (see Appendix 1.2). It thus follows from the discussion at the end of Section 4.2 that the coefficients a_K in Equation (1) must have unit values, i.e. $a_K = +1$ for any K.

If p is the probability that the samples of the received signal are corrupted by impulsive noise, then the combined PDF of the noise samples is

$$p_n(x) = q \, p_w(x) + p \, p_z(x) \tag{7}$$

where $q = 1-p$, $p_w(x)$ is the Gaussian noise PDF and $p_z(x)$ is the PDF of the noise samples affected by at least one noise impulse. In what follows both $p_w(x)$ and $p_z(x)$ are assumed to be symmetric, unimodal, PDF's which are completely known. The probability p is also assumed known.

Due to the purely random occurrence of the noise pulses in time, the probability $p_M(i)$ of having i samples corrupted by impulsive noise in a sequence of M signal samples is given by the well known binomial distribution:

---

* See Section 4.2, Equation (78).

$$p_M(i) = \binom{M}{i} p^i q^{M-i} \qquad (8)$$

In this chapter only small values of M are considered, namely $M \leqslant 6$, since for higher values the system becomes very inefficient in terms of transmission rate and thus is not suitable for data transmission. If a low M gives an unacceptably high error probability the combination with coding appears to be the best alternative. This point will be considered further in Chapter VII.

It is also further assumed that the signal-to-Gaussian-noise ratio (SGNR) defined by

$$\rho_{dB} = 10 \log_{10} \frac{E_s}{\sigma_w^2}$$

(σ_w^2 being the variance of the Gaussian noise) is greater than 12 dB in which case the error probability of the receiver in the presence of Gaussian noise alone is much less than 10^{-5} and thus most errors occur when impulsive noise is present.

5.2.2 The noise detector

As explained in Section 5.1, the noise detector in Fig. 5.1 aims at detecting the presence of the impulsive component of the noise in the background formed by the transmitted signal and the white Gaussian noise. In the following analysis it is assumed that this aim is to be achieved by using only the information contained in the samples of the received waveform at the instants $t_n = nT$ (n being an integer). The optimum detector would in general be expected to process continuously the received waveform but its analysis is naturally much more difficult than that of the suboptimum detector considered below.

Let the samples delivered by the sampler in Fig. 5.1 be termed S_i ($i = 0, 1, 2, \ldots, M-1$) and let the parameter θ_i indicate the presence ($\theta_i = 1$) or absence ($\theta_i = 0$) of the impulsive disturbance at the i^{th} sample. We can then write

$$S_i = A\phi_i + w_i + u_i \theta_i \qquad (9)$$

where $A = \sqrt{E_s}$ is the signal sample magnitude*, $\phi_i = \pm 1$ accounts for its polarity, w_i is the white Gaussian noise sample and $u_i\theta_i$ is the impulsive component of the noise. Instead of Equation (9), it will be found more convenient to write

$$S_i = \begin{cases} A\phi_i + w_i & \text{if } \theta_i = 0 \\ A\phi_i + z_i & \text{if } \theta_i = 1 \end{cases} \tag{10}$$

where w_i and z_i are distributed according to the PDF's $p_w(x)$ and $p_z(x)$ respectively. As defined above

$$\begin{aligned} &P[\theta_i = 1] = p \\ \text{and} \quad &P[\theta_i = 0] = 1 - p = q \end{aligned} \tag{11}$$

In order to calculate the required likelihood ratio we first note that

$$\begin{aligned} P[S_i/\theta_i = 0;\ \phi_i] &= p_w(S_i - A\phi_i) \\ P[S_i/\theta_i = 1;\ \phi_i] &= p_z(S_i - A\phi_i) \end{aligned} \tag{12}$$

and therefore

$$P[S_i/\theta_i = 0] = \sum_{\phi_i = \pm 1} P[\phi_i]\, p_w(S_i - A\phi_i) \tag{13}$$

$$P[S_i/\theta_i = 1] = \sum_{\phi_i = \pm 1} P[\phi_i]\, p_z(S_i - A\phi_i)$$

The likelihood ratio on which the detector is based is by definition [5-1]

$$\Lambda(S_i) = \frac{P[S_i/\theta_i = 1]}{P[S_i/\theta_i = 0]} \tag{14}$$

If $\hat{\theta}_i$ is the decision made about the value of θ_i we can express the receiver action in the following terms:

---

* See Section 4.2, Equation (58), where A_s means the same as A.

$$\begin{aligned} &\text{If } \Lambda(S_i) > \lambda \qquad \text{decide} \quad \hat{\theta}_i = 1; \\ &\text{if } \Lambda(S_i) < \lambda \qquad \text{decide} \quad \hat{\theta}_i = 0. \end{aligned} \tag{15}$$

As is well known [5-1], the threshold λ can be expressed as follows:

$$\lambda = \frac{qC_f}{pC_m} = \frac{q}{p}\gamma \tag{16}$$

where C_f is the cost of deciding $\hat{\theta}_i = 1$ when actually $\theta_i = 0$ and C_m is the cost of deciding $\hat{\theta}_i = 0$ when actually $\theta_i = 1$. A zero value is assumed for the cost of any correct decision. For the purpose of minimizing the probability of error in the signal detection, making $C_f = C_m$ does not necessarily lead to the optimal receiver. This question will not be pursued further at this point but will be taken up later in this chapter when the performance of the overall receiver is considered.

In the remainder of this chapter it will be assumed that

$$P[\phi_i = +1] = P[\phi_i = -1] = \tfrac{1}{2} \tag{17}$$

In view of Equation (14) it is thus possible to write

$$\Lambda(S_i) = \frac{p_z(S_i+A) + p_z(S_i-A)}{p_w(S_i+A) + p_w(S_i-A)} \tag{18}$$

Since $p_z(x)$ and $p_w(x)$ are symmetric unimodal PDF's it follows that*

$$\Lambda(S_i) = \Lambda(-S_i) \tag{19}$$

and that

$$\Lambda(0) = \frac{p_z(A)}{p_w(A)} \tag{20}$$

In the cases of interest, the probability of the event $z_i > A$ is much higher than that of the event $w_i > A$ and thus

$$\Lambda(0) \gg 1 \tag{21}$$

---

* The symmetry expressed by Equation (19) is a direct consequence of Equation (17).

By comparing Equations (9) and (10) it can be concluded that $z_i = w_i + u_i$ and thus

$$C_z(\omega) = C_w(\omega).C_u(\omega),$$

where C_z, C_w and C_u are the characteristic functions (CHF's) of the random variables z, w and u respectively. Therefore,

$$\begin{aligned} p_z(0) &= \frac{1}{2\pi}\int_{-\infty}^{\infty} C_w(\omega)C_u(\omega)d\omega \\ &\leqslant \frac{1}{2\pi}\int_{-\infty}^{\infty} C_w(\omega)\,|C_u(\omega)|\,d\omega \\ &\leqslant \frac{1}{2\pi}\int_{-\infty}^{\infty} C_w(\omega)d\omega = p_w(0), \end{aligned} \tag{22}$$

where the second inequality follows from the fact that $|C_u(\omega)| \leqslant 1$. From Equation (18) we obtain

$$\Lambda(A) = \frac{p_z(0) + p_z(2A)}{p_w(0) + p_w(2A)} \tag{23}$$

In most practical situations

$$\frac{p_w(2A)}{p_w(0)} \leqslant \frac{p_z(2A)}{p_z(0)} \leqslant 1 \tag{24}$$

and thus

$$\frac{p_z(2A)}{p_w(2A)} \geqslant \frac{p_z(0)}{p_w(0)}.$$

If $a \leqslant p_z(2A)$ is such that

$$\frac{a}{p_w(2A)} = \frac{p_z(0)}{p_w(0)} = \frac{a + p_z(0)}{p_w(2A) + p_w(0)}$$

then, in view of relations (22) to (24),

$$\frac{p_z(0)}{p_w(0)} \leqslant \Lambda(A) \leqslant 2\frac{p_z(0)}{p_w(0)} \leqslant 2 \tag{25}$$

There are cases, like those studied in Section 5.3, where the reason behind relations (21) and (24) also implies that

$$\Lambda(A) \ll 1. \tag{26}$$

The previous considerations serve to justify the typical graph of function $\Lambda(x)$ shown in Fig. 5.2. From this figure it can be seen that the decision rule expressed by relations (15) can be reformulated in the following terms:

$$\begin{aligned} &\text{If } -\varepsilon_1 < |S_i| - A < \varepsilon_2 \text{ decide } \hat{\theta}_i = 0 \\ &\text{otherwise decide } \hat{\theta}_i = 1. \end{aligned} \tag{27}$$

The new thresholds ε_1 and ε_2 are obviously positive functions of the threshold λ in the decision rule (15).

The performance of the noise detector can be described by the probabilities

$$\alpha = P\left[\hat{\theta}_i = 1 \,|\, \theta_i = 0\right] \tag{28}$$

and

$$\beta = P\left[\hat{\theta}_i = 0 \,|\, \theta_i = 1\right] \tag{29}$$

In view of equation (19) α can be expressed in the following manner:

$$\alpha = 1 - \alpha_+ - \alpha_- \tag{30}$$

where

$$\alpha_+ = P\left[\hat{\theta}_i = 0,\ S_i > 0 \mid \theta_i = 0,\ \phi_i = +1\right] \tag{31}$$

and

$$\alpha_- = P\left[\hat{\theta}_i = 0,\ S_i < 0 \mid \theta_i = 0,\ \phi_i = +1\right] \tag{32}$$

If σ_w^2 is the variance of the Gaussian noise samples then

$$\alpha_+ = \tfrac{1}{2}\,\mathrm{erf}\left(\frac{\varepsilon_1}{\sigma_w\sqrt{2}}\right) + \tfrac{1}{2}\,\mathrm{erf}\left(\frac{\varepsilon_2}{\sigma_w\sqrt{2}}\right) \tag{33}$$

and

$$\alpha_- = \tfrac{1}{2}\,\mathrm{erfc}\left(\frac{2A-\varepsilon_1}{\sigma_w\sqrt{2}}\right) - \tfrac{1}{2}\,\mathrm{erfc}\left(\frac{2A+\varepsilon_2}{\sigma_w\sqrt{2}}\right) \tag{34}$$

Since usually $A \gg \sigma_w$, it is assumed hereafter that $\alpha_- \ll \alpha_+$ and therefore that

$$\begin{aligned} \alpha &\simeq 1 - \alpha_+ \\ &\simeq \tfrac{1}{2}\,\mathrm{erfc}\left(\frac{\varepsilon_1}{\sigma_w\sqrt{2}}\right) + \tfrac{1}{2}\,\mathrm{erfc}\left(\frac{\varepsilon_2}{\sigma_w\sqrt{2}}\right) \end{aligned} \tag{35}$$

Also, in view of Equation(19) it follows that

$$\beta = \beta_+ + \beta_- \tag{36}$$

where

$$\beta_+ = P\left[\hat{\theta}_i = 0,\ S_i > 0 \mid \theta_i = 1,\ \phi_i = +1\right] \tag{37}$$

and

$$\beta_- = P\left[\hat{\theta}_i = 0,\ S_i < 0 \mid \theta_i = 1,\ \phi_i = +1\right] \tag{38}$$

These probabilities can be expressed in terms of the exceedence probability function (EPF) of the random variables Z_i/K_z, K_z being some appropriate dispersion parameter* of $p_z(x)$. Since this EPF is given by

$$Q_z(y) = K_z \int_y^\infty p_z(K_z x)dx \tag{39}$$

it follows that

$$\beta_+ = 1 - Q_z\left(\frac{\varepsilon_1}{K_z}\right) - Q_z\left(\frac{\varepsilon_2}{K_z}\right) \tag{40}$$

and

$$\beta_- = Q_z\left(\frac{2A-\varepsilon_1}{K_z}\right) - Q_z\left(\frac{2A+\varepsilon_2}{K_z}\right) \tag{41}$$

In the following subsection it is shown that the error probability at the receiver output is a function of the above-defined probabilities. It is important to note at this stage that these probabilities can be readily expressed in terms of the following parameters:

(a) Signal-to-Gaussian-noise ratio (SGNR):

$$\rho = \frac{A}{\sigma_w} \tag{42}$$

(b) Signal-to-impulsive-noise ratio (SINR):

$$\mu = \frac{A}{K_z} \tag{43}$$

(c) Impulsive-to-Gaussian-noise ratio (IGNR):

$$\zeta = \frac{K_z}{\sigma_w} = \frac{\rho}{\mu} \tag{44}$$

---

* In the numerical examples considered later, if the variance σ_z^2 of $p_z(x)$ is finite then $K_z = \sigma_z$. Otherwise K_z is assumed to be the median of $|Z_i|$.

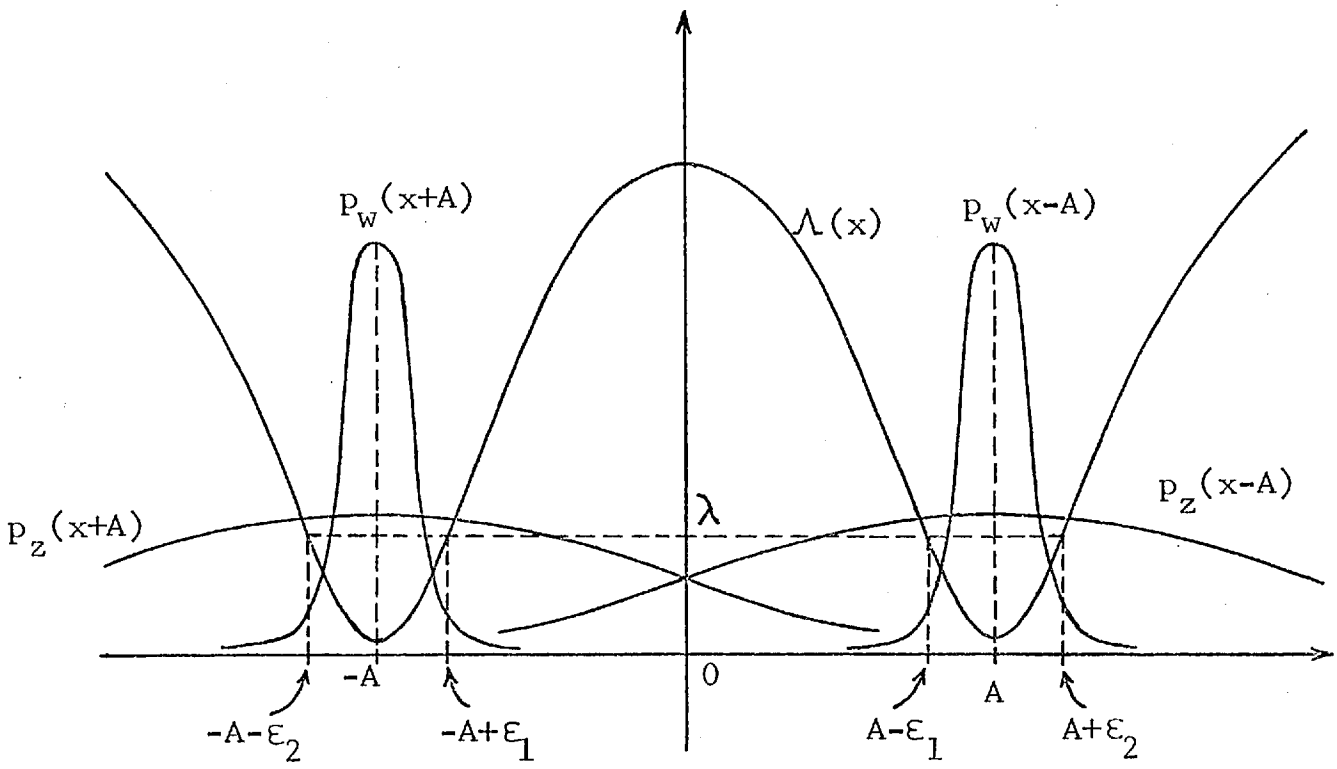
$p_w(x+A)$
$\Lambda(x)$
$p_w(x-A)$
$p_z(x+A)$
λ
$p_z(x-A)$
-A
0
A
$-A-\varepsilon_2$
$-A+\varepsilon_1$
$A-\varepsilon_1$
$A+\varepsilon_2$

Fig. 5.2

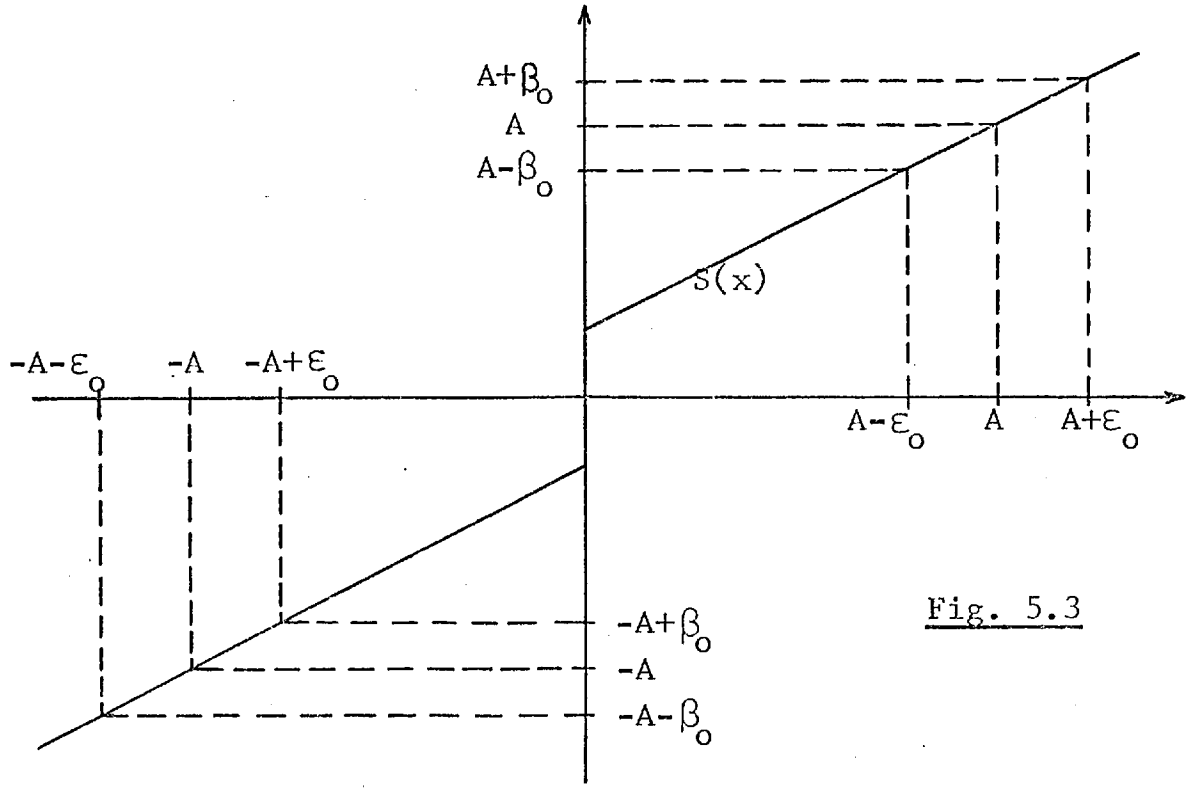
$A+\beta_o$
A
$A-\beta_o$
S(x)
$-A-\varepsilon_o$
-A
$-A+\varepsilon_o$
$A-\varepsilon_o$
A
$A+\varepsilon_o$
$-A+\beta_o$
-A
$-A-\beta_o$

Fig. 5.3

(d) The ratios $\delta_1 = \varepsilon_1/\sigma_w$ and $\delta_2 = \varepsilon_2/\sigma_w$.

5.2.3 The double-path detector

As outlined in Section 5.1 the noise detector studied above produces two outputs,

$$g_i = S_i.(1 - \hat{\theta}_i) \tag{45}$$

and

$$h_i = S_i.\hat{\theta}_i \tag{46}$$

which are directed to the blocks S and T (Fig. 5.1) respectively. Let d_i denote the i^{th} transmitted digit (0 or 1) and $\hat{d}_i$ denote the corresponding binary digit produced at the receiver output. It will be assumed henceforth that

$$\phi_i = \begin{cases} +1 & \text{if } d_i = 0 \\ -1 & \text{if } d_i = 1. \end{cases} \tag{47}$$

In terms of the notation in Fig. 5.1 the performance of the double-path detector can be described as follows:

$$\hat{d}_i = \begin{cases} K_i = 0 & \text{if } X = \sum_{i=0}^{M-1} S(g_i) \geqslant X_1 > 0 \\ K_i = 1 & \text{if } X \leqslant X_2 < 0 \\ \eta_i & \text{if } X_2 < X < X_1, \end{cases} \tag{48}$$

X_1 and X_2 being the thresholds of the null-zone detector. In the last case the null-zone detector produces an erasure symbol (i.e. $K_i = x$) and the decision rule is

$$\hat{d}_i = \eta_i = \begin{cases} 0 & \text{if } Y = \sum_{i=0}^{M-1} T(h_i) > 0 \\ 1 & \text{if } Y \leqslant 0. \end{cases} \tag{49}$$

In view of Equation (19) it can be seen that the error probability P_e of the receiver in Fig. 5.1 is the same whether $d_i = 0$ or $d_i = 1$, that is

$$P_e = P\left[\hat{d}_i = 1 \mid \phi_i = +1\right] = P\left[\hat{d}_i = 0 \mid \phi_i = -1\right] \quad (50)$$

Therefore, by assuming that a message element $d_i = 0$ was transmitted, the error probability, P_e, can be expressed as follows:

$$P_e = P_{eu} + P_x P_{ex} \quad (51)$$

where P_{eu} and P_x are the probabilities of obtaining a 1 and an erasure symbol x, respectively, at the output of the upper branch, and P_{ex} is the probability of obtaining a 1 at the output of the lower branch when an erasure symbol is delivered by the upper branch. In terms of the notation in Fig. 5.1, these probabilities can be defined formally as follows:

$$P_{eu} = P\left[K_i = 1 \mid \phi_i = +1\right] \quad (52)$$

$$P_x = P\left[K_i = x \mid \phi_i = +1\right] \quad (53)$$

$$P_{ex} = P\left[\eta_i = 1 \mid K_i = x, \phi_i = +1\right] \quad (54)$$

To obtain an expression for P_e in terms of the receiver parameters is, in the general case, an intractable problem. In order to understand better the difficulties involved, let it be assumed for ease of exposition that $\varepsilon_1 = \varepsilon_2 = \varepsilon_0$ and that the block S in Fig. 5.1 has the transfer function shown in Fig. 5.3. In this case $S(g_i) = \pm A + v_i$ for some v_i such that $|v_i| < \beta_0$ and thus the output from the accumulator 1 (Fig. 5.1) can be written as follows:

$$\sum_{i=0}^{M-1} S(g_i) = KA + \delta_K$$

where $K = 0, \pm 1, \pm 2, \ldots, \pm M$ and

$$|\delta_K| < M\beta_0,$$

the meaning of β_0 being explained in Fig. 5.3. When $K \neq 0$ the null-zone detector should decide in favour of 0 or 1 according to the sign of K ($K_i = 0$ if $K>0$ and $K_i = 1$ if $K<0$). However, if $K = 0$, all the information about the signal has

been destroyed by the noise and thus an erasure symbol should be produced. The determination of the optimum thresholds for the null-zone detector is a quite difficult problem unless the slope of the straight lines in Fig. 5.3 is chosen such that $M\beta_0 \leq A/2$. In fact, only in this case is it possible to decide without error whether $K = 0$ or $K \neq 0$. For this reason it will be assumed henceforth that the receiver is of the simplified form in which the block S shown in Fig. 5.1 is assumed to be a hard limiter, i.e.

$$S(g_i) = \begin{cases} +A & \text{if } g_i > 0 \\ -A & \text{if } g_i < 0. \end{cases} \tag{55}$$

In this case, $\beta_0 = 0$.

Since usually the SGNR $\rho_{dB} > 12$ dB, the performance of the lower branch of the receiver will be essentially determined by the impulsive component of the noise. Thus, the input h_i to the block T in Fig. 5.1 can be drawn directly from the sampler output. The corresponding block diagram is shown in Fig. 5.4, where the noise detector and the transfer function $S(g_i)$ have been merged into the block R defined by:

$$R(S_i) = \begin{cases} +A & \text{if } -\varepsilon_1 < S_i - A < \varepsilon_2 \\ -A & \text{if } -\varepsilon_2 < S_i + A < \varepsilon_1 \\ 0 & \text{otherwise.} \end{cases} \tag{56}$$

The null-zone detector thus produces an erasure symbol x when its input is zero and a symbol 0 or 1 when its input is positive or negative, respectively. It is important to note that in Fig. 5.4 the path passing through the block T is exactly the single-path detector discussed in Section 3.4. The upper branch is intended to improve the performance by exploiting the non-continual nature of the noise n(t) as already explained in Section 5.1.

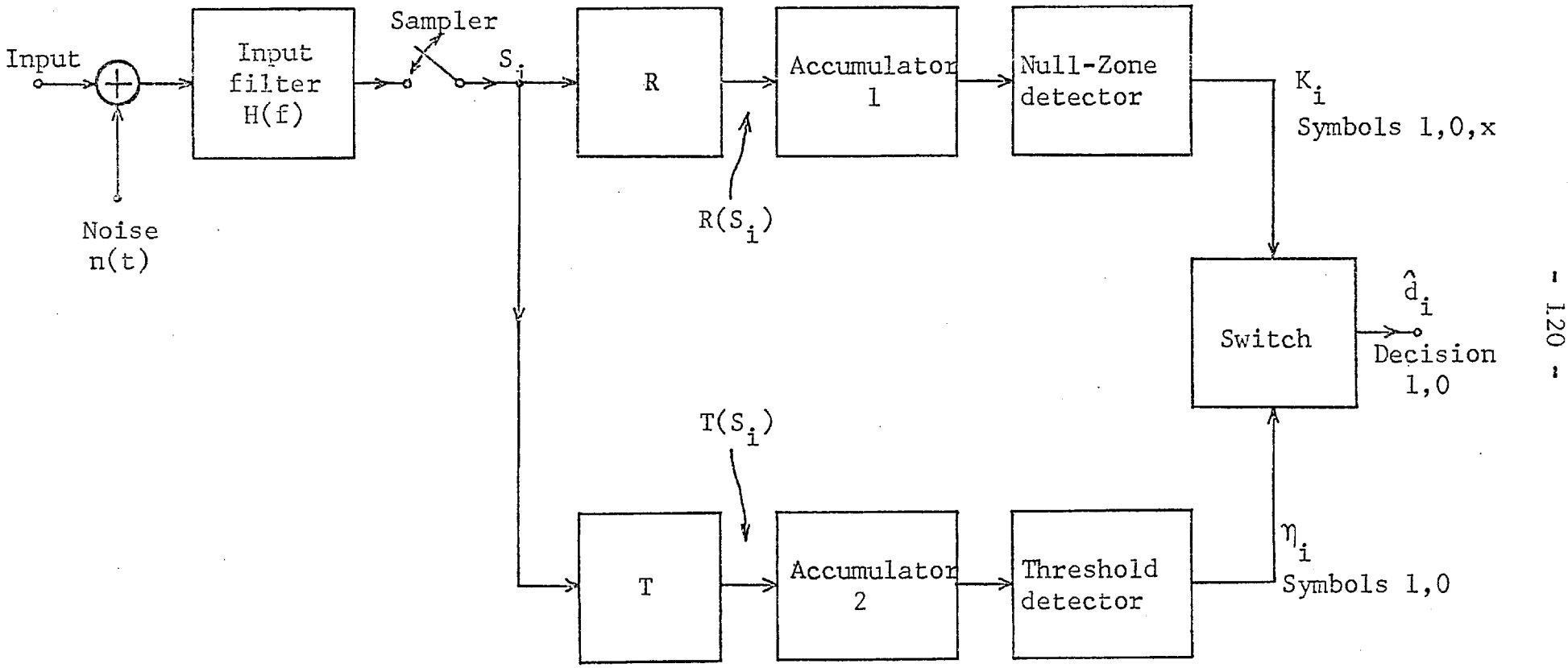

Fig. 5.4: Simplified version of the receiver.

Now let $P_{e\ell}$ be defined as the probability of error at the output of the lower branch of the receiver and P_{ez} as the probability of error at the same point when the noise at the output of the sampler in Fig. 5.4 is replaced by a continual noise of PDF $p_z(x)$. Hence

$$P_{e\ell} = P[\eta_i = 1 \mid d_i = 0] \tag{57}$$

and P_{ez} is the value taken by $P_{e\ell}$ when $p = 1$. The numerical results presented in Section 5.3 support the following important relations

$$P_{ex} \simeq P_{ez} \tag{58}$$

$$P_x P_{ex} < P_{e\ell} < P_{ex} \tag{59}$$

Relation (58) means that, in most cases where the upper branch fails to reach a decision, all the M samples are affected by impulse noise, assuming of course that the noise detector is performing sufficiently well. The same numerical results referred to above show that for low SINR's the two terms in Equation (51) are such that

$$P_{eu} \ll P_x P_{ex} \tag{60}$$

This relation, together with (58), suggests a means of making the receiver adaptive in cases in which p changes with time. In these cases the parameters ε_1 and ε_2 would be chosen so as to minimize the erasure probability P_x which can be estimated during the actual operation of the receiver. This question will be considered again in Section 5.3. It can be further concluded that the performance of the whole receiver depends mainly on the performance of the noise detector through the value of P_x and on the design of the block T in Fig. 5.4 through the value of $P_{ex} \simeq P_{ez}$.

The expressions for calculating the probabilities defined by Equations (52) to (54) will now be derived. Let (see equation (45))

$$P_+ = P\left[g_i > 0 \mid \phi_i = +1\right] \tag{61}$$

$$P_- = P\left[g_i < 0 \mid \phi_i = +1\right] \tag{62}$$

and

$$P_o = P\left[g_i = 0 \mid \phi_i = +1\right] \tag{63}$$

According to Equation (45), if $g_i = 0$, then either $\hat{\theta}_i = 1$ or $S_i = 0$, the latter event having a zero probability. If the definitions of the probabilities in Equations (30) and (36) are taken into account then it follows that

$$\begin{aligned} P_o &= P\left[\hat{\theta}_i = 1\right] \\ &= q\alpha + p(1-\beta) \end{aligned} \tag{64}$$

$$\begin{aligned} P_+ &= P\left[\hat{\theta}_i = 0,\ S_i > 0 \mid \phi_i = +1\right] \\ &= q\alpha_+ + p\beta_+ \end{aligned} \tag{65}$$

and

$$\begin{aligned} P_- &= P\left[\hat{\theta}_i = 0,\ S_i < 0 \mid \phi_i = +1\right] \\ &= 1 - P_o - P_+ \\ &= q\alpha_- + p\beta_- \end{aligned} \tag{66}$$

If now, in the expansion*

$$(P_- + P_o + P_+)^M = \sum_{i=1}^{L} N_i \, P_-^{\ell_i} \, P_o^{m_i} \, P_+^{n_i} \tag{67}$$

the terms in which $\ell_i > n_i$ are selected P_{eu} is obtained and if the terms in which $\ell_i = n_i$ are selected P_x is obtained. Thus:

$$P_{eu} = \sum_{i=1}^{F} F_i \, P_-^{a_i} \, P_o^{b_i} \, P_+^{c_i}, \qquad a_i > c_i \tag{68}$$

and

$$P_x = \sum_{i=1}^{G} G_i \, P_-^{d_i} \, P_o^{e_i} \, P_+^{f_i}, \qquad d_i = f_i \tag{69}$$

An algorithm for computing P_{eu} and P_x is presented in Appendix 2.1. If $\alpha \ll 1$ and $p\beta \ll q$ then, as shown in the same appendix

---

* If for $i \neq K$ either $\ell_i \neq \ell_K$ or $m_i \neq m_K$ or both, it can be shown that $L = \frac{1}{2}(M+1)^K(M+2)$. Obviously $\ell_i + m_i + n_i = M$ for any i.

the product $P_x P_{ex}$ is given with good approximation by

$$P_x P_{ex} \simeq \sum_{i=1}^{G} G_i \, P_-^{d_i} \, P_o^{e_i} \, P_+^{f_i} \, E_{e_i}(e_i A) \qquad (70)$$

where $E_n(x)$ is the exceedence probability function (EPF) of the sum of n independent random variables each one of these being the response of the block T in Fig. 5.4 to a noise sample z_j with PDF $p_z(x)$. Since the derivation of the relations (68) to (70) is based on a trinomial probability distribution [see Equation (67)] it follows that they are only valid when the signal samples corrupted by impulsive noise are distributed in time in a purely random way.

The numerical examples studied in Section 5.3 show that if $\sigma_z \gg A$ the values of ε_1 and ε_2 that minimize the error probability P_e are very close to each other. Therefore, it is important from a practical point of view to consider the sub-optimum receiver where

$$\varepsilon_1 = \varepsilon_2 = \varepsilon_0$$

and ε_0 is chosen so as to minimize the error probability P_e. Even in this simpler case it has not been found possible to obtain an expression for the optimum value ε_0 owing to analytical difficulties. In the next section the optimization of the receiver is carried out with the help of computational techniques.

If it is assumed that the SINR μ is very small, the order of magnitude of the optimum value of ε_0 can easily be obtained. In fact, from Equations (40) and (41) it follows that

$$\lim_{K_z \to \infty} \beta_+ = \lim_{K_z \to \infty} \beta_- = 0$$

and thus, according to Equations (64) to (66),

$$\lim_{\mu \to 0} P_+ = q\alpha_+$$

$$\lim_{\mu \to 0} P_- = q\alpha_-$$

$$\lim_{\mu \to 0} P_0 = p + q\alpha$$

If $\varepsilon_1 = \varepsilon_2 = \varepsilon_0$ in Equation (34) and it is assumed that $\varepsilon_0 \ll 2A$ then it can readily be shown that

$$\alpha_- \simeq \frac{\varepsilon_0}{\sigma_w}\sqrt{\frac{2}{\pi}}\exp(-2\frac{A^2}{\sigma_w^2}) \tag{71}$$

Relation (35) can now be written as

$$\alpha \simeq \operatorname{erfc}(\frac{\varepsilon_0}{\sigma_w\sqrt{2}}) \tag{72}$$

If the SGNR ρ is high enough (say, $\rho_{dB} > 12$ dB) relation (71) shows that α_- will have a negligible value and thus all terms in Equation (69) will be negligible except that for which $d_i = f_i = 0$. Moreover, since $a_i \geq 1$, all terms in Equation (68) are very small. According to relation (58)

$$\lim_{\mu \to 0} P_{ex} \simeq \lim_{\mu \to 0} P_{ez} = \tfrac{1}{2}$$

It thus follows that

$$\lim_{\mu \to 0} P_e \simeq \tfrac{1}{2} \lim_{\mu \to 0} P_x$$

$$\simeq \tfrac{1}{2} \lim_{\mu \to 0} P_o^M = \tfrac{1}{2}(p + q\alpha)^M$$

For small α

$$\lim_{\mu \to 0} P_e \simeq \tfrac{1}{2} p^M(1 + M\frac{q\alpha}{p})$$

and thus, if $M\alpha \ll p$, the performance is close to the best that can be expected. More specifically, if

$$M \operatorname{erfc}(\frac{\varepsilon_0}{\sigma_w\sqrt{2}}) = \frac{p}{10} \tag{73}$$

then P_e can be written as

$$P_e \simeq \tfrac{1}{2} p^M \tag{74}$$

Another important limiting case is that in which the Gaussian-noise variance σ_w^2 is negligible. From Equations (33) and (34) it follows that

$$\lim_{\sigma_w \to 0} \alpha_+ = 1 \quad \text{and} \quad \lim_{\sigma_w \to 0} \alpha_- = 0.$$

Therefore, according to Equations (40), (41), (65) and (66),

$$\lim_{\rho \to \infty} P_+ = 1 - 2p\,Q_z\left(\frac{\varepsilon_0}{K_z}\right) \tag{75}$$

$$\lim_{\rho \to \infty} P_- = p\,Q_z\left(\frac{2A-\varepsilon_0}{K_z}\right) - p\,Q_z\left(\frac{2A+\varepsilon_0}{K_z}\right) \tag{76}$$

Let μ_o and μ_1 be defined as the values of the SINR for which

$$\left[\frac{d}{d\varepsilon_0} P_x\right]_{\varepsilon_0=0} \geqslant 0 \quad \text{if} \quad \mu \leqslant \mu_0 = \frac{A_o}{K_z}$$

and

$$\left[\frac{d}{d\varepsilon_0} P_e\right]_{\varepsilon_0=0} \geqslant 0 \quad \text{if} \quad \mu \leqslant \mu_1 = \frac{A_1}{K_z}$$

the values of P_x and P_e being those obtained for $\sigma_w = 0$. Thus it can be stated that P_x (or P_e) attains a minimum value at $\varepsilon_0 = +0$ provided that $\mu \leqslant \mu_0$ (or $\mu \leqslant \mu_1$). For higher SINR's this minimum value will be attained at some $\varepsilon_0 > 0$. In Appendix 2.2 it is shown that

$$p = \frac{X_{1j}}{X_{1j} - jY + MX_{0j}\,\varphi(\mu_j)}, \qquad j = 0, 1. \tag{77}$$

where

$$\varphi(\mu) = 1 + \frac{P_z(0)}{P_z(2A)}$$

$$Y = \sum_{i=1}^{F} \xi(a_i - 1).F_i$$

$$X_{Kj} = \sum_{i=1}^{G} \xi(d_i - K).G_i.\left[\xi(j) + jE_{e_i}(e_i.A_j)\right]$$

$$\xi(n) = \begin{cases} 1 & \text{if } n = 0 \\ 0 & \text{if } n \neq 0 \end{cases}$$

the notation of Equations (68) to (70) being assumed. The above relations are sufficient to enable the functions

$\mu_o = f_o(p)$ and $\mu_1 = f_1(p)$ to be plotted for any value of $M > 1$. These functions are plotted in Figs. 5.5 and 5.6 for $M = 2$ and $M = 3$ and for the following forms of $p_z(x)$:

(a) Case Study 1 - Gaussian PDF:

$$p_z(x) = \frac{1}{\sigma_z\sqrt{2\pi}} \exp(-\frac{x^2}{2\sigma_z^2}) \tag{78}$$

(b) Case Study 2 - Cauchy PDF:

$$p_z(x) = \frac{\beta}{\pi} \frac{1}{\beta^2 + x^2} \tag{79}$$

The dispersion parameter K_z has been given the values α_z and β, respectively. The computations have shown that the values of μ_o and μ_1 for $M > 3$ are greater than those given by the graphs in Figs. 5.5 and 5.6 for the same value of p.

By using Equations (75) and (76) it can be concluded that for $\sigma_w = 0$ and $\varepsilon_0 = +0$

$$P_+ = q, \qquad P_- = 0 \tag{80}$$

and thus $P_0 = 1 - P_+ - P_- = p$. Equations (68) and (69) will thus give

$$P_{eu} = 0, \text{ and } P_x = p^M. \tag{81}$$

The previous value of P_x shows that the upper branch of the detector only fails to reach a decision when all the M received samples are affected by impulsive noise. Therefore, in this case

$$P_{ex} = P_{ez} \tag{82}$$

It should be noted that if $\mu \longrightarrow 0$ then relation (74) becomes an exact equality.

The previous results can be summarized by saying that if $\sigma_w = 0$ and $\varepsilon_0 = +0$ then $\alpha = \beta = 0$ and thus the noise detector performs ideally. When Gaussian noise is present the noise

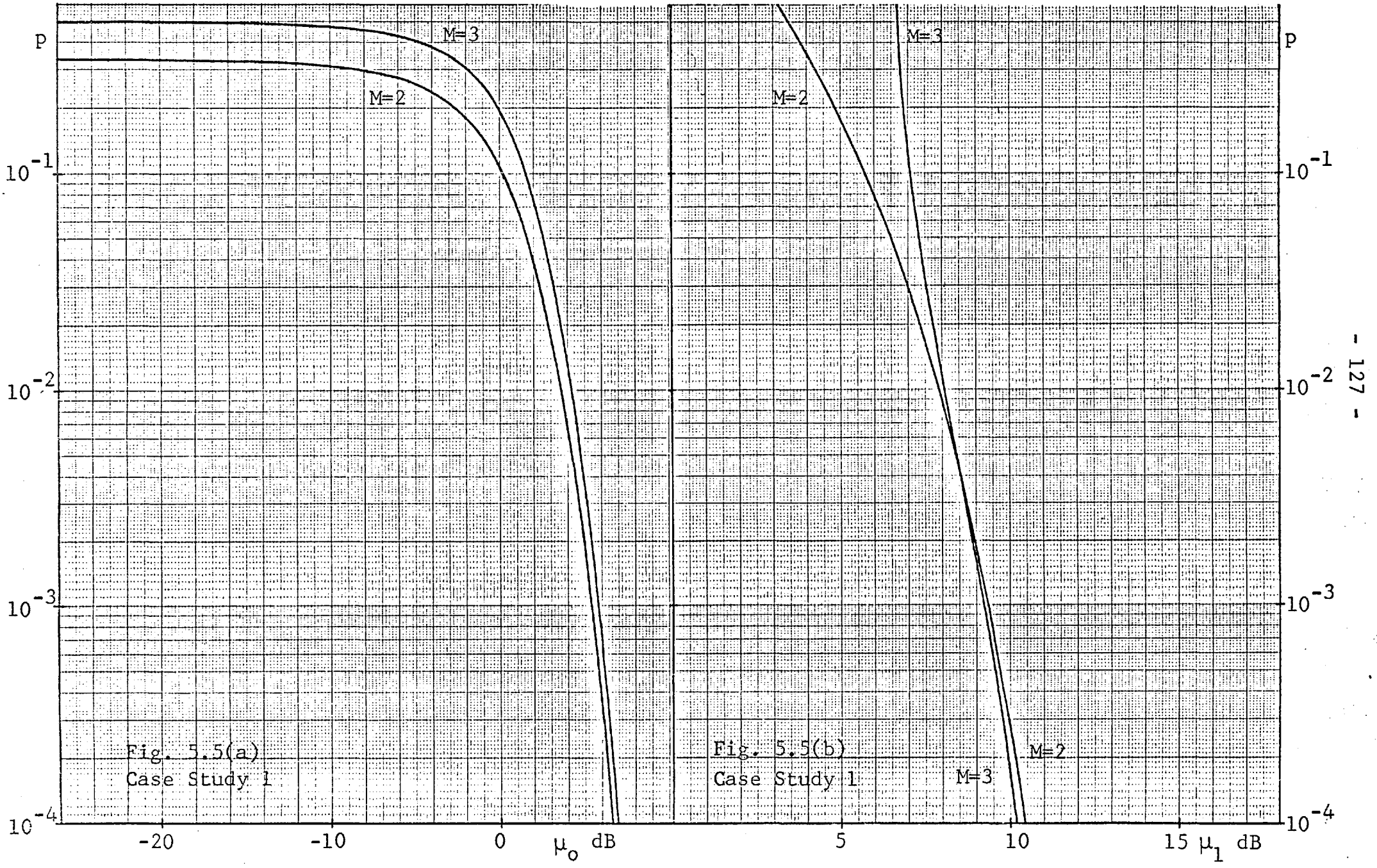
p
M=3
M=2
10^{-1}
10^{-2}
10^{-3}
10^{-4}
-20
-10
0
μ_o dB
Fig. 5.5(a)
Case Study 1
p
M=3
M=2
5
10
15 μ_1 dB
Fig. 5.5(b)
Case Study 1
M=2
M=3

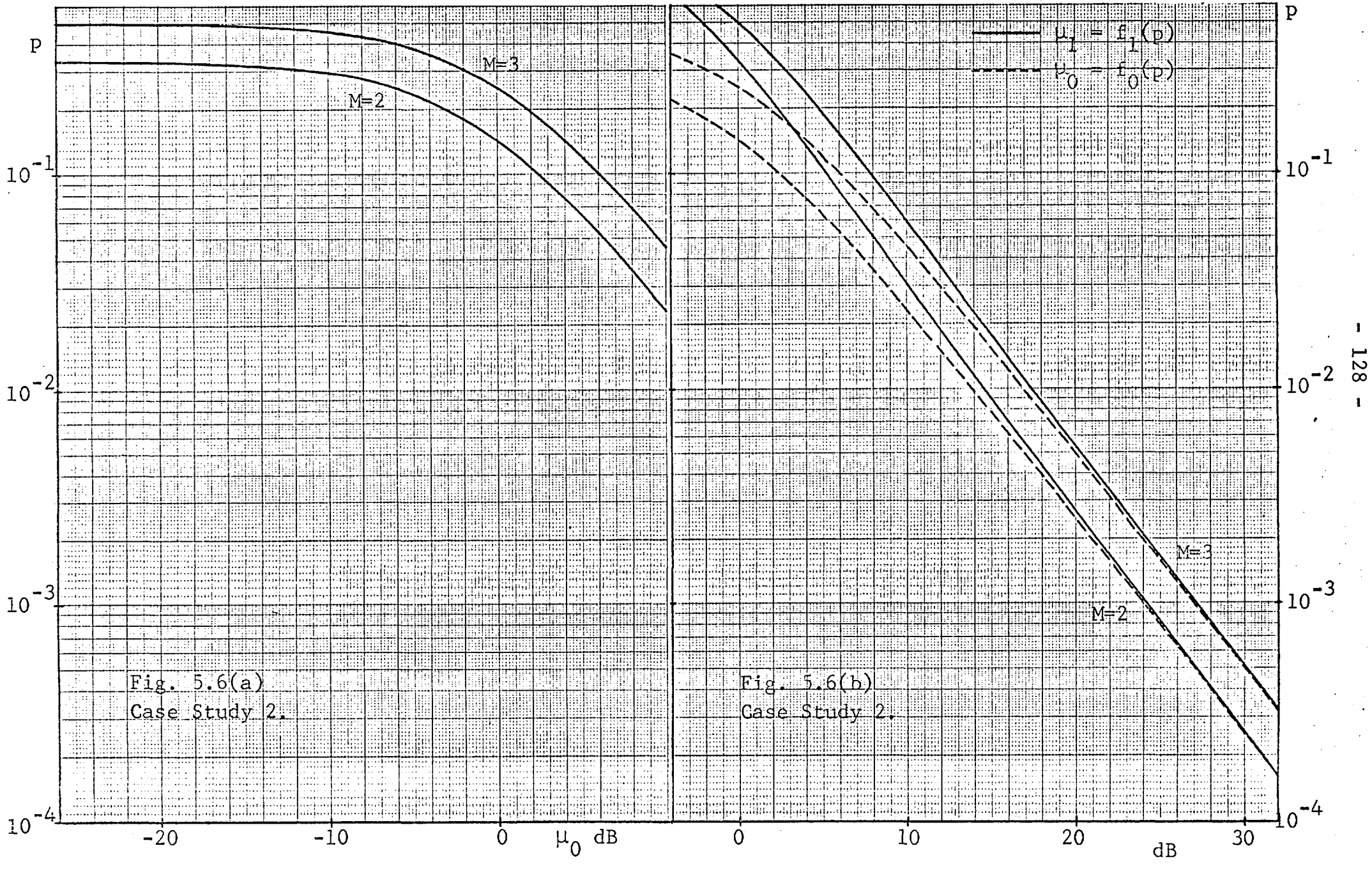

Fig. 5.6(a)
Case Study 2.

Fig. 5.6(b)
Case Study 2.

detector should be designed so as to obtain* (if possible)

$$P[\theta_i = 0, \quad \hat{\theta}_i = 1] = q\alpha \ll 1 \tag{83}$$

and

$$P[\theta_i = 1, \quad \hat{\theta}_i = 0] = p\beta \ll 1. \tag{84}$$

These conditions mean that the upper branch of the detector will accept most samples corrupted by Gaussian noise alone and virtually none of those corrupted by impulsive noise. It thus follows from these conditions that

$$P_e \simeq P_x . P_{ez}, \tag{85}$$

where

$$P_x \simeq p^M. \tag{86}$$

If the SINR μ is low enough, conditions (83) and (84) can be satisfied with the noise detector described in Section 5.2.2. If this is not the case, an attempt should be made to develop more efficient noise detectors as suggested at the end of Section 5.1. In any case

$$P_e \gtrsim p^M . P_{ez} = P_{LB}, \tag{87}$$

where the value P_{LB} corresponds to ideal performance of the noise detector ($\alpha = \beta = 0$).**

5.3 DISCUSSION OF NUMERICAL RESULTS

In this section the analysis will be continued for the two cases referred to in Section 5.2, namely:

(a) Case Study 1

In this case the noise samples affected by impulsive noise are assumed to follow the Gaussian PDF of Equation (78). With $K_z = \sigma_z$ in Equation (39) it follows that

$$Q_z(y) = \tfrac{1}{2}\, \mathrm{erfc}\left(\frac{y}{\sqrt{2}}\right) \tag{88}$$

---

* Note that if, by varying ε_o, the probability α decreases then β increases and vice versa.

** If $\mu_{dB} \gg 0$ dB the error probability P_e can be slightly lower than P_{LB} as the numerical results in the next section show.

(b) Case Study 2

In this case the noise samples affected by impulsive noise obey the Cauchy PDF of Equation (79). With K_z defined as the median of the random variable $|z|$ then

$$K_z = \beta \tag{89}$$

and Equation (39) gives

$$Q_z(y) = \frac{1}{2} - \frac{1}{\pi} \operatorname{tg}^{-1} y. \tag{90}$$

Case 1 is presumed to be a favourable one due to the fast variation of $p_z(x)$ for high x. On the other hand, since the Cauchy distribution has an infinite variance, Case 2 must be a rather unfavourable one.

In both cases the block T in the diagram of Fig. 5.4 has been assumed linear, i.e.

$$T(x) = x. \tag{91}$$

In Case 1 this would be the optimum shape for T(x), if the presence of impulsive noise could be detected with no error, and is obviously nearly optimum if conditions (83) and (84) are satisfied. In fact, under these conditions the noise detecting operation is nearly ideal and therefore the lower branch of the receiver processes a stream of samples corrupted by an almost continual noise with PDF $p_z(x)$. As shown in Section 3.4, the optimization of the block T of the receiver thus leads in Case 2 to the following nonlinear transfer function*:

$$T(x) = \log \frac{p_z(x - A)}{p_z(x + A)} = \log \frac{\beta^2 + (x + A)^2}{\beta^2 + (x - A)^2} \tag{92}$$

---

* See Section 3.4, Equation (9).

Since the determination of the noise PDF at the output of such nonlinear device is too difficult a task to be done analytically, only the linear transfer function is considered in this chapter. The performance that can be obtained by using a nonlinear block T will be estimated in Chapter VI with the help of Monte Carlo techniques.

The fact that both the Gaussian and the Cauchy distributions are stable* makes it very easy to find the expressions of the EPF $E_n(y)$ involved in relation (70), in the case where $T(x) = x$. These expressions give:

Case Study 1:

$$E_n(nA) = \tfrac{1}{2}\,\mathrm{erfc}\left(\frac{A}{\sigma_z}\sqrt{\frac{n}{2}}\right) = Q_z(\mu\sqrt{n}), \qquad \mu = \frac{A}{\sigma_z}. \tag{93}$$

Case Study 2:

$$E_n(nA) = \frac{1}{2} - \frac{1}{\pi}\,\mathrm{tg}^{-1}\frac{A}{\beta} = Q_z(\mu), \qquad \mu = \frac{A}{\beta}. \tag{94}$$

As can be seen, in Case 2 $E_n(nA)$ turns out to be independent of n.

In the graphs presented in Chapter IV the SINR was defined as ratio of r.m.s. values, i.e.

$$\psi_{dB} = 20\,\log_{10}\frac{A}{\sigma_z\sqrt{p}} = \mu_{dB} - 10\,\log_{10}p. \tag{95}$$

It was shown in that chapter that the smear-desmear technique gives a significant improvement only if

$$\psi_{dB} \gg -10\,\log_{10}p, \tag{96}$$

that is, if

$$\mu = \frac{A}{\sigma_z} \gg 1. \tag{97}$$

---

* For the definition of stable distribution, see Ref. [5-2].

In this chapter interest is centred only on the low SINR cases, that is to say, those cases where

$$\mu_{dB} \ll 0 \text{ dB} \tag{98}$$

while still maintaining a SGNR $\rho_{dB} > 12$ dB, so as to have the impulsive noise as the only important cause of errors.

Consider now the analysis of the graphs presented below paying particular attention to the differences and similarities between the two cases being studied. These graphs can be grouped into several classes which may be described as follows.

A) Graphs giving the values (in dB) of the ratios $\delta_1 = \varepsilon_1/\sigma_w$ and $\delta_2 = \varepsilon_2/\sigma_w$ that minimize the error probability, P_e, versus $\zeta_{dB} = \rho_{dB} - \mu_{dB}$, for several values of ρ_{dB}.

These graphs are shown in Figs. 5.7 and 5.8 for Case 1 and in Figs. 5.9 and 5.10 for Case 2. It should be recalled here that the abcissa of these graphs is the impulsive-to-Gaussian noise ratio (IGNR) defined by Equation (44). As in all the other graphs presented below, the following high value of p has been assumed:

$$v_1 = -\log p = \tfrac{1}{8},$$

that is,

$$p = 0.118.$$

It can be concluded that, in the low SINR cases defined by relation (98), the parameters ε_1 and ε_2 differ very little from each other and can thus be set to a common value ε_0 without significantly affecting the receiver performance.

B) Graphs giving the value of the minimum error probability corresponding to the ratios $\delta_1 = \varepsilon_1/\sigma_w$ and $\delta_2 = \varepsilon_2/\sigma_w$ given by the graphs of class (A).

These graphs are shown in Fig. 5.11. They show that

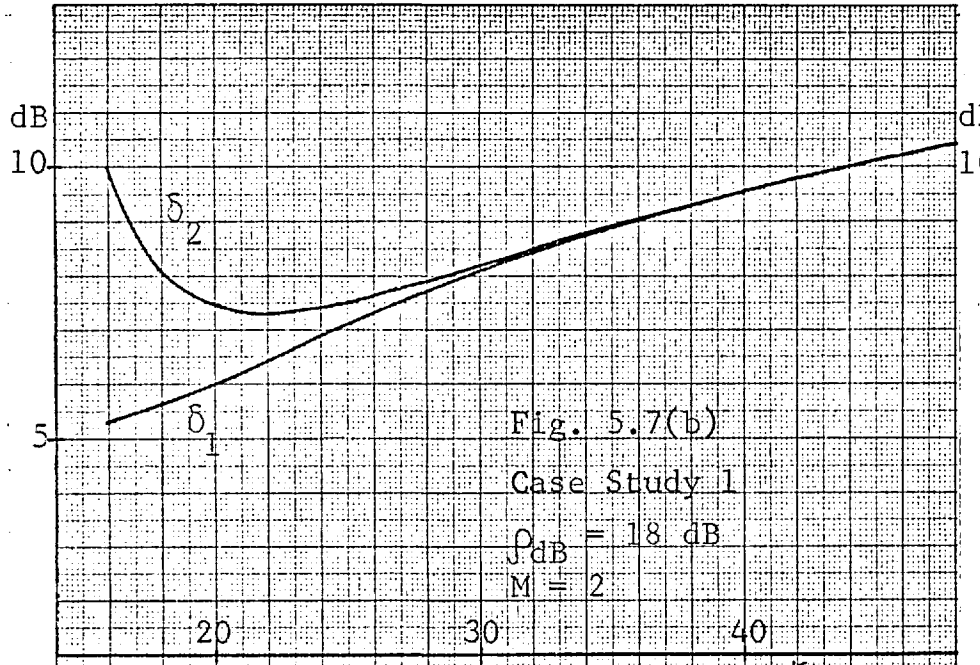

Fig. 5.7(b)
Case Study 1
ρ_{dB} = 18 dB
M = 2

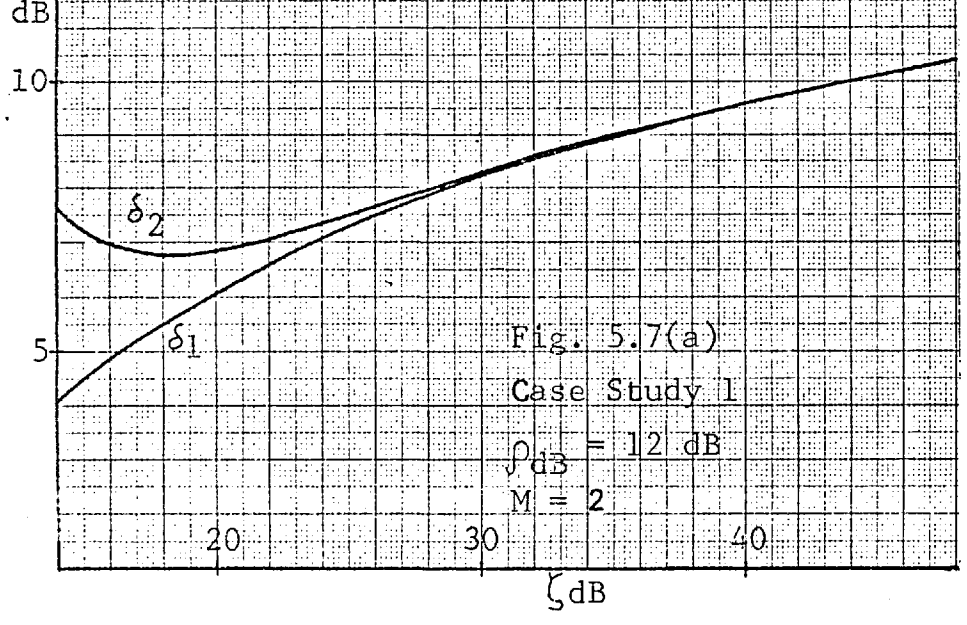

Fig. 5.7(a)
Case Study 1
ρ_{dB} = 12 dB
M = 2

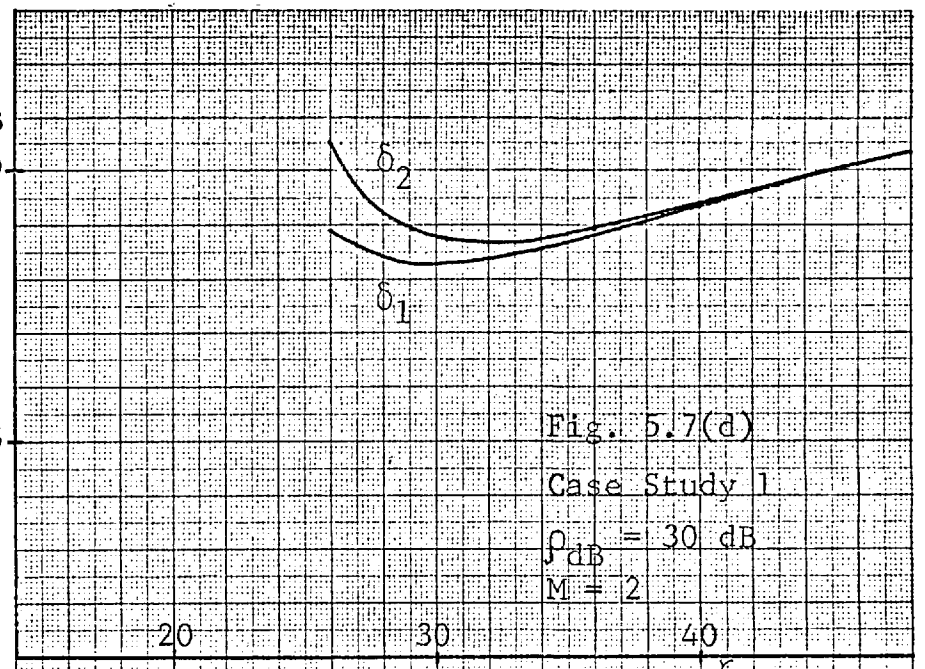

Fig. 5.7(d)
Case Study 1
ρ_{dB} = 30 dB
M = 2

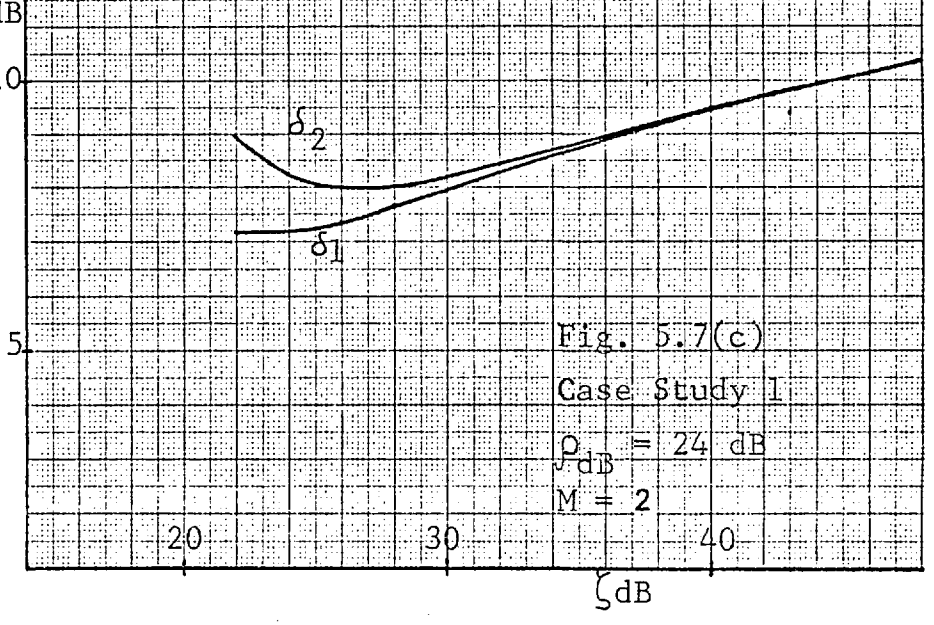

Fig. 5.7(c)
Case Study 1
ρ_{dB} = 24 dB
M = 2

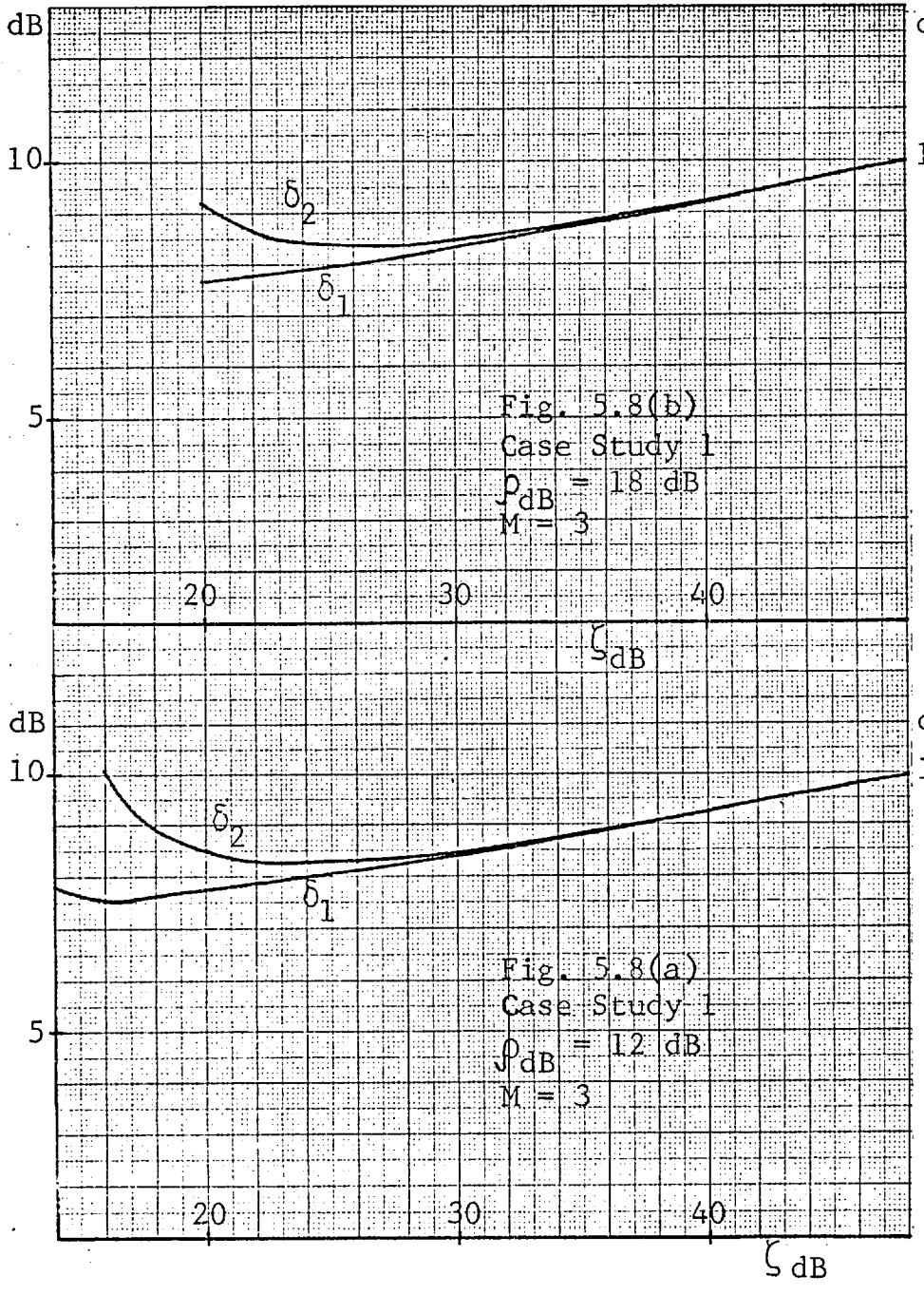

Fig. 5.8(b)
Case Study 1
ρ_{dB} = 18 dB
M = 3

Fig. 5.8(a)
Case Study 1
ρ_{dB} = 12 dB
M = 3

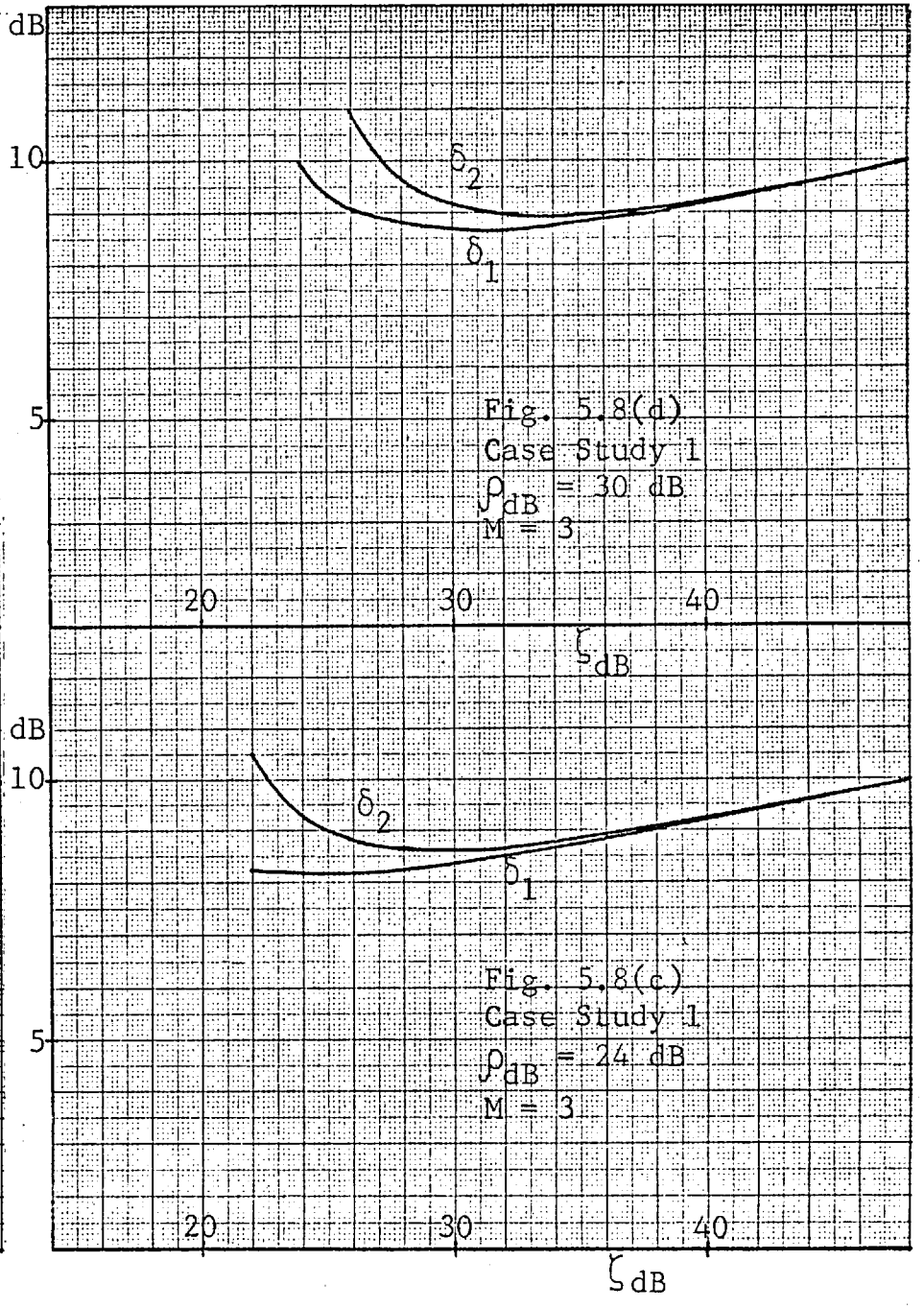

Fig. 5.8(d)
Case Study 1
ρ_{dB} = 30 dB
M = 3

Fig. 5.8(c)
Case Study 1
ρ_{dB} = 24 dB
M = 3

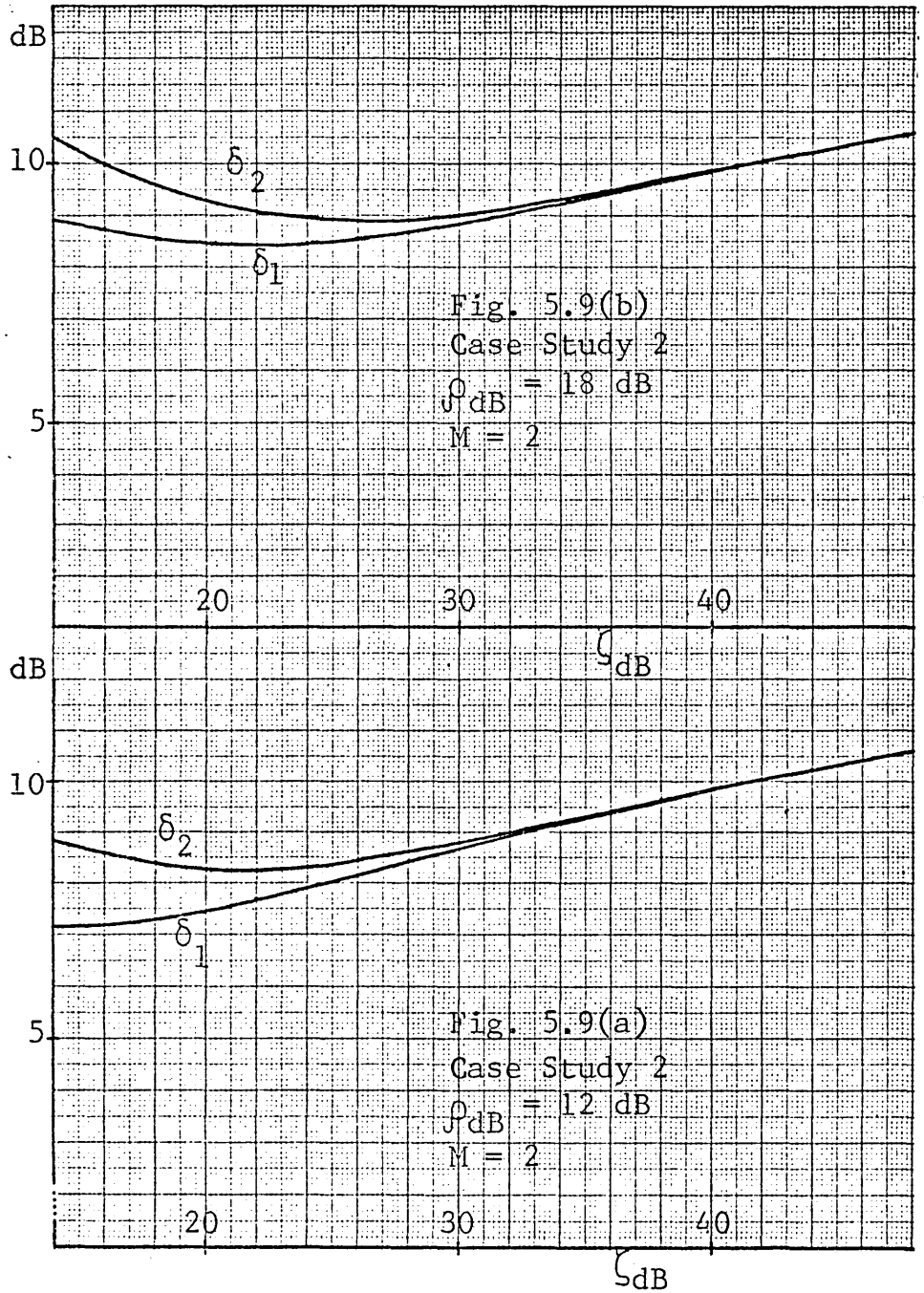

Fig. 5.9(b)
Case Study 2
ρ_{dB} = 18 dB
M = 2

Fig. 5.9(a)
Case Study 2
ρ_{dB} = 12 dB
M = 2

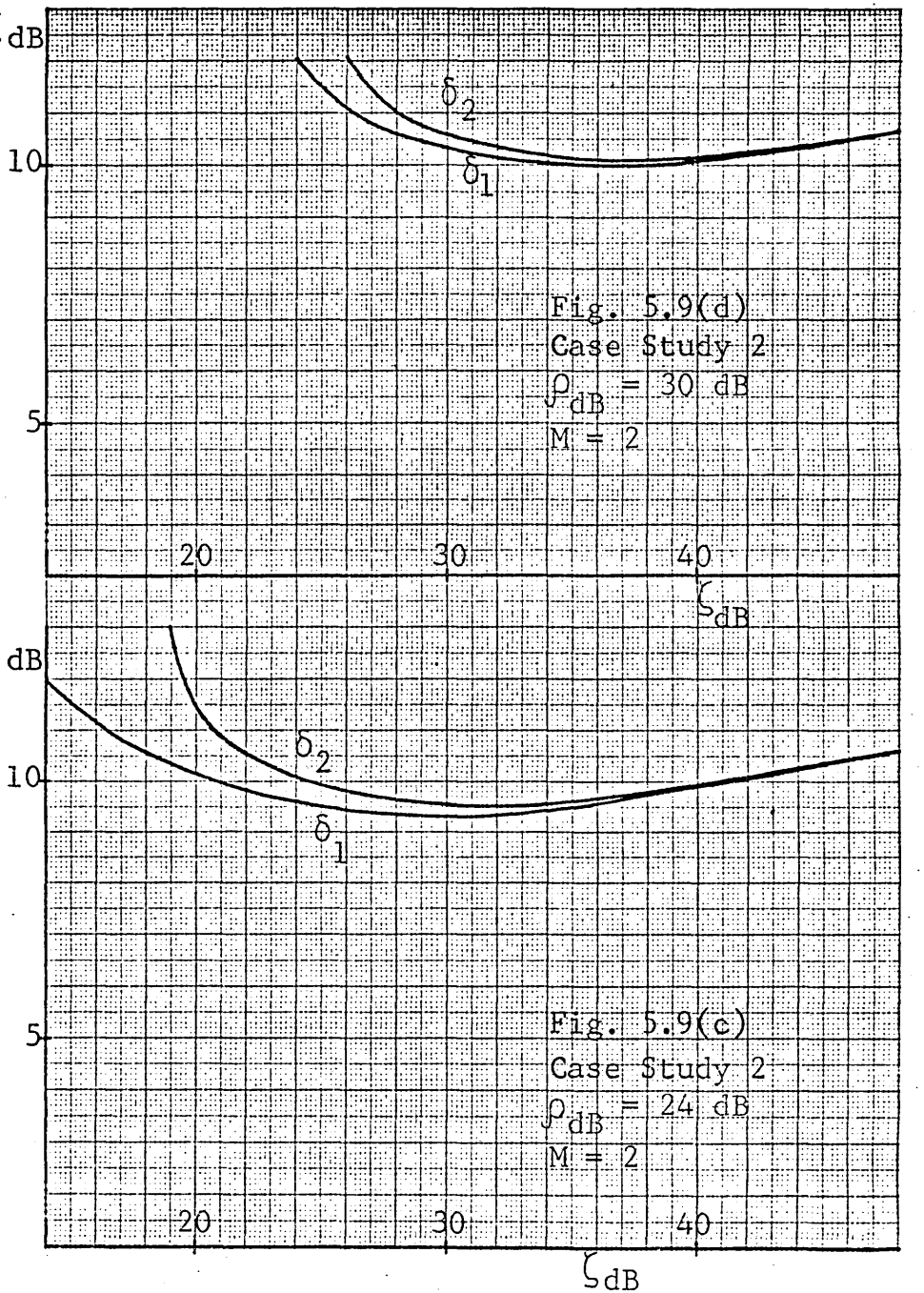

Fig. 5.9(d)
Case Study 2
ρ_{dB} = 30 dB
M = 2

Fig. 5.9(c)
Case Study 2
ρ_{dB} = 24 dB
M = 2

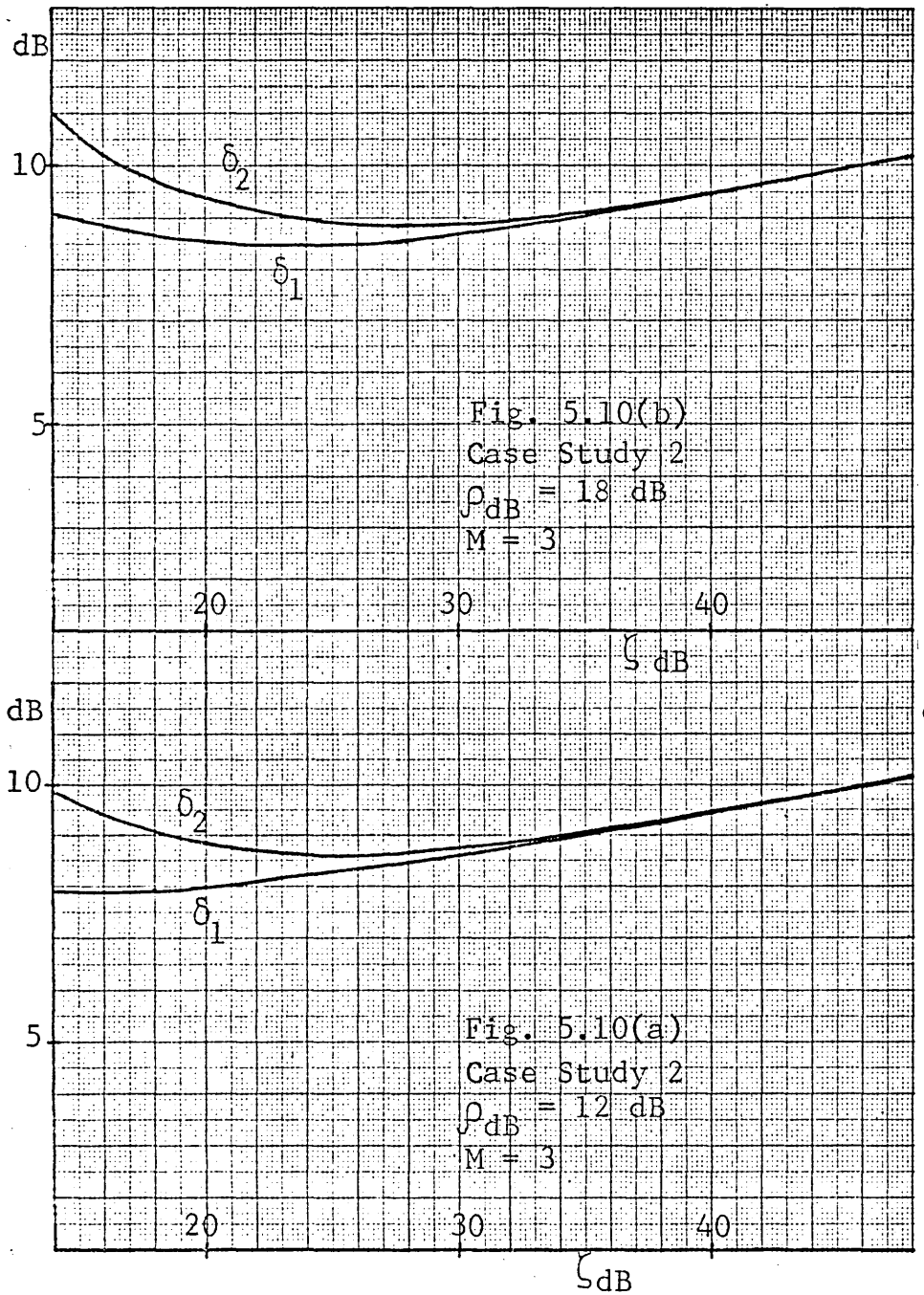

Fig. 5.10(b)
Case Study 2
ρ_{dB} = 18 dB
M = 3

Fig. 5.10(a)
Case Study 2
ρ_{dB} = 12 dB
M = 3

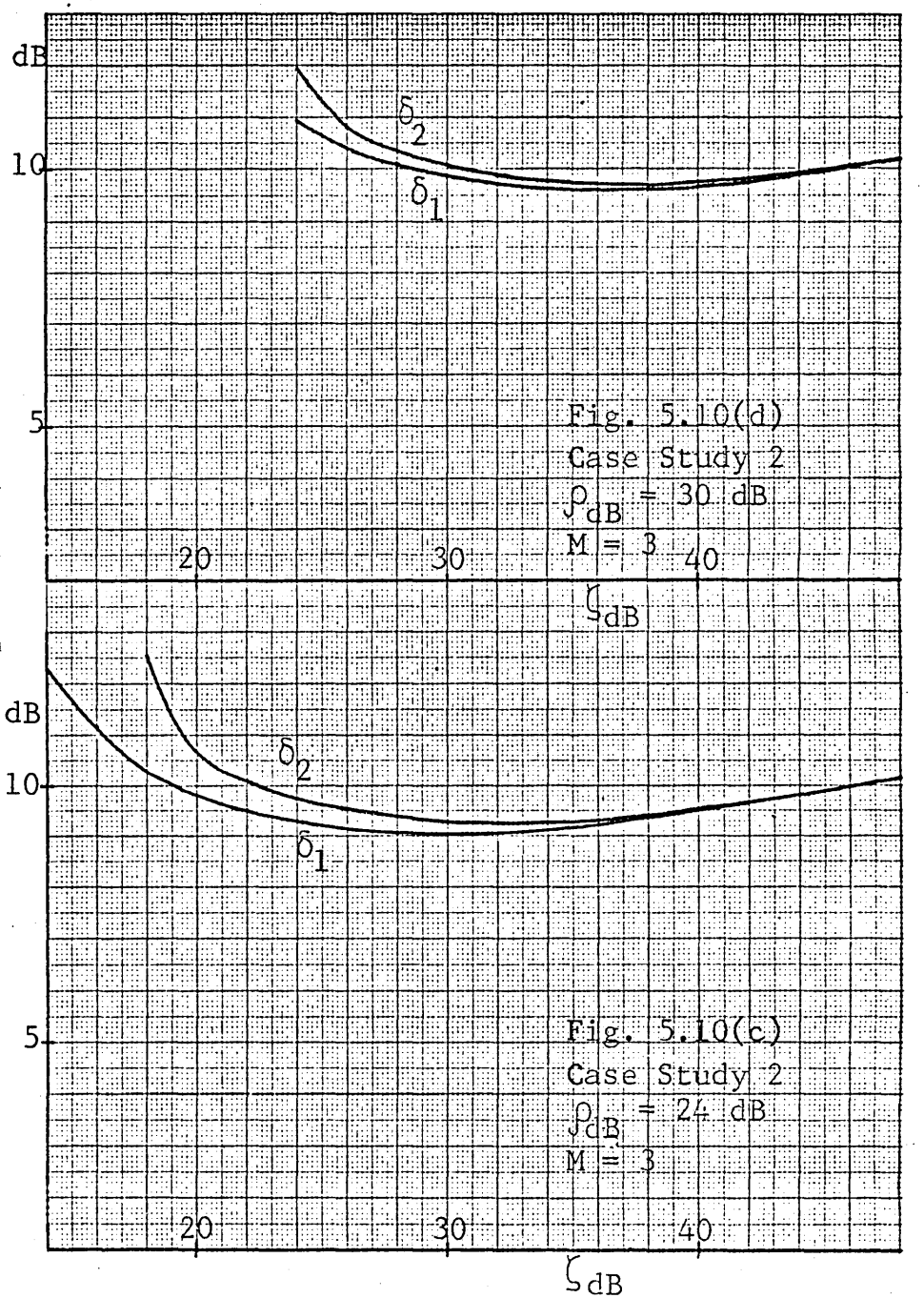

Fig. 5.10(d)
Case Study 2
ρ_{dB} = 30 dB
M = 3

Fig. 5.10(c)
Case Study 2
ρ_{dB} = 24 dB
M = 3

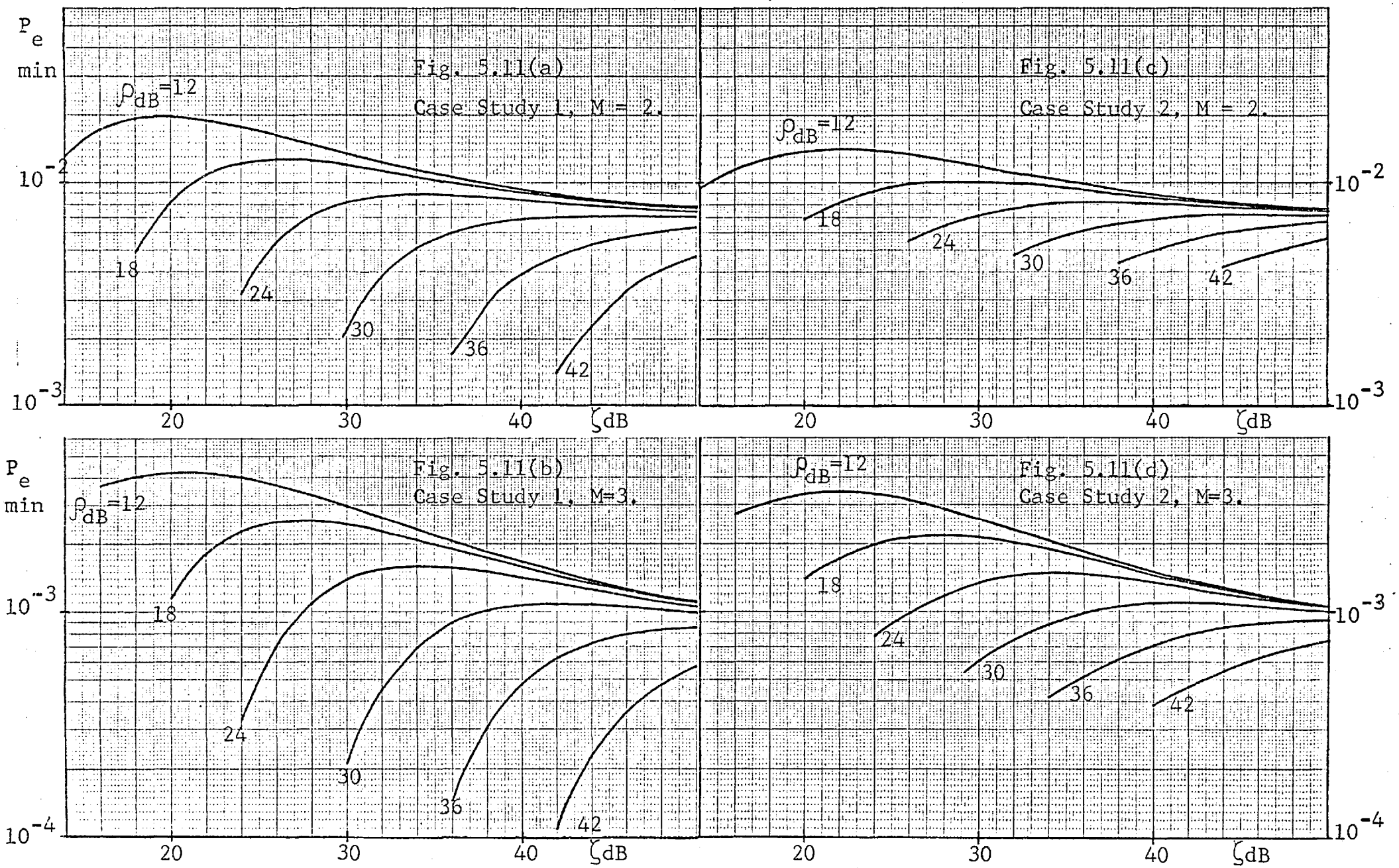
Fig. 5.11(a)
Case Study 1, M = 2.
Fig. 5.11(c)
Case Study 2, M = 2.
Fig. 5.11(b)
Case Study 1, M=3.
Fig. 5.11(d)
Case Study 2, M=3.
P_e min
ρ_{dB}=12
18
24
30
36
42
10^{-2}
10^{-3}
10^{-4}
20
30
40
ζ_{dB}

for high values of the IGNR ζ very little can be gained by increasing the SGNR ρ.

C) Graphs giving the value of the erasure probability, P_x, under the conditions of the previous graphs.

These graphs are shown in Fig. 5.12 and are quite similar in shape to those of the minimum error probability.

D) Graphs giving the parameters [see Equation (18)]:

$$\gamma_1 = \frac{p}{q}\Lambda(A - \varepsilon_1) \tag{99}$$

and

$$\gamma_2 = \frac{p}{q}\Lambda(A + \varepsilon_2) \tag{100}$$

calculated under the conditions of the above graphs.

These graphs are shown in Figs. 5.13 and 5.14 for Case 1 and in Figs. 5.15 and 5.16 for Case 2. They show that for $\mu_{dB} \ll 0$ dB the parameters γ_1 and γ_2 differ very little from each other. This means that for very low SINR μ the optimal receiver must indeed be preceded by a noise detector as shown in Fig. 5.1. In other words, the receiver structure of Fig. 5.1 is asymptotically optimal as the IGNR ζ tends to infinity.

All graphs in classes (A) to (D) were computed by using a minimization subroutine to minimize the function $P_e = f(\varepsilon_1, \varepsilon_2)$ defined by Equations (51), (68) and (70). In all graphs discussed below the parameters ε_1 and ε_2 are assumed to be set to a common value ε_0.

E) Graphs giving the value (in dB) of the ratio $\delta = \varepsilon_0/\sigma_w$ that minimize the error probability P_e, versus the IGNR ζ_{dB}, for several values of the SGNR ρ_{dB}.

These graphs are presented in Fig. 5.17 and show that if condition (98) is satisfied the optimum value of ε_o can be obtained with good approximation by using the curve corresponding to $\rho_{dB} = 12$ dB. If $p = 0.118$ then Equation (73) gives the following values of δ_{dB}:

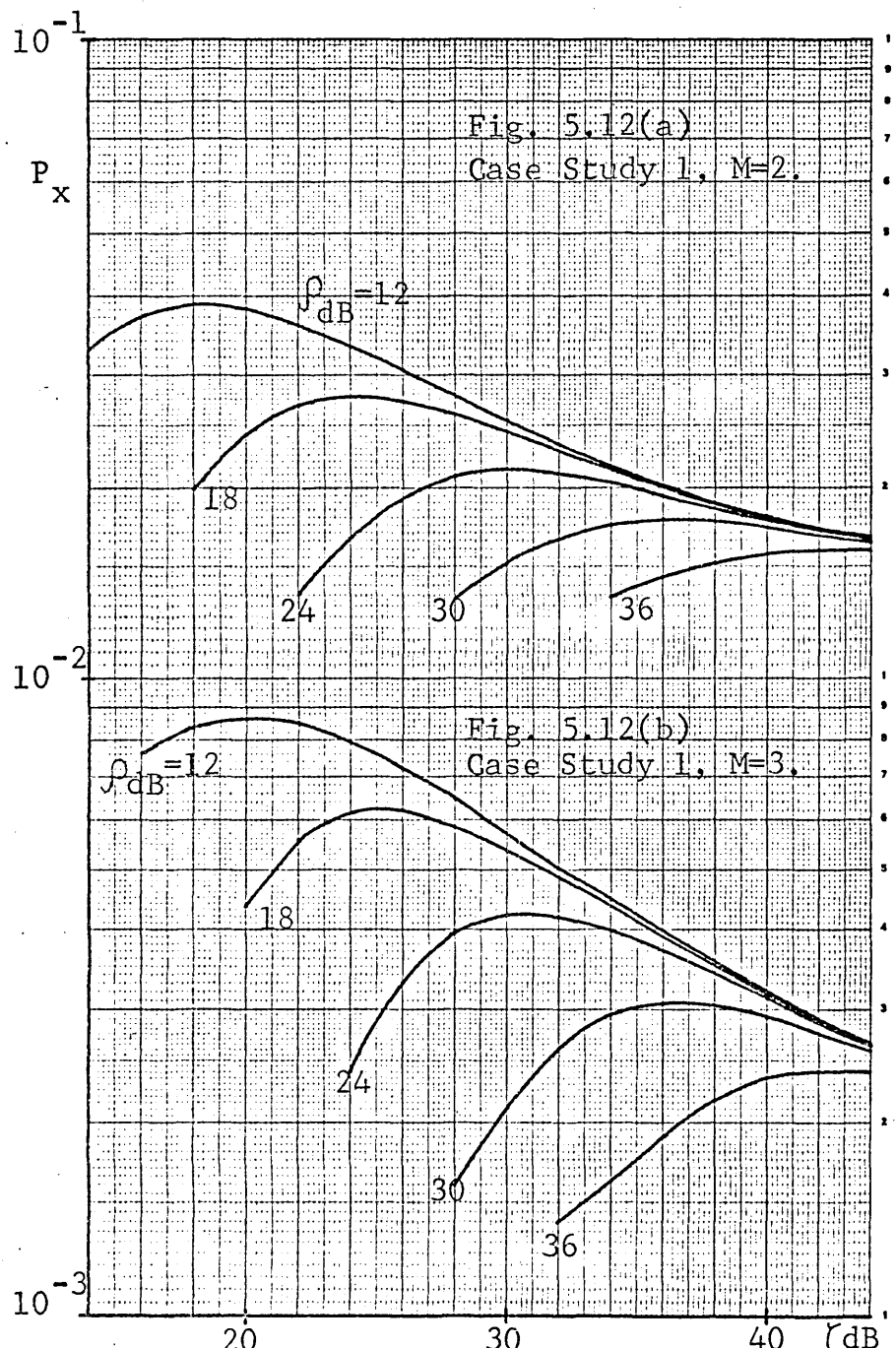

Fig. 5.12(a)
Case Study 1, M=2.

Fig. 5.12(b)
Case Study 1, M=3.

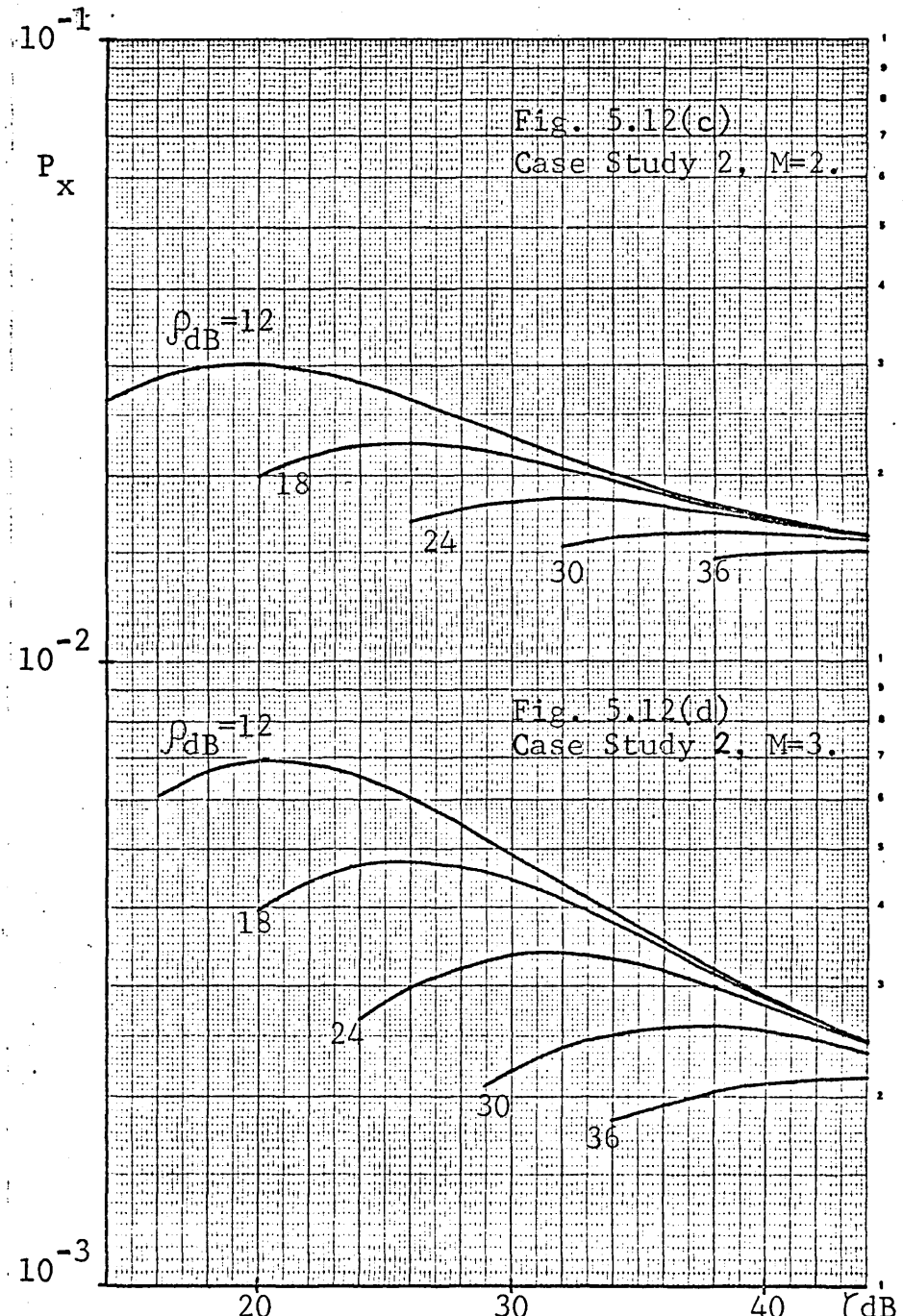

Fig. 5.12(c)
Case Study 2, M=2.

Fig. 5.12(d)
Case Study 2, M=3.

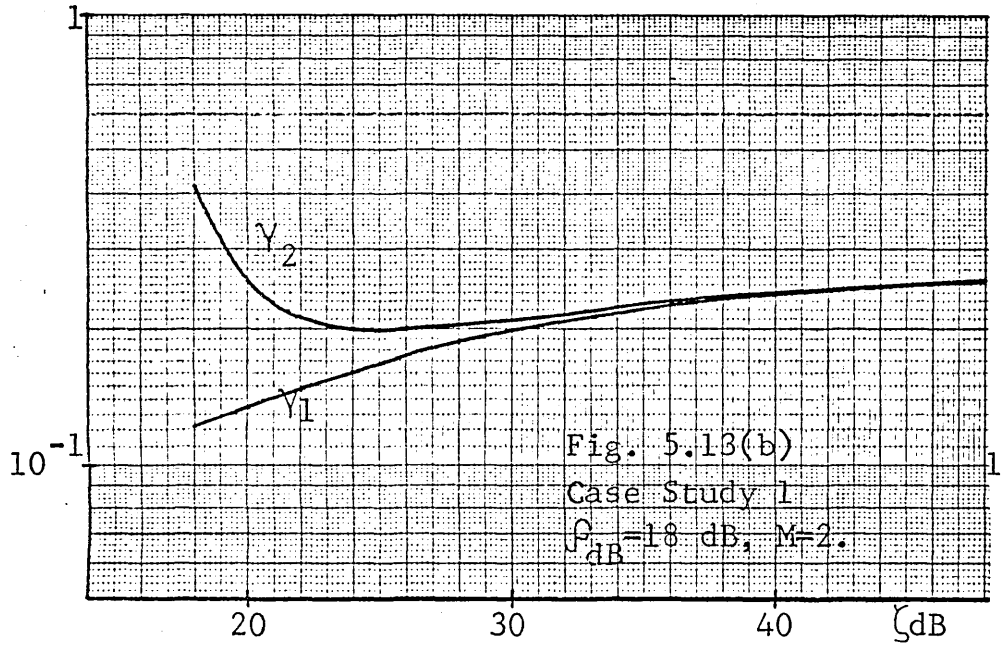

Fig. 5.13(b)
Case Study 1
ρ_{dB}=18 dB, M=2.

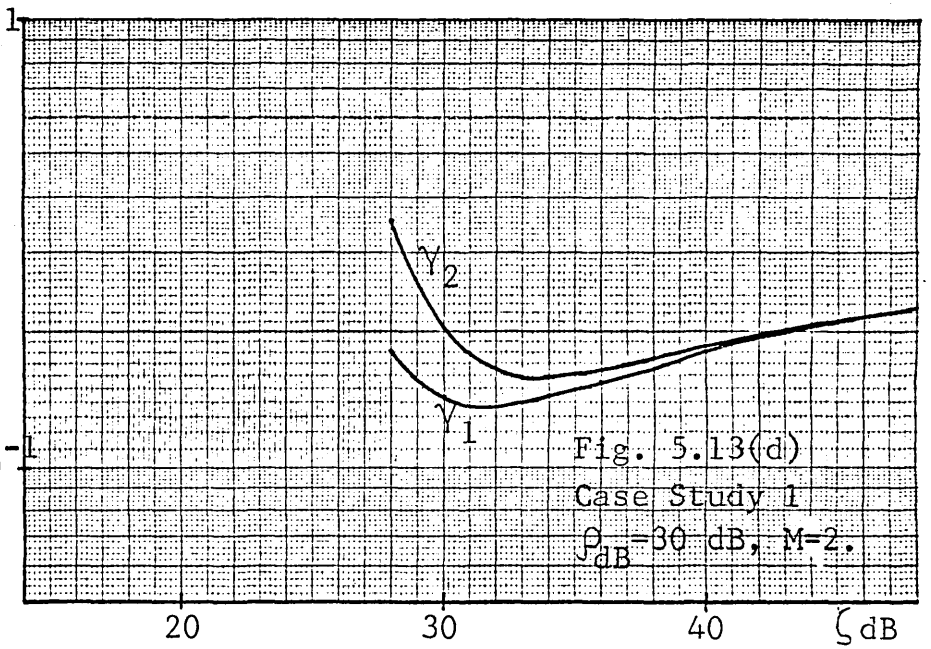

Fig. 5.13(d)
Case Study 1
ρ_{dB}=30 dB, M=2.

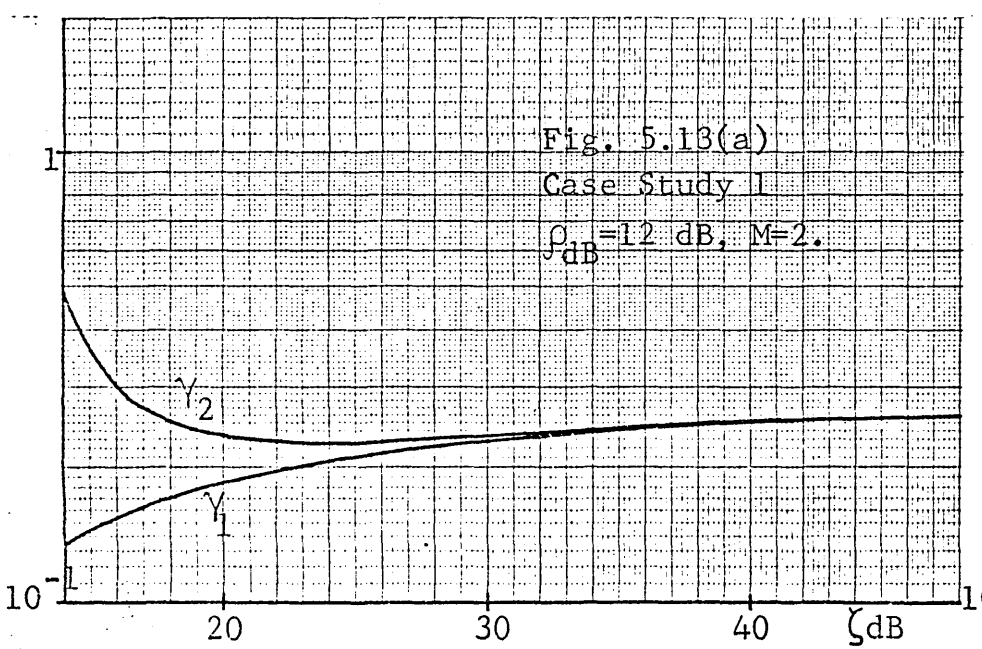

Fig. 5.13(a)
Case Study 1
ρ_{dB}=12 dB, M=2.

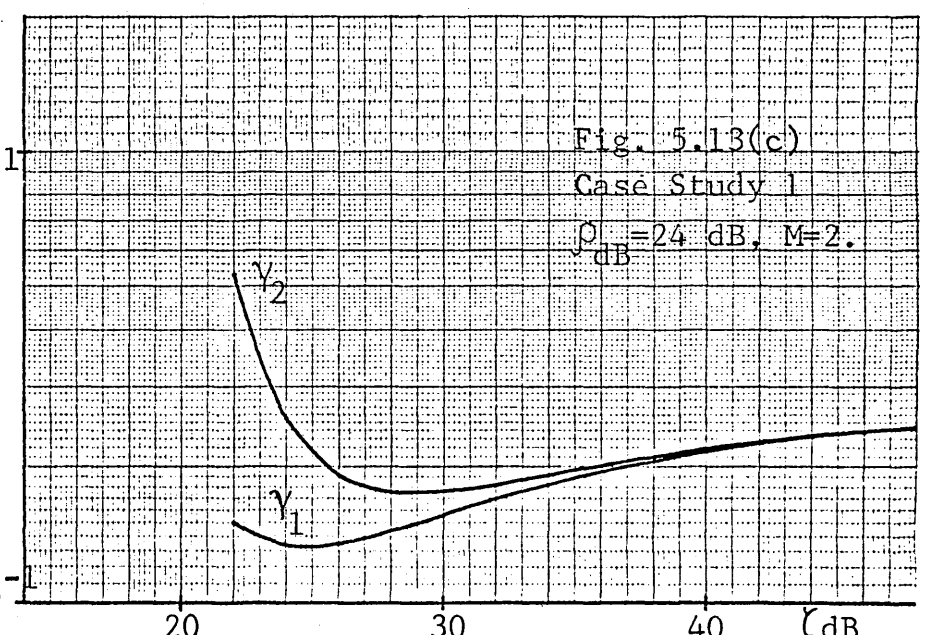

Fig. 5.13(c)
Case Study 1
ρ_{dB}=24 dB, M=2.

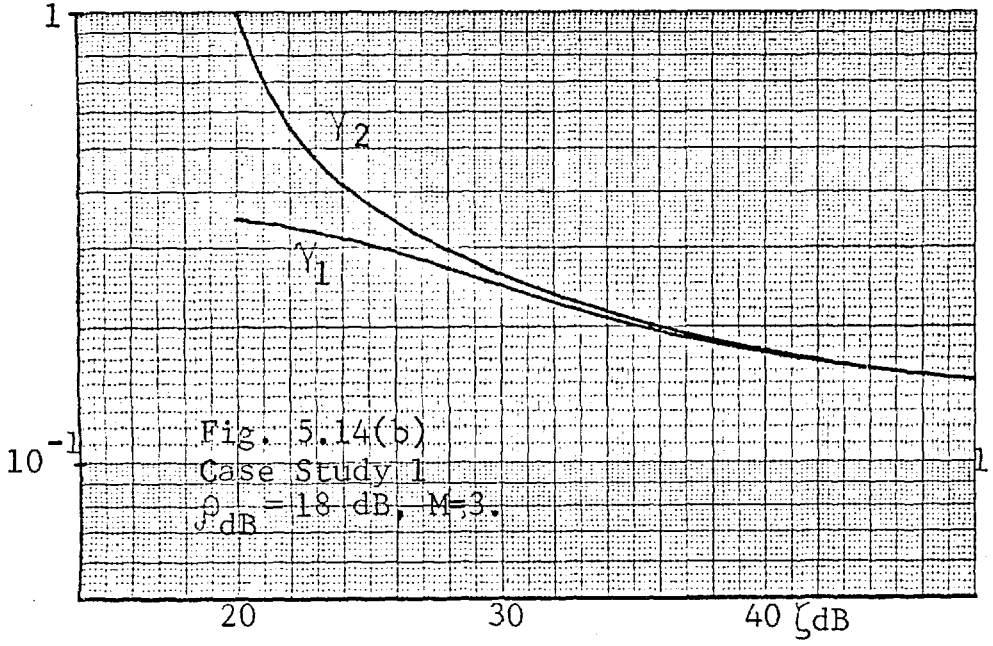

Fig. 5.14(b)
Case Study 1
ρ_{dB} = 18 dB, M=3.

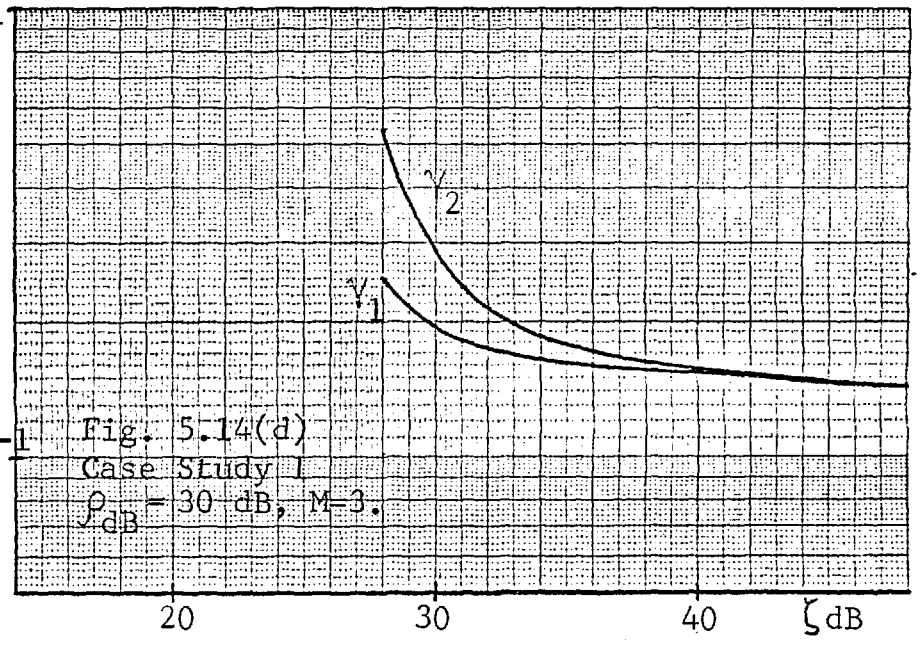

Fig. 5.14(d)
Case Study 1
ρ_{dB} = 30 dB, M=3.

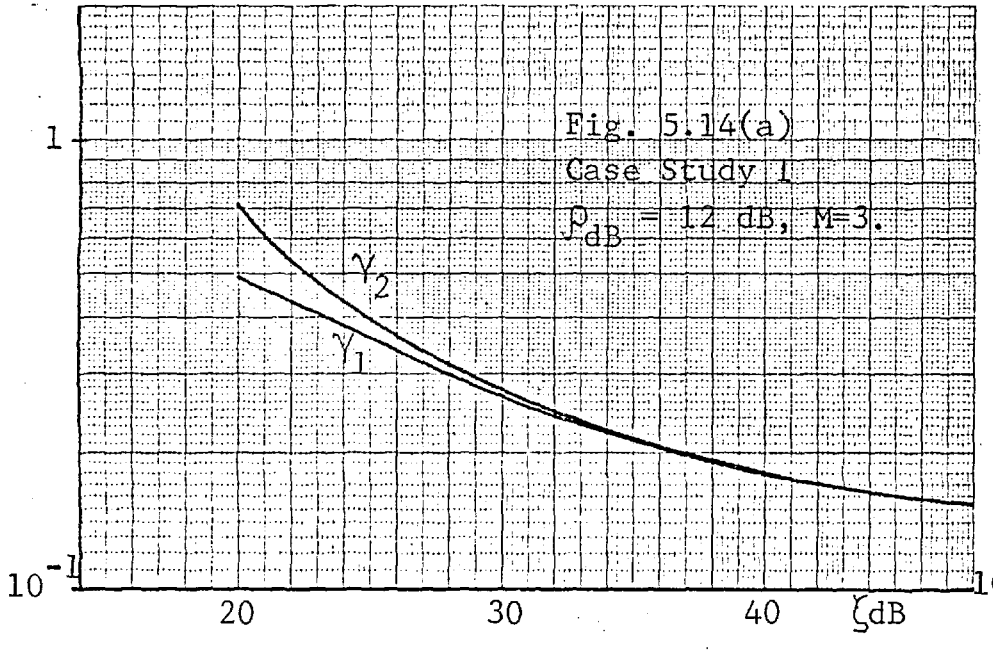

Fig. 5.14(a)
Case Study 1
ρ_{dB} = 12 dB, M=3.

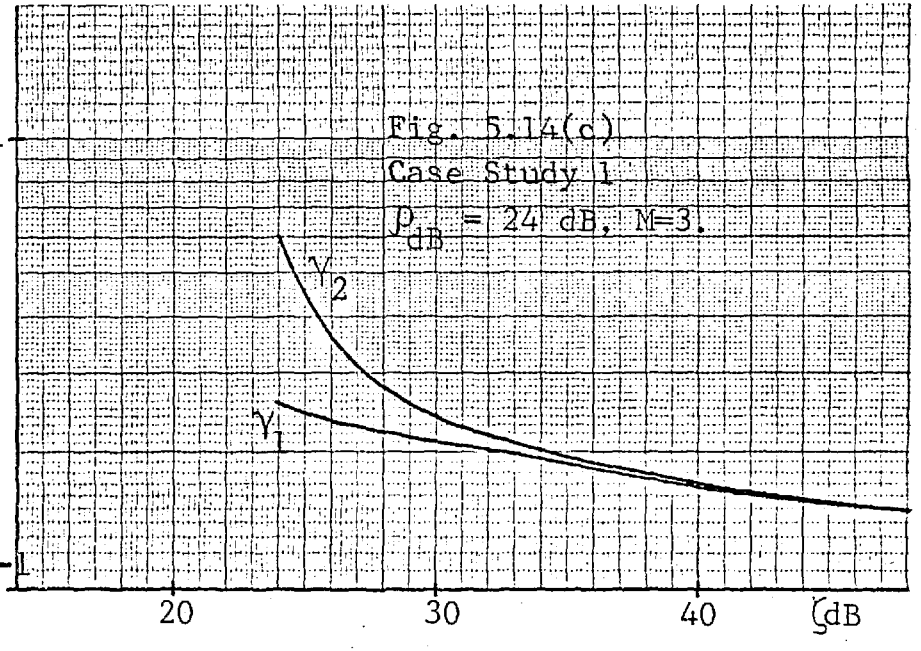

Fig. 5.14(c)
Case Study 1
ρ_{dB} = 24 dB, M=3.

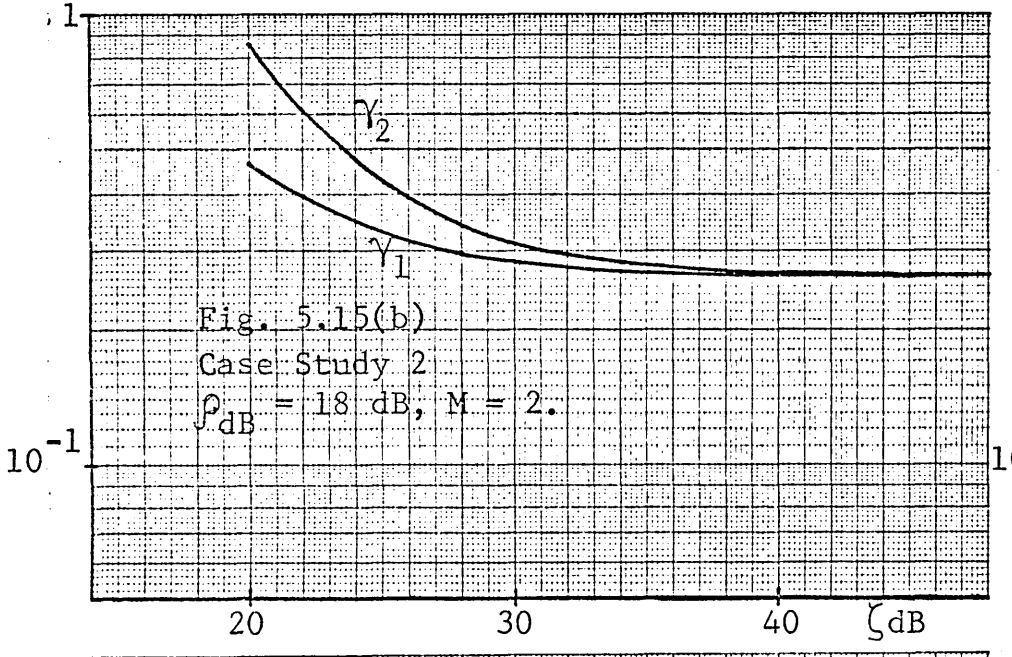

Fig. 5.15(b)
Case Study 2
ρ_{dB} = 18 dB, M = 2.

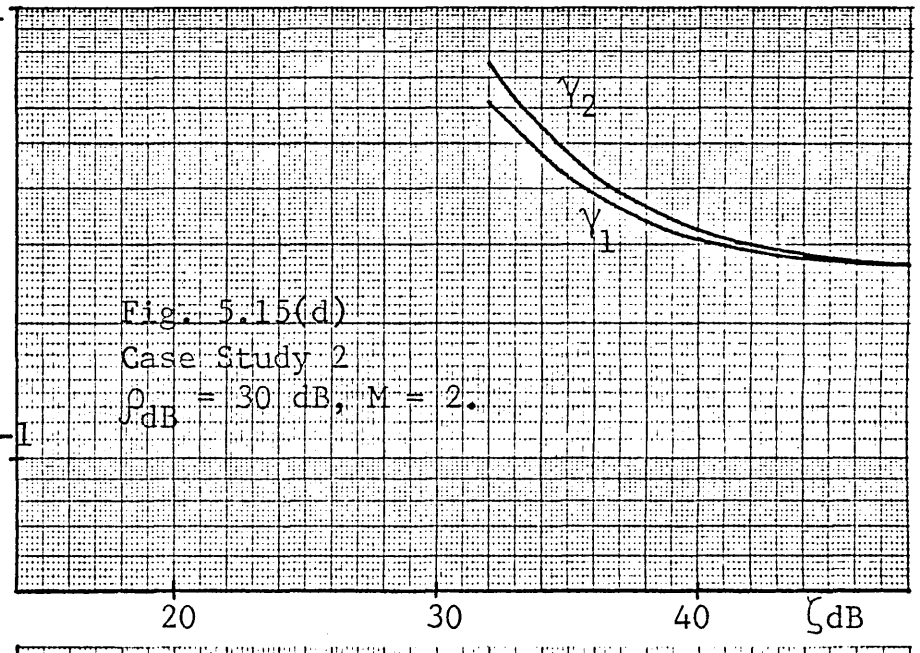

Fig. 5.15(d)
Case Study 2
ρ_{dB} = 30 dB, M = 2.

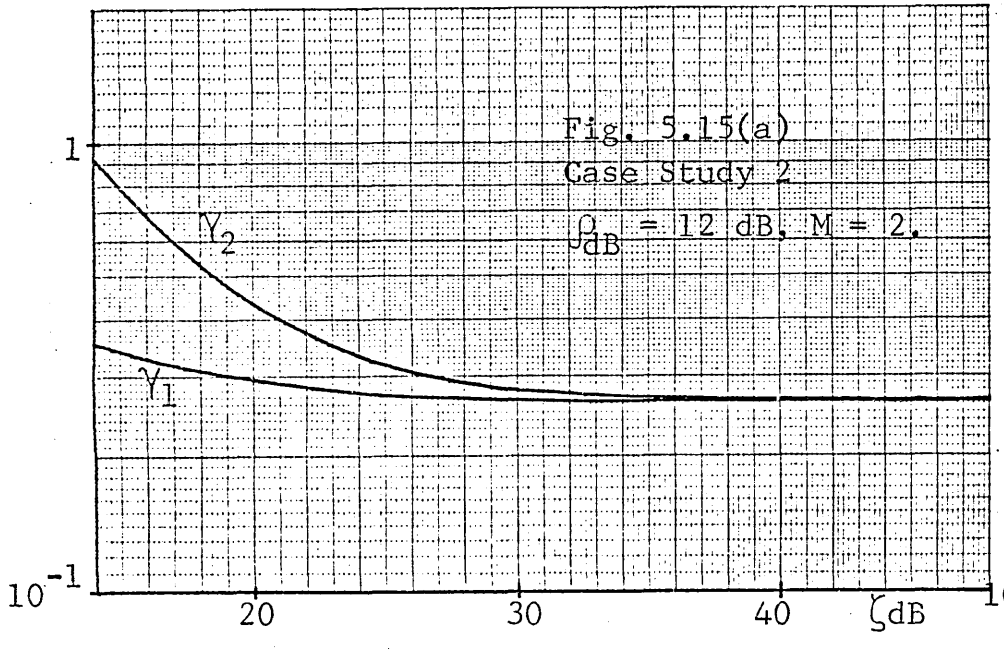

Fig. 5.15(a)
Case Study 2
ρ_{dB} = 12 dB, M = 2.

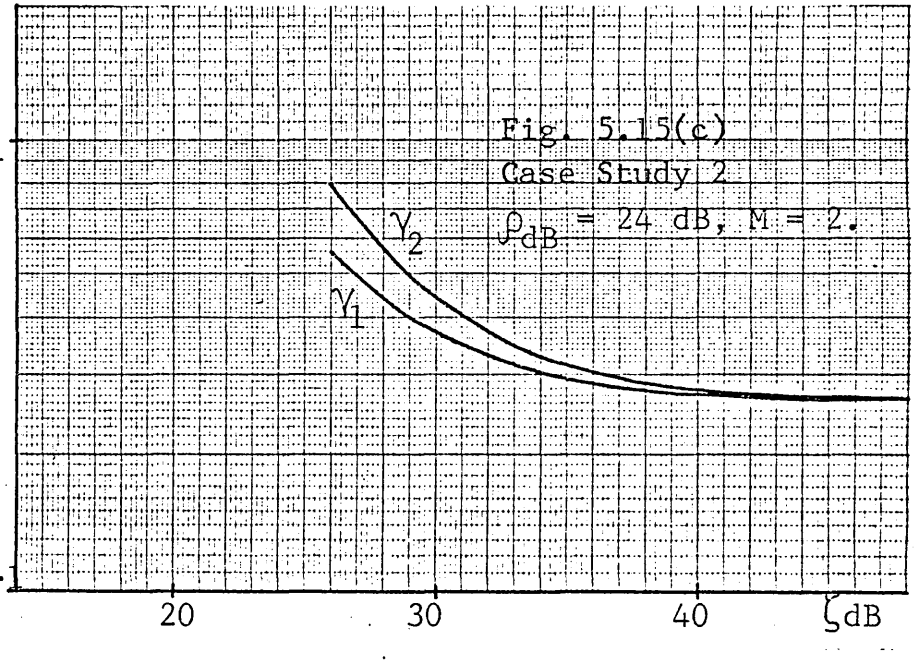

Fig. 5.15(c)
Case Study 2
ρ_{dB} = 24 dB, M = 2.

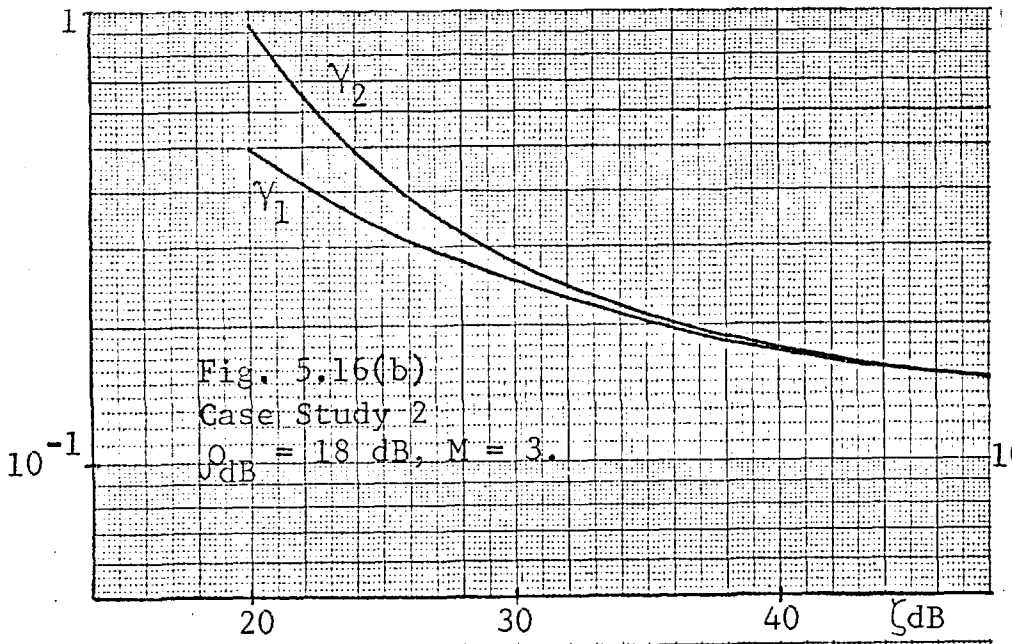

Fig. 5.16(b)
Case Study 2
ρ_{dB} = 18 dB, M = 3.

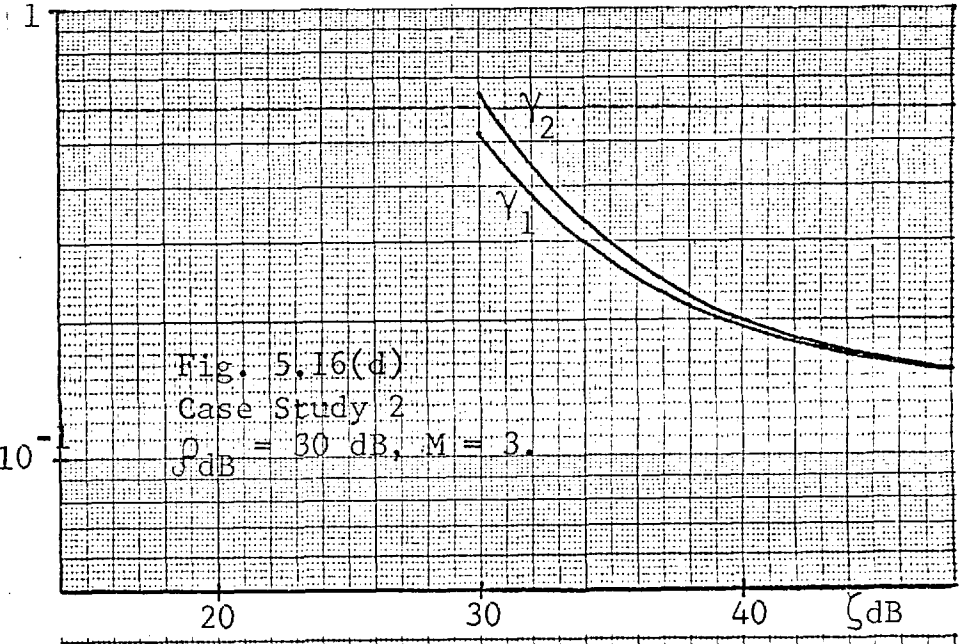

Fig. 5.16(d)
Case Study 2
ρ_{dB} = 30 dB, M = 3.

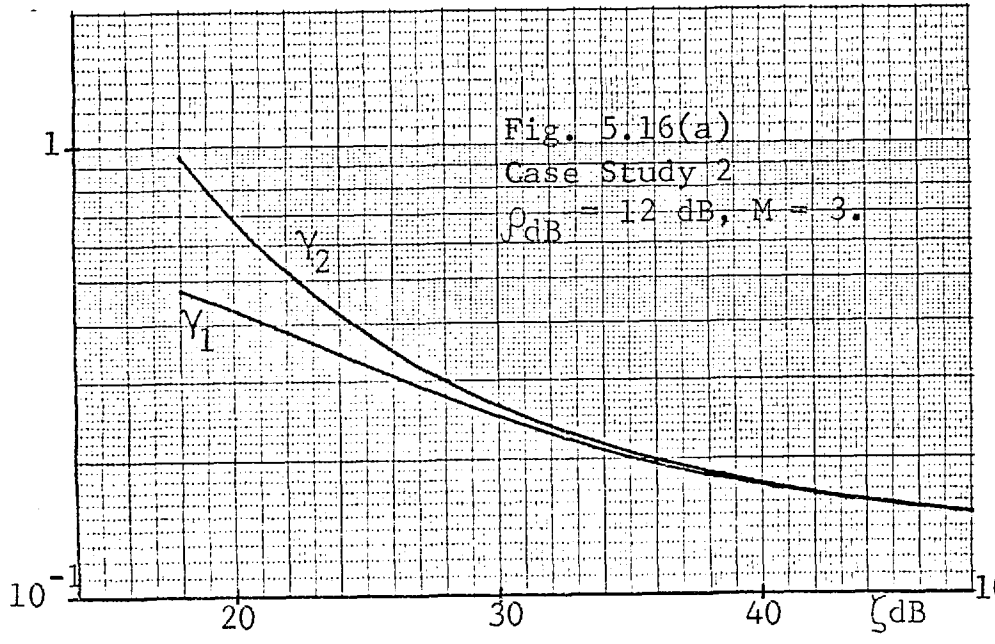

Fig. 5.16(a)
Case Study 2
ρ_{dB} = 12 dB, M = 3.

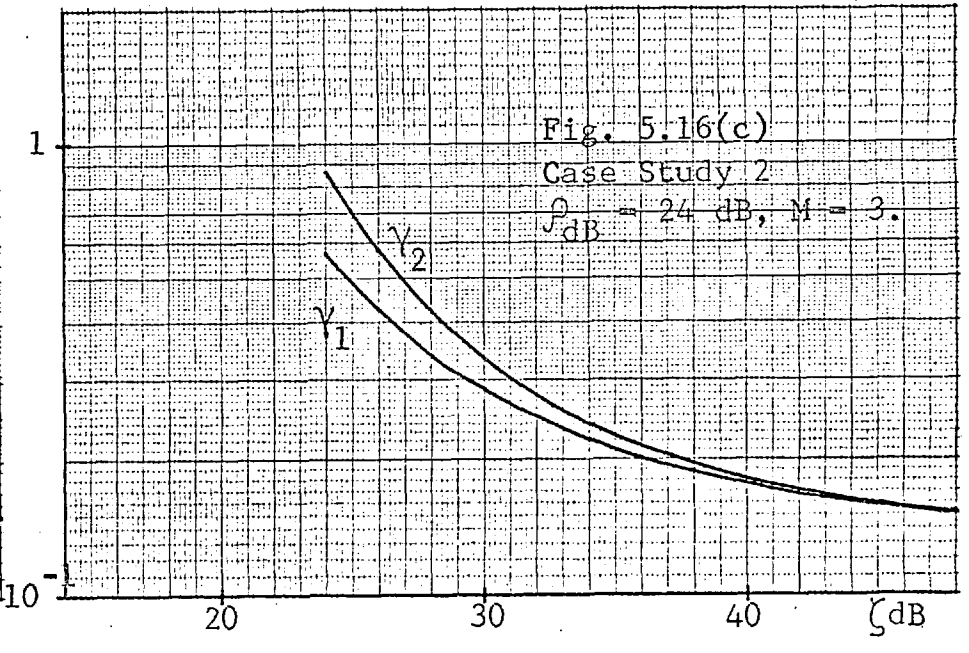

Fig. 5.16(c)
Case Study 2
ρ_{dB} = 24 dB, M = 3.

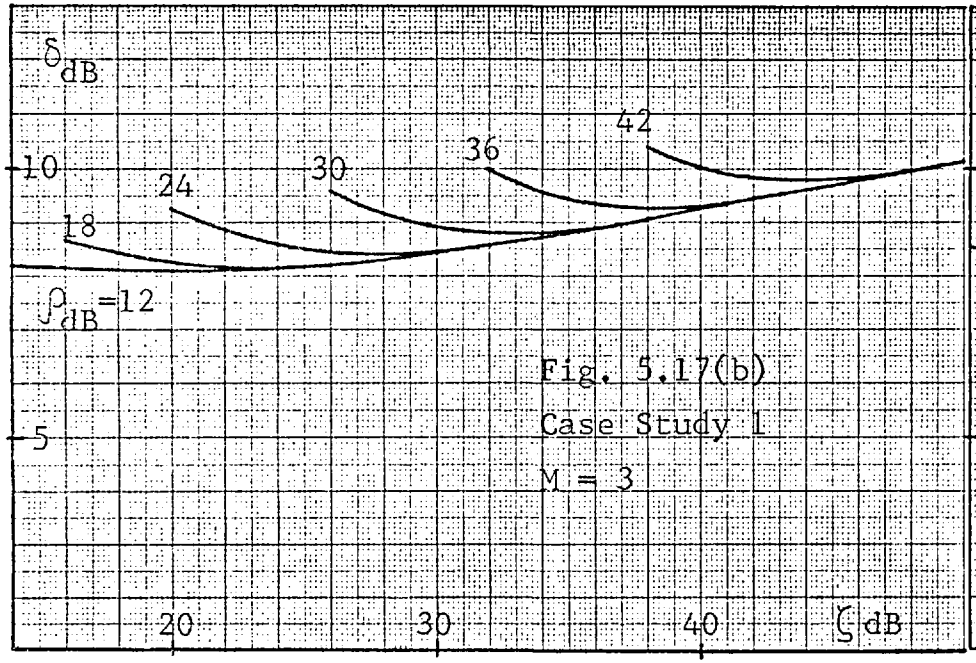

Fig. 5.17(b)
Case Study 1
M = 3

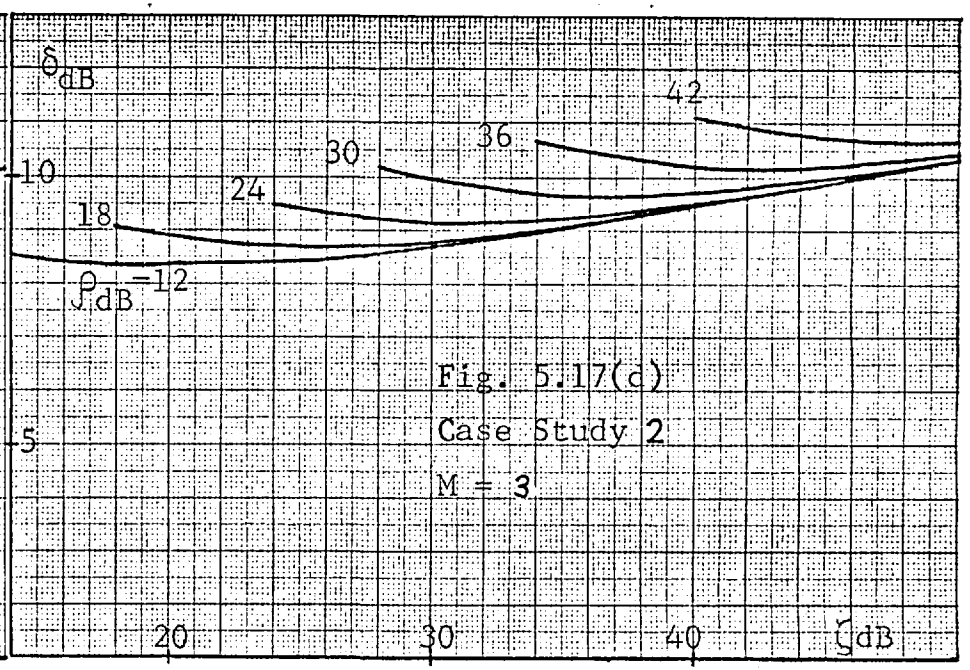

Fig. 5.17(d)
Case Study 2
M = 3

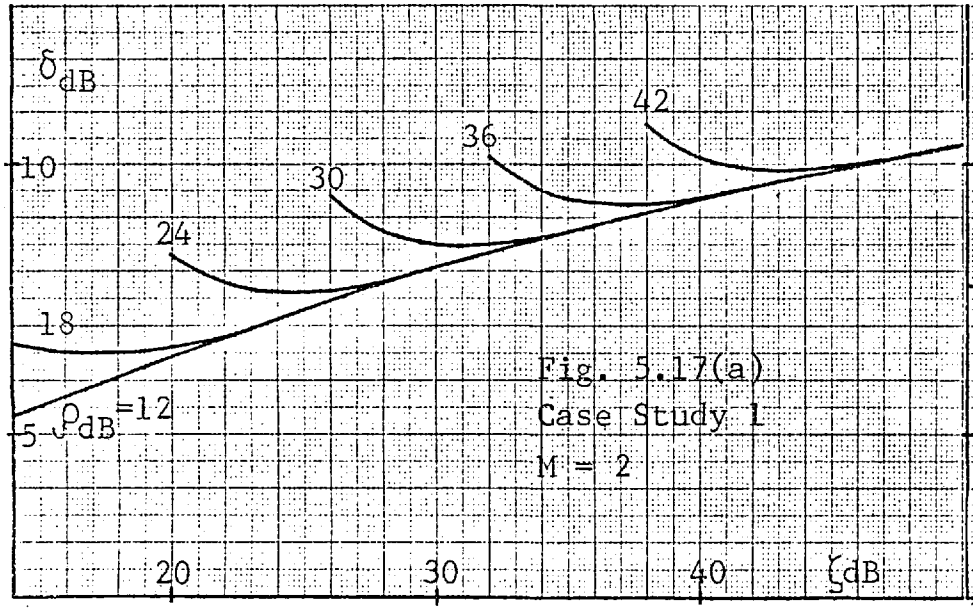

Fig. 5.17(a)
Case Study 1
M = 2

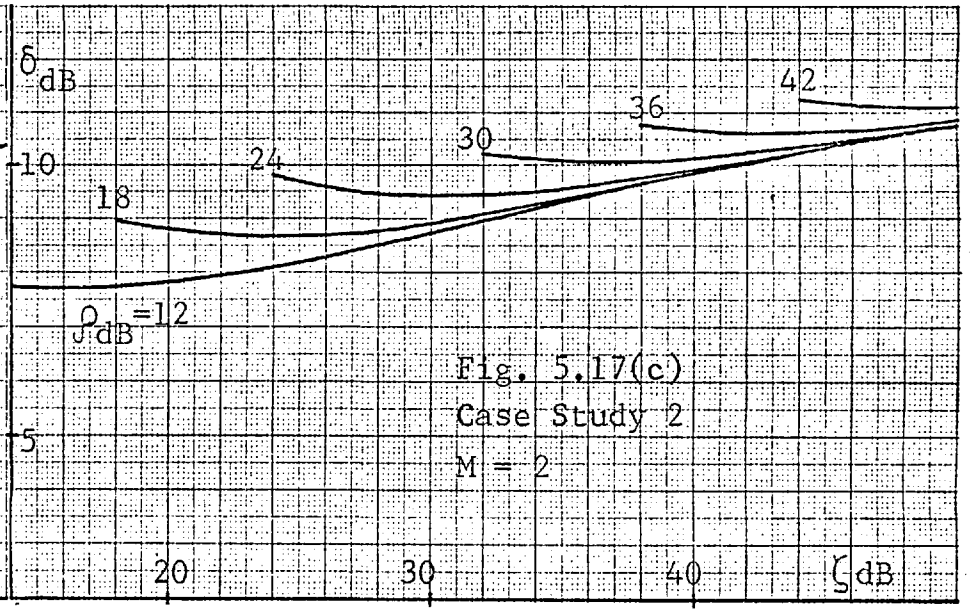

Fig. 5.17(c)
Case Study 2
M = 2

M	2	3	4	5	6
δ_{dB}	8.8	9.2	9.4	9.6	9.8

As can be seen, these values of δ_{dB} are quite close to each other and to those given by the graphs in class (E).

F) Graphs giving the minimum error probability corresponding to the value of ε_0 given by the graphs in the previous class. These are shown in Fig. 5.18 and can be seen to give practically the same values as those in Fig. 5.11. Therefore the restriction $\varepsilon_1 = \varepsilon_2 = \varepsilon_0$ has no practical consequences in the range of parameters considered.

G) Graphs giving the erasure probability, P_x, corresponding to the minimum error probability.

These graphs are presented in Fig. 5.19. Here again the values given by these graphs are very close to those given by the graphs of Fig. 5.12.

H) Graphs giving the value (in dB) of the ratio $\delta = \varepsilon_0/\sigma_w$ that minimizes the erasure probability P_x.

These graphs are presented in Fig. 5.20 and have a similar shape to those shown in Fig. 5.17. When $\mu_{dB} \ll 0$ dB the optimum value of δ is practically independent of ρ and is very close to the value given by Equation (73). On the other hand, if $\mu_{dB} \gg 0$ dB the minimization of P_x leads to $\delta = \rho$, that is, ε_o attains its maximum value, A.

I) Graphs giving the minimum erasure probability, $P_{x_{min}}$.

These graphs are shown in Fig. 5.21 and can be seen to give values which are practically identical to those given by the graphs of Fig. 5.19.

J) Graphs giving the error probability corresponding to the minimum erasure probability given by the previous graphs.

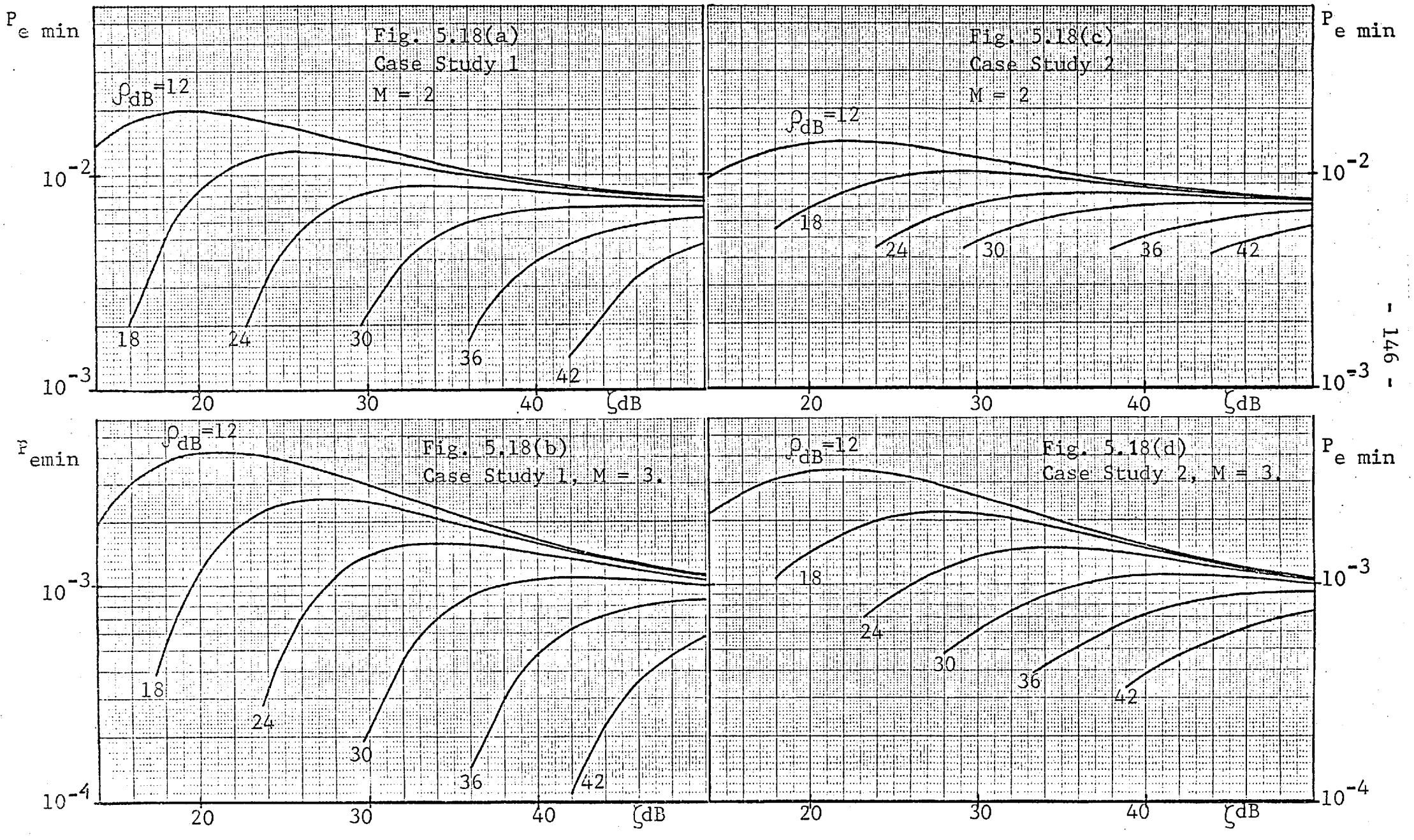
Fig. 5.18(a)
Case Study 1
M = 2
ρ_{dB}=12
$P_{e\ min}$
10^{-2}
10^{-3}
18
24
30
36
42
20
30
40
ζ_{dB}
Fig. 5.18(c)
Case Study 2
M = 2
ρ_{dB}=12
$P_{e\ min}$
10^{-2}
10^{-3}
18
24
30
36
42
20
30
40
ζ_{dB}
Fig. 5.18(b)
Case Study 1, M = 3.
ρ_{dB}=12
P_{emin}
10^{-3}
10^{-4}
18
24
30
36
42
20
30
40
ζ_{dB}
Fig. 5.18(d)
Case Study 2, M = 3.
ρ_{dB}=12
$P_{e\ min}$
10^{-3}
10^{-4}
18
24
30
36
42
20
30
40
ζ_{dB}

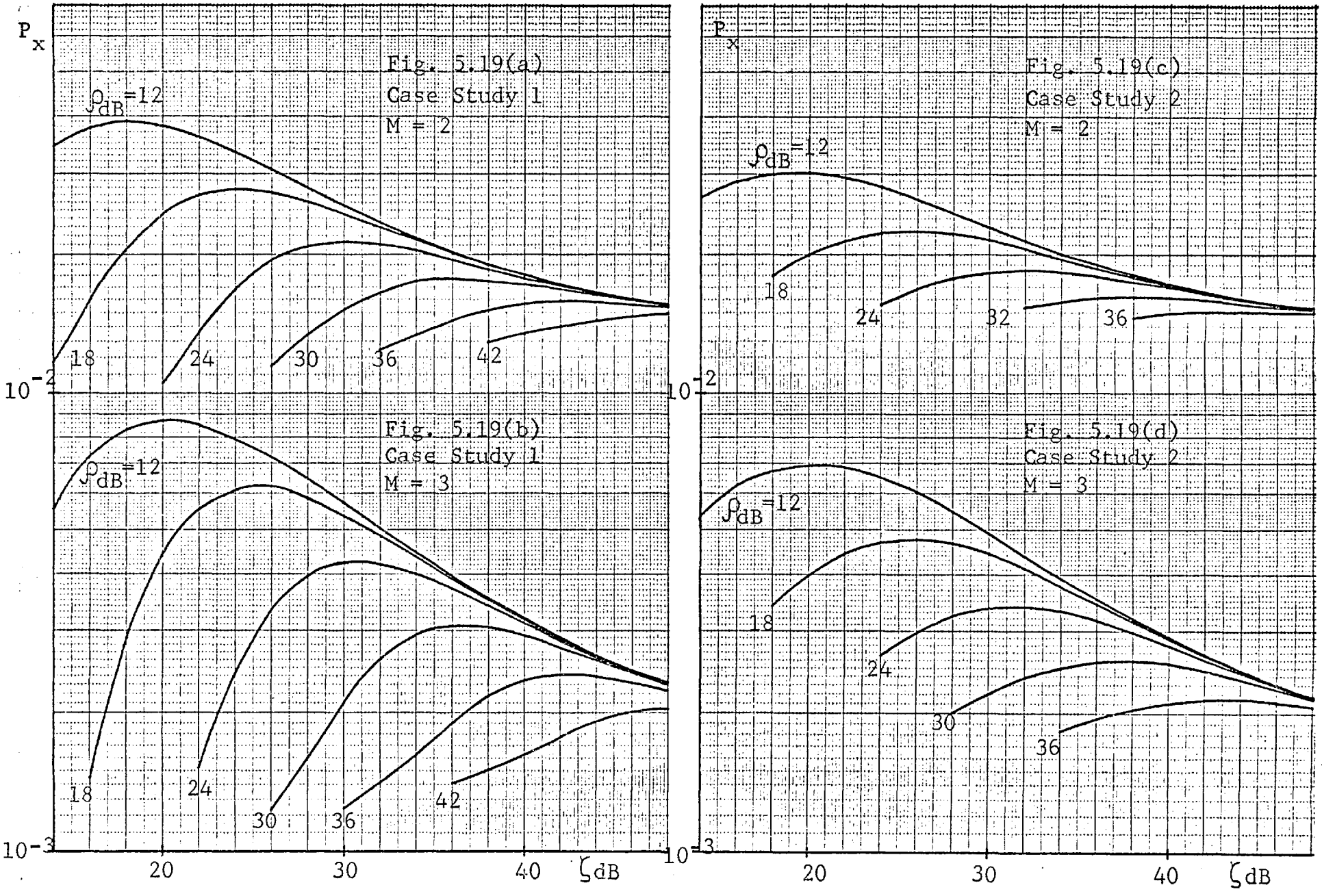
P_x
Fig. 5.19(a)
Case Study 1
M = 2
ρ_{dB}=12
18
24
30
36
42
10^{-2}
Fig. 5.19(b)
Case Study 1
M = 3
ρ_{dB}=12
18
24
30
36
42
10^{-3}
20
30
40
ζ_{dB}
P_x
Fig. 5.19(c)
Case Study 2
M = 2
ρ_{dB}=12
18
24
32
36
10^{-2}
Fig. 5.19(d)
Case Study 2
M = 3
ρ_{dB}=12
18
24
30
36
10^{-3}
20
30
40
ζ_{dB}

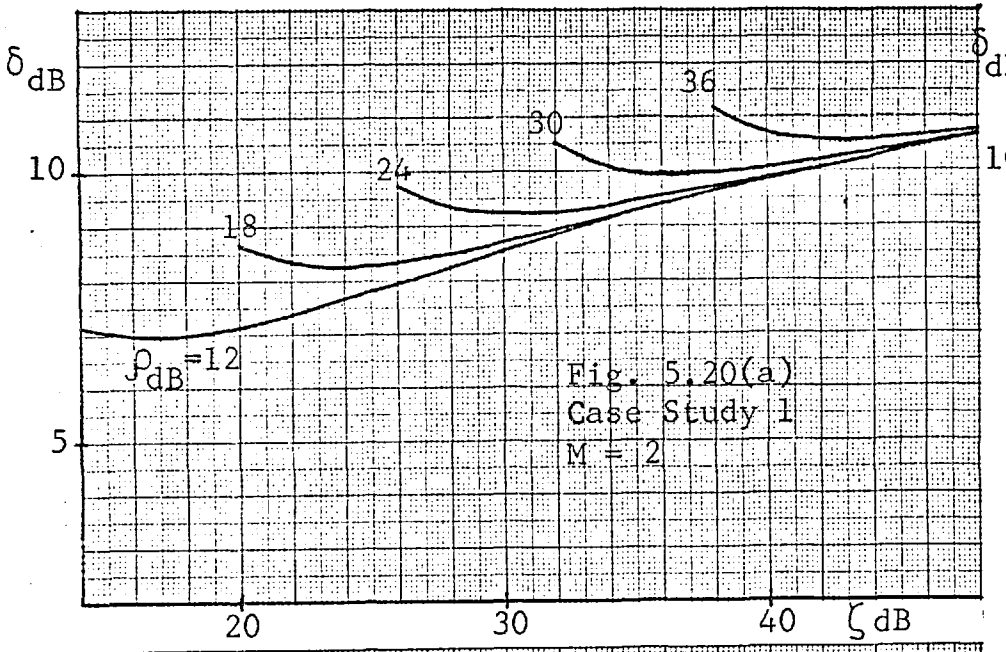

Fig. 5.20(a)
Case Study 1
M = 2

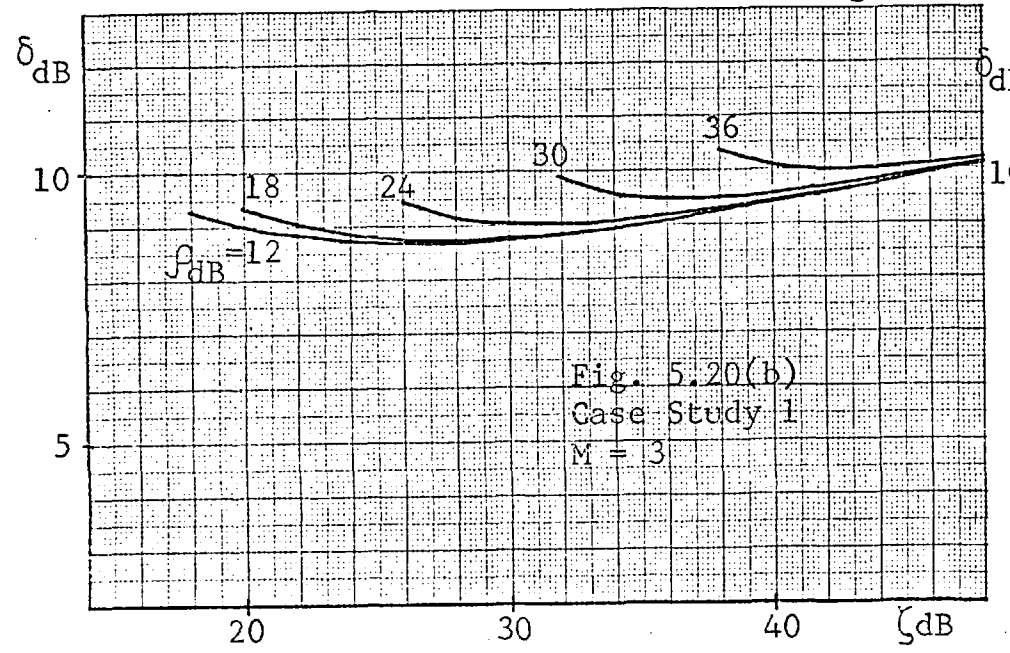

Fig. 5.20(b)
Case Study 1
M = 3

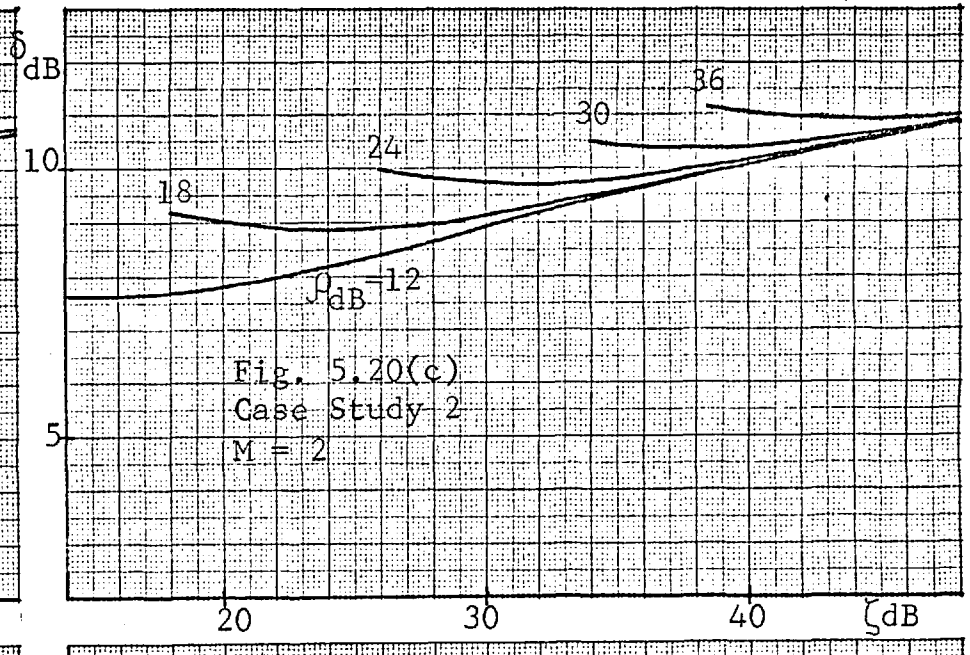

Fig. 5.20(c)
Case Study 2
M = 2

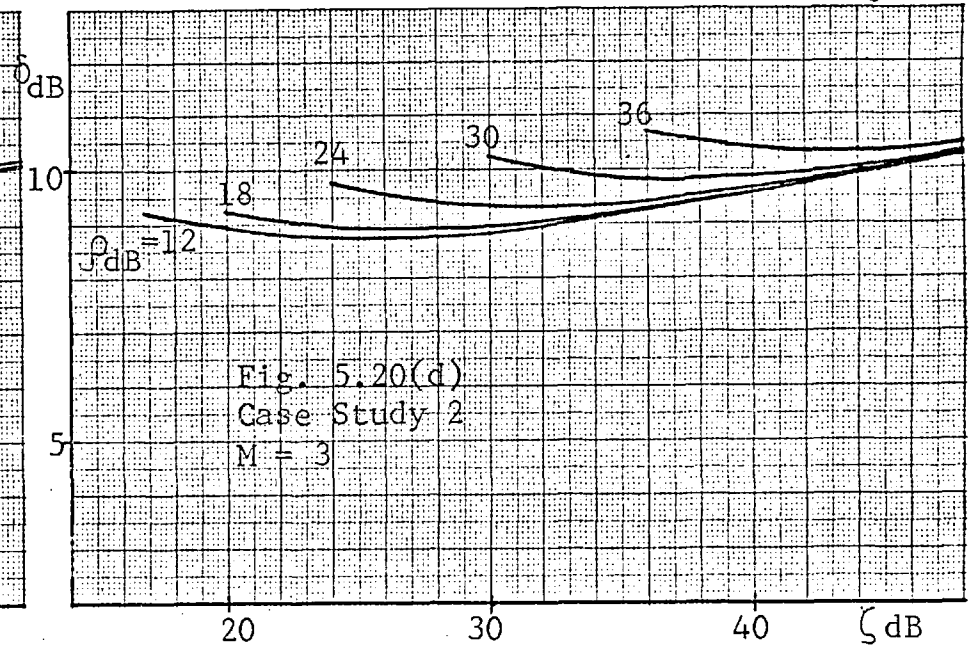

Fig. 5.20(d)
Case Study 2
M = 3

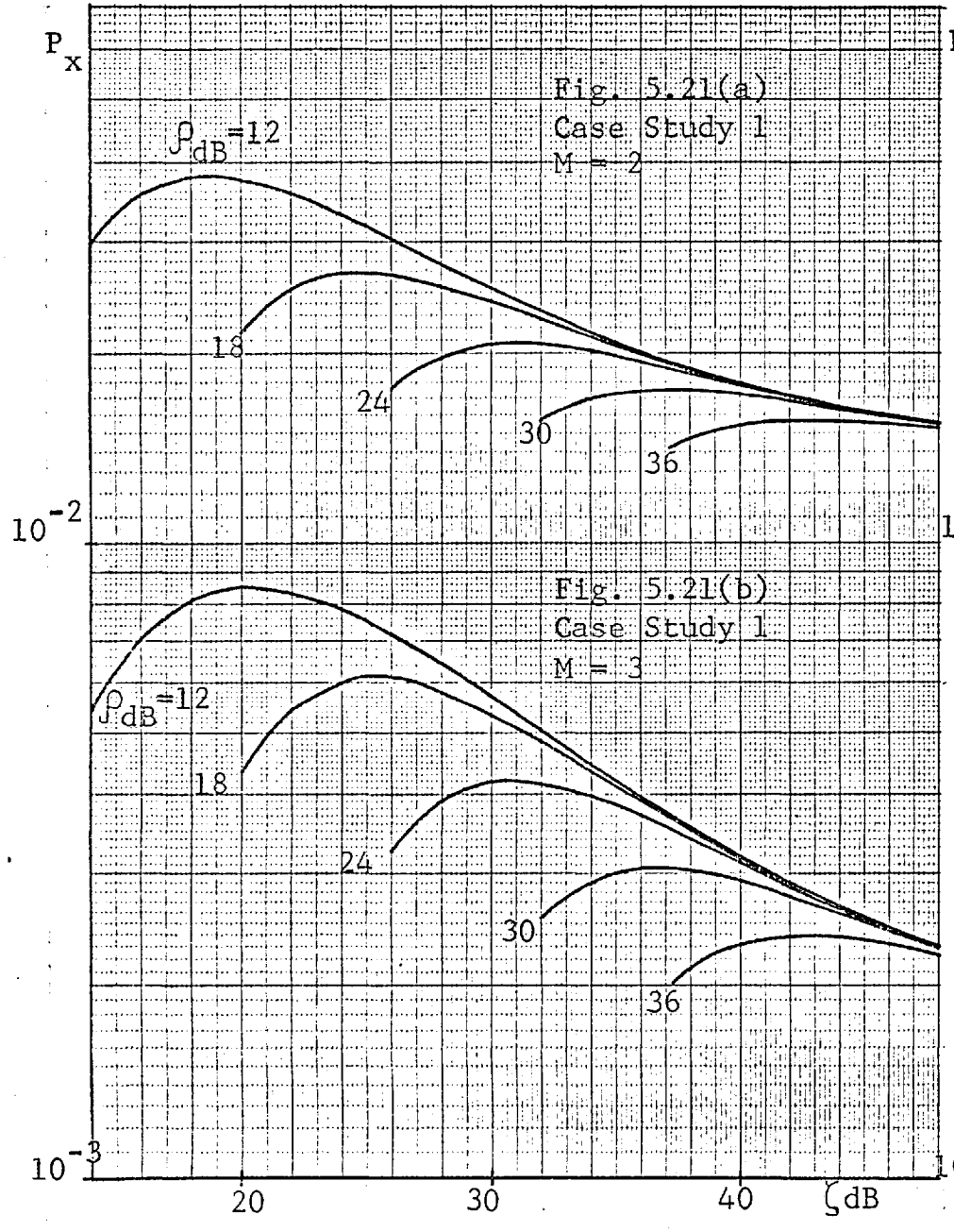

Fig. 5.21(a)
Case Study 1
M = 2

Fig. 5.21(b)
Case Study 1
M = 3

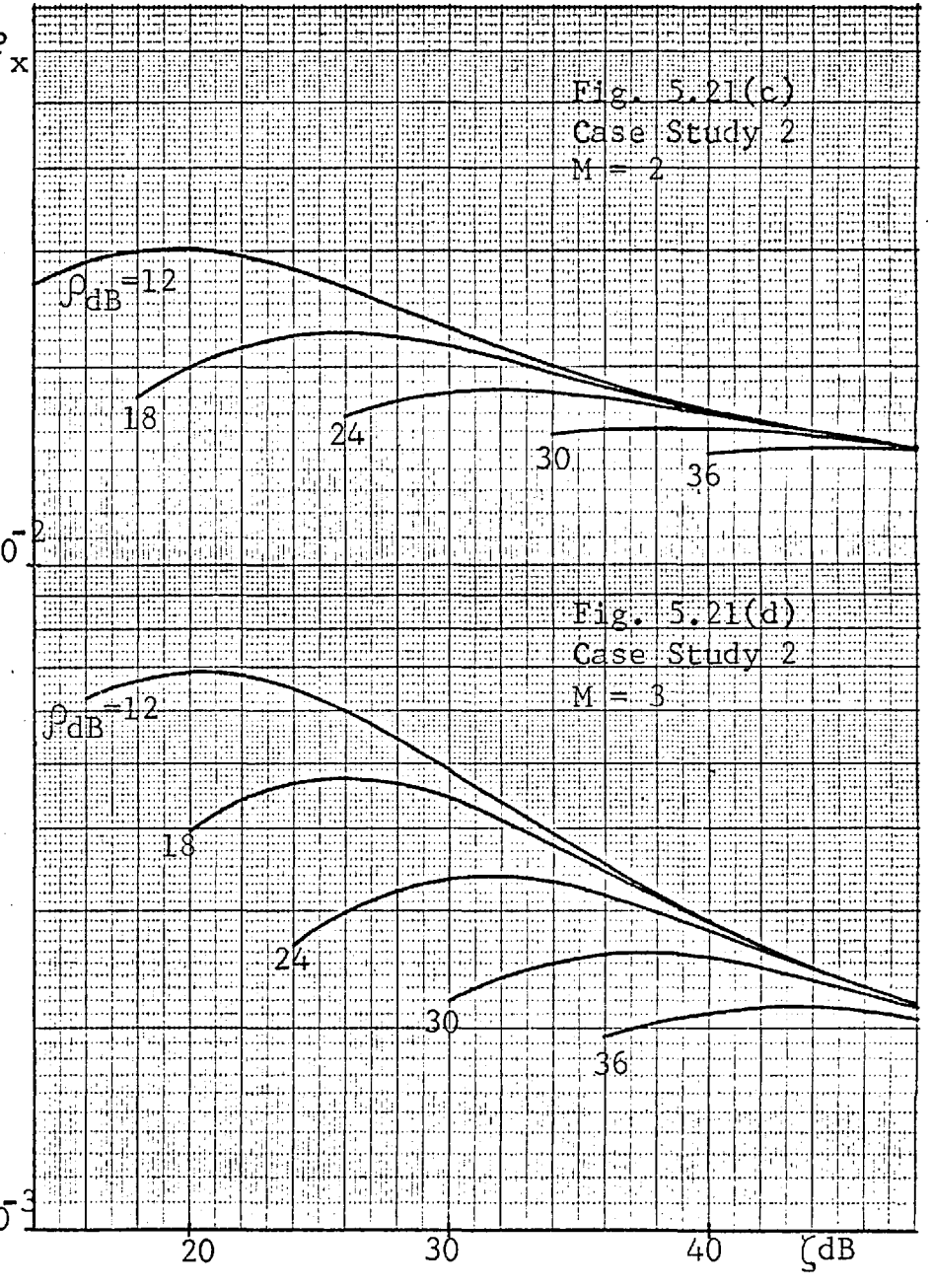

Fig. 5.21(c)
Case Study 2
M = 2

Fig. 5.21(d)
Case Study 2
M = 3

These graphs are shown in Fig. 5.22 and can be seen to give values which are practically identical to those plotted in the graphs of Fig. 5.18. It can thus be concluded from the graphs discussed above that if

$$\rho_{dB} > 12 \text{ dB} \quad \text{and} \quad \mu_{dB} < 0 \text{ dB}$$

then the minimization of the erasure probability P_x, as a function of ε_0, will lead to an error probability P_e very close to the minimum given by the graphs in class B.

In the graphs discussed below, each curve corresponds to a fixed value of the parameter ε_0.

K) Graphs giving the error probability P_e versus the SGNR ρ_{dB}, for a fixed value of the IGNR ζ_{dB}.

These graphs are shown in Figs. 5.23, 5.24 and 5.25 for the values ζ_{dB} = 20.0, 32.0 and 44.0 dB, respectively. In each graph the continuous curves correspond to a value $\delta = \varepsilon_o/\sigma_w$ close to the optimum for the assumed ζ_{dB} and ρ_{dB} = 12 dB; the dots correspond to δ_{dB} - 3.0 dB and the small circles correspond to δ_{dB} + 3.0 dB. It can be seen that the error probability exhibits a quite shallow minimum as a function of δ.

L) Graphs giving the erasure probability P_x under the same conditions as the graphs in class K.

These graphs are presented in Figs. 5.26, 5.27 and 5.28 and the graphical conventions are the same as for the graphs of class K. The curves of P_x show a point of inflexion at $\rho_{dB} \simeq \zeta_{dB}$, that is, $\mu_{dB} \simeq 0$ dB. The difference between the values of P_x at a low and a high value of ρ_{dB} decreases as ζ_{dB} increases, and for high values of ζ_{dB} relation (86) is valid for any ρ_{dB} within the range of interest, in accordance with the theory of Subsection 5.2.3.

M) Graphs giving the error probability of the upper branch of the receiver, P_{eu}, under the conditions of the two previous classes of graphs.

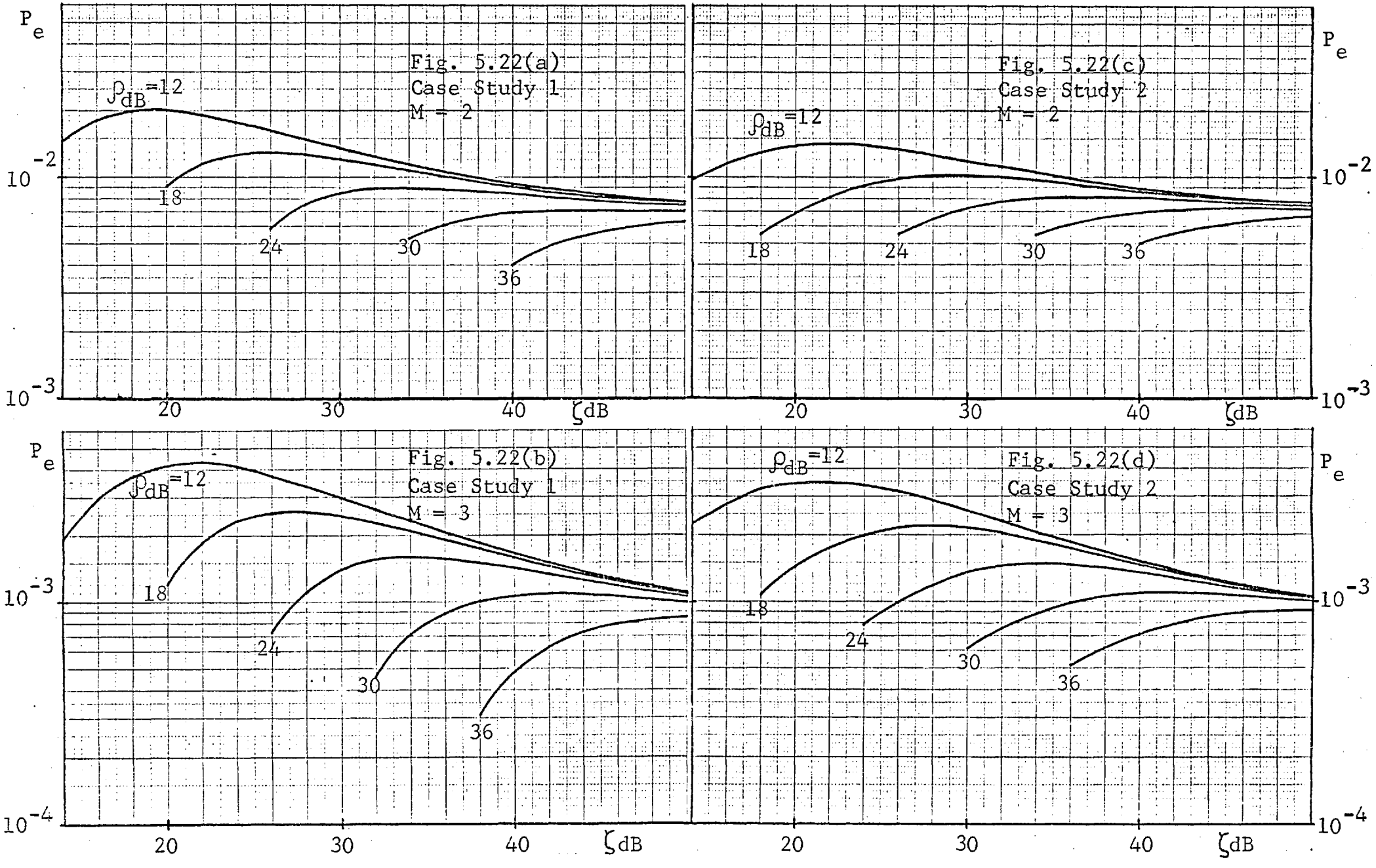
Fig. 5.22(a)
Case Study 1
M = 2
ρ_{dB}=12
18
24
30
36
P_e
10^{-2}
10^{-3}
20
30
40
ζ_{dB}
Fig. 5.22(c)
Case Study 2
M = 2
ρ_{dB}=12
18
24
30
36
P_e
10^{-2}
10^{-3}
20
30
40
ζ_{dB}
Fig. 5.22(b)
Case Study 1
M = 3
ρ_{dB}=12
18
24
30
36
P_e
10^{-3}
10^{-4}
20
30
40
ζ_{dB}
Fig. 5.22(d)
Case Study 2
M = 3
ρ_{dB}=12
18
24
30
36
P_e
10^{-3}
10^{-4}
20
30
40
ζ_{dB}

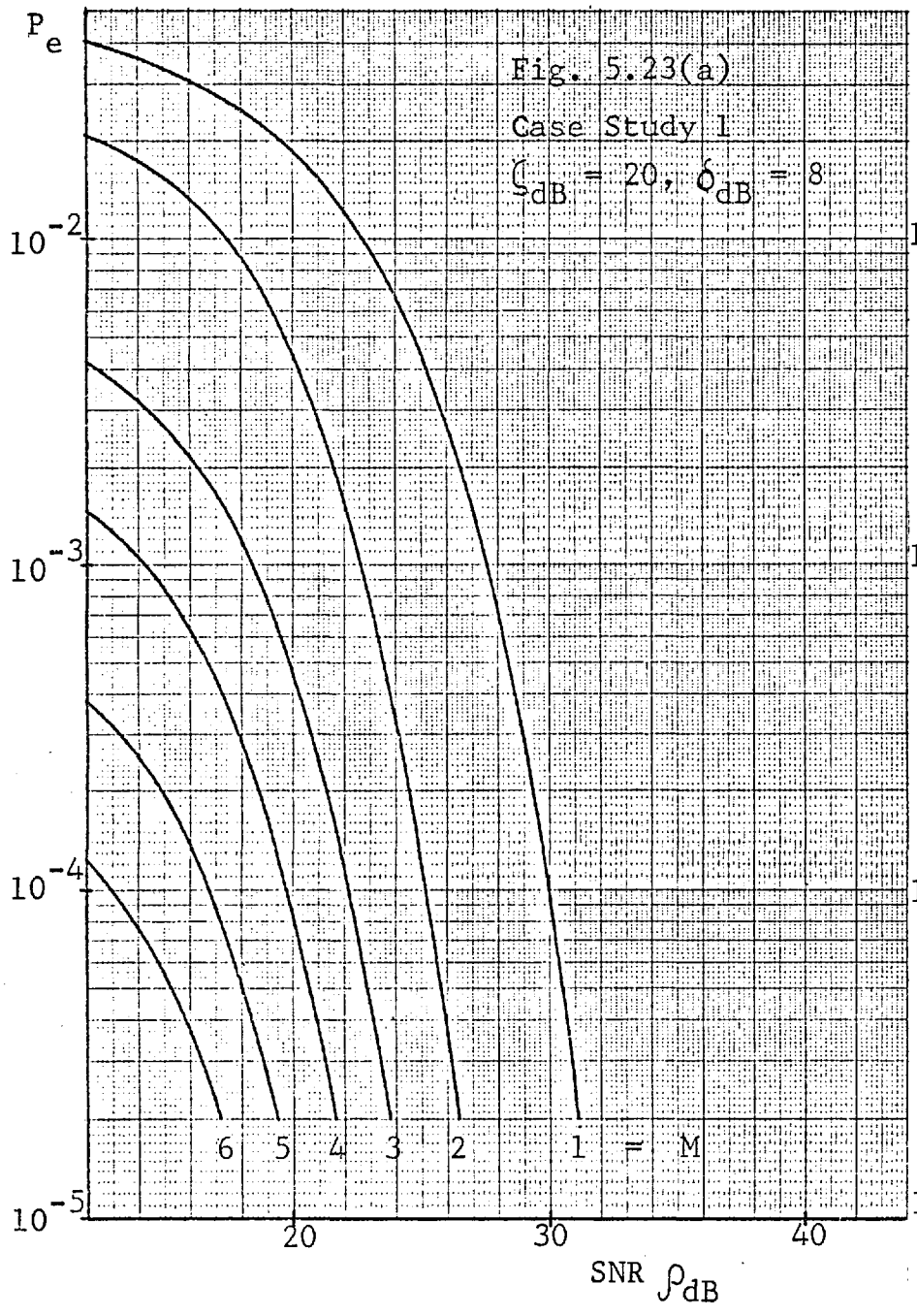

Fig. 5.23(a)
Case Study 1
$\zeta_{dB} = 20$, $\delta_{dB} = 8$

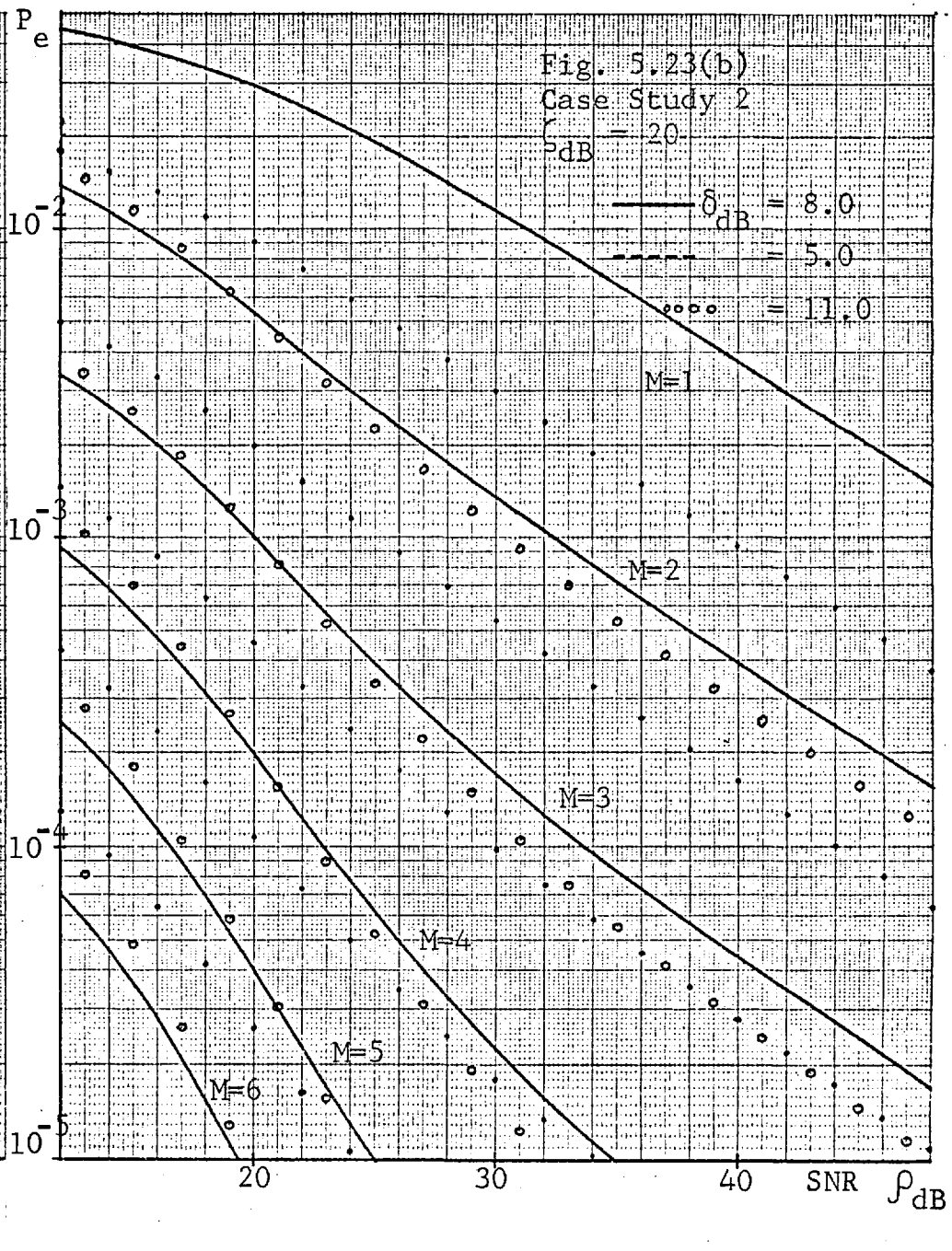

Fig. 5.23(b)
Case Study 2
$\zeta_{dB} = 20$
——— $\delta_{dB} = 8.0$
– – – = 5.0
°°°° = 11.0

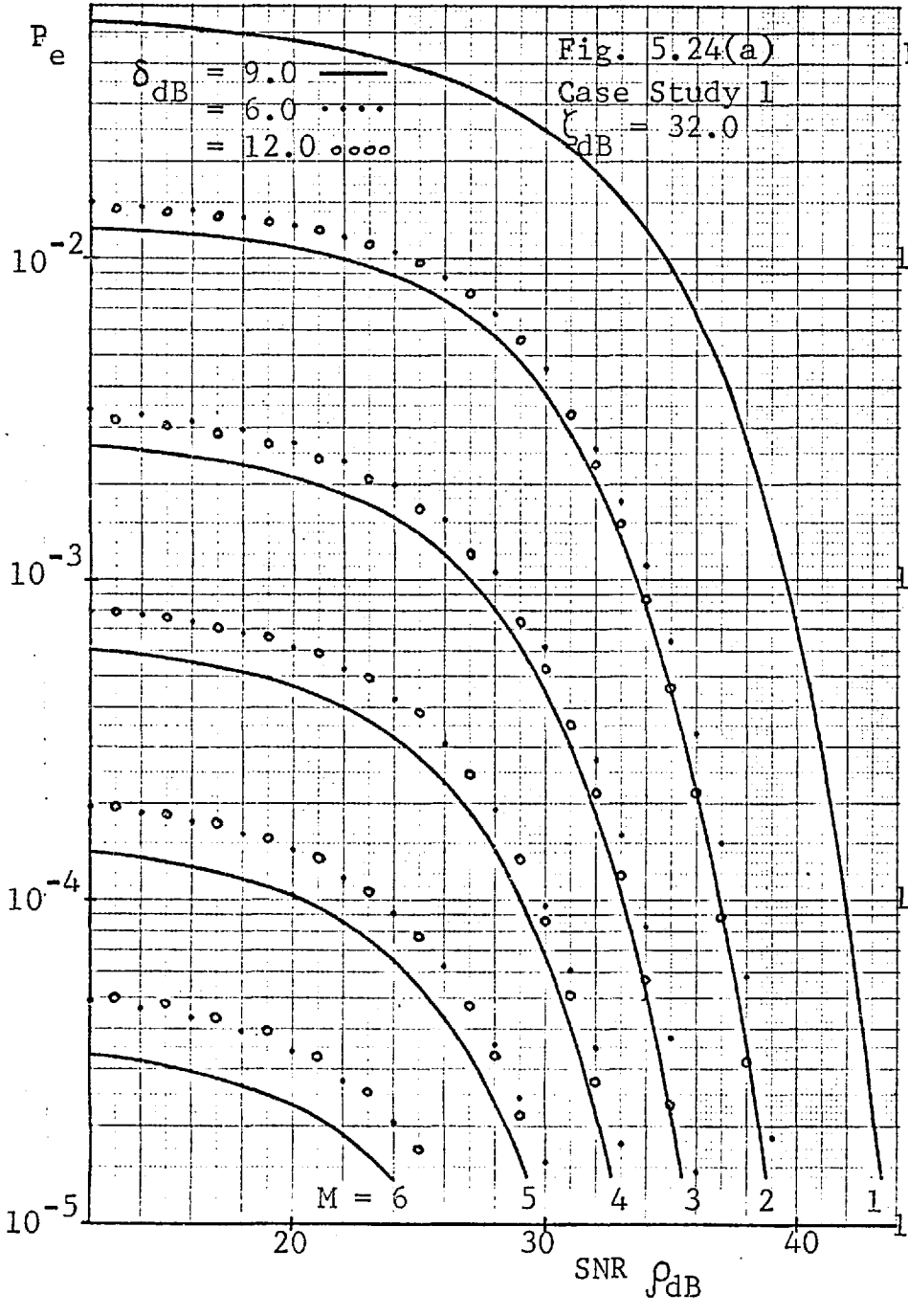
Fig. 5.24(a)
Case Study 1
ζ_{dB} = 32.0
δ_{dB} = 9.0
= 6.0
= 12.0
P_e
10^{-2}
10^{-3}
10^{-4}
10^{-5}
M = 6
5
4
3
2
1
20
30
40
SNR ρ_{dB}

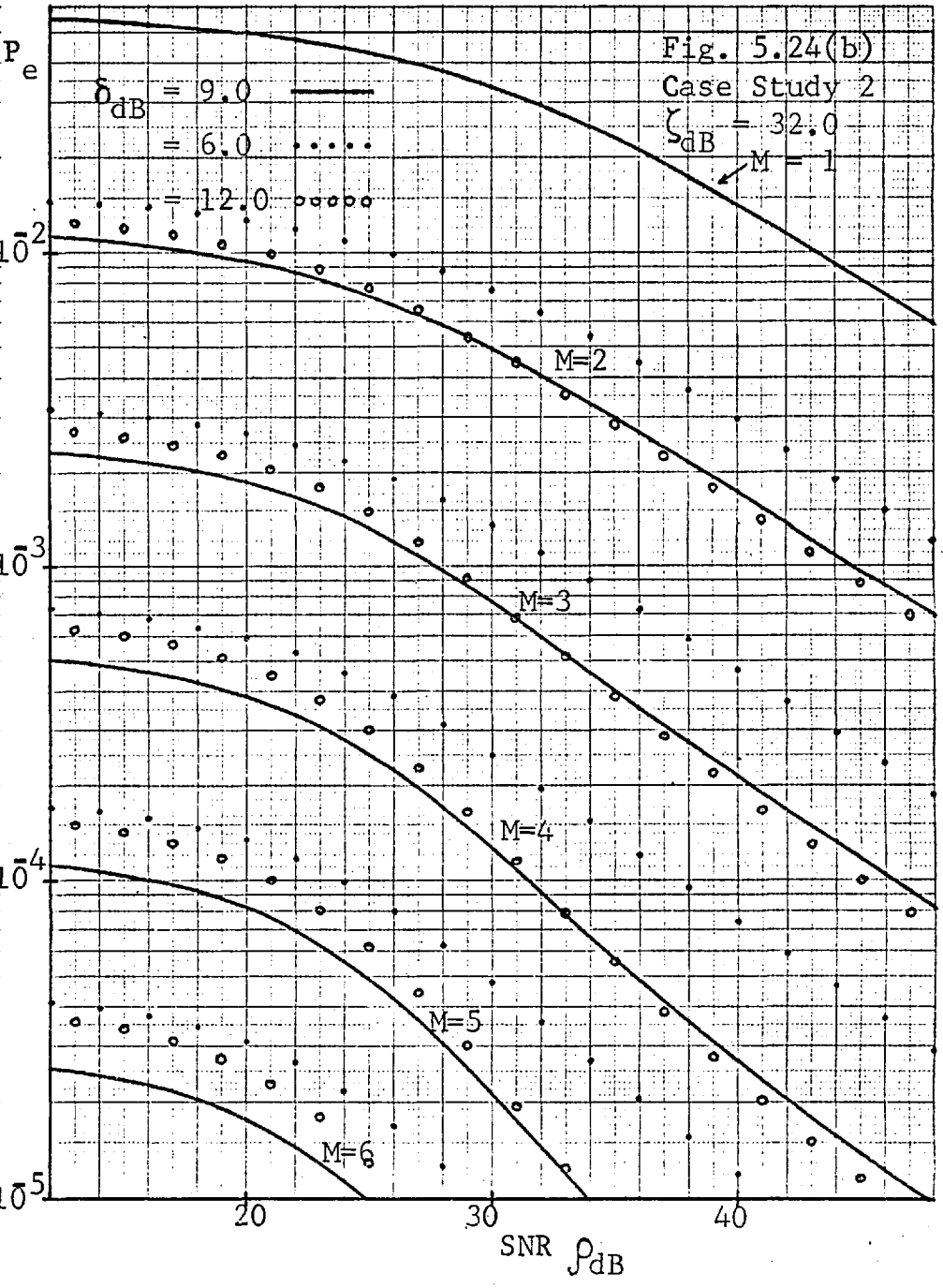
Fig. 5.24(b)
Case Study 2
ζ_{dB} = 32.0
δ_{dB} = 9.0
= 6.0
= 12.0
P_e
M = 1
M=2
M=3
M=4
M=5
M=6
10^{-2}
10^{-3}
10^{-4}
10^{-5}
20
30
40
SNR ρ_{dB}

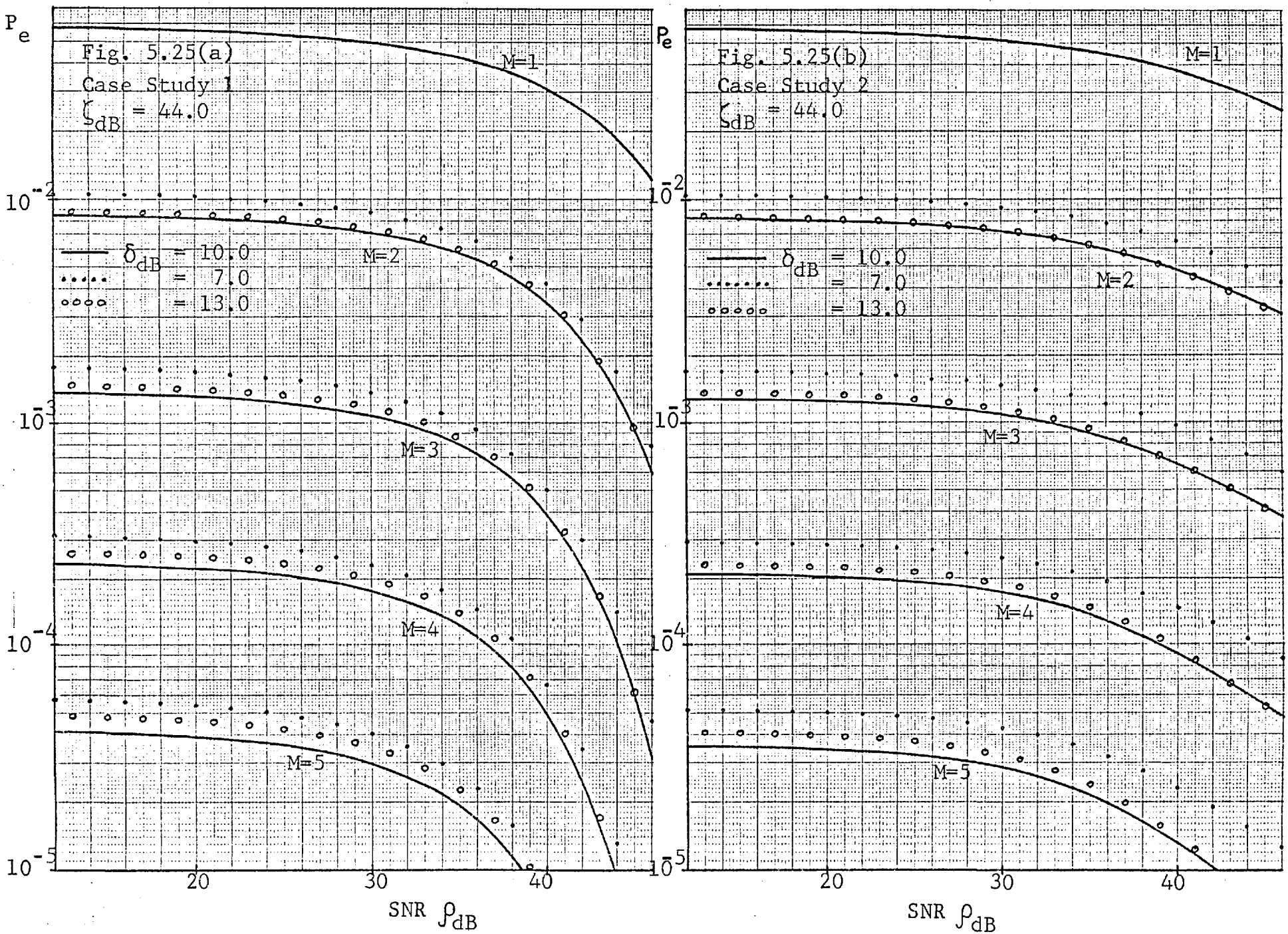
Fig. 5.25(a)
Case Study 1
ζ_{dB} = 44.0
P_e
M=1
M=2
M=3
M=4
M=5
δ_{dB} = 10.0
= 7.0
= 13.0
10^{-2}
10^{-3}
10^{-4}
10^{-5}
20
30
40
SNR ρ_{dB}
Fig. 5.25(b)
Case Study 2
ζ_{dB} = 44.0
P_e
M=1
M=2
M=3
M=4
M=5
δ_{dB} = 10.0
= 7.0
= 13.0
10^{-2}
10^{-3}
10^{-4}
10^{-5}
20
30
40
SNR ρ_{dB}

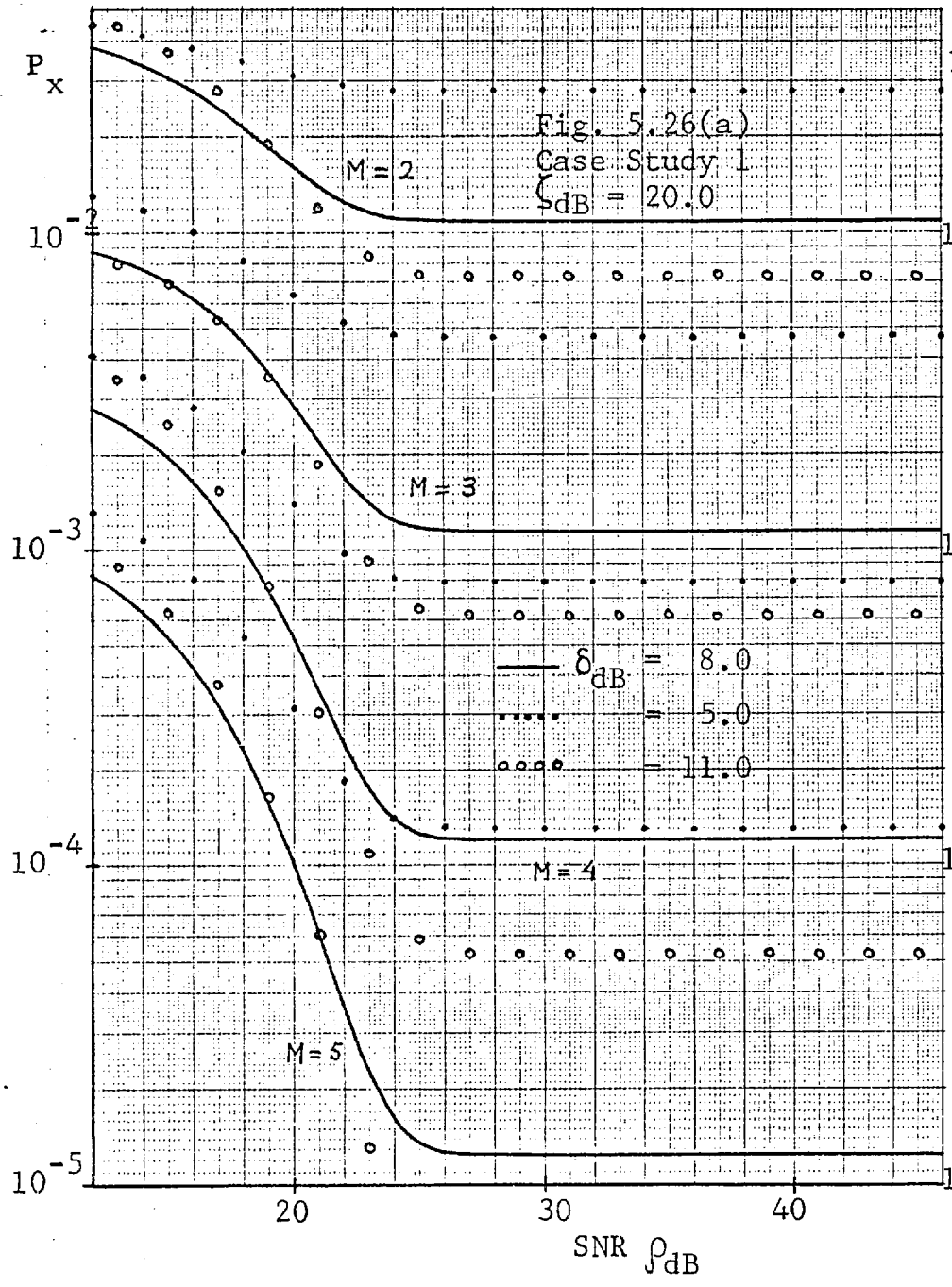
P_x
Fig. 5.26(a)
Case Study 1
ζ_{dB} = 20.0
M = 2
M = 3
M = 4
M = 5
10^{-2}
10^{-3}
10^{-4}
10^{-5}
δ_{dB} = 8.0
= 5.0
= 11.0
20
30
40
SNR ρ_{dB}

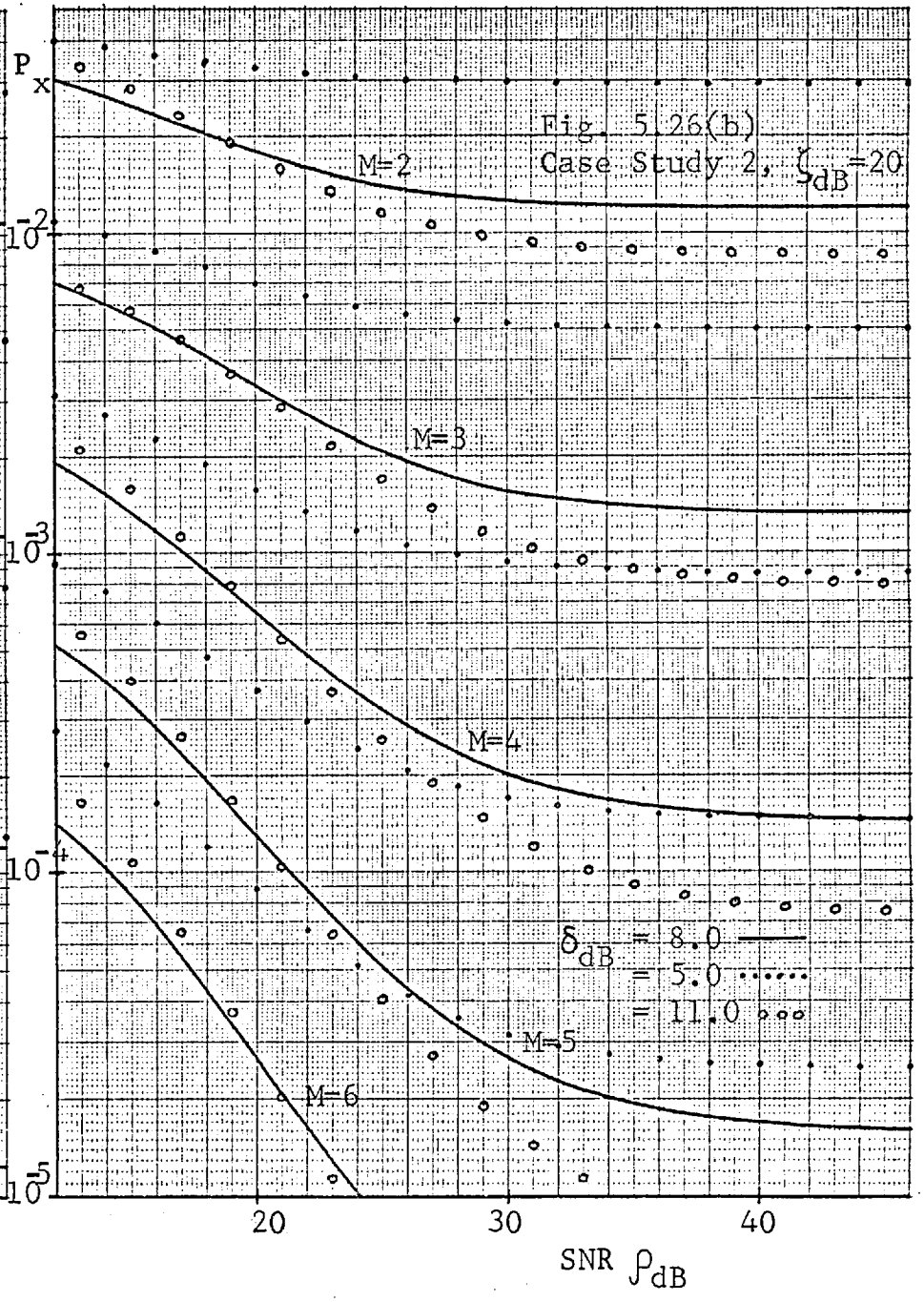
P_x
Fig. 5.26(b)
Case Study 2, ζ_{dB} =20
M=2
M=3
M=4
M=5
M=6
10^{-2}
10^{-3}
10^{-4}
10^{-5}
δ_{dB} = 8.0
= 5.0
= 11.0
20
30
40
SNR ρ_{dB}

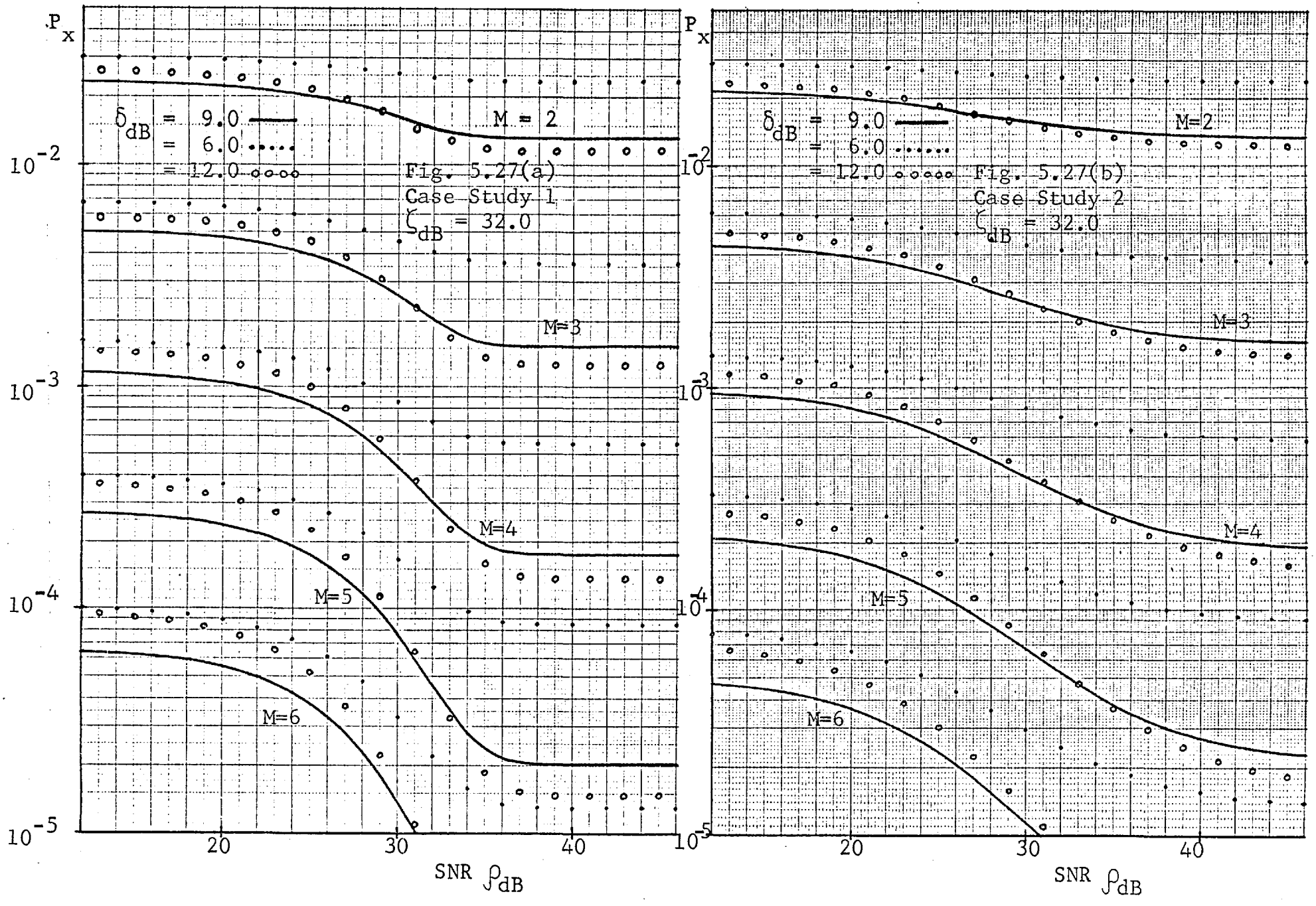
P_x
δ_{dB} = 9.0
= 6.0
= 12.0
M = 2
M=3
M=4
M=5
M=6
Fig. 5.27(a)
Case Study 1
ζ_{dB} = 32.0
10^{-2}
10^{-3}
10^{-4}
10^{-5}
20
30
40
SNR ρ_{dB}
P_x
δ_{dB} = 9.0
= 6.0
= 12.0
M=2
M=3
M=4
M=5
M=6
Fig. 5.27(b)
Case Study 2
ζ_{dB} = 32.0
10^{-2}
10^{-3}
10^{-4}
10^{-5}
20
30
40
SNR ρ_{dB}

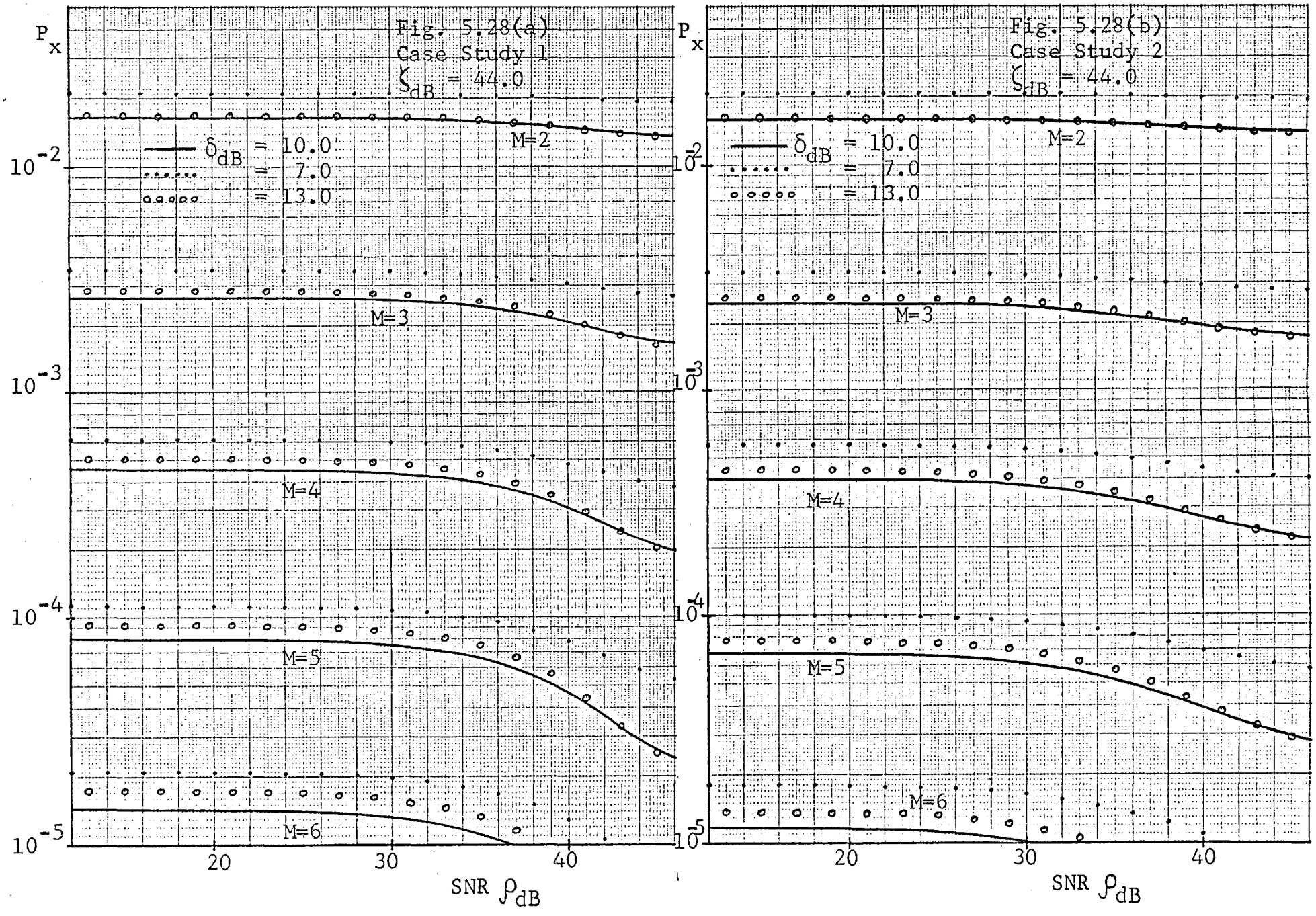
Fig. 5.28(a)
Case Study 1
ζ_{dB} = 44.0
P_x
δ_{dB} = 10.0
= 7.0
= 13.0
M=2
M=3
M=4
M=5
M=6
10^{-2}
10^{-3}
10^{-4}
10^{-5}
20
30
40
SNR ρ_{dB}
Fig. 5.28(b)
Case Study 2
ζ_{dB} = 44.0
P_x
δ_{dB} = 10.0
= 7.0
= 13.0
M=2
M=3
M=4
M=5
M=6
10^{-2}
10^{-3}
10^{-4}
10^{-5}
20
30
40
SNR ρ_{dB}

They are shown in Figs. 5.29 and 5.30. By comparing them with the graphs of class K it can be concluded that, within the range of parameters considered, the contribution of the upper branch of the receiver for the error probability is always smaller than the contribution of the lower branch, that is,

$$P_{eu} < P_x . P_{ex}.$$

For high values of ζ_{dB} it can be further concluded that P_{eu} is negligible compared with P_e.

N) Graphs giving the probability P_{ex} defined in subsection 5.2.3 and calculated with the help of relations (69) and (70).

These graphs are shown in Fig. 5.31 for Case 1 and in Fig. 5.32 for Case 2. In view of Equation (94) it is easy to conclude that in Case 2

$$P_{ex} \simeq \frac{1}{2} - \frac{1}{\pi} tg^{-1} \mu, \qquad (101)$$

and thus the P_{ex} curves in Fig. 5.32 are horizontal translations of each other.

O) Graphs giving the error probability $P_{e\ell}$ at the output of the lower branch of the receiver.

These graphs are presented in Fig. 5.33 for Case 1 and in Fig. 5.32 for Case 2. The method used for calculating $P_{e\ell}$ is explained in Appendix 2.3. It should be noted that the curves for ζ_{dB} = 32 dB can be obtained from those for ζ_{dB} = 44 dB by translating the latter 12 dB to the left. The same method can be used for any other $\zeta_{dB} < 44$ dB for reasons explained in Appendix 2.3. It is important to note that $P_{e\ell}$ is the error probability of a linear receiver which bases its decision on a long signal, as in the case of Chapter IV. Fig. 5.33 shows again that to render the noise Gaussian by accumulating noise samples is only beneficial for high SINR. Moreover, Fig. 5.32 shows that the use of long signals cannot be of any help in the case of a Cauchy amplitude distribution.

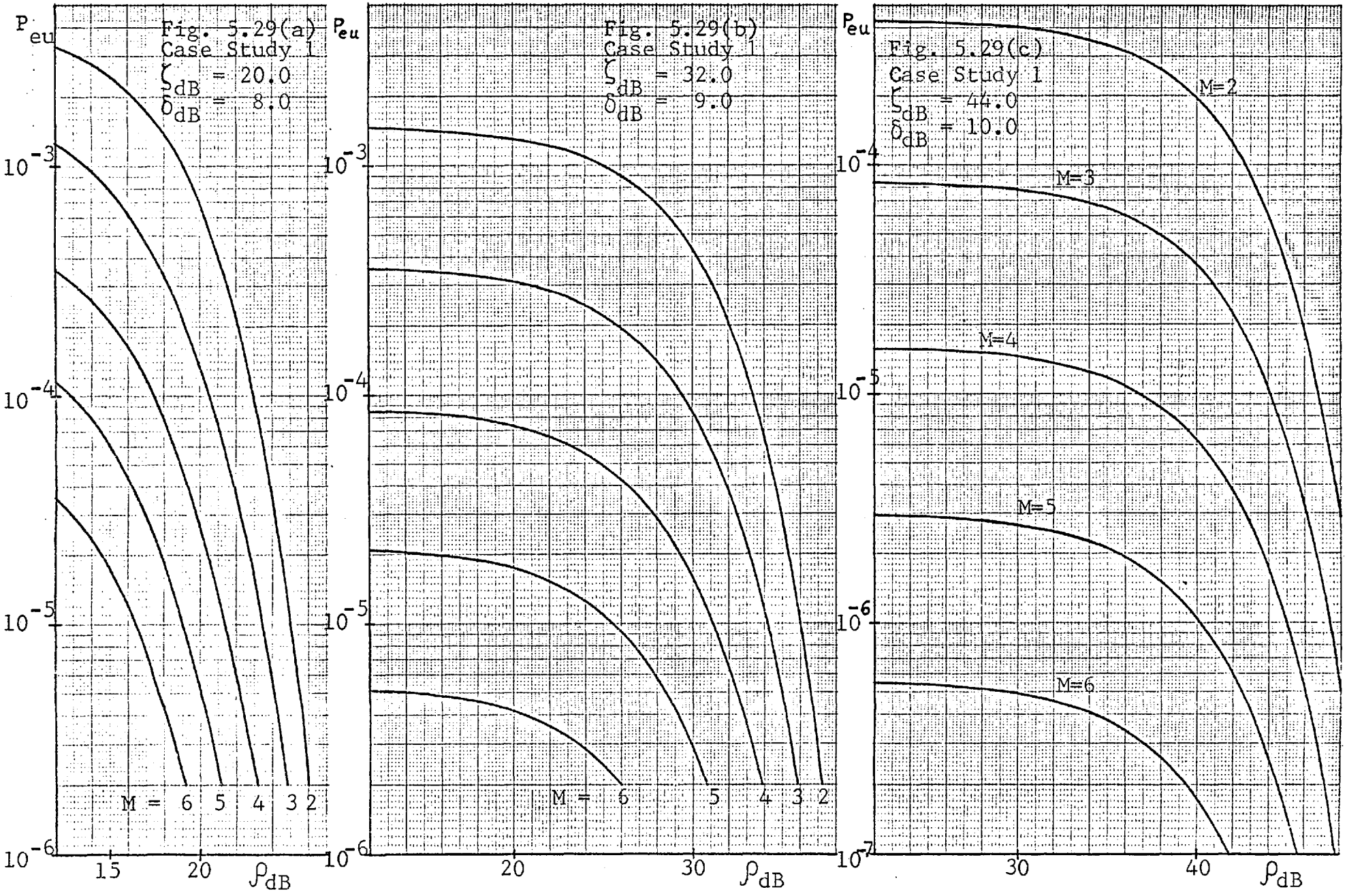
Fig. 5.29(a)
Case Study 1
ζ_{dB} = 20.0
δ_{dB} = 8.0
P_{eu}
10^{-3}
10^{-4}
10^{-5}
10^{-6}
M = 6 5 4 3 2
15
20
ρ_{dB}
Fig. 5.29(b)
Case Study 1
ζ_{dB} = 32.0
δ_{dB} = 9.0
P_{eu}
10^{-3}
10^{-4}
10^{-5}
10^{-6}
M = 6 5 4 3 2
20
30
ρ_{dB}
Fig. 5.29(c)
Case Study 1
ζ_{dB} = 44.0
δ_{dB} = 10.0
P_{eu}
10^{-4}
10^{-5}
10^{-6}
10^{-7}
M=2
M=3
M=4
M=5
M=6
30
40
ρ_{dB}

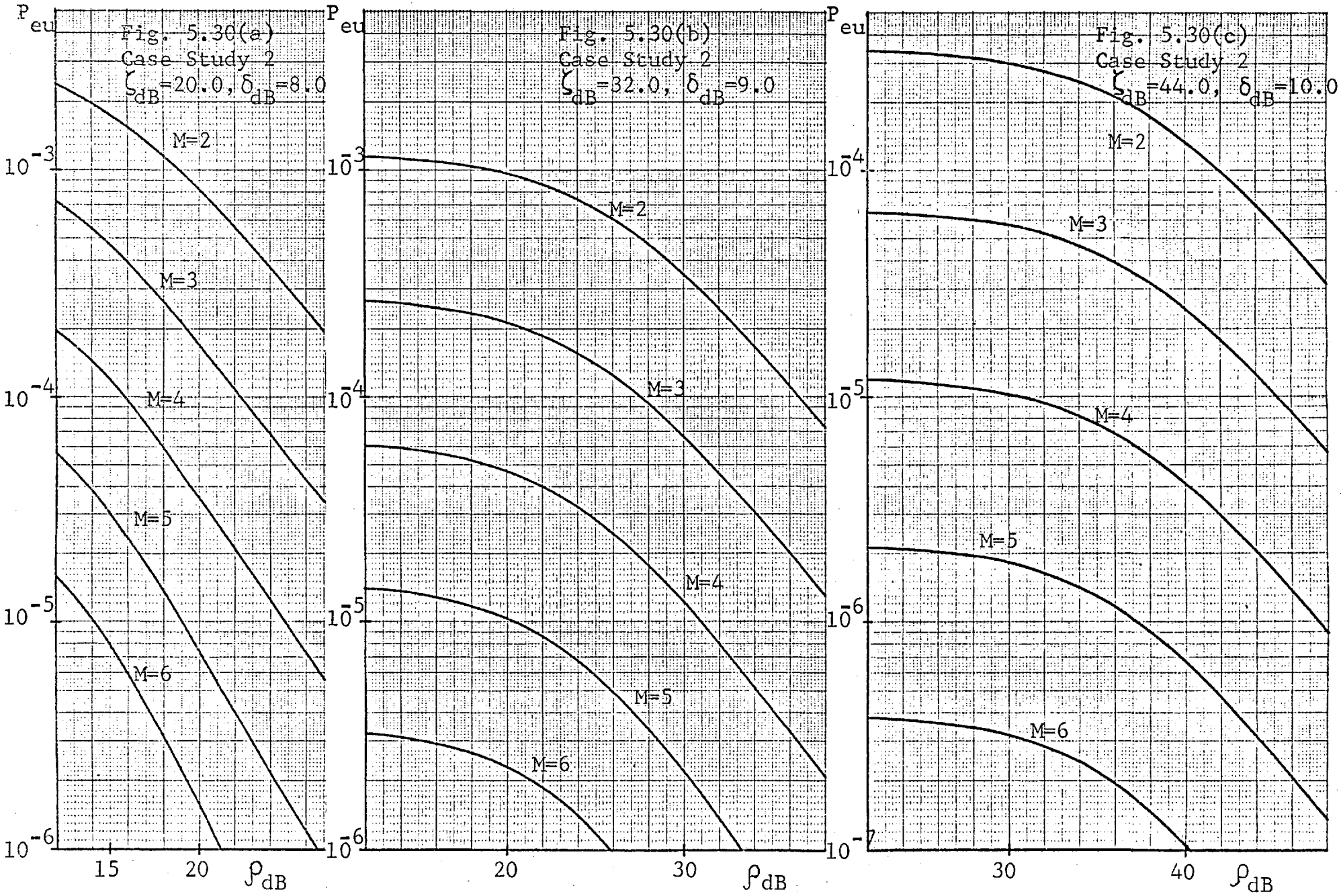
Fig. 5.30(a)
Case Study 2
ζ_{dB}=20.0, δ_{dB}=8.0
P_{eu}
10^{-3}
10^{-4}
10^{-5}
10^{-6}
M=2
M=3
M=4
M=5
M=6
15
20
ρ_{dB}
Fig. 5.30(b)
Case Study 2
ζ_{dB}=32.0, δ_{dB}=9.0
P_{eu}
10^{-3}
10^{-4}
10^{-5}
10^{-6}
M=2
M=3
M=4
M=5
M=6
20
30
ρ_{dB}
Fig. 5.30(c)
Case Study 2
ζ_{dB}=44.0, δ_{dB}=10.0
P_{eu}
10^{-4}
10^{-5}
10^{-6}
10^{-7}
M=2
M=3
M=4
M=5
M=6
30
40
ρ_{dB}

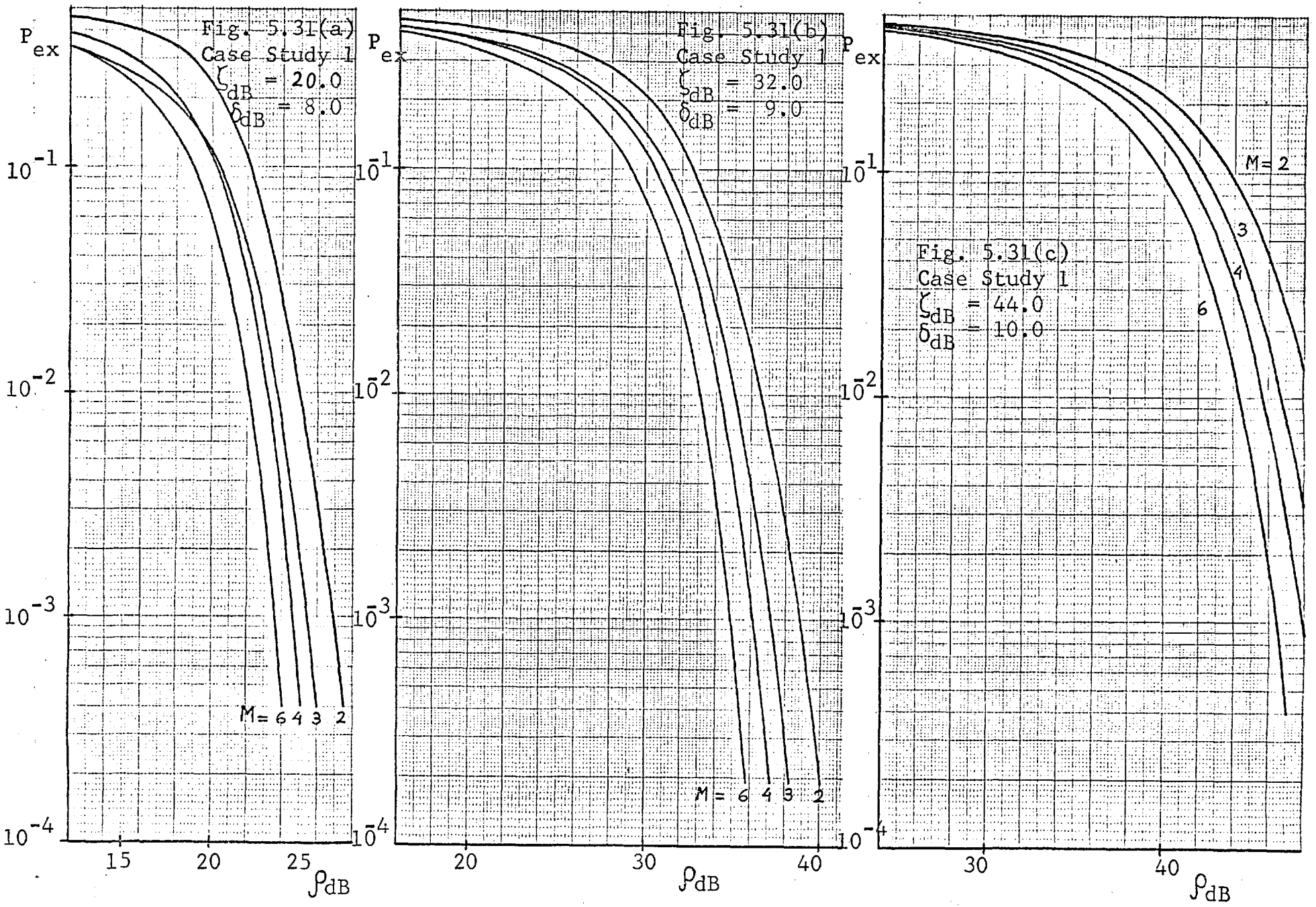
Fig. 5.31(a)
Case Study 1
ζ_{dB} = 20.0
δ_{dB} = 8.0
P_{ex}
10^{-1}
10^{-2}
10^{-3}
10^{-4}
M = 6 4 3 2
15
20
25
ρ_{dB}
Fig. 5.31(b)
Case Study 1
ζ_{dB} = 32.0
δ_{dB} = 9.0
P_{ex}
10^{-1}
10^{-2}
10^{-3}
10^{-4}
M = 6 4 3 2
20
30
40
ρ_{dB}
Fig. 5.31(c)
Case Study 1
ζ_{dB} = 44.0
δ_{dB} = 10.0
P_{ex}
10^{-1}
10^{-2}
10^{-3}
10^{-4}
M = 2
3
4
6
30
40
ρ_{dB}

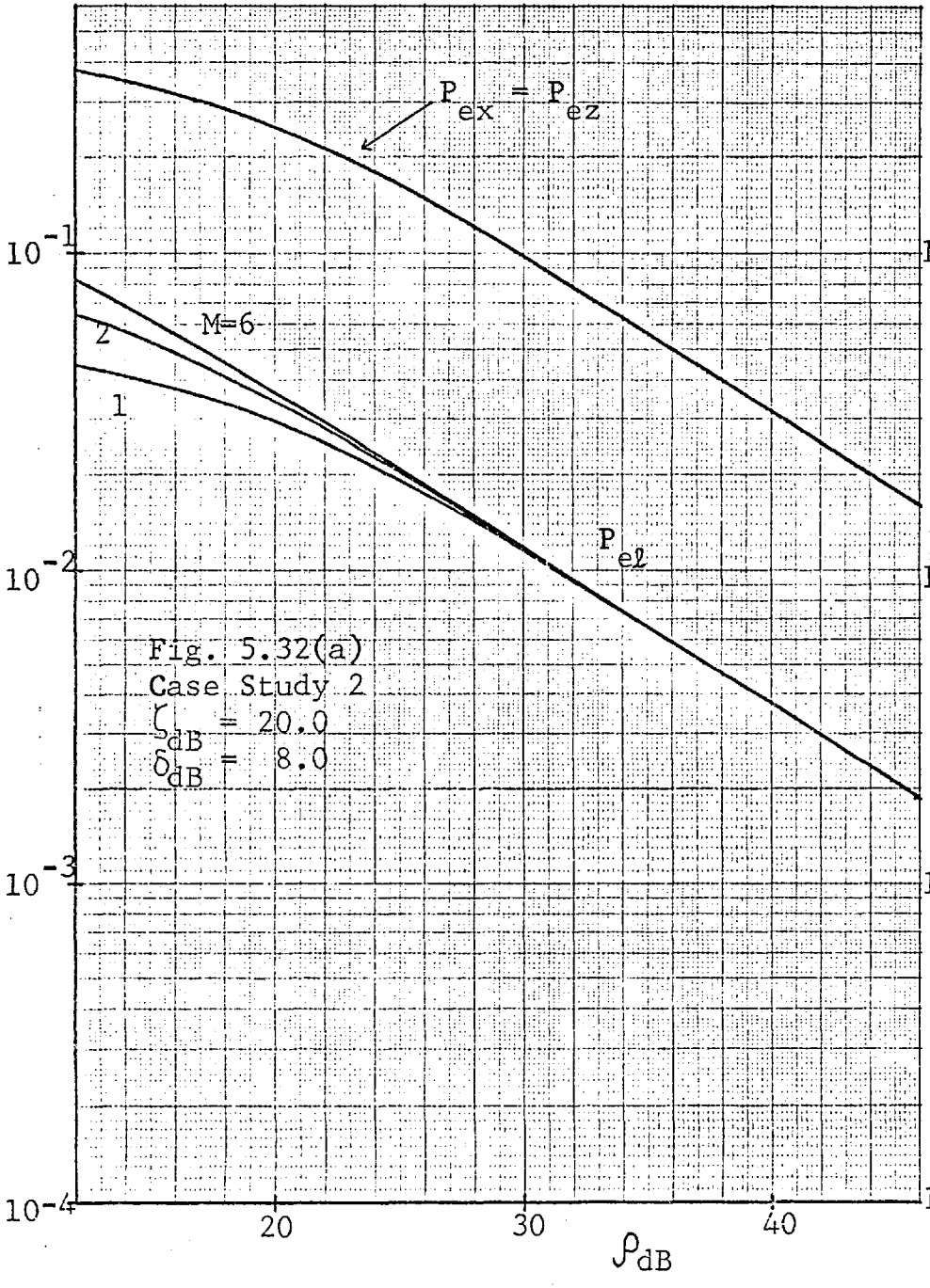

Fig. 5.32(a)
Case Study 2
$\zeta_{dB} = 20.0$
$\delta_{dB} = 8.0$

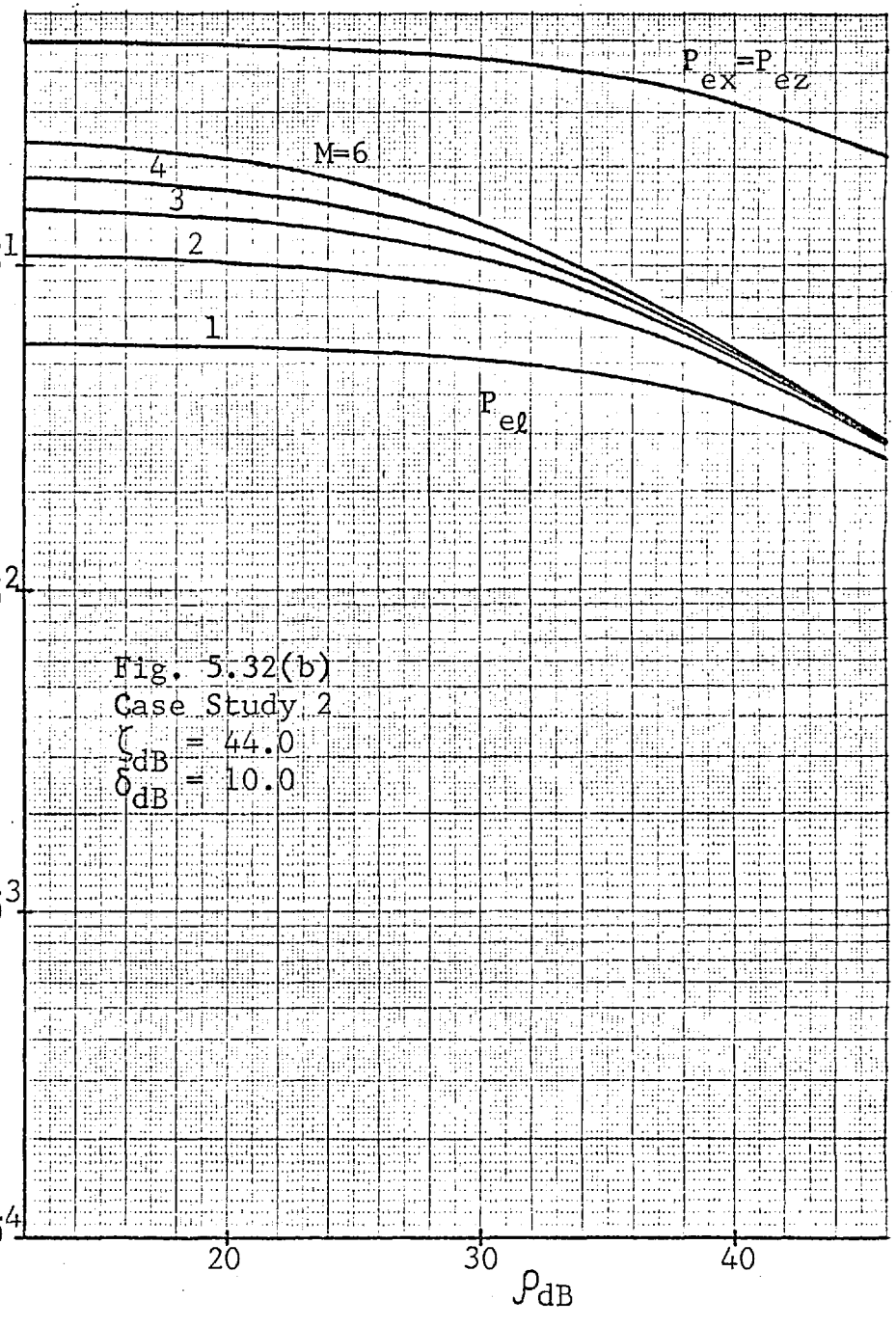

Fig. 5.32(b)
Case Study 2
$\zeta_{dB} = 44.0$
$\delta_{dB} = 10.0$

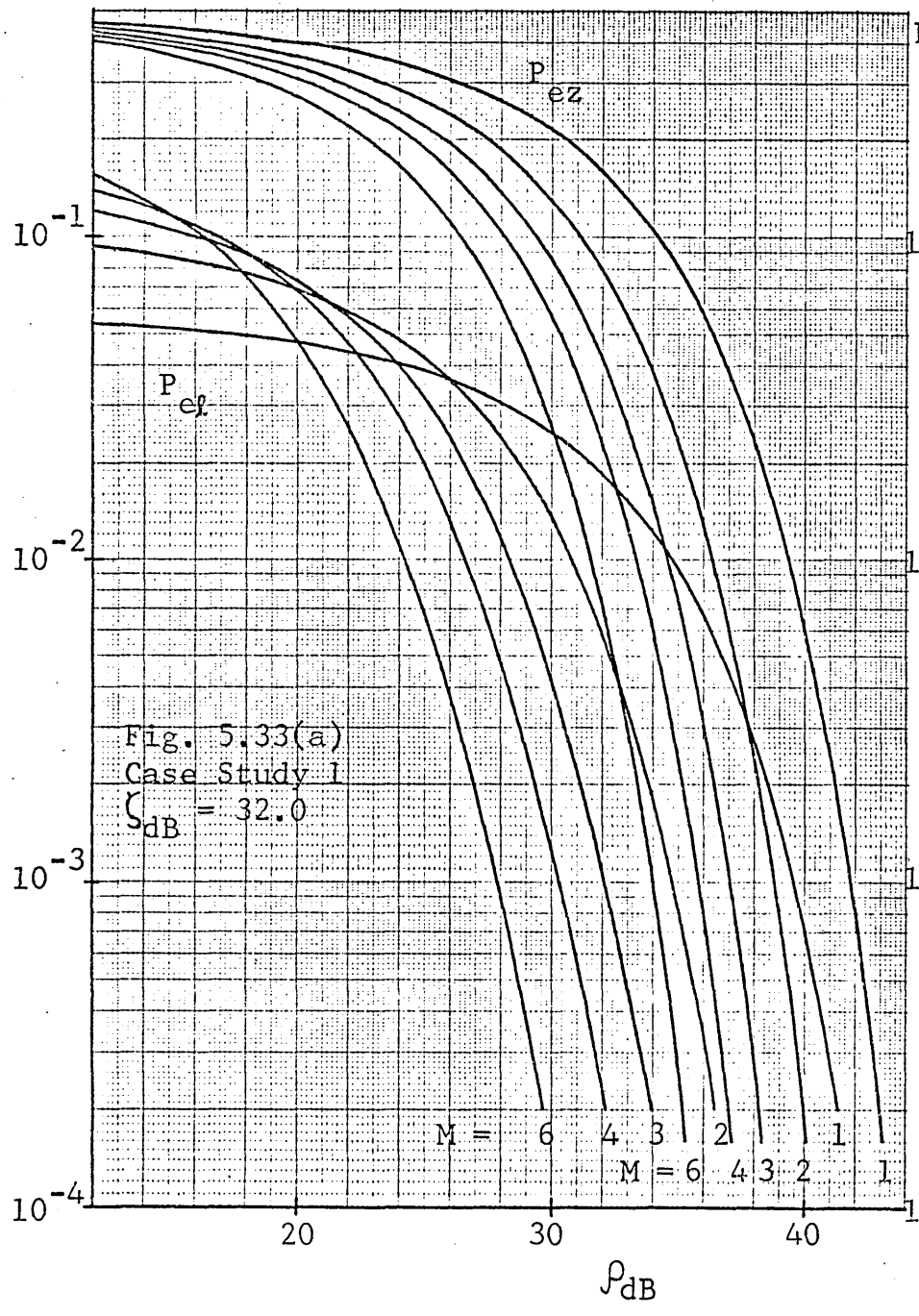

Fig. 5.33(a)
Case Study 1
$\zeta_{dB} = 32.0$

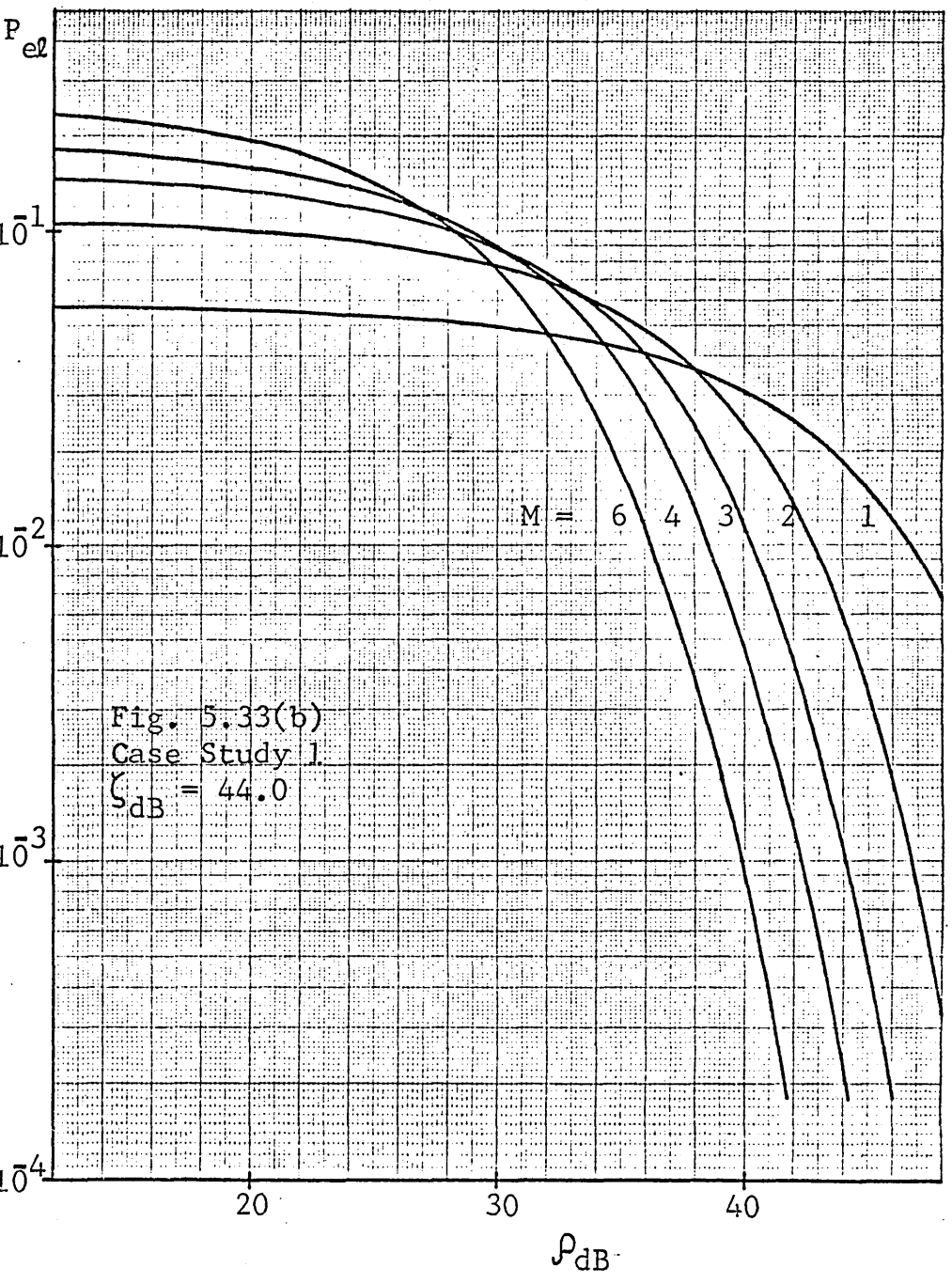

Fig. 5.33(b)
Case Study 1
$\zeta_{dB} = 44.0$

P) Graphs giving the error probability P_{ez} at the output of the lower branch of the receiver shown in Fig. 5.4, when all samples are corrupted by impulsive noise, that is, when p = 1.

These graphs are shown in Fig. 5.33(a) for Case 1 and in Fig. 5.32 for Case 2. The expressions for P_{ez} are given in Appendix 2.3. As can be seen, P_{ez} is only a function of p, M and μ. In view of relation (101) it follows that in Case 2

$$P_{ez} \simeq P_{ex}.$$

This relation is also true in Case 1, as can be seen by comparing the graphs in Figs. 5.33(a) and 5.31. These graphs give a value of P_{ex} slightly higher than the value of P_{ez}, which is due to the error of the approximation given by relation (70). Since the noise detector makes some errors in detecting the presence of the samples corrupted by impulsive noise it follows that P_{ex} is the value of $P_{e\ell}$ corresponding to a value of p less than unity. Therefore, in the cases where the conditions (83) and (84) are satisfied the actual value of P_{ex} is slightly smaller than P_{ez} and the relation

$$P_e \simeq P_{eu} + P_x P_{ez} \qquad (102)$$

thus gives a tight upper bound on P_e. This point will be taken up again in Chapter VI where relation (102) is shown to give a good approximation, with the help of the results of Monte Carlo simulations.

Q) Graphs giving the error probability P_{LB} defined by Equation (87).

These graphs are shown in Fig. 5.34. By comparing them with the graphs of Fig. 5.18 it can be seen that if $\mu_{dB} \ll 0$ dB, ζ_{dB} is not very high and M is large then P_{LB} can be much smaller than P_e, which means that in such case an improvement in the design of the noise detector may be worthwhile. It

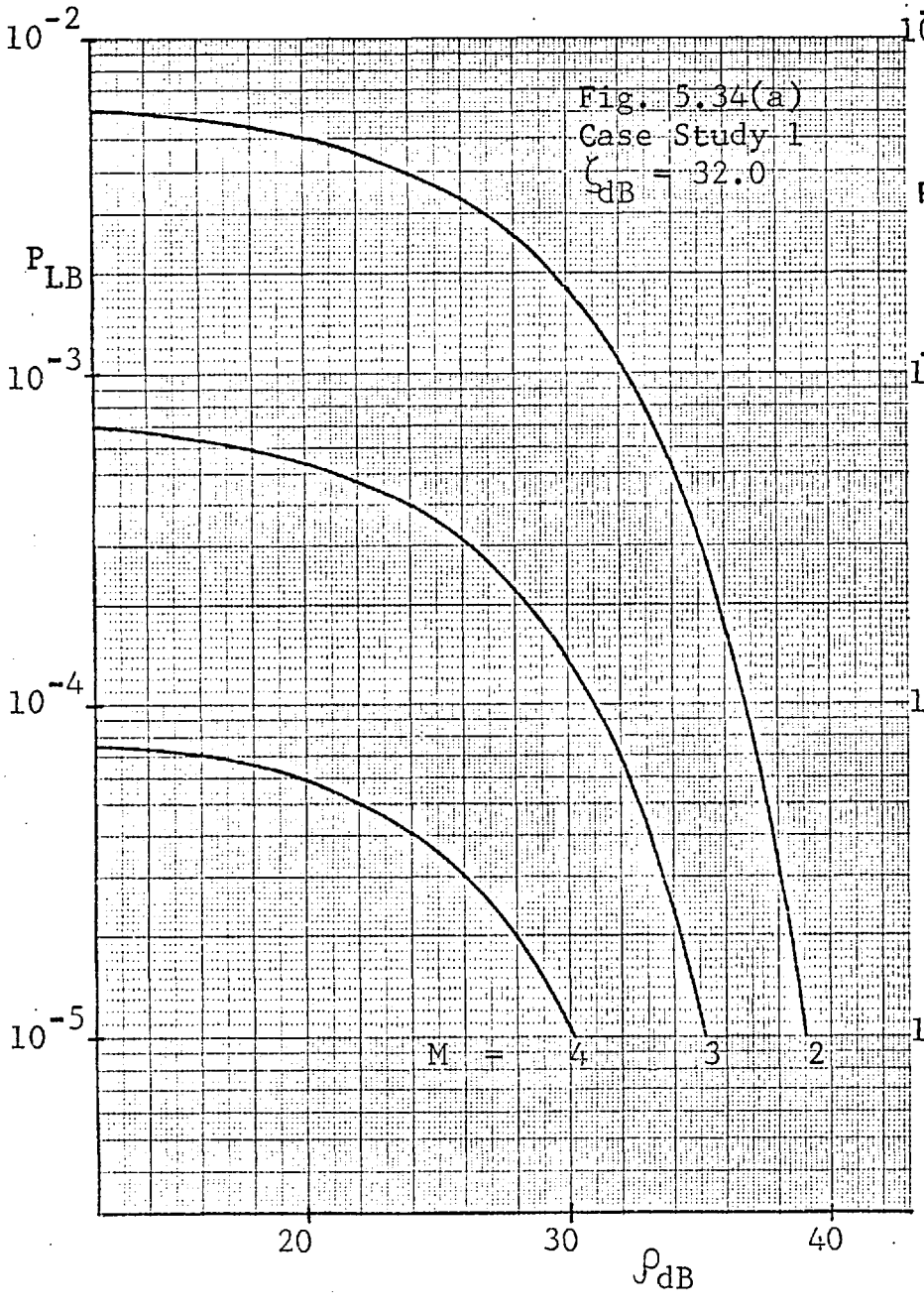
Fig. 5.34(a)
Case Study 1
ζ_{dB} = 32.0
P_{LB}
10^{-2}
10^{-3}
10^{-4}
10^{-5}
M = 4
3
2
20
30
40
ρ_{dB}

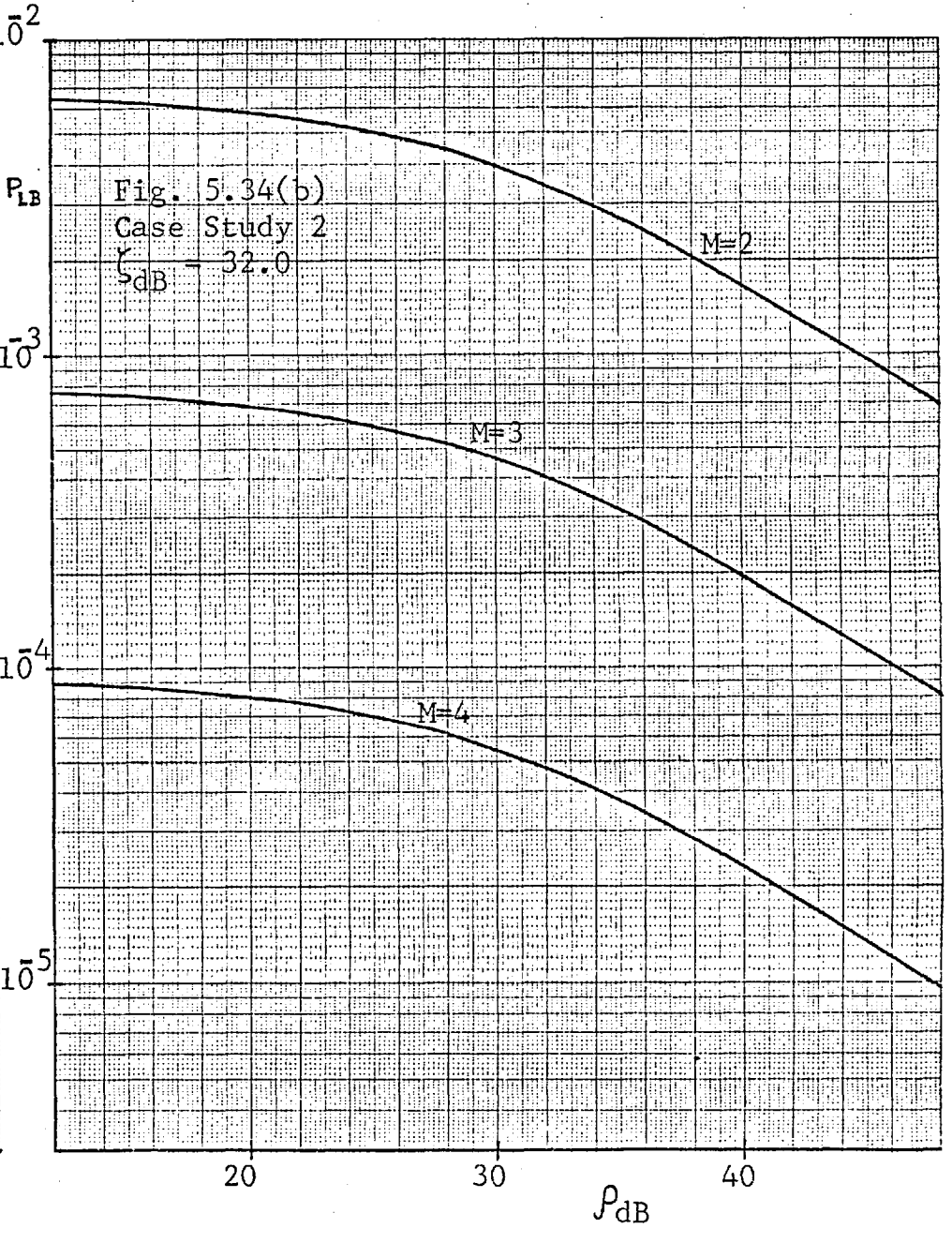
Fig. 5.34(b)
Case Study 2
ζ_{dB} = 32.0
P_{LB}
10^{-2}
10^{-3}
10^{-4}
10^{-5}
M=2
M=3
M=4
20
30
40
ρ_{dB}

can also be seen that, for high ρ_{dB} and low ζ_{dB}, the error probability P_e can be slightly lower than P_{LB} because

$$P_x \simeq P_o^M \simeq p^M(1 - \beta)^M < p^M.$$

R) Graphs giving the value (in dB) of the ratio $\delta = \varepsilon_o/\sigma_w$ that minimizes the error probability P_{eu} at the output of the receiver upper branch.

These graphs are shown in Fig. 5.35. In Case 2 the value of δ is almost independent of the SGNR ρ. By comparison with the graphs in Fig. 5.20 it can be concluded that, if $\rho_{dB} \geq$ 18 dB, the value of δ that minimizes P_{eu} is smaller than the value of δ that minimizes P_x. In view of relation (102), the value of δ that minimizes P_e thus lies between these two values. The fact that, for any fixed $\rho_{dB} > 12$ dB,

$$\lim_{\zeta \to \infty} (P_{eu}/P_e) = 0 \qquad (103)$$

means that the receiver that minimizes the erasure probability P_x is asymptotically optimal as $\mu \longrightarrow 0$. However, the numerical results show that in both of the cases studied the receiver is nearly optimal whenever $\mu_{dB} \leq 0$ dB.

This section is concluded by noting that for high ζ the performance of the receiver in the presence of both types of impulsive noise considered are nearly identical. However, if ζ is low and ρ is high the error probability in Case 1 is much lower than that in Case 2. This stems from the fact that the Gaussian PDF has short tails compared with the Cauchy PDF.

5.4 CONCLUSIONS

The numerical results discussed in the previous section permit a few conclusions to be drawn that are valid in both of the cases considered. These conclusions are also believed to be valid for any other amplitude distribution of the impulsive noise

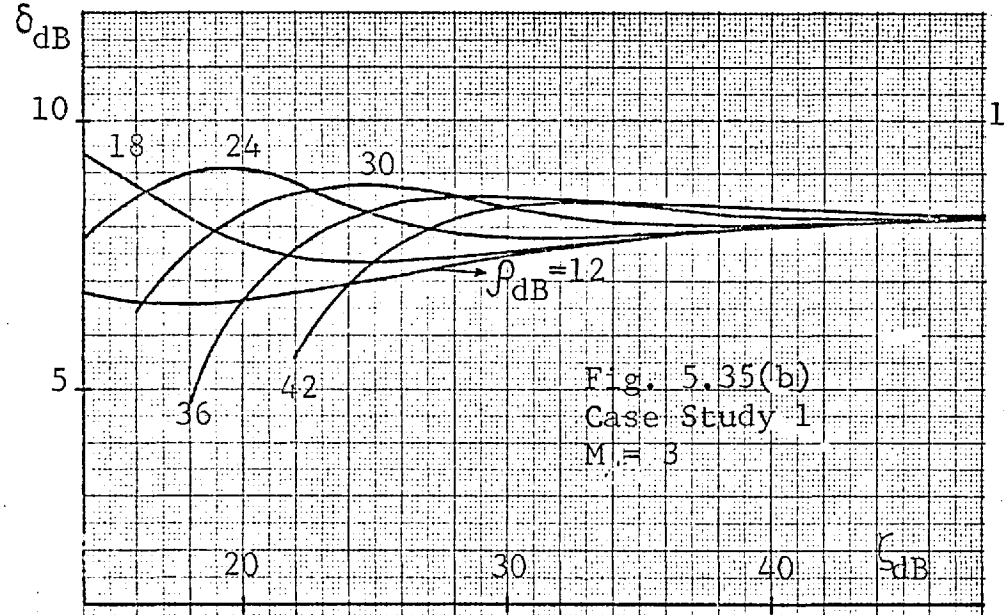

Fig. 5.35(b)
Case Study 1
M = 3

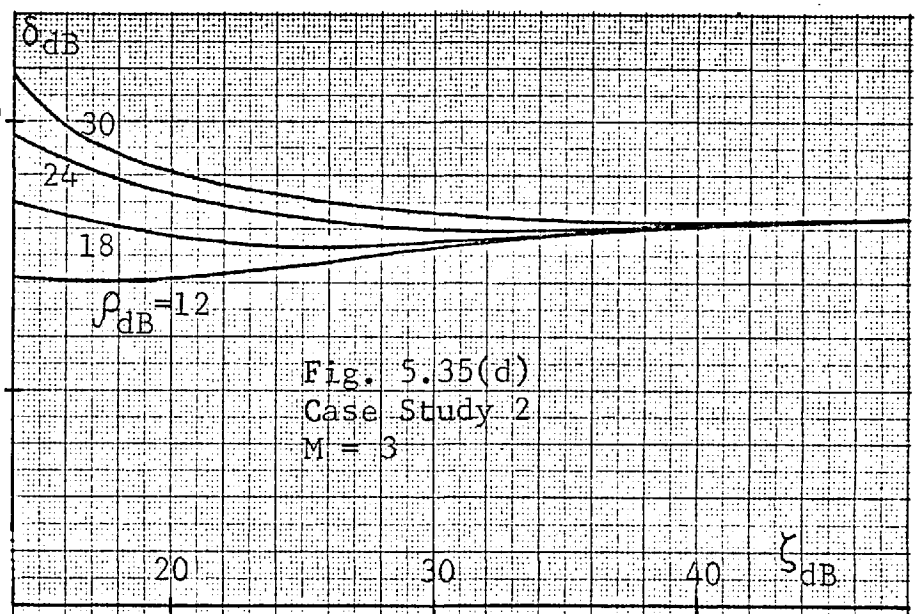

Fig. 5.35(d)
Case Study 2
M = 3

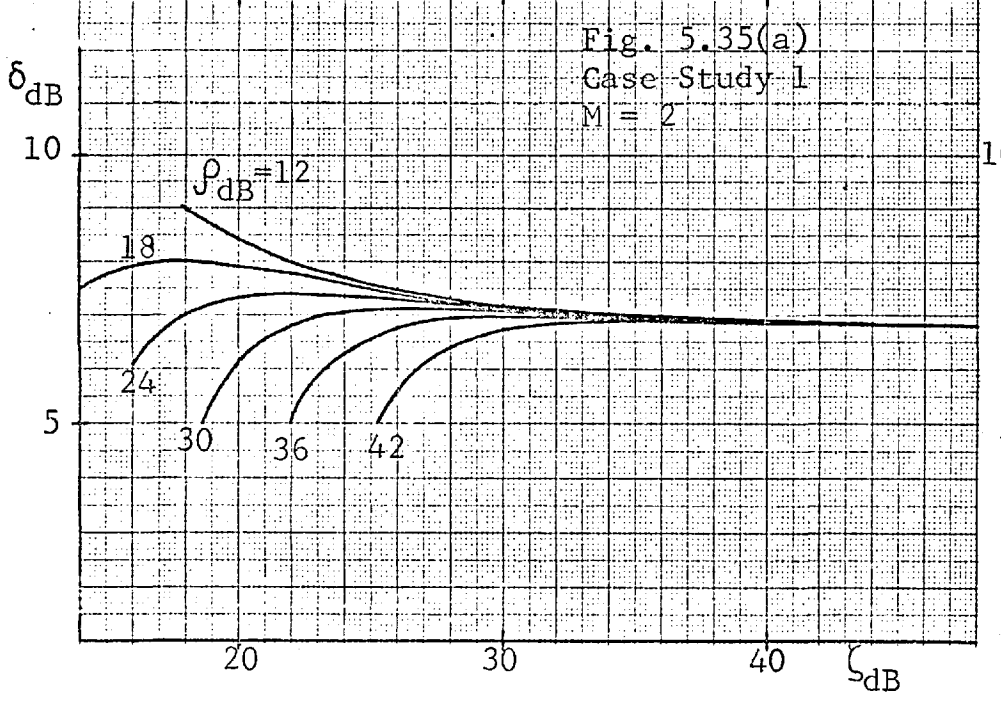

Fig. 5.35(a)
Case Study 1
M = 2

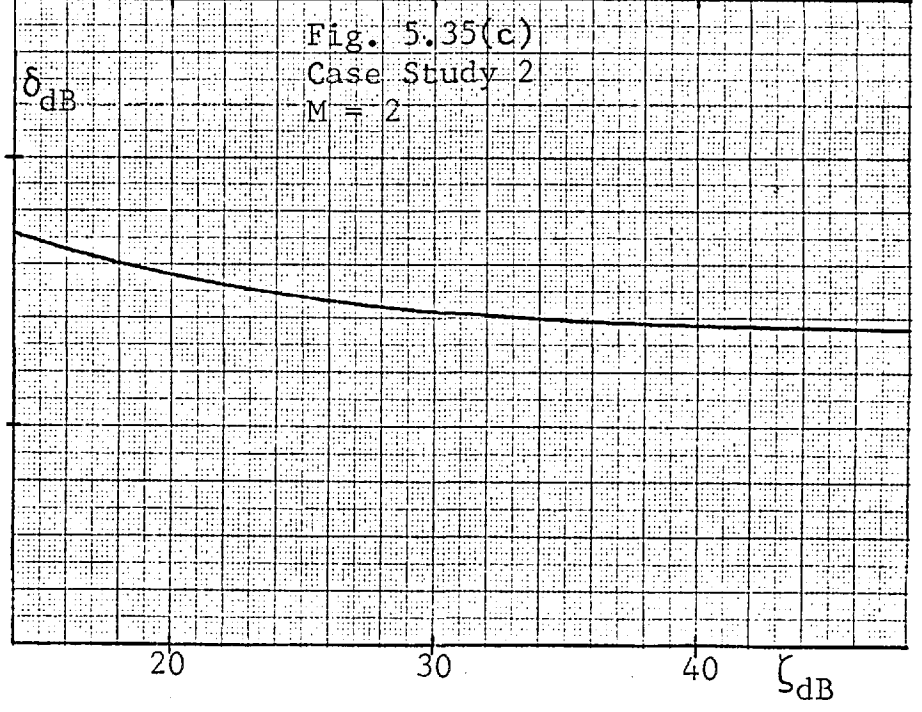

Fig. 5.35(c)
Case Study 2
M = 2

component. The conclusions are as follows*:

(a) If the SINR $\mu_{dB} < 0$ dB, the receiver thresholds ε_1 and ε_2 can be set to the same value ε_0 without significantly affecting the performance.

(b) The double-path receiver is asymptotically optimal as $\mu \longrightarrow 0$. In different terms, if $\mu_{dB} \ll 0$ dB, the values of the likelihood ratio $\Lambda(S_i)$ defined by Equation (14), when $S_i = A \pm \varepsilon_o$ and ε_o is given the optimum value, are nearly equal and thus the noise detection operation can be described with good approximation by relations (15).

(c) If $\mu_{dB} < 0$ dB, the error probability P_e is given with good approximation by

$$P_e = P_{eu} + P_x . P_{ez} \qquad (104)$$

where P_{eu} is the error probability at the output of the receiver upper branch, P_x is the erasure probability at the same point, and P_{ez} is the error probability at the output of the receiver lower branch when this branch is subjected to a continual noise with the same amplitude distribution as the impulsive noise component. It can therefore be concluded from relation (104) that the lower branch of the receiver must be designed as an optimal receiver to overcome a continual noise, which will usually be non-Gaussian.

(d) If $\mu_{dB} < 0$ dB, the minimization of P_x as a function of ε_0 leads to a value of P_e very close to the minimum the receiver can achieve. This is related to the fact that both P_{eu} and P_x show quite shallow minima at values of ε_0 close to each other. Since an estimate of P_x is easy to obtain while the receiver is operating, the adaptive receiver that tries to minimize P_x seems quite easy to implement. Since

---

* As in the previous sections, it is assumed here that the SGNR $\rho_{dB} > 12$ dB.

$$\lim_{\mu \to 0} P_e = \frac{1}{2} P_x,$$

this adaptive receiver will be asymptotically optimal as $\mu \longrightarrow 0$.

(e) If $\mu_{dB} \ll 0$ dB, the minimum erasure probability is only slightly greater than the probability of M consecutive signal samples being corrupted by impulsive noise. In the case in which the impulsive noise samples occur independently, with probability p, it is possible to write

$$\lim_{\mu \to 0} P_x = p^M.$$

(f) Let a group of K consecutive samples of impulsive noise be called a burst. If $\bar{K}$ is the average burst length and $\bar{n}$ is the average burst-free interval then the probability p of a signal sample being corrupted by impulsive noise is given by

$$p = \frac{\bar{K}}{\bar{K} + \bar{n}}$$

If it happens that $\bar{n} \geqslant \bar{K} \gg M$ and thus most bursts have lengths much greater than M, then the fraction of pulse sequences of length M which are fully corrupted by impulsive noise is approximately equal to p, and thus independent of M. Therefore, in this case

$$\lim_{\mu \to 0} P_e \simeq \frac{p}{2}.$$

Under such conditions a scrambler-descrambler pair would be necessary in order to randomize the occurrence of the impulsive noise samples at the input of the receiver, and thus make $\bar{K} \ll M$. In the limit where a perfect randomization is attained

$$\bar{K} = \frac{1}{1 - p} \quad \text{and} \quad \bar{n} = \frac{1}{p},$$

since in this case the burst length will follow a geometric distribution, i.e.

$$P[K = i] = (1 - p)p^{i-1},$$

and the burst-free interval will follow the same type of

distribution, i.e.

$$P[n = i] = p(1 - p)^{i-1}$$

These points will be developed further in Chapter VI.

CHAPTER VI

COMPUTER SIMULATION OF THE IMPULSIVE NOISE CHANNEL

I can, if the worst comes to the worst, still realize that the Good Lord may have created a world in which there are no natural laws. In short, a chaos. But that there should be statistical laws with definite solutions, i.e. laws that compel the Good Lord to throw the dice in each individual case, I find highly disagreeable.

A. Einstein, quoted in C. Seelig, "Albert Einstein".

6.1 THE SIMULATION PROBLEM

In several situations considered previously, particularly in Chapter V, problems arose whose numerical solutions could not be obtained by direct computation. The reasons for the difficulty were that either analytical expressions were not available or direct computation based on existing expressions required too much computer-time.

A way out of these difficulties is sometimes offered by the so-called Monte-Carlo techniques. In this case the solution is attained in four steps:

(a) generation of the transmitted data sequence;

(b) generation of the noise, which is then combined linearly with the transmitted signal to obtain the received signal;

(c) application of the detection operation to the received signal so as to obtain the received data sequence;

(d) comparison of this sequence with the transmitted one to count the number of errors that have occurred, from which the required estimate of the error probability is then readily derived.

It is assumed throughout this chapter that the transmitted data sequence is binary and thus step (a) above requires in general the use of a binary pseudo-random generator. However, in all cases studied in this chapter the probability of detecting a digit in error is the same whether it is a "zero" or a "one" and, therefore, it is possible and convenient to assume that the transmitter sends a sequence of identical digits (say, zeros). It is also assumed in this chapter that the receiver processes samples of the received signal. Therefore, step (b) of the simulation procedure can be accomplished by using a pseudo-random number generator to generate the noise samples, which

are then combined linearly with the corresponding samples of the transmitted signal.

The generation of the noise samples usually takes most of the computer-time in the simulation procedure. Since in order to obtain a sufficiently accurate estimate of the error probability it is usually necessary to use a long transmitted data sequence, the noise structure must be simple enough to permit its generation in a reasonable amount of time. In what follows an attempt is made to simplify the structure of the impulsive noise by maintaining in the simulated time-series only those characteristics of the actual noise which appear to affect significantly the performance of the communication system under test.

Before the simulation experiment starts it is very desirable to have an estimate of the number of transmitted digits required to estimate the error probability with a prescribed accuracy. Assuming for simplicity that the errors are statistically independent events, the number of errors in n digits obeys a binomial distribution of mean $n P_e$ and variance $nP_e(1-P_e)$, where P_e is the probability of error. For sufficiently large n this distribution becomes approximately Gaussian and thus the probability of a given number of errors can be easily determined. The relative error in estimating P_e is given by $(x - nP_e)/(nP_e)$, where x is the number of observed errors. This relative error has an approximately Gaussian distribution with zero mean and standard deviation $\sqrt{(1-P_e)/(nP_e)}$. Thus, to find the probability P of maintaining a given level of accuracy α it is necessary to determine n from the equation

$$P = \text{Prob}\left[\left|\frac{x-nP_e}{nP_e}\right| \leq \alpha\right]$$

$$\simeq \frac{1}{\sqrt{2\pi}} \int_{-K\alpha}^{K\alpha} \varepsilon^{-t^2/2}\, dt = \varphi(K\alpha) \qquad (1)$$

where $K = \sqrt{\frac{nP_e}{1-P_e}}$.

This can be written in the form

$$K = \frac{1}{\alpha}\varphi^{-1}(P) \qquad (2)$$

or

$$n = K^2 \frac{1-P_e}{P_e} \qquad (3)$$

Therefore, if P = 90% and $\alpha = 0.1$ then

$$n \simeq \frac{300}{P_e} \qquad (4)$$

The author's experience is that, in order not to exceed an acceptable amount of computer-time, it is impossible to estimate error probabilities of an order of magnitude less than 10^{-3}.

In the remainder of this chapter the theory for simulation of certain kinds of impulsive noise is developed and this is then used to tackle some of the problems which were not solved in previous chapters.

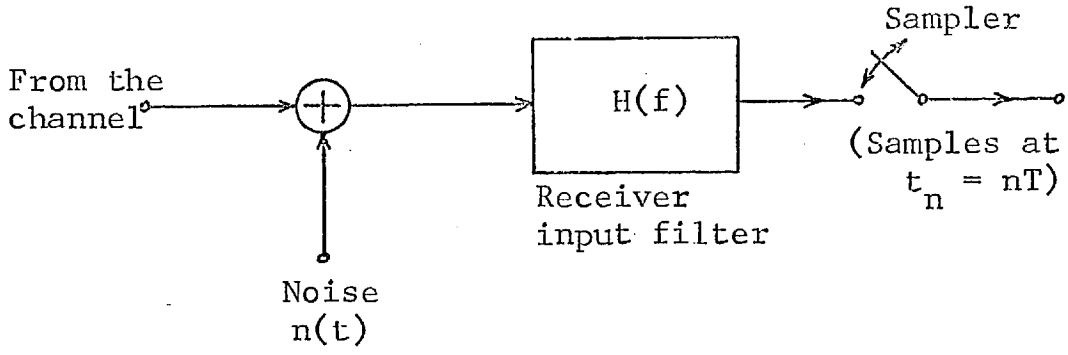

Fig. 6.1

6.2 SIMULATION OF IMPULSIVE NOISE

6.2.1 Poisson impulse noise

An attempt will now be made to find a procedure for implementing a pseudo-random number generator capable of producing a sequence of numbers having the same statistical properties as the sequence of noise samples at the sampler output in Fig. 6.1.

In this figure it is assumed that n(t) is an ideal Poisson impulse noise, that is

$$n(t) = \sum_{i=-\infty}^{\infty} r_i \, \delta(t - \tau_i) \tag{5}$$

where the τ_i form a sequence of purely random instants to which corresponds a fixed average repetition rate of ν impulses per second. This means that the time intervals between impulses, $T_i = \tau_{i+1} - \tau_i$, obey an exponential distribution with PDF

$$p_T(x) = \begin{cases} \nu \, \varepsilon^{-\nu x}, & x > 0 \\ 0, & x < 0 \end{cases} \tag{6}$$

It is possible to show that, under these circumstances, the number N(t) of pulses occurring in the interval (t_o, t_o+t) is distributed according to the Poisson law, i.e.

$$P[N(t)=K] = \varepsilon^{-\nu t} \frac{(\nu t)^K}{K!} \tag{7}$$

Let $\{u_i\}$ be the sequence of noise samples at the sampler output in Fig. 6.1. As stated in Chapter II, the first-order PDF $p_u(x)$ of the u_i's has a characteristic function (CHF) $F_u(\omega)$ given by

$$F_u(\omega) = \exp\left\{\nu \int_{-\infty}^{\infty} [F_r(\omega h(t)) - 1] \, dt\right\} \tag{8}$$

where $F_r(\omega)$ is the CHF of the impulse intensities (areas) r_i appearing in Equation (5), and h(t) is the impulse response of the receiver input filter. Throughout this chapter it is assumed that the PDF $p_r(x)$ corresponding to the CHF $F_r(\omega)$ is a symmetric unimodal PDF, thus having a zero mean. It follows immediately from Equations (15) and (16) in Chapter II that

$$E[u_i] = 0 \tag{9}$$

and

$$E[u_i u_K] = \nu \cdot E[r_i^2] \cdot \int_{-\infty}^{\infty} h(t+iT)h(t+KT)dt \tag{10}$$

where the variances $E[r_i^2]$ are assumed to have the same finite value. Assuming, as in Chapters IV and V, that h(t) is a

Nyquist pulse, it becomes apparent that $\{u_i\}$ is an uncorrelated time-series with zero mean, no matter what other statistical properties are assumed for $\{r_i\}$. Hence

$$\sigma_u^2 = \nu\sigma_r^2 . \int_{-\infty}^{\infty} h^2(t)dt \qquad (11)$$

where σ_u^2 and σ_r^2 are the variances of $p_u(x)$ and $p_r(x)$ respectively. It is possible, without any loss of generality, to assume that

$$\int_{-\infty}^{\infty} h^2(t)dt = 1 \qquad (12)$$

and hence $\sigma_u^2 = \nu\sigma_r^2$. (13)

In what follows it is assumed that the transfer function H(f) is real and hence h(t) = h(-t). By defining the waveforms*

$$f(t) = h(t)\, G_a(\tfrac{t}{T}) \qquad (14)$$

$$g(t) = h(t) - f(t) \qquad (15)$$

$F_u(\omega)$ can be factorized as follows:

$$F_u(\omega) = F_x(\omega).F_y(\omega) \qquad (16)$$

where

$$F_x(\omega) = \exp\left\{\nu\int_{-T/2}^{T/2} [F_r(\omega f(t)) - 1]\,dt\right\} \qquad (17)$$

and

$$F_y(\omega) = \exp\left\{\nu\int_{-\infty}^{\infty} [F_r(\omega g(t)) - 1]\,dt\right\} \qquad (18)$$

If it is noted that the filter in Fig. 6.1 can be replaced by two filters in parallel, as shown in Fig. 6.2, it becomes obvious that $F_x(\omega)$ and $F_y(\omega)$ are the CHF's of the noise samples due to the impulse responses f(t) and g(t), respectively. It is easy to see that the samples $\{x_i\}$, resulting from f(t), and the samples $\{y_i\}$, resulting from g(t), have zero means and variances given by

$$\sigma_x^2 = \sigma_u^2\,\eta^2 \qquad (19)$$

---

* $G_a(x) = 1$ if $|x| < 0.5$ and zero otherwise.

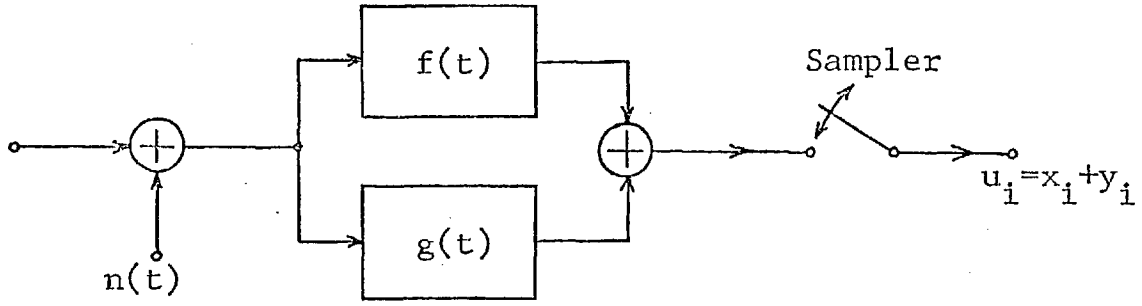

Fig. 6.2

and

$$\sigma_y^2 = \sigma_u^2 (1 - \eta^2) \tag{20}$$

respectively, where

$$\eta^2 = \int_{-T/2}^{T/2} h^2(t)dt. \tag{21}$$

Moreover, it can easily be seen that

$$\lim_{\omega \to \infty} F_x(\omega) = \exp(-\nu T) = q = 1-p \tag{22}$$

and

$$\lim_{\omega \to \infty} F_y(\omega) = 0. \tag{23}$$

In Equation (22) the parameter q is clearly the probability of a sampling instant not being affected by any noise pulse of shape f(t). Since f(t) is limited to a time interval of duration T, it is obvious that the samples $\{x_i\}$ are statistically independent. The same is not true, in general, for the samples $\{y_i\}$ which, according to Equation (23), belong to a continual noise. Furthermore, it cannot be concluded from Equation (16) that the samples $\{x_i\}$ are statistically independent from the samples $\{y_i\}$*.

If the Nyquist pulse h(t) is fairly well designed, the energy fraction η^2 will be very close to unity and thus $\sigma_y^2 \ll \sigma_x^2$. When a background Gaussian noise of variance σ_w^2 is present its samples will be included in $\{y_i\}$ thus making

$$\sigma_y^2 = \sigma_w^2 + \sigma_u^2 (1 - \eta^2) \tag{24}$$

---

* See Ref. [6-1], page 113.

The term $\sigma_u^2(1 - \eta^2)$ may in some practical cases be of the same order of magnitude as σ_w^2.

The error probability P_{e1} at the sampling instants where the continual noise component is present alone and the error probability P_{e2} at the sampling instants where the non-continual component is also present are sketched in Fig. 6.3.

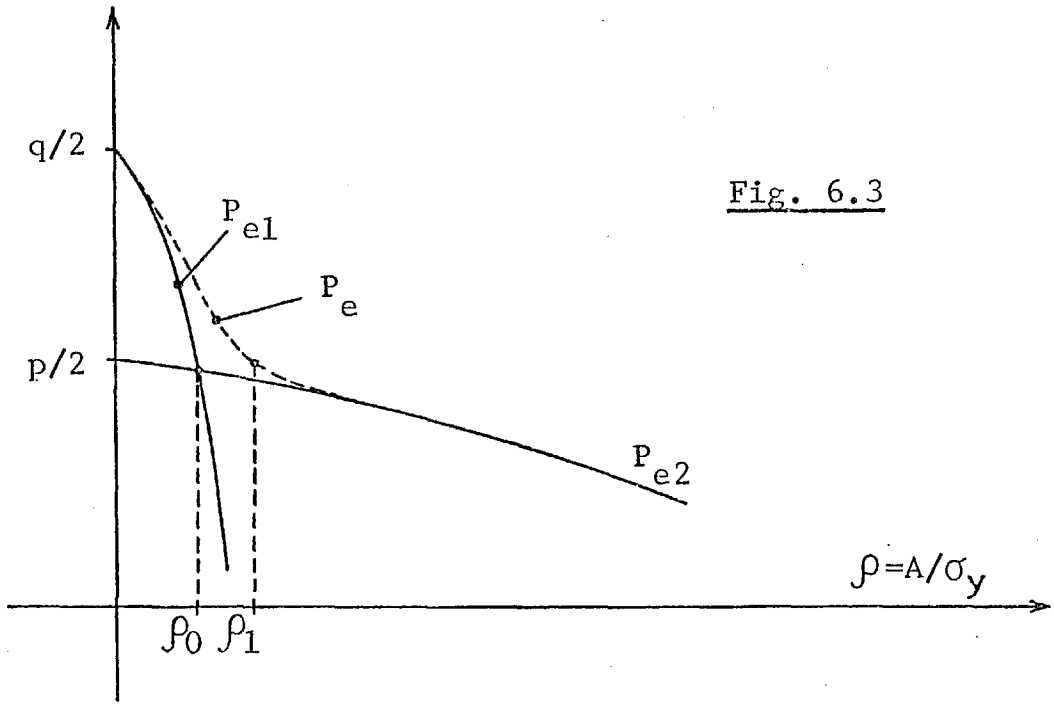

Fig. 6.3

If $\sigma_x \gg \sigma_y$ the SNR ρ_o at the point where the curves P_{e1} and P_{e2} cross each other is approximately given by

$$\frac{1}{2}\operatorname{erfc}\left(\frac{\rho_o}{\sqrt{2}}\right) \simeq \frac{p}{2q}, \qquad (25)$$

assuming that the continual noise component can be closely approximated by a Gaussian process of variance σ_y^2. With the help of Equation (25), Table 6.1 can be obtained.

TABLE 6.1

p	ρ_o	$(\rho_o)_{dB}$
1/8	1.47	3.3
1/32	2.15	6.7
1/128	2.66	8.5

The total error probability $P_e = P_{e1} + P_{e2}$ is indicated in Fig. 6.3 by a broken line. In practice the SNR ρ is greater than the value ρ_1 corresponding to a point* near the elbow of the curve P_e in Fig. 6.3. Under these conditions P_e is closely approximated by P_{e2} and thus it is only necessary to simulate the sequence of statistically independent samples $\{x_i\}$. The way in which this can be done will now be examined.

Following a similar approach to that used in Section 4.2.4, it is possible to define a normalized impulse response

$$\begin{aligned} f_1(t) &= \sqrt{T}\, f(tT) \\ &= \sqrt{T}\, h(tT)\, G_a(t) \end{aligned} \tag{26}$$

and a normalized repetition rate

$$\nu_1 = \nu T. \tag{27}$$

It thus follows that

$$F_x(\omega) = \exp\left\{\nu_1 \int_{-\frac{1}{2}}^{\frac{1}{2}} \left[F_r\left(\frac{\omega}{\sqrt{T}}\, f_1(t)\right) - 1\right] dt\right\} \tag{28}$$

The noise samples at the output of a filter with impulse response $f_1(t)$ are

$$x_{1i} = \sqrt{T}\, x_i \tag{29}$$

and therefore their CHF is given by

$$\begin{aligned} F_{x1}(\omega) &= F_x(\sqrt{T}\,\omega) \\ &= \exp\left\{\nu_1 \left[F_{s1}(\omega) - 1\right]\right\} \end{aligned} \tag{30}$$

where

$$F_{s1}(\omega) = \int_{-\frac{1}{2}}^{\frac{1}{2}} F_r(\omega\, f_1(t))\, dt. \tag{31}$$

It is obvious that $F_{s1}(\omega)$ is the CHF of any noise sample which is due to one and only one noise pulse of shape $f_1(t)$. Since

$$\int_{-\frac{1}{2}}^{\frac{1}{2}} f_1^2(t)\, dt = \eta^2 \tag{32}$$

---

* In many important cases the value of ρ_1 is about 15 dB or less.

it can readily be shown that the variance of $F_{s1}(\omega)$ is $\sigma_{s1}^2 = \sigma_r^2 \eta^2$. Moreover, because $x_{1i} = \sqrt{T}\, x_i$, the variance of x_{1i} is

$$\sigma_{x1}^2 = \nu_1 \sigma_r^2 \eta^2 \tag{33}$$

Obviously, the system performance is not altered when the filter in Fig. 6.1 is replaced by a normalized filter of impulse response

$$h_1(t) = \sqrt{T}\, h(tT), \tag{34}$$

since the signal and the noise at the sampler output are scaled by the same factor $\sqrt{T}$.

If it is now assumed that $f_1(t)$ is a symmetric unimodal pulse shape, as shown in Fig. 6.4, the following functions can be defined:

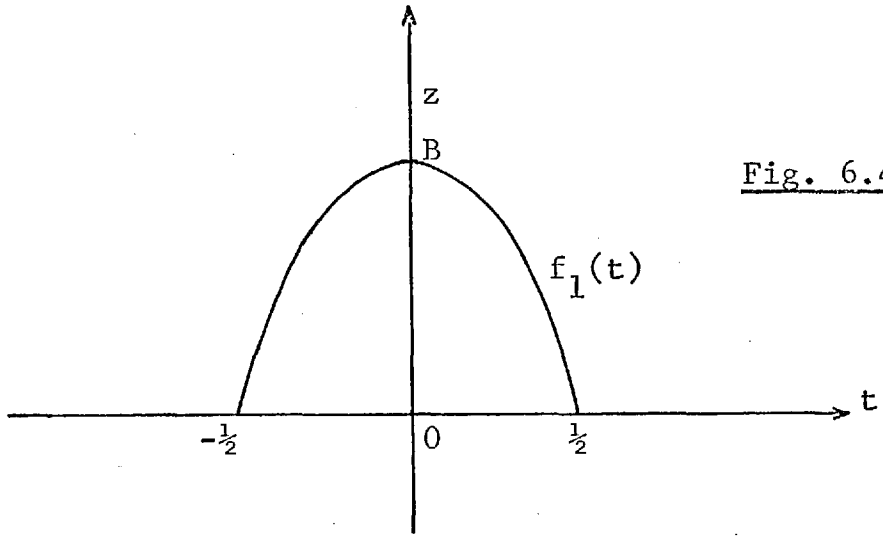

Fig. 6.4

$$z = f_1(t), \qquad 0 \leqslant t \leqslant \tfrac{1}{2} \tag{35}$$

and

$$t = r(z), \qquad 0 \leqslant z \leqslant B. \tag{36}$$

It is thus possible to express $F_{s1}(\omega)$ as follows:

$$F_{s1}(\omega) = 2 \int_0^{\frac{1}{2}} F_r(\omega f_1(t))dt$$

$$= \int_0^B F_r(\omega z)g(z)dz \tag{37}$$

where the function

$$g(z) = -2r'(z) \tag{38}$$

is assumed non-negative within the interval $0 \leqslant z \leqslant B$ and zero outside. By observing that

$$\int_0^B g(z)dz = -2\left[r(B) - r(0)\right] = 1 \tag{39}$$

it can be concluded that $g(z)$ is a probability density function. Now let

$$z = B\sqrt{v} \tag{40}$$

so that

$$F_{s1}(\omega) = \int_0^1 F_r(\omega B\sqrt{v})\ p(v)dv \tag{41}$$

where the PDF $p(v)$ is given by

$$\begin{aligned} p(v) &= -2\,\frac{d}{dv}\left[r(B\sqrt{v})\right] \\ &= -\frac{B}{\sqrt{v}}\,r'(B\sqrt{v}) \\ &= \frac{B}{2\sqrt{v}}\,g(B\sqrt{v}), \end{aligned} \tag{42}$$

and thus

$$g(z) = \frac{2z}{B^2}\,p\left(\frac{z^2}{B^2}\right) \tag{43}$$

Due to the similarity between Equations (37) and (41) it is obvious that

$$\begin{aligned} \overline{v^\alpha} &= \int_0^1 v^\alpha\ p(v)dv \\ &= \frac{1}{B^{2\alpha}} \int_0^1 (B\sqrt{v})^{2\alpha}\ p(v)dv \\ &= \frac{2}{B^{2\alpha}} \int_0^{\frac{1}{2}} \left[f_1(t)\right]^{2\alpha} dt. \end{aligned} \tag{44}$$

In particular,

$$\overline{v} = \frac{\eta^2}{B^2} \tag{45}$$

The EPF of p(v) is given by

$$Q(x) = \int_x^1 p(v)dv$$
$$= -2\left[\, r(B\sqrt{v})\right]_x^1$$
$$= 2\, r\,(B\sqrt{x}). \qquad (46)$$

An important case is the one where h(t) is time-limited to the interval (-T/2, T/2) and thus $\eta^2 = 1$. In this case h(t) is a Nyquist pulse if and only if the PDF p(v) is symmetric with centre of symmetry $v = \frac{1}{2}$. The proof of this property is presented in Appendix 3.1. Moreover, since under these conditions $\bar{v} = \frac{1}{2}$, it follows from Equation (45) that $B = \sqrt{2}$.

It is a well-known result of probability theory* that if the random variable X has PDF p(x) then the random variable

$$U = Q(X) = \int_X^\infty p(x)dx \qquad (47)$$

is uniformly distributed in the interval $[0,1]$. Conversely, if U is uniformly distributed in $[0,1]$ then $X = Q^{-1}(U)$ has PDF

$$p(x) = |Q'(x)|. \qquad (48)$$

Therefore, according to Equations (35), (36) and (46), given the random variable (RV) $U \sim U(0,1)$** the RV

$$V = \frac{1}{B^2} f_1^2\left(\frac{U}{2}\right) \qquad (49)$$

has the PDF p(v) defined in Equation (42) and

$$Z = \left|f_1\left(\frac{U}{2}\right)\right| = B\sqrt{V} \qquad (50)$$

has the PDF g(z) defined in Equation (43).

The position has now been reached where the procedure for generating the non-continual time-series $\{x_{1i}\} = \{x_i\sqrt{T}\}$ can be set as follows:

---

* See Ref. [6-1], page 146.

** $Y \sim U(0,1)$ means that Y is a RV uniformly distributed in $[0,1]$.

(a) Generate an integer $k \geq 0$ which obeys the Poisson law

$$P_k = \varepsilon^{-\nu_1} \frac{\nu_1^k}{k!} \tag{51}$$

(b) If $k > 0$ generate a random number (RN) R_1 with the PDF $p_r(x)$ of the impulse intensities r_i in Equation (5) and a RN V_1 with the help of Equation (49) [or a RN Z_1 with the help of Equation (50)] and then form the product

$$S_1 = B R_1 \sqrt{V_1} \tag{52a}$$

$$[\text{or } S_1 = R_1 Z_1]. \tag{52b}$$

This RN S_1 has a PDF $p_{s1}(x)$ which corresponds to the CHF $F_{s1}(\omega)$ in Equation (37).

(c) If $k > 1$ generate another $(k-1)$ RN's with PDF $p_{s1}(x)$ and add up the k independent RN's to obtain

$$X_1 = \sum_{i=1}^{k} S_i, \qquad k > 0 \tag{53}$$

When $k = 0$, set $X_1 = 0$. The RN X_1 has the CHF $F_{x1}(\omega)$ since Equation (30) can be written in the following form

$$F_{x1}(\omega) = \sum_{k=0}^{\infty} P_k F_{s1}^k(\omega). \tag{54}$$

It should be noticed that in cases where the PDF $P_{s1}(x)$ can be found in closed form there may be a simpler means of generating the RN's S_i. The previous method differs from that used in Ref. [6-2]. In this reference the overlap of the noise pulses of shape h(t) is taken into account even when the time interval between those pulses is longer than T seconds. Responses from at most fifty noise impulses distributed in time according to Equation (6) are accumulated at every sampling instant. This method manages to take into account the statistical dependence between impulsive noise samples but it turns out that

it consumes more computer-time than the procedure described above. The considerations made previously about Fig. 6.3 indicate that very little difference between the results of the two methods is to be expected under practical conditions.

An alternative approach to simulating Poisson impulse noise is that used in Chapter V. In fact the non-continual noise samples can be expressed as follows

$$x_{1i} = u_{1i}\,\theta_i, \tag{55}$$

where the θ_i's form a zero-one process defining the time-distribution of the non-continual noise component and are such that

$$P[\theta_i = 0] = q = \exp(-\nu_1) \tag{56}$$

and

$$P[\theta_i = 1] = p = 1 - q \tag{57}$$

Since Equation (30) can be written in the form

$$F_{x_1}(\omega) = q + p\,F_{u_1}(\omega) \tag{58}$$

where

$$F_{u_1}(\omega) = \frac{q}{p}\left[\exp(\nu_1 F_{s_1}(\omega)) - 1\right] \tag{59}$$

it becomes clear that Equation (59) gives the CHF of the time-series $\{u_{1i}\}$. Notice that, as in Equation (23),

$$\lim_{\omega \to \infty} F_{u_1}(\omega) = 0 \tag{60}$$

From Equation (58) the relation between the PDF's can be derived:

$$p_{x_1}(x) = q\,\delta(x) + p\,p_{u_1}(x). \tag{61}$$

In the cases where h(t) is time-limited to $[-T/2, T/2]$ it is obvious that $p_{u_1}(x)$ is the impulsive noise PDF at those sampling instants where at least one noise pulse is present.

Let N consecutive sampling instants be considered and the number k of those where $\theta_i = 1$ be counted. It is obvious

that k obeys the binomial distribution

$$p_N(k) = \binom{N}{k} p^k q^{N-k} \tag{62}$$

This characterizes the purely random nature of the time-distribution of the Poisson impulse noise. It can also be characterized by the distribution of the burst lengths. A burst is defined as a run of ones in the zero-one process $\{\theta_i\}$ and thus the probability of a burst of length $k \geq 1$ obeys the geometric distribution

$$P_k = q\, p^{k-1} \tag{63}$$

If now a gap is defined as a run of zeros, it follows that the probability of a gap of length $n \geq 1$ is

$$Q_n = p\, q^{n-1} \tag{64}$$

Therefore, if a procedure is known for generating the RN's k, n and u_i another method is available of simulating the Poisson impulse noise.

It is well-known that

$$E[k] = \sum_{k=1}^{\infty} k\, P_k = 1 + \frac{p}{q} = \bar{k} \tag{65}$$

$$E[n] = \sum_{n=1}^{\infty} n\, Q_n = 1 + \frac{q}{p} = \bar{n} \tag{66}$$

Therefore, it follows that

$$\frac{\bar{k}}{\bar{k} + \bar{n}} = p \tag{67}$$

as would be expected.

6.2.2 Non-Poisson impulse noise

As has already been pointed out in Chapter II, if the distribution of the times of occurrence τ_i in Equation (5) is non-Poisson the study of the first-order distribution of the

noise becomes too difficult to be of general practical interest. However, cases frequently arise in practice where the noise pulses tend to bunch more than they do in Poisson impulse noise. In other words, the average burst length $\bar{k}$ and the average gap length $\bar{n}$ tend to be greater than they are in Poisson impulse noise for the same given ratio

$$p = \frac{\bar{k}}{\bar{k} + \bar{n}} \tag{68}$$

In order to gain insight into the performance of data communication systems when the impulsive noise departs from the Poisson case, a class of burst noises will now be considered which appears as a natural generalization of the Poisson impulse noise. It is first assumed that the PDF of the white* time-series $\{u_{1i}\}$ in Equation (55) can be well approximated by some known PDF $p_{u1}(x)$. For the distributions of the burst and gap lengths, respectively, the following negative binomial distributions are taken:

$$P_k = \binom{-v}{k-1} (-p)^{k-1} q^v \tag{69}$$

$$Q_n = \binom{-r}{n-1} (-q)^{n-1} p^r \tag{70}$$

where $k, n \geq 1$, $v, r > 0$ and $p+q = 1$. Note that

$$\binom{-v}{k} (-1)^i = \binom{v+i-1}{i}. \tag{70}$$

It is well-known that

$$\bar{k} = 1 + v \frac{p}{q} \tag{72}$$

$$\bar{n} = 1 + r \frac{q}{p} \tag{73}$$

It is further assumed that these average lengths satisfy Equation (68), or equivalently,

$$\frac{\bar{k}}{\bar{n}} = \frac{p}{q}, \tag{74}$$

for any positive v and r. It necessarily follows that

---

* $\{u_{1i}\}$ is called white if its elements are statistically independent and identically distributed.

$$v = 1 + \frac{q}{p}(r - 1) \tag{75}$$

Therefore, if $v = 1$ it follows that $r = 1$; that is to say, Equations (63) and (64) are obtained as a special case. From Equations (73) and (74):

$$\bar{k} = r + \frac{p}{q}. \tag{76}$$

As can be seen, under the previous conditions the time distribution of the impulsive noise is completely defined by the two average lengths $\bar{k}$ and $\bar{n}$, since they determine the parameters p, v and r of the PDF's (69) and (70). Always in practical situations $v \geqslant 1$ and thus $r \geqslant 1$, also. Since usually $p \ll 1$ it is concluded from Equation (76) that r is approximately equal to the average burst length.

The CHF's corresponding to the PDF's (69) and (70) are respectively

$$F(\omega) = q^v \varepsilon^{j\omega} (1 - p \varepsilon^{j\omega})^{-v} \tag{77}$$

and

$$G(\omega) = p^r \varepsilon^{j\omega} (1 - q \varepsilon^{j\omega})^{-r}. \tag{78}$$

From these CHF's one can easily derive Equations (72) and (73) and also

$$\overline{k^2} = (\bar{k})^2 + pv/q^2 \tag{79}$$

$$\overline{n^2} = (\bar{n})^2 + qr/p^2 \tag{80}$$

The continual part of the noise is assumed to be white Gaussian noise.

6.3 EXAMPLES OF SIMULATION

In this section five simulation experiments are described, the aim of which is to provide insight into problems stated in Chapters IV and V, which could not be solved by using the methods developed in those chapters. Each experiment was

carried out twice and 50,000 received signal and noise samples were used each time. In any of the experiments the two error probabilities obtained for every SNR and number of pulse repetitions M were found to be very close to each other and for this reason only their arithmetic mean is plotted in the graphs presented below. Both sequences of noise samples were generated with the help of a single generator of pseudo-random numbers from a uniform distribution and it was ensured that the uniform random numbers used to generate the second sequence came immediately after those used in the generation of the first noise sequence.

The five simulation experiments were carried out using a single computer program whose structure is described in Appendix 3.2. The generation of the required pseudo-random numbers is discussed in the same appendix.

6.3.1 Experiment 1

This experiment was designed to test the results of Case Study 2 described in Section 5.3. Thus, the block T in the lower branch of the receiver was assumed to be linear i.e.

$$T(x) = x. \tag{81}$$

The impulsive noise samples were assumed to obey a Cauchy distribution.

In the graphs shown in Fig. 6.5 each small circle represents the arithmetic mean of the two error probabilities computed for a certain SNR and M = 1, 2 or 3; the continuous curves are the same as those shown in Fig. 5.24(b). It can be seen that the methods of this chapter and Chapter V lead to values of the error probability which are practically identical.

6.3.2 Experiment 2

This is a repetition of experiment 1 under the conditions of Case Study 1 described in Section 5.3. The values of the

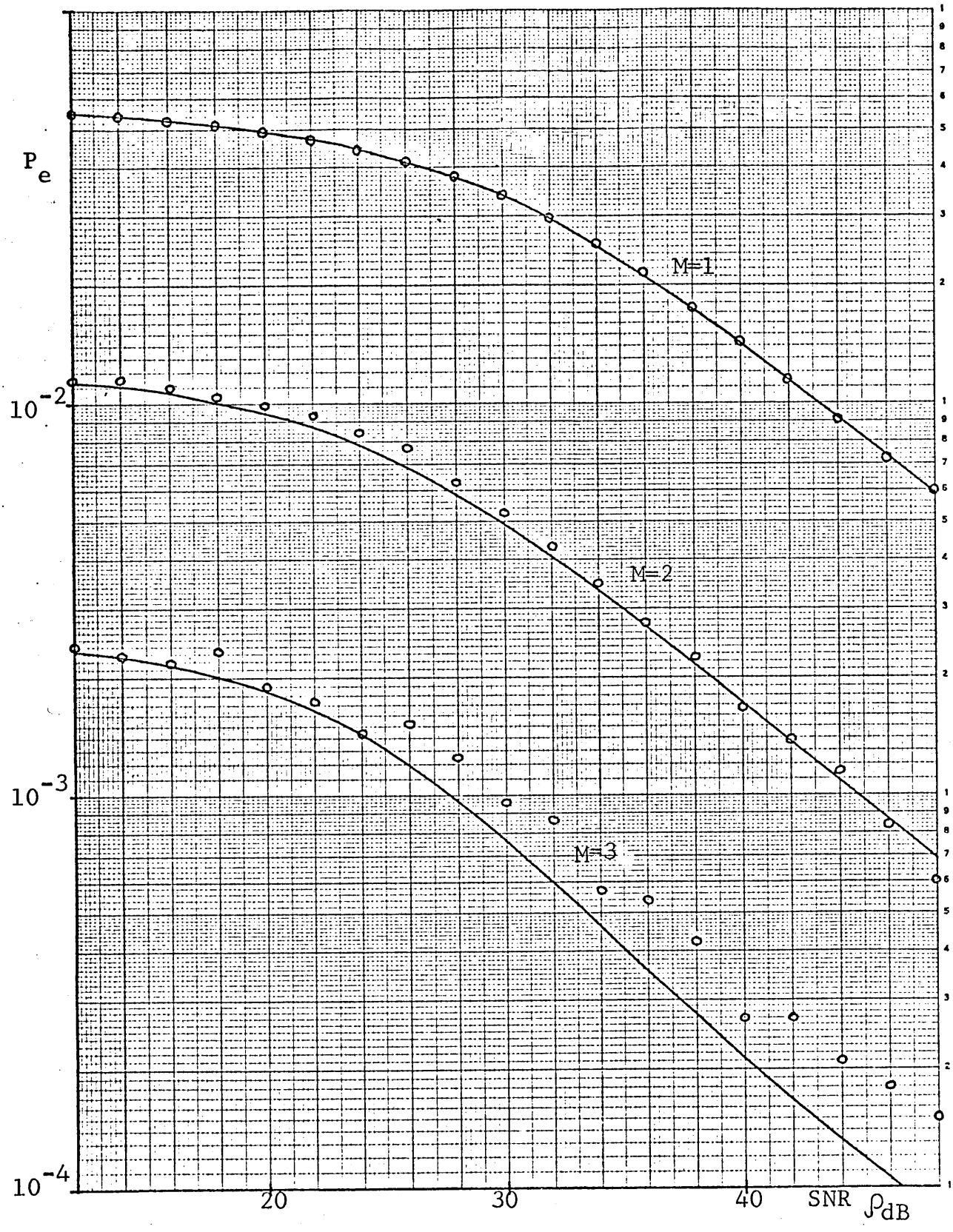

Fig. 6.5 $p = 0.118$

$\zeta_{dB} = 32.0$ dB

$\delta_{dB} = 9.0$ dB

parameters and the results are shown in Fig. 6.6, where the continuous curves correspond to the approximation*

$$P_e \simeq P_{eu} + P_x P_{ez} \qquad (82)$$

and were obtained with the help of the graphs plotted in Figs. 5.28(a), 5.29(c) and 5.33(a). The approximation given by Equation (82) is thus quite good both in experiments 1 and 2.

6.3.3. Experiment 3

The only difference with respect to experiment 1 is that in the present case

$$T(x) = \log \frac{\beta^2 + (x + A)^2}{\beta^2 + (x - A)^2} \qquad (83)$$

i.e. the block T of the receiver is nearly optimum provided the impulsive noise detection is done with a small percentage of errors**. As in experiments 1 and 4, it is assumed that $\beta = 1$ and thus A is identical to the SINR μ. Moreover, as in experiments 1 and 2, it has been assumed that

$$V_1 = -\log p = 1/8 \qquad (84)$$

The small circles in Fig. 6.7 represent the arithmetic mean of the two error probabilities obtained for every SINR and value of M; the continuous curves are the same as in Fig. 6.5. It is obvious that, in the range of values of μ considered, optimization of the block T of the receiver yields very little gain and that this gain increases as μ increases.

6.3.4 Experiment 4

This experiment was intended to test the performance of the receiver of experiment 1 in the presence of the non-Poisson type of impulsive noise described by Equations (69) and

---

* See Chapter V, relation (102).

** See in Chapter V the discussion about Equation (92).

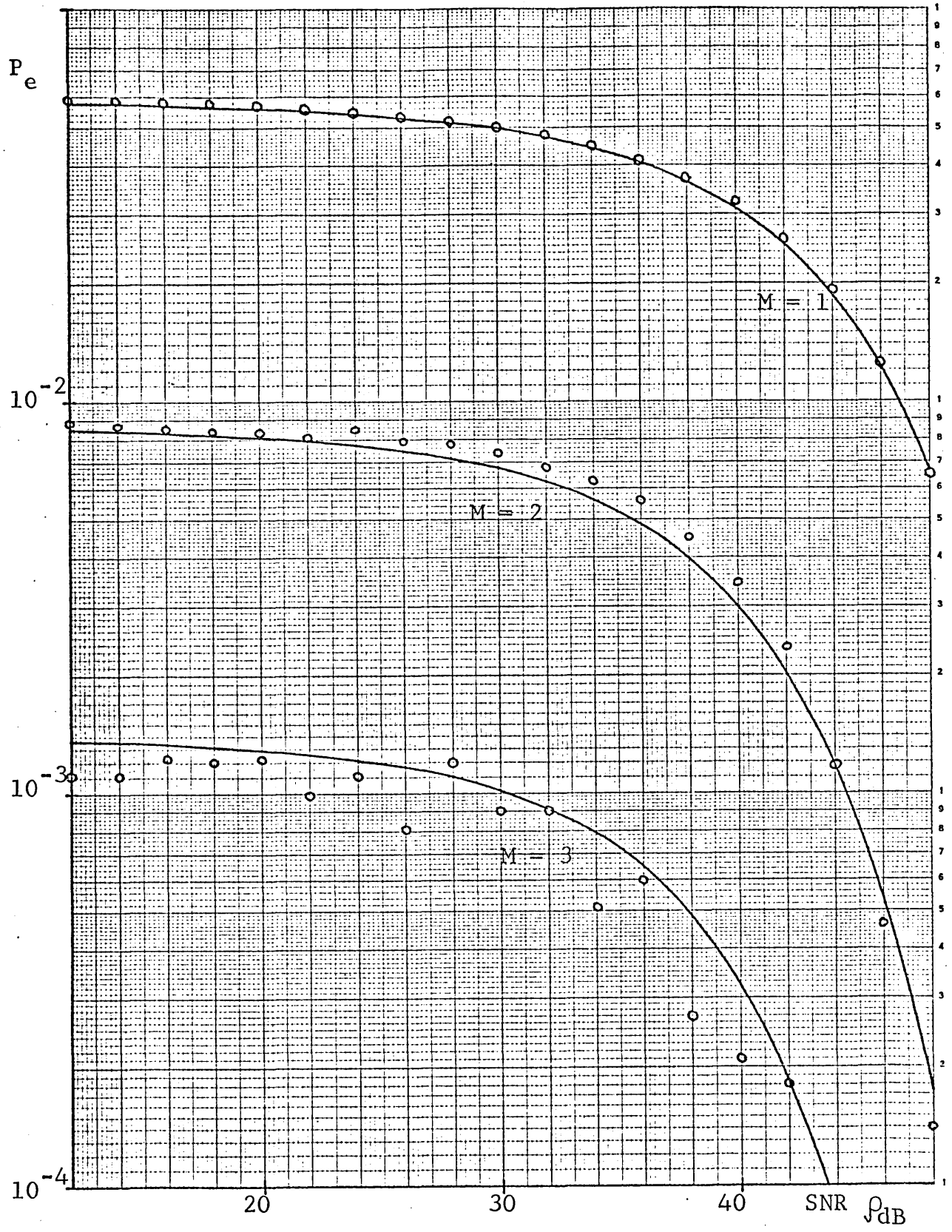

Fig. 6.6

p = 0.118
ζ_{dB} = 44.0 dB
δ_{dB} = 10.0 dB

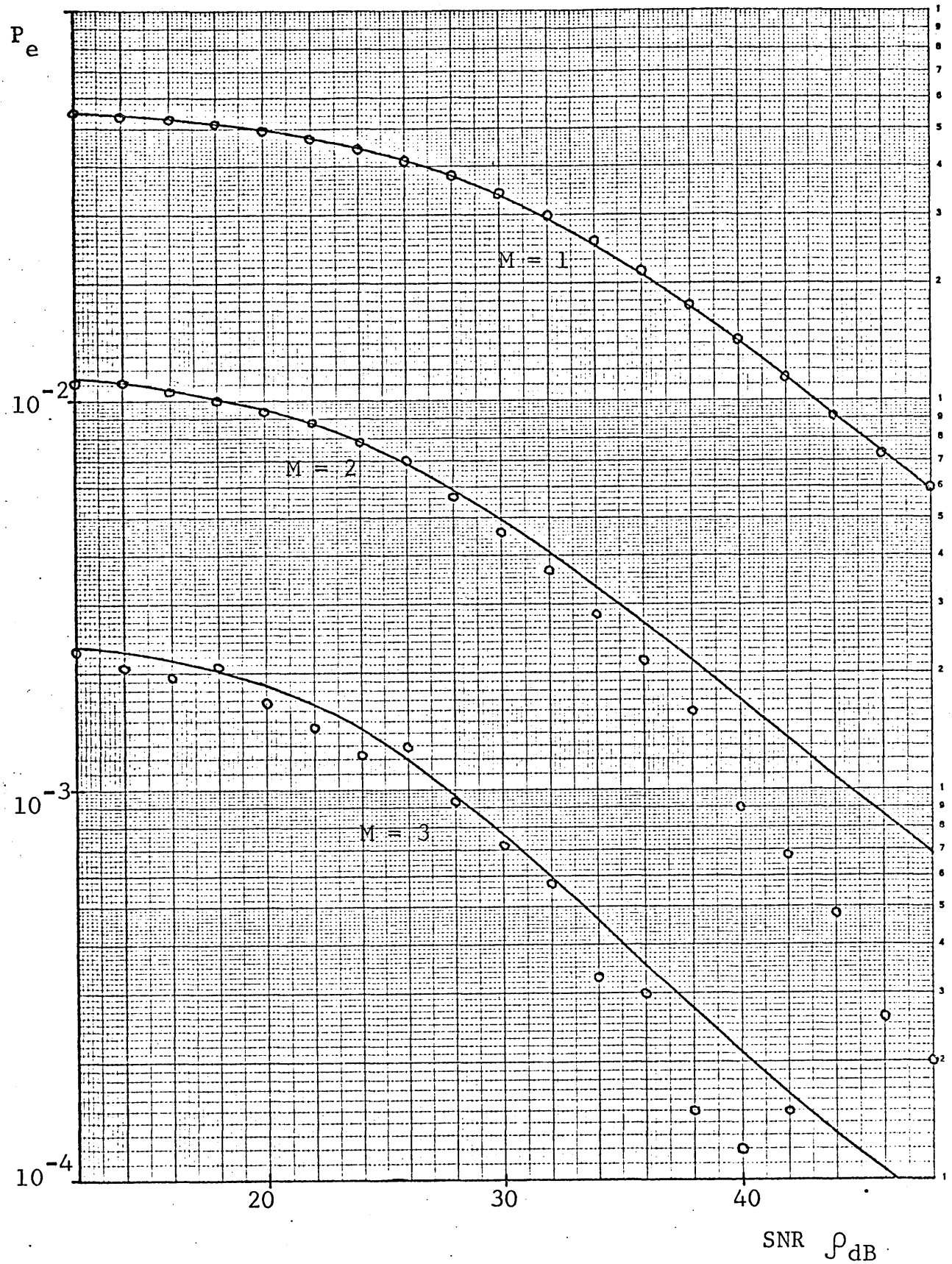

Fig. 6.7

p = 0.118
ζ_{dB} = 32.0 dB
δ_{dB} = 9.0 dB

(70). As in experiments 1 and 3 it was assumed that the samples of impulsive noise obey a Cauchy distribution* of parameter β and that

$$\eta = 1$$

$$\zeta_{dB} = \left(\frac{\beta}{\sigma_w}\right)_{dB} = 32.0 \text{ dB}$$

and

$$\delta_{dB} = \left(\frac{\varepsilon_0}{\sigma_w}\right)_{dB} = 9.0 \text{ dB}.$$

Moreover, it was assumed that $p = 1/8$ and the cases $r = 2$, 4, 8 and 16 were considered as well as the Poisson case $r = 1$. In Figs. 6.8 to 6.12 the continuous curves were obtained by the method of Chapter V for the case $r = 1$ and each dot, circle or cross represents the arithmetic mean of two error probabilities obtained by the Monte-Carlo method. It is obvious that for each value of M and a given SINR the error probability increases as r increases and that the limit as $r \longrightarrow \infty$ does not depend on M, as explained in Section 5.4(f). This limit is attained virtually as soon as $r \gg M$.

6.3.5 Experiment 5

This experiment was designed to test the performance of the smear-desmear technique studied in Chapter IV in the presence of a non-Poisson noise distributed in time according to Equations (69) and (70) and whose samples follow a Laplace distribution of variance σ_x^2. No Gaussian noise was assumed present (i.e. $\sigma_w^2 = 0$) and, as in the four previous experiments, $\eta = 1$. In the case where $r = 1$ (Poisson noise) the method of Chapter IV can be used to compute the error probability by substituting in Equation (105) of that chapter

$$\phi_1(\omega) = q + p\, F_x(\omega) \qquad (85)$$

where $F_x(\omega)$ is the Laplace CHF:

---

* See Chapter V, Equation (79).

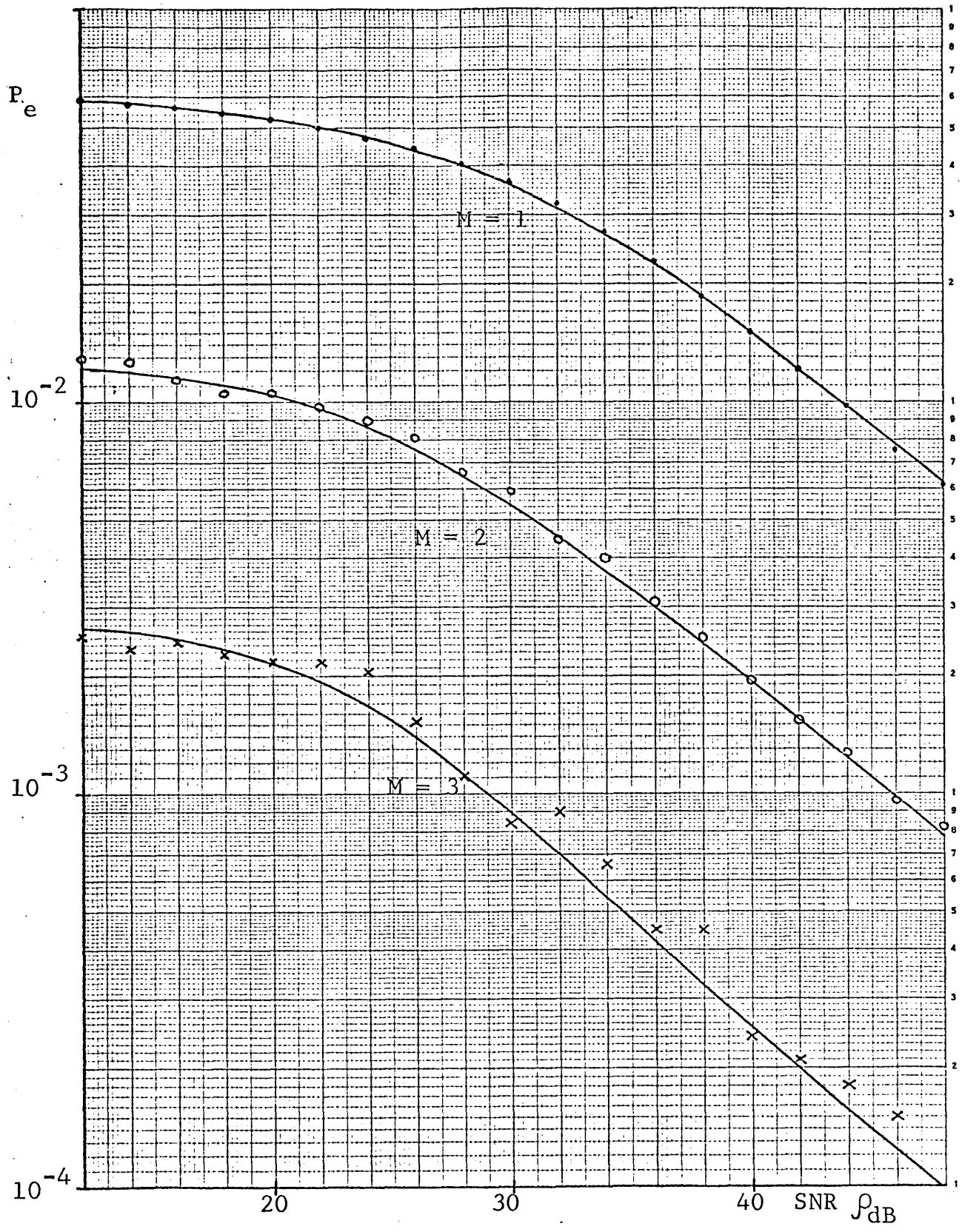

Fig. 6.8

$p = \frac{1}{8}$,
$\zeta_{dB} = 32.0$ dB
$\delta_{dB} = 9.0$ dB
$r = 1$ (Poisson noise)

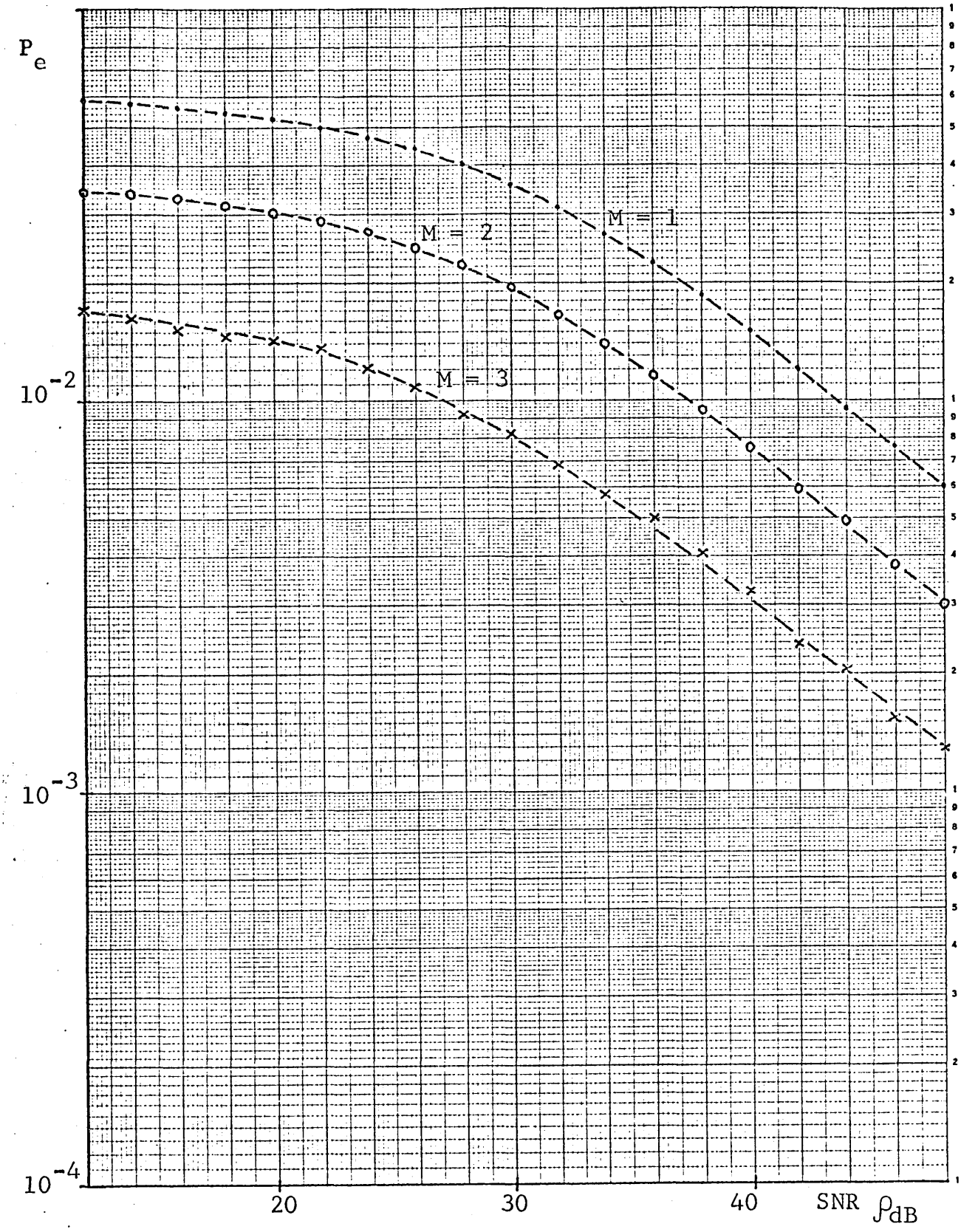

Fig. 6.9

$p = \frac{1}{8}$
$\zeta_{dB} = 32.0$ dB
$\delta_{dB} = 9.0$ dB
$r = 2$

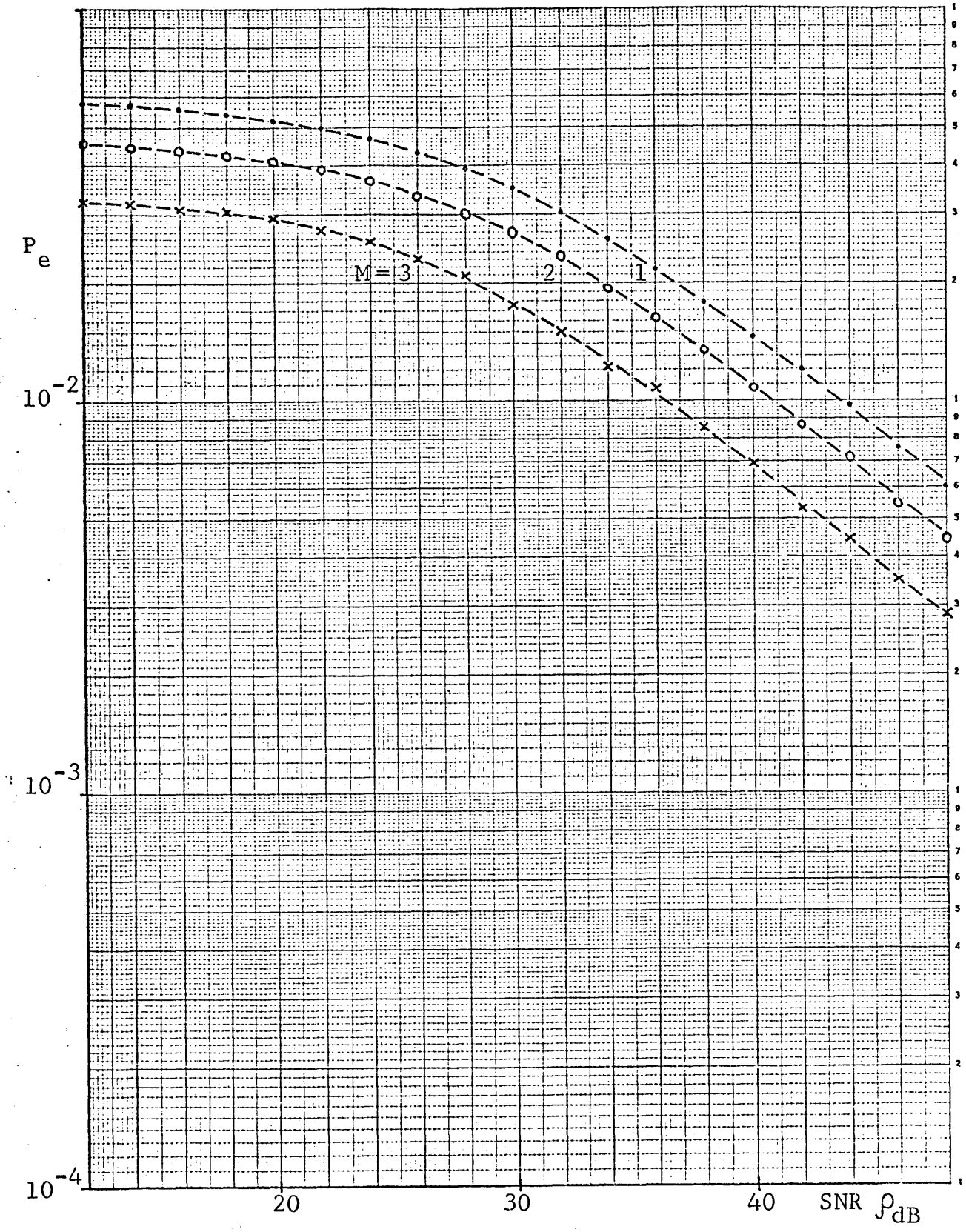

Fig. 6.10

$p = \frac{1}{8}$
$\zeta_{dB} = 32.0$ dB
$\delta_{dB} = 9.0$ dB
$r = 4.$

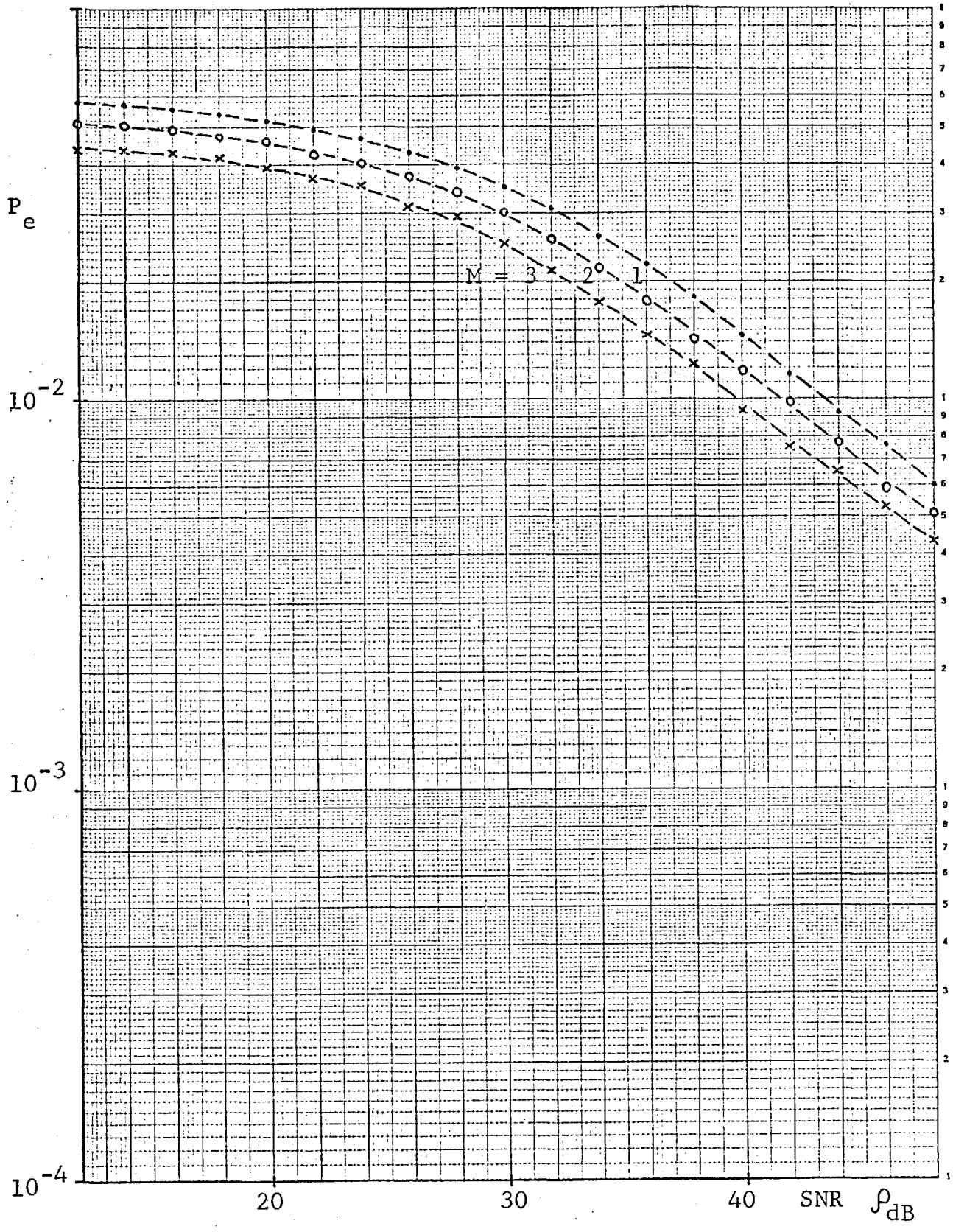

Fig. 6.11

$p = \frac{1}{8}$
$\zeta_{dB} = 32.0$ dB
$\delta_{dB} = 9.0$ dB
$r = 8$

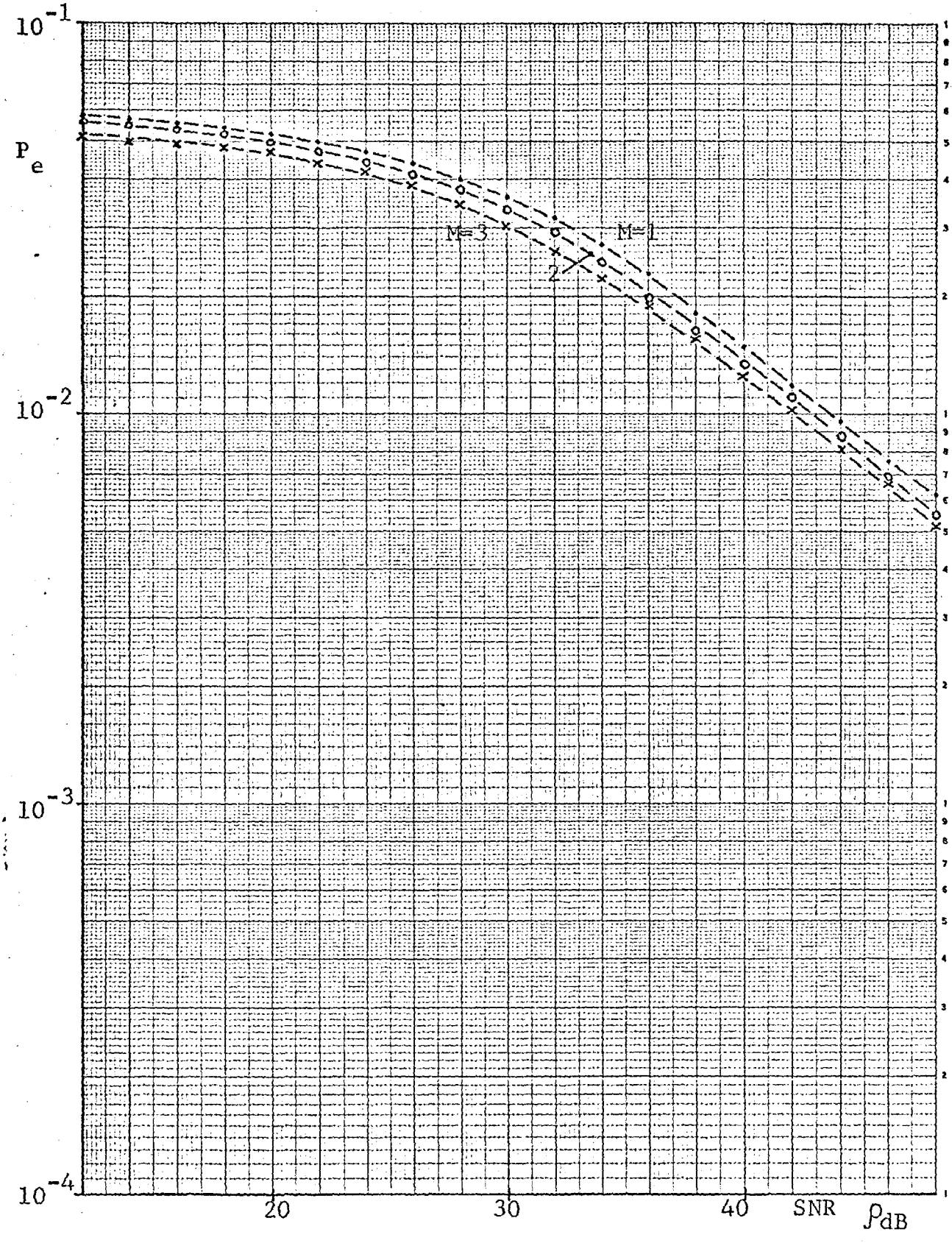

Fig. 6.12

$p = \frac{1}{8}$
$\zeta_{dB} = 32.0$ dB
$\delta_{dB} = 9.0$ dB
$r = 16$

$$F_x(\omega) = (1 + \frac{\sigma_x^2 \omega^2}{2})^{-1} \qquad (86)$$

and

$$\sigma_x^2 = \frac{1}{pN} \qquad (87)$$

In Fig. 6.13 the continuous curves were obtained by the previous method. In Figs. 6.13 to 6.18 each dot represents the arithmetic mean of two error probabilities obtained by simulation for N = 1, 2, 4, 8 or 16 and a given value of the SINR

$$\psi = \frac{A_s}{\sigma_x \sqrt{p}} \qquad (88)$$

where A_s, as already defined in Chapter IV, is the magnitude of the signal samples at the input of the decision device. As in experiment 4, it was assumed that p = 1/8.

By comparing the graphs shown in Figs. 6.13 to 6.18 it can be seen that, as the average burst length increases, the curves corresponding to different values of N become closer. This fact means that, for a required level of error probability (lower than, say, 10^{-3}), the SNR improvement corresponding to a given N will become smaller and smaller as the impulsive noise deviates more and more from the purely random case. Moreover, the harmful effect caused by the smear-desmear technique, for low SINR, gets weaker as the average length $\bar{k}$ of the noise bursts increases.

6.4 CONCLUSIONS

From the examples of simulation studied in the previous section the following important statements can be derived, which are believed to be valid under much broader conditions than those assumed in Section 6.3:

(a) The efficiency of the rate reduction method studied in Chapter V decreases as the average length $\bar{k}$ of the impulsive noise bursts increases. If $\bar{k} \gg M > 1$ the error probability is very close to that obtained for M = 1. Therefore, the addition

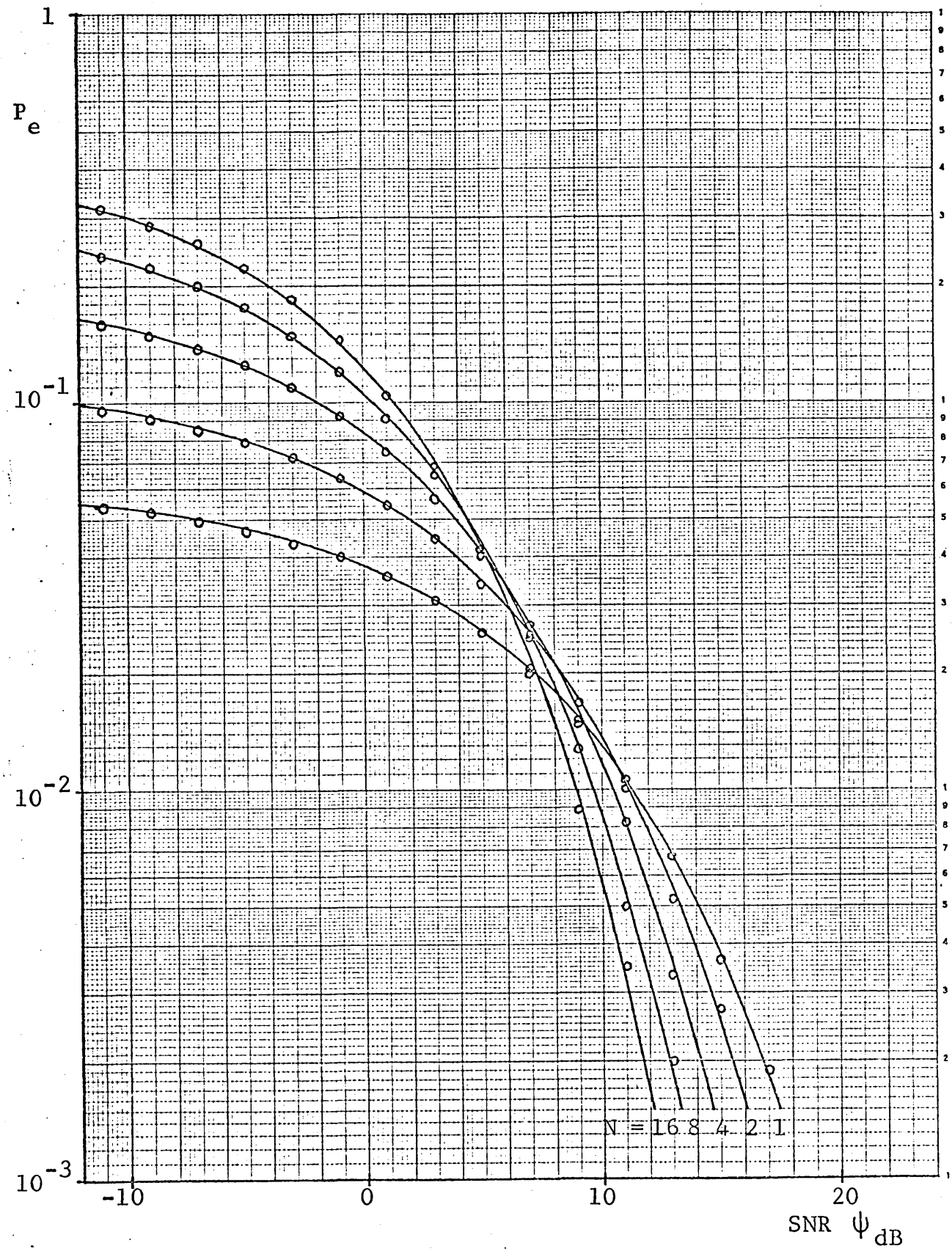

Fig. 6.13 $p = \frac{1}{8}$, $r = 1$ (Poisson noise)

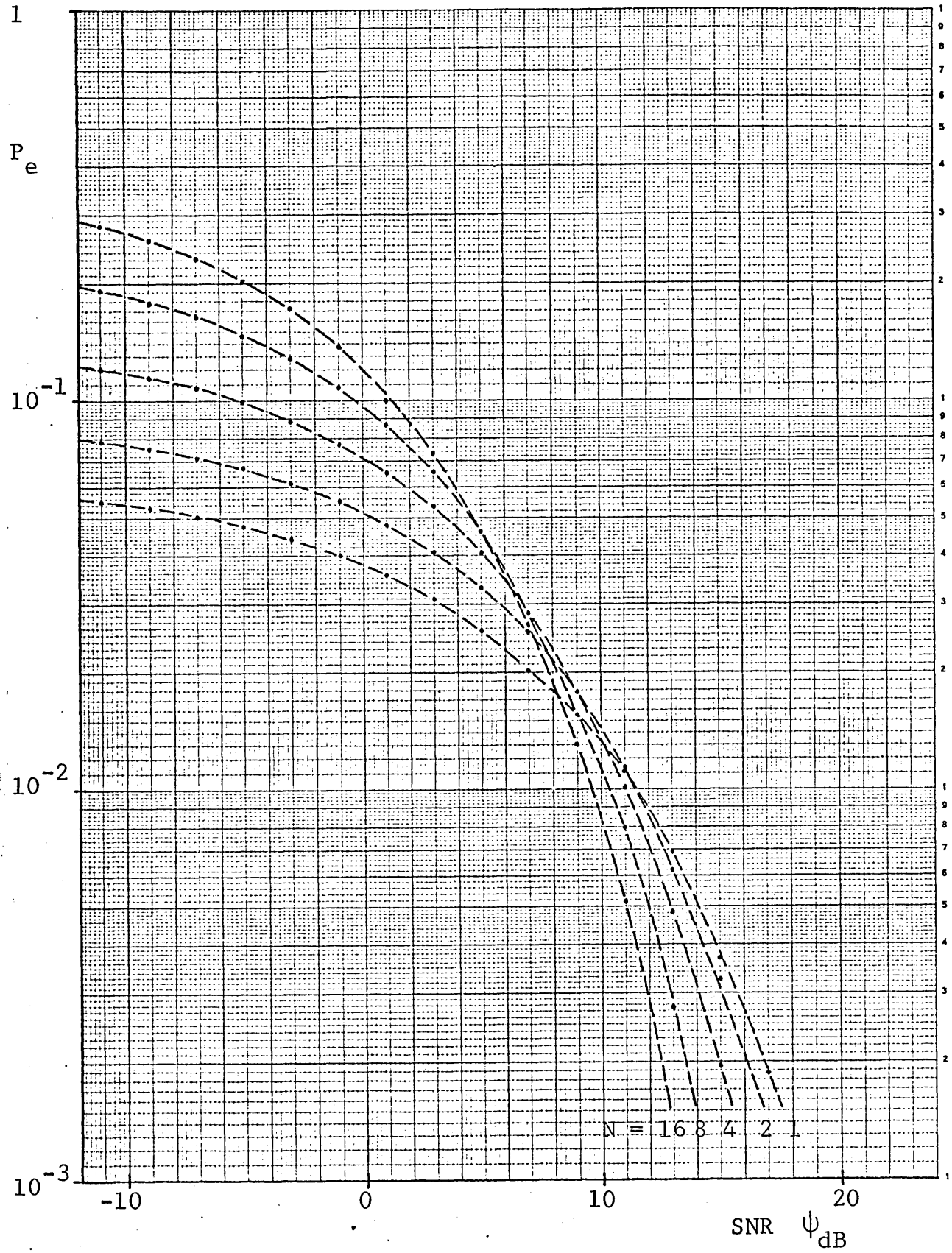

Fig. 6.14 $p = \frac{1}{8}$, $r = 2$.

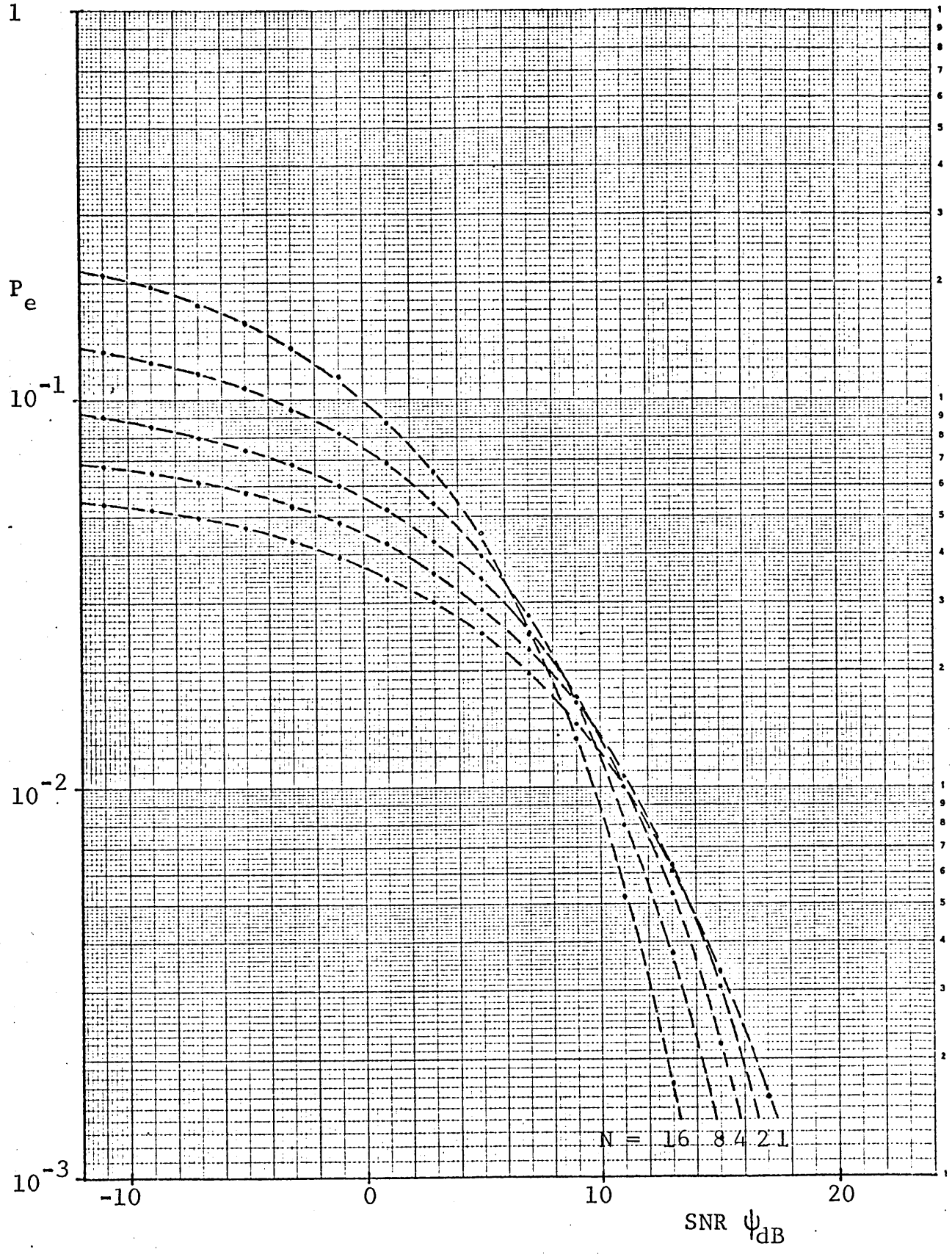

Fig. 6.15 $p = \frac{1}{6}$, $r = 4$.

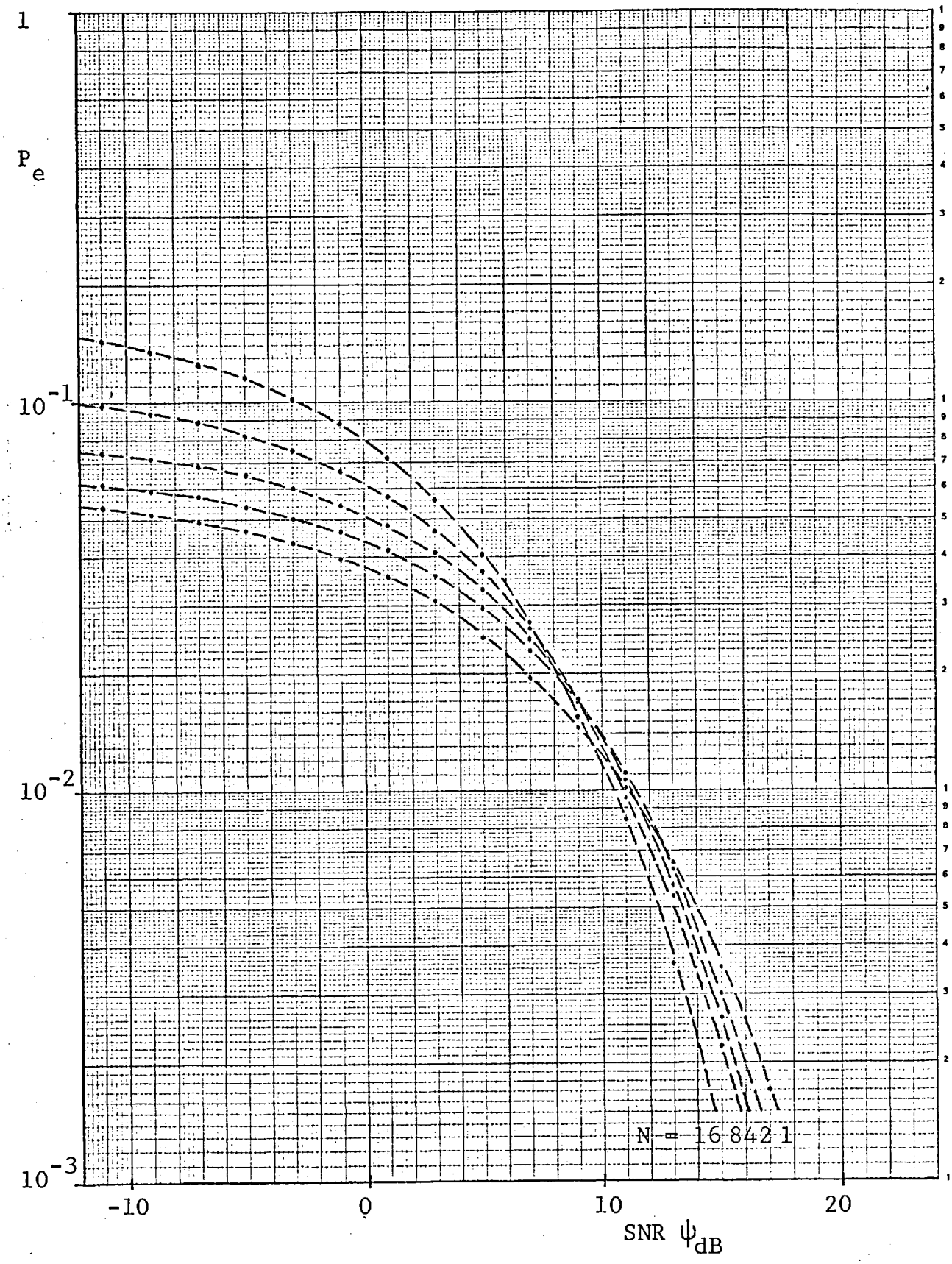

Fig. 6.16 $p = \frac{1}{8}$, $r = 8$.

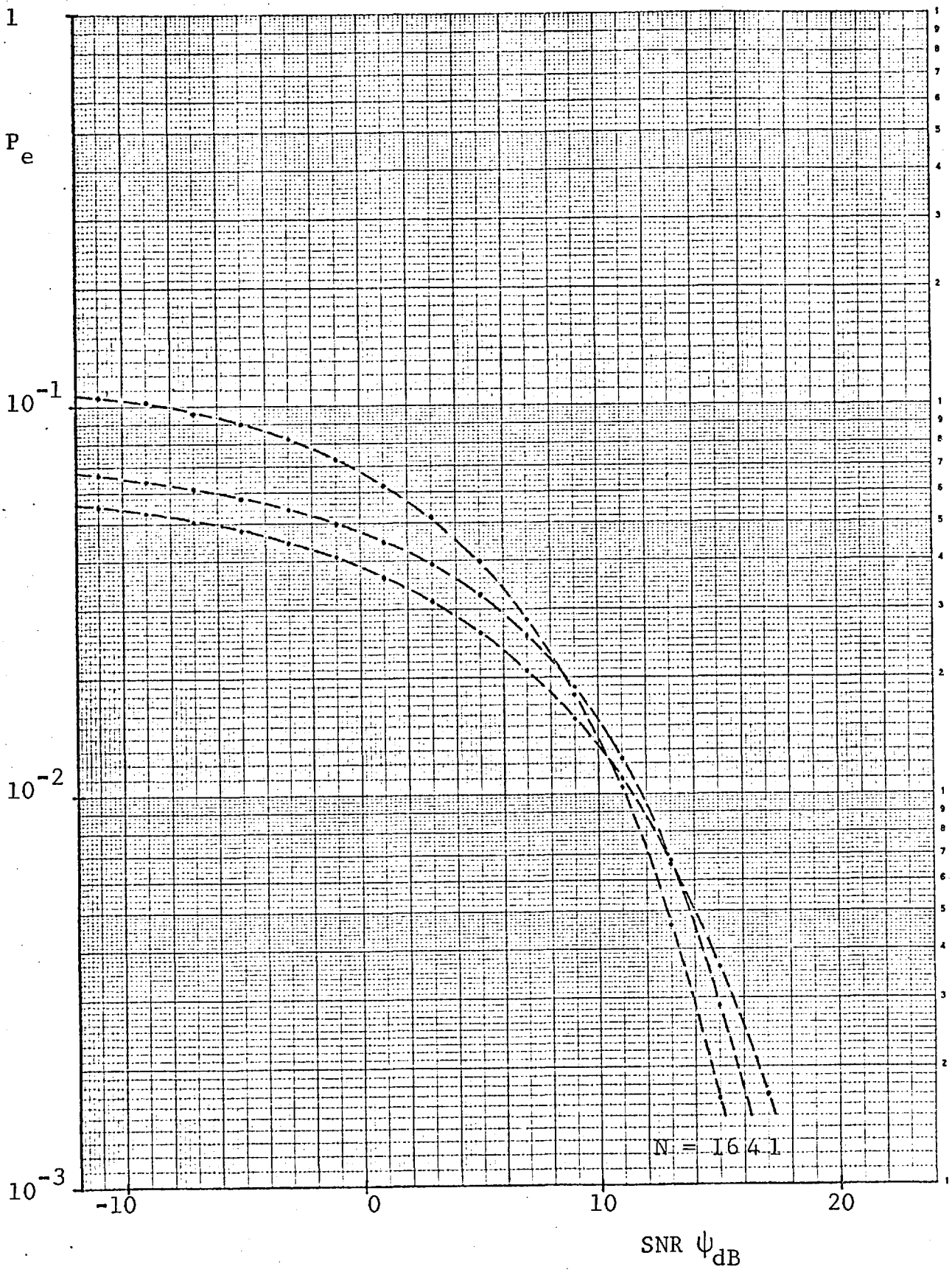

Fig. 6.17 $p = \frac{1}{8}$, $r = 16$.

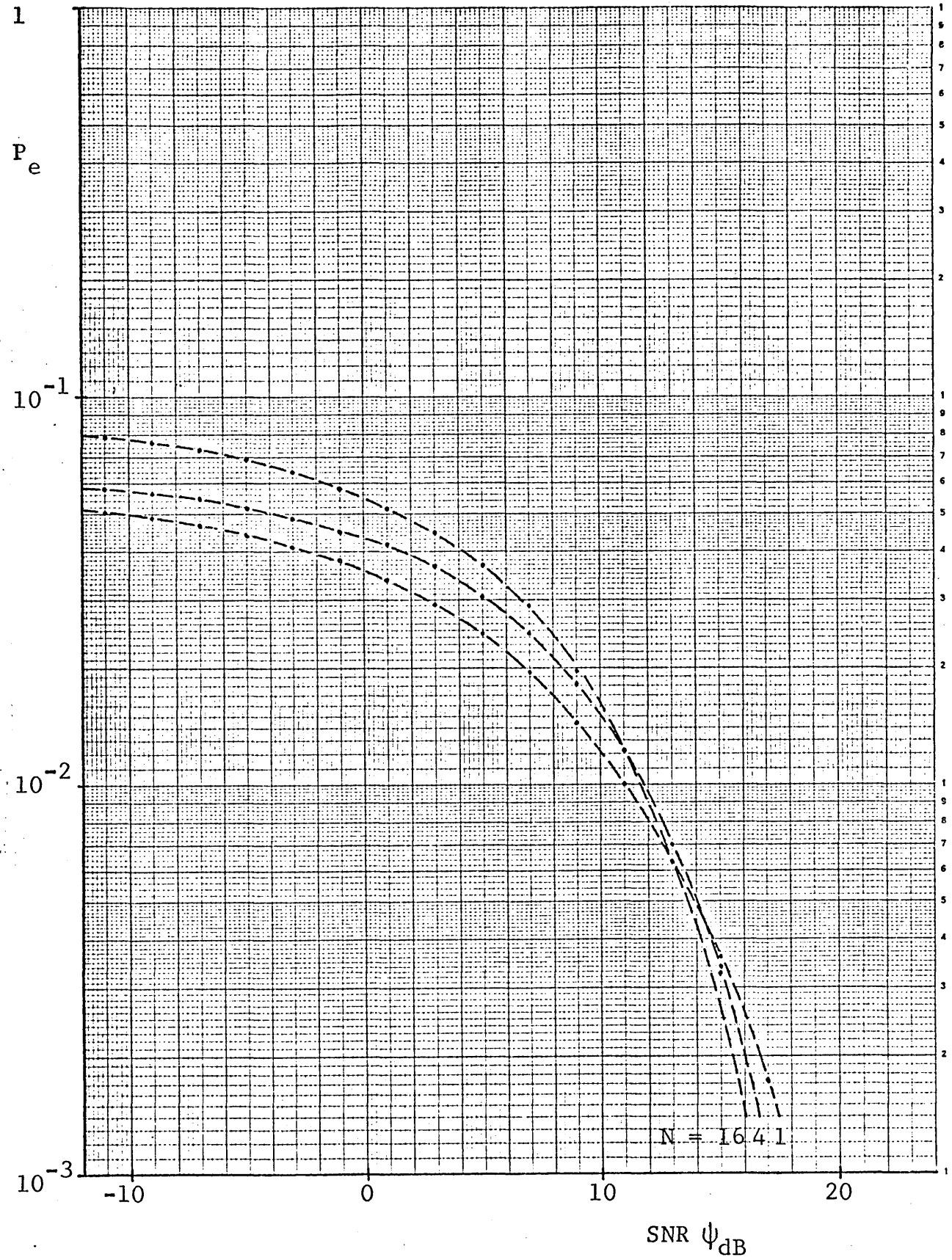

Fig. 6.18 $p = \frac{1}{8}$, $r = 32$.

of a scrambler-descrambler pair to the data system will significantly improve the efficiency in the presence of a strongly non-Poisson impulse noise, provided the noise-sample density p is low enough.

(b) The error probability estimated by the Monte-Carlo method is very close to the value given by Equation (82) for those cases where $\mu_{dB} \lesssim 0$ dB. This statement is believed to be valid for any type of impulsive noise since the definitions of P_{eu}, P_x and P_{ez} are independent of the particular amplitude or time distribution assumed for the noise.

(c) When $\mu_{dB} \lesssim 0$ dB the optimization of the block T shown in Fig. 5.4 has a practically negligible effect on the error probability. As μ_{dB} increases the probability P_{ez} in Equation (82) will decrease and the relative reduction in P_{ez} will increase.

(d) In the case of the smear-desmear technique developed in Chapter IV, the effect of a non-Poisson impulse noise is to reduce the SNR improvement obtained with a given value of N in the presence of Poisson impulse noise. This can be explained in the following way: for very low SNR each noise pulse is very likely to cause an error by itself and thus the bunching of the noise pulses will reduce the fraction of data bits which they affect, and consequently will reduce the error probability; on the other hand, if the SNR is well above the threshold of improvement the noise samples in a burst strengthen the capability of each other to cause an error, thereby resulting in a higher error probability than in the Poisson case. Here again the use of a scrambler-descrambler pair will prove beneficial in the range of SNR's where the technique turns out to be useful. The importance attached to the Poisson impulse noise in Chapters IV and V is thus justified.

CHAPTER VII

THE USE OF CODING IN VERY NOISY CHANNELS

Use not vain repetitions,
as the heathen do: for they
think that they shall be heard
for their much speaking.

The New Testament, St. Matthew,
6.7.

7.1 INTRODUCTION

It may be concluded from the results of Chapter V that in the cases where the SINR μ is low and the density p of impulsive noise samples is high (say, in the order of 10^{-1}), the attainment of a low error rate (i.e. less than 10^{-5} bit-error rate) at the receiver output gives rise to a transmission rate factor* that may be considered to be too low for many data transmission applications. Alternatively, in these cases, an attempt can be made to achieve the desired bit-error rate by using a powerful forward error-correcting code alone. If, however, the errors to be corrected occur randomly at a rate as high as, say, 10^{-1}, achievement of an output bit-error rate lower than 10^{-5} demands the use of a code with a rate that may be lower than that obtained by pulse repetition, for the same output bit-error rate. For this reason it is proposed in this chapter to use a combination of the repetition method (Chapter V) with a forward error-correcting code**. If, as in most practical circumstances, the errors to be corrected tend to cluster in bursts or bursts of bursts, a random error-correcting code will not perform well and a single-burst or multiburst error-correcting code must therefore be used. A major shortcoming of these non-random error-correcting codes is the high sensitivity of their performance to the details of the bit-error structure. For this reason only random error-correcting codes are considered henceforth and the errors from the channel are assumed to have been randomized before decoding by some scrambling (reordering) operation on the data pulses prior to transmission, followed by restoration of the original ordering prior to decoding at the receiver. This scrambling-descrambling operation is intended to make the channel appear to the decoder as a random-error channel.

---

* Transmission rate factor is the ratio between the actual transmission rate and the channel capacity.

** All the random error-correcting codes considered in this chapter are binary linear block codes.

The combination of the repetition method with a random error-correcting code may be described as follows (see Fig. 7.1 for functional diagram). A binary information stream is presented to the encoder, k bits at a time. The encoder adds n-k redundant check bits such that up to t random errors can be corrected by the decoder placed at the receiver terminal. Prior to transmission, each bit of the coded data stream is repeated M times and the resulting data stream is made to pass through an interleaver which is the unit used in practice to perform the scrambling operation referred to above. At the receiving terminal the received samples are unscrambled by passing them through a second interleaver unit referred to in Fig. 7.1 as the descrambler. The samples are then presented to the double-path detector developed in Chapter V, which makes a decision based on each sequence of M samples, and the resulting binary data stream is then passed on to the decoder for error correction.

An interleaver can be described by a rectangular array of digital storage elements with R rows and S columns. At the transmitting terminal the data is read into the interleaver on a row-by-row basis and when the array is full the data is read out on a column-by-column basis. Thus, adjacent bits in a block of S bits at the input of the interleaver are separated in transmission by R-1 bits. At the receiving terminal the data is fed into the descrambler on a column-by-column basis and is then restored to its original ordering by reading out on a row-by-row basis. Since the descrambler is normally implemented by a digital device, it will have to be preceded by an analog-to-digital converter. The number of binary storage elements in the descrambler is B_u = RSN, where RS is the total number of quantized samples that can be stored in it and N is the number of elements occupied by each sample. It is possible to reduce the total storage capacity needed by performing both the interleaving and the descrambling operations in two steps, as

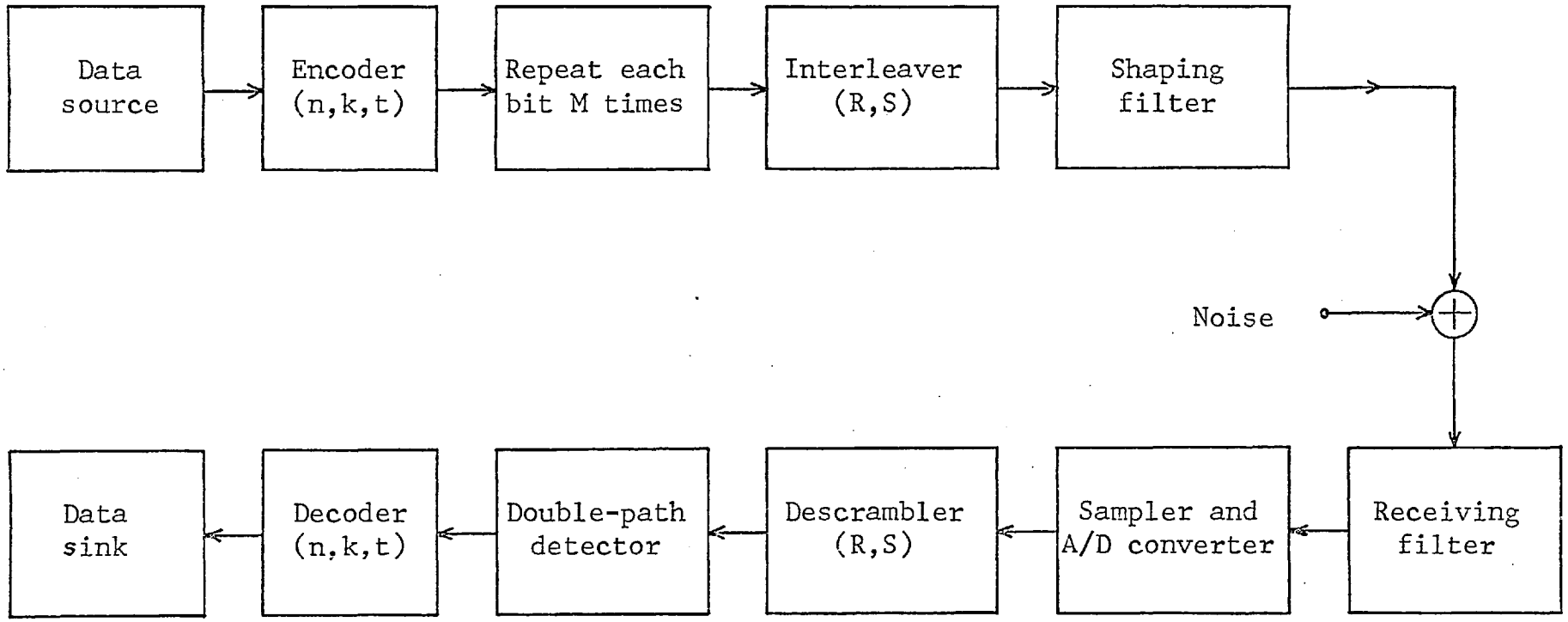
Data source
Encoder (n,k,t)
Repeat each bit M times
Interleaver (R,S)
Shaping filter
Noise
Receiving filter
Sampler and A/D converter
Descrambler (R,S)
Double-path detector
Decoder (n,k,t)
Data sink

Fig. 7.1

indicated in Fig. 7.2. In this figure the interleaver unit alters the ordering of the coded data stream, the restoration to the original ordering being carried out at the receiver, before decoding, by descrambler 2. The second interleaving operation entails simply repeating each block of n_3 bits M times with descrambler 1 at the receiver reassembling the received samples corresponding to M identical transmitted bits before presentation of these to the double-path detector. If, as pointed out in Ref. [7-2], the number n_2 of columns in the interleaver in Fig. 7.2 is equal to the code block length n, then, from the point of view of consecutive errors, the interleaving operation redefines the code as $(n_1 n, n_1 k, n_1 t)$. This means that when a burst of $n_1 t$ errors occurs within an interleaved block of $n_1 n$ bits at the input of descrambler 2 (Fig. 7.2), then at the decoder input these errors are dispersed over n_1 code words with t in each word, and can therefore be corrected. By suitably choosing the interleaving factor n_1 it is possible to reduce the number of code words with more than t errors (while decreasing the number of words with no errors) and thus allow the random error-correcting code to provide a significant reduction in received-data error-rate. The design of the scrambling operations thus entails the choice of interleaving factors n_1 and n_3 which maximize the randonmess of the impulsive noise locations at the input of the double-path detector and the randonmess of the error locations at the decoder input, given the encoding parameters n, k and M, the maximum permitted transmission delay, the maximum complexity allowed for the interleaver-descrambler units and, of course, the time statistics of the impulsive noise. The details of the design can be found in Refs. [7-1, 2, 8]. In these references interleaved block coding is shown to be one of the best techniques for combating burst-type error patterns. Pierce et al. [7-8] noted that "only bit-interleaved block coding (has) consistently provided significant performance gains over the

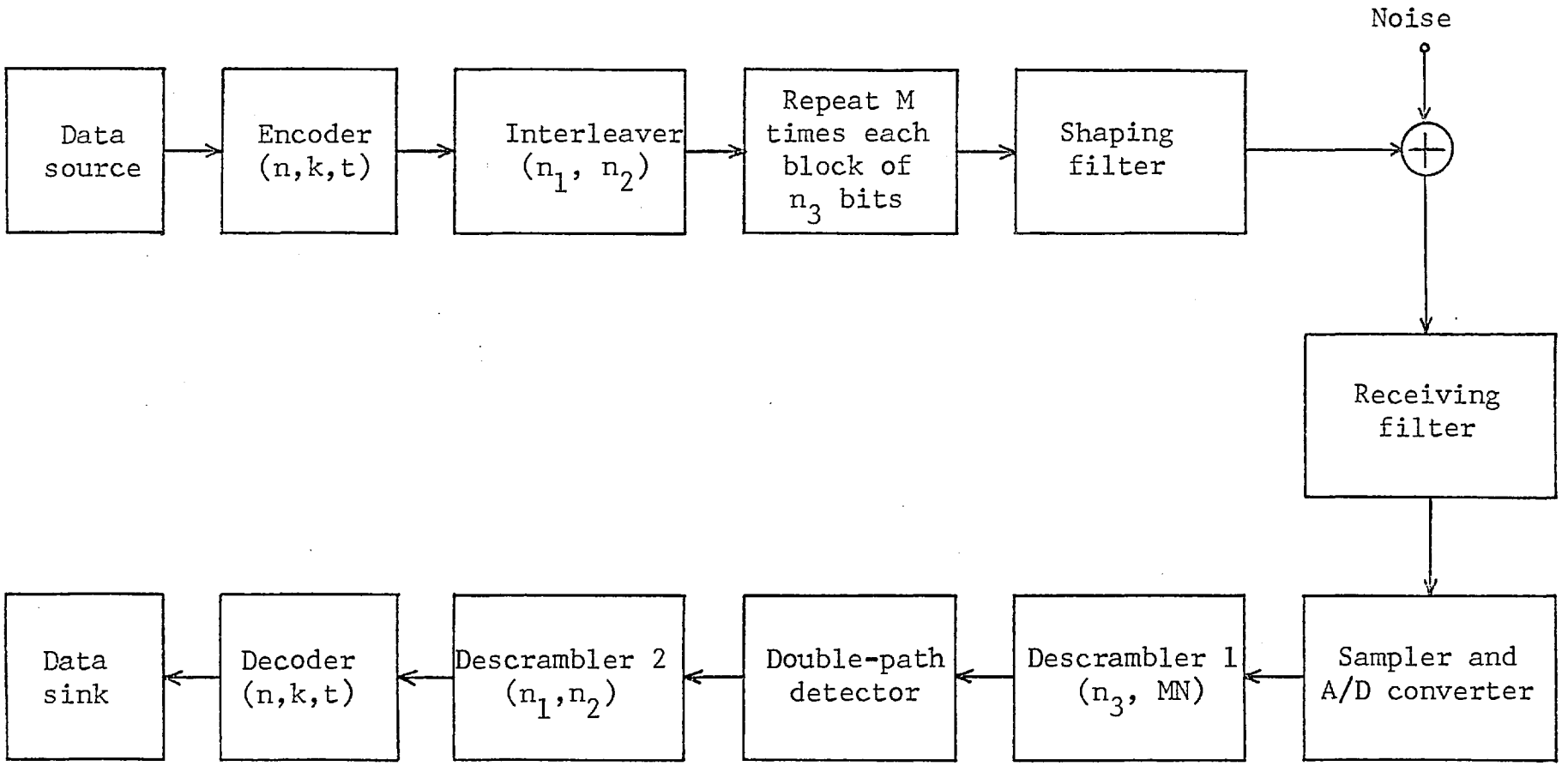
Noise
Data source
Encoder (n,k,t)
Interleaver (n_1, n_2)
Repeat M times each block of n_3 bits
Shaping filter
Receiving filter
Sampler and A/D converter
Descrambler 1 (n_3, MN)
Double-path detector
Descrambler 2 (n_1,n_2)
Decoder (n,k,t)
Data sink

Fig. 7.2

entire range of HF modem-channel conditions considered".

It is important to point out that an interleaver is not necessarily implemented by an array of digital storage elements. It is obviously more convenient in practice to use the so-called synchronous interleavers [7-9] in which a symbol is read out each each time a symbol is read in.

In the following sections no limitations are imposed on transmission delay or system complexity and it is assumed that the time statistics of the noise or the errors at the points of interest can be considered nearly random in order to assure a good performance of the double-path detector and the decoder. In Section 7.2 bounds on the improvement factor* of the decoder are derived, which are later used in Section 7.3 to analyze the performance of the overall system.

7.2 BOUNDS ON THE DECODER PERFORMANCE

The exact calculation of the bit-error probability P_e at the output of the decoder in Fig. 7.2 is in general a very difficult task [7-10]. If, however, some restrictions on the error distribution and the type of decoder are made, reasonably tight bounds on P_e can be easily derived. In the following, it is assumed that the bit-errors occur independently at the decoder input. Moreover, it is assumed that the decoder produces at the output the k information bits of the codeword U closest, in the Hamming sense, to the received n-tuple V if U and V differ in t positions or less; otherwise the decoder will just let through the first k bits of the received block V. Although sub-optimum, this decoder is believed to provide an estimate of P_e which is sufficiently accurate for the purposes of this chapter. As a matter of fact, it is known that the most efficient decoders only attempt to correct up to t errors [7-11].

---

* The improvement factor is defined as the average fraction of input errors corrected by the decoder.

Let us now compare the above-defined decoder with the so-called maximum-likelihood decoder, which, under the assumed conditions, minimizes the error probability [7-12]. The maximum-likelihood decoder will, in any case, decode the received block into that codeword that differs from it in the fewest positions. If the number of errors e in the received block is not greater than t, the above decoding rule is never ambiguous because there is always one and only one codeword at a minimum distance e from the received block. Thus, in this case ($e \leqslant t$) all errors will be corrected. Given an arbitrary n-tuple V whose nearest codeword U_1 is at a distance i, either no other codeword is at a distance i from V or at least one more codeword U_2 is at a distance i from V. It is thus possible to define A_i as the number of n-tuples of the first type and B_i as the number of n-tuples of the second type, for a fixed minimum distance i (from some codeword). From the above considerations it follows that

$$B_i = 0 \qquad \text{for } i \leqslant t$$

and that A_o is the number of codewords, that is

$$A_o = 2^k.$$

Moreover, in the code standard array [7-13] the number of cosets whose coset leader has weight i is given by $(A_i + B_i)2^{-k}$. Given one of these cosets, if there are in it two or more n-tuples of minimum weight any one of them may be taken as coset leader. Thus, there are $A_i 2^{-k}$ cosets for which the coset leader is the only n-tuple in the coset having a minimum weight i and $B_i 2^{-k}$ cosets each with more than one word of minimum weight.

If e errors occur and $e > t$ all errors will be corrected at the decoder if an n-tuple of the first type with a minimum distance $i = e$ is received. For n-tuples of the second type having a minimum distance $i = e$ the decoding rule is ambiguous and correct decoding is not always achieved. For those cases

where the received n-tuple has a minimum distance $i < e$ correct decoding is never possible. In order to obtain bounds on P_e for the maximum-likelihood decoder the probabilities of these three events must therefore be known or at least bounded. Since this knowledge is not readily obtainable in the general case, it is necessary to consider the suboptimum decoder defined above. As stated above, this decoder first finds the minimum distance i from the received n-tuple V to a codeword and then either produces the information bits of some codeword nearest to V if $i \leq t$, or the first k bits of the received n-tuple if $i > t$. It thus follows that incorrect decoding can only occur if the number of errors e in V is greater than t and that three cases are then possible:

(a) $i = e$ and the average number of errors at the decoder output is then $\varepsilon_1 = ke/n$;

(b) $t < i < e$ and the average number of output errors is then the same as in (a), i.e. $\varepsilon_2 = ke/n$;

(c) $i < e$, $i < t$ and the average number of output errors ε_3 is then bounded as follows*:

$$dk/n \leq \varepsilon_3 \leq (2e - 1)k/n$$

where $d = 2t + 1$ is the minimum distance of the code. If the input errors occur independently with probability p_1, the bit-error probability P_e at the decoder output is therefore bounded as follows:

$$P_e > \frac{1}{n} \sum_{e=t+1}^{d} e\binom{n}{e} p_1^e (1 - p_1)^{n-e} + \frac{d}{n} \sum_{e=d+1}^{n} \binom{n}{e} p_1^e (1-p_1)^{n-e}$$

and

$$P_e < \frac{2}{n} \sum_{e=t+1}^{n} e\binom{n}{e} p_1^e (1 - p_1)^{n-e}.$$

---

* The upper bound follows from the triangle inequality [7-14].

On defining $q_1 = 1 - p_1$ and

$$E(n,\ r,\ p_1) = \sum_{i=r}^{n} \binom{n}{i} p_1^i\ q_1^{n-i}$$

it can be shown that

$$\frac{1}{n} \sum_{i=t+1}^{n} i\binom{n}{i}\ p_1^i\ q_1^{n-i} = p_1\ E(n-1,\ t,\ p_1)$$

The bounds given above then become

$$P_e > p_1\ E(n-1,\ t,\ p_1) - p_1\ E(n-1,\ d,\ p_1) + \frac{d}{n}\ E(n,\ d+1,\ p_1) \qquad (1)$$

and

$$P_e < 2p_1\ E(n-1,\ t,\ p_1) \qquad (2)$$

Since the binomial exceedence probabilities $E(n,r,p_1)$ satisfy the following relation

$$n\ E(n-1,t,p_1) = (n-t)E(n,t,p_1) + t\ E(n,t+1,p_1)$$

the lower bound (1) can therefore be rewritten

$$P_e > p_1 E(n-1,t,p_1) + q_1 E(n-1,d,p_1) - (1-\frac{d}{n})\ E(n,d,p_1).$$

Since in all practical situations $t > p_1 n$, the contribution from the last two terms of the lower bound is very small compared to the first term. Thus it is possible to write

$$P_e \gtrsim p_1 E(n-1,t,p_1). \qquad (3)$$

By comparing the bounds (2) and (3) it may thus be concluded that the above method provides a fairly accurate estimate of the bit-error rate at the output of the suboptimum decoder.

7.3 EVALUATION OF THE SYSTEM PERFORMANCE

From the results of Chapter V it can be concluded that the bit-error probability p_1 at the input of the decoder in Fig. 7.2 is bounded as follows

$$p_1 < p^M/2,$$

p being that fraction of received samples in which the impulsive noise occurs with an amplitude high enough to cause an error. In this section a worst-case analysis is done by assuming that*

$$p_1 = p^M/2 \tag{4}$$

and

$$P_e = 2p_1 E(n-1, s, p_1). \tag{5}$$

Given the values of n, M and p it is possible to calculate the minimum value of the argument s for which the value of P_e given by Equation (5) is smaller than, say, 10^{-5}. Then, by using the table** in Ref. [7-7], the parameters (n,k,t), $t \geqslant s$, of some existing code can be found which maximize (or nearly maximize) the overall transmission rate

$$R = \frac{k}{Mn} \text{ bits per transmitted pulse.} \tag{6}$$

This procedure was used to obtain Table 7.1 where it is assumed that, for some integer $i \geqslant 1$, $p = 2^{-i}$ and thus

$$p_1 = 2^{-j}, \qquad j = Mi + 1. \tag{7}$$

From Table 7.1 values of R can be derived corresponding to several values of n and M. These values of R are presented in Table 7.2. The parameters of the best cyclic codes under the conditions of Table 7.1, together with the optimum value of M and the rate R achieved, are shown in Table 7.3.

It is interesting to compare the values of R shown in Tables 7.2 and 7.3 with the capacity of the binary symmetric channel between the encoder output and the decoder input. This capacity, in bits per transmitted pulse, is given by

$$C_M = (1 + p_1 \log_2 p_1 + q_1 \log_2 q_1)/M \tag{8}$$

where $p_1 = 1 - q_1$ is given in Equation (4). If $p_1 = 2^{-j}$ it can be shown that

---

* A limit situation where Equation (4) is exactly satisfied is considered in the last pages of subsection 5.2.3.

** The modifications to this table due to results from Refs. [7-3,4,5,6] have been taken into account.

n \ Mi	1	2	3	4	5	6	7	8	9	10	11	12
7	-	-	-	-	1,3	1,3	1,2	1,2	1,2	1,2	1,2	1,2
9	-	-	-	1,4	1,3	1,3	^{B}2,2	2,2	2,2	2,2	2,2	2,2
15	-	-	1,7	1,5	^{B}2,4	^{A}5,3	5,3	^{A}7,2	7,2	7,2	7,2	7,2
17	-	-	1,7	2,5	3,4	6,3	6,3	^{B}9,2	9,2	9,2	9,2	9,2
21	-	-	1,8	^{B}2,6	^{B}5,4	10,3	10,3	12,2	12,2	12,2	12,2	12,2
23	-	1,11	1,8	2,6	5,5	6,4	^{B}12,3	14,2	14,2	14,2	14,2	14,2
25	-	1,12	1,8	3,6	6,5	7,4	12,3	15,2	15,2	15,2	15,2	15,2
27	-	1,12	1,9	5,6	7,5	9,4	14,3	17,2	17,2	17,2	17,2	17,2
31	-	1,13	2,9	^{A}6,7	^{A}11,5	12,4	^{A}16,3	^{A}21,2	21,2	21,2	21,2	21,2
33	-	1,14	^{B}2,10	6,7	^{B}11,5	^{B}13,4	18,3	^{B}22,2	22,2	22,2	22,2	22,2
35	-	1,14	2,10	7,7	13,5	15,4	20,3	24,2	24,2	24,2	24,2	24,2
39	-	1,15	^{B}2,11	9,7	16,5	19,4	23,3	28,2	28,2	28,2	28,2	28,2
41	-	1,16	3,11	6,8	13,6	^{B}21,4	25,3	25,3	30,2	30,2	30,2	30,2
43	-	1,16	3,11	7,8	^{B}15,6	22,4	27,3	27,3	31,2	31,2	31,2	31,2
45	-	1,17	^{B}4,11	9,8	15,6	24,4	29,3	29,3	33,2	33,2	33,2	33,2
47	-	1,17	3,12	10,8	16,6	25,4	31,3	31,3	35,2	35,2	35,2	35,2
49	-	1,17	4,12	12,8	18,6	26,4	32,3	32,3	37,2	37,2	37,2	37,2
51	-	1,18	5,12	12,8	^{B}19,6	24,5	34,3	34,3	39,2	39,2	39,2	39,2
55	-	1,19	6,13	12,9	22,6	28,5	38,3	38,3	43,2	43,2	43,2	43,2
57	-	1,19	6,13	14,9	24,6	30,5	33,4	40,3	45,2	45,2	45,2	45,2
63	1,31	1,21	^{A}7,14	^{B}19,9	^{B}28,7	^{A}36,5	^{A}39,4	^{B}46,3	^{A}51,2	51,2	51,2	51,2
65	1,32	2,21	8,14	18,10	29,7	37,5	41,4	47,3	^{B}53,2	53,2	53,2	53,2
127	1,54	4,33	^{A}29,21	^{A}43,14	^{A}71,9	^{A}85,6	^{A}92,5	^{A}106,3	106,3	^{A}113,2	113,2	113,2
255	1,94	^{A}21,55	^{A}47,33	^{A}115,21	^{A}155,13	^{A}187,9	^{A}207,6	^{A}223,4	^{A}231,3	^{A}239,2	239,2	239,2
511	1,170	^{A}31,96	^{A}130,55	^{A}241,33	^{A}340,20	^{A}394,13	^{A}439,8	^{A}457,6	^{A}475,4	^{A}484,3	^{A}493,2	493,2
1023	1,315	^{A}111,172	^{A}278,96	^{A}523,55	^{A}708,32	^{A}838,19	^{A}903,12	^{A}943,8	^{A}973,5	^{A}983,4	^{A}993,3	^{A}1003,2

TABLE 7.1: VALUES (k,s)

$p=2^{-i}$; $p_1=p^{M/2}$; $2p_1E(n-1,s,p_1)<10^{-5}\leqslant 2p_1E(n-1,s-1,p_1)$.

A: BCH codes; B: other cyclic codes.

n	M	i=1	2	3	4	5	6	7	8	9	10
15	1	-	-	0.066	0.066	0.133	0.333	0.333	0.466	0.466	0.466
	2	-	0.033	0.166	0.233	0.233	0.233	0.233			
	3	0.022	0.111	0.155	0.155	0.155					
	4	0.016	0.116	0.116							
	5	0.026	0.093	0.093							
	6	0.055	0.077								
	7	0.047	0.066								
	8	0.058									
21	1	-	-	0.047	0.095	0.238	0.476	0.476	0.571	0.571	0.571
	2	-	0.047	0.238	0.286	0.286	0.286	0.286			
	3	0.016	0.158	0.190	0.190	0.190					
	4	0.024	0.143	0.143							
	5	0.047	0.114	0.114							
	6	0.079	0.095								
	7	0.068	0.820								
	8	0.071									
23	1	-	0.043	0.043	0.087	0.217	0.261	0.522	0.609	0.609	0.609
	2	0.022	0.043	0.130	0.304	0.304	0.304	0.304			
	3	0.014	0.087	0.203	0.203	0.203					
	4	0.022	0.152	0.152							
	5	0.043	0.122	0.122							
	6	0.043	0.101								
	7	0.074	0.087								
	8	0.065									
31	1	-	0.032	0.064	0.193	0.354	0.387	0.516	0.677	0.677	0.677
	2	0.016	0.096	0.193	0.338	0.338	0.338	0.338			
	3	0.021	0.129	0.225	0.225	0.225					
	4	0.048	0.169	0.169							
	5	0.070	0.135	0.135							
	6	0.064	0.113								
	7	0.074	0.097								
	8	0.085									
63	1	0.016	0.016	0.111	0.301	0.444	0.571	0.619	0.730	0.809	0.809
	2	0.008	0.151	0.285	0.365	0.405	0.405	0.405			
	3	0.037	0.190	0.270	0.270	0.270					
	4	0.075	0.182	0.202							
	5	0.088	0.162	0.162							
	6	0.095	0.135								
	7	0.088	0.115								
	8	0.091									
127	1	0.008	0.031	0.228	0.338	0.559	0.669	0.724	0.834	0.834	0.890
	2	0.016	0.169	0.334	0.417	0.445	0.445	0.445			
	3	0.076	0.223	0.278	0.296	0.296					
	4	0.085	0.209	0.222							
	5	0.112	0.178	0.178							
	6	0.112	0.148								
	7	0.103	0.127								
	8	0.104									
255	1	0.004	0.082	0.184	0.451	0.608	0.733	0.812	0.874	0.906	0.937
	2	0.045	0.225	0.366	0.437	0.468	0.468	0.468			
	3	0.061	0.244	0.302	0.312	0.312					
	4	0.112	0.218	0.234							
	5	0.121	0.187	0.187							
	6	0.122	0.156								
	7	0.116	0.134								
	8	0.109									
511	1	0.002	0.060	0.254	0.472	0.665	0.771	0.859	0.894	0.930	0.947
	2	0.030	0.236	0.335	0.447	0.474	0.482	0.482			
	3	0.085	0.257	0.310	0.322	0.322					
	4	0.118	0.223	0.241							
	5	0.133	0.189	0.193							
	6	0.128	0.161								
	7	0.123	0.138								
	8	0.112									
1023	1	-	0.108	0.272	0.511	0.692	0.819	0.882	0.922	0.951	0.961
	2	0.054	0.255	0.409	0.461	0.480	0.490	0.490			
	3	0.091	0.273	0.317	0.326	0.326					
	4	0.127	0.230	0.245							
	5	0.138	0.192	0.196							
	6	0.136	0.163								
	7	0.126	0.140								
	8	0.115									

TABLE 7.2: VALUES OF R=K/(Mn) DERIVED FROM TABLE 7.1

If $Mi \geqslant 16$ $\therefore$ $p_1 < 10^{-5}$ and R=1/M.

TABLE 7.3: Parameters for the best cyclic codes

Upper values: k,t,M; lower value: maximum rate R = k/(Mn); t ⩾ s (see Table 7.1)
A: BCH codes B: other cyclic codes

n \ i	1	2	3	4	5	6	7	8	9	10
15	7,2,8 0.058 A	7,2,4 0.116	5,3,2 0.116 A	7,2,2 0.233	7,2,2 0.233	5,3,1 0.333	5,3,1 0.333	7,2,1 0.466	7,2,1 0.466	7,2,1 0.466
21	9,3,6 0.071 B	9,3,3 0.143	9,3,2 0.214	12,2,2 0.286 B	12,2,2 0.286	9,3,1 0.428	9,3,1 0.428	12,2,1 0.571	12,2,1 0.571	12,2,1 0.571
23	12,3,7 0.074 B	12,3,4 0.130	12,3,3 0.174	12,3,2 0.261	12,3,2 0.261	12,3,2 0.261	12,3,1 0.522	12,3,1 0.522	12,3,1 0.522	12,3,1 0.522
31	21,2,8 0.085 A	21,2,4 0.169	21,2,3 0.225	21,2,2 0.338	11,5,1 0.354 A	11,5,1 0.354	16,3,1 0.516 A	21,2,1 0.677	21,2,1 0.677	21,2,1 0.677
63	36,5,6 0.095 A	36,5,3 0.190	36,5,2 0.285	46,3,2 0.365 B	28,7,1 0.444 B	36,5,1 0.571	39,4,1 0.619 A	46,3,1 0.730	51,2,1 0.809 A	51,2,1 0.809
127	85,6,6 0.112 A	85,6,3 0.223	85,6,2 0.334	106,3,2 0.417 A	71,9,1 0.559 A	85,6,1 0.669	92,5,1 0.724A	106,3,1 0.834	106,3,1 0.834	113,2,1 0.890A
255	187,9,6 0.122 A	187,9,3 0.224	187,9,2 0.336	115,21,1 0.451 A	155,13,1 0.608 A	187,9,1 0.733	207,6,1 0.812 A	223,4,1 0.874 A	231,3,1 0.906 A	239,2,1 0.937 A
511	340,20,5 0.133 A	394,13,3 0.257 A	394,13,2 0.385	241,36,1 0.472 A	340,20,1 0.665	394,13,1 0.771	439,8,1 0.859 A	457,6,1 0.894 A	475,4,1 0.930 A	484,3,1 0.947 A
1023	708,34,5 0.138 A	838,19,3 0.273 A	838,19,2 0.409	523,55,1 0.511 A	708,34,1 0.692	838,19,1 0.819	903,12,1 0.882 A	943,8,1 0.922 A	973,5,1 0.951 A	983,4,1 0.961 A

$$C_M \simeq \frac{1 - p_1(j + 1.442)}{M}, \quad j \geqslant 5.$$

In Table 7.4 the values of C_M are given for several values of p and M. It can be seen that for large n and $p = \frac{1}{2}$, the value M = 5 entails a rate reduction with respect to the case where M = 1 of at least

$$\frac{C_5}{C_1} \cdot 100\% = 93.6\%.$$

Similarly, for $p = \frac{1}{4}$ and M = 3,

$$\frac{C_3}{C_1} \cdot 100\% = 68.2\%$$

and for $p = \frac{1}{8}$ and M = 2,

$$\frac{C_2}{C_1} \cdot 100\% = 70.5\%.$$

In practice, by using a powerful BCH code ($n \geqslant 127$) the following results can be achieved:

$$R/C_1 \gtrsim 0.5 \quad \text{if} \quad 1/64 < p \leqslant \tfrac{1}{2},$$

and

$$R/C_1 > 0.7 \quad \text{if} \quad 2 \times 10^{-3} < p \leqslant 1/64,$$

and at the same time an error probability P_e lower than 10^{-5} at the data sink can be ensured. In Refs. [7-1,8] a value $R/C_1 \simeq 0.50$ is considered acceptable in practice if the channel error rate p/2 lies between 10^{-2} and 10^{-3}. By using the system described in this chapter it is possible to satisfy the same requirement in cases where the channel error rate is much higher.

If coding is not used it is necessary that

$$M \geqslant \frac{16}{-\log_2 p}$$

in order to achieve

$$P_e = p_1 < 10^{-5}.$$

The maximum rates attainable in this case are shown in Table 7.5. As can be seen, the transmission rates shown in Table 7.3 for small n are quite close to those in Table 7.5. Thus, combination of the repetition method with an error-correcting

TABLE 7.4

Values of C_M given by Equation (8)

M \ P	1/2	1/4	1/8	1/16	1/32	1/64	1/128	1/256
1	0.188	0.456	0.662	0.799	0.883	0.934	0.963	0.980
2	0.228	0.400	0.467	0.490	0.497	0.499	0.499	0.499
3	0.220	0.311	0.329	0.333	0.333	0.333	0.333	0.333
4	0.200	0.245	0.249	0.249	0.249	0.249	0.249	0.249
5	0.176	0.199	0.199	0.199	0.199	0.199	0.199	0.199
6	0.155	0.166	0.166	0.166	0.166	0.166	0.166	0.166
7	0.137	0.142	0.142	0.142	0.142	0.142	0.142	0.142
8	0.122	0.124	0.124	0.124	0.124	0.124	0.124	0.124

TABLE 7.5

$M \geqslant 16/(-\log_2 p) = a, \quad M < a + 1, \quad P_e = p^{M/2} < 10^{-5}$

$-\log_2 p$	1	2	3	4	5	6	7	8	9	10
M	16	8	6	4	4	3	3	2	2	2
R=1/M	0.062	0.125	0.166	0.250	0.250	0.333	0.333	0.500	0.500	0.500

code can only increase the rate significantly if the code length is large. By using a powerful code the transmission rate can be increased by a factor of about 2, with respect to the case where the repetition method is used alone.

7.4 CONCLUSIONS

If the probability p of a received signal sample being corrupted by a strong impulsive noise is high, the analysis of the previous section shows that the best form of error control from the point of view of transmission rate is an optimized combination of the repetition method developed in Chapter V with error-correcting coding. In fact, by comparing Tables 7.2 and 7.5 it can be seen that for each value of n there is a probability p_o such that if $p > p_o$ the rate corresponding to M = 1 and the best binary linear code is lower than the rate obtained with the repetition method alone. As can be seen, p_o increases as n increases; for example:

$$n = 15 \quad \therefore \quad p_o \simeq 1/64$$
$$n = 1023 \quad \therefore \quad p_o \simeq 1/8.$$

It can be further concluded that for $p \gtrsim p_o$ and n small (say, $n \simeq 20$) the combination of the repetition method with coding provides a transmission rate close to that achieved with the repetition method alone (although for different values of $M>1$). However, by choosing a large code length a significant increase in transmission rate can be achieved in cases where $p \gtrsim p_o$. For lower values of p and arbitrary code length it turns out that the maximum transmission rate is obtained for M = 1.

More specifically, if a BCH code of length $n \geqslant 127$ is used, it is possible to choose the parameters n, k and M in such a way that the transmission rate $R = k/(Mn)$ meets the following requirements*:

---

* C_1 is the capacity of the binary channel when only one pulse is transmitted per symbol (M = 1).

$$R/C_1 \gtrsim 0.5 \quad \text{if} \quad 1/64 < p \leqslant \tfrac{1}{2}$$

and

$$R/C_1 > 0.7 \quad \text{if} \quad 2 \times 10^{-3} < p \leqslant 1/64$$

while the error probability at the decoder output is kept below 10^{-5}. The previous requirements are normally considered acceptable in practice [7-1,8].

As explained in Section 7.1, the previous statements are only valid if the impulse noise samples at the input of the double-path detector and the bit errors at the decoder input can be assumed to occur independently. In order to satisfy these conditions with good enough approximation it will often be necessary to perform an interlacing operation on the encoded data sequence prior to transmission. As explained in Section 7.1, interlacing is usually easier to implement in two steps: first by placing an interleaver at the output of the encoder, and secondly by transmitting the M pulses corresponding to a given data bit at a wide distance apart.

CHAPTER VIII

CONCLUSIONS

> And suppose we solve all the problems it presents. What happens? We end up with more problems than we started with. Because that's the way problems propagate their species. A problem left to itself dries up or goes rotten. But fertilize a problem with a solution - you'll hatch out dozens.
>
> N.F. Simpson, "A Resounding Tinkle"

8.1 SUMMARY OF CONTRIBUTIONS

Most of the conclusions arising out of the work described in the previous four chapters have already been summarized there. In this chapter the original results of the investigation are reviewed with the same general approach as that adopted in Chapter I, and using the terminology and notation introduced in that chapter.

8.1.1 Smearing technique

In Chapter IV the transmitter was assumed to send through the channel, every LT seconds, one of 2^L signal waveforms of the form

$$s_i(t - kLT) = \sum_{j=1}^{L} \alpha_{ij} f_j(t - kLT) \qquad (1)$$

$(i = 0, 1, \ldots, 2^L-1; \quad k = 0, 1, 2, \ldots)$ where $\alpha_{ij} = \pm 1$ and* [see Fig. 1.2(a)]

$$f_j(t) = \sum_{\ell=0}^{N-1} a_{j\ell} y(t - \ell T). \qquad (2)$$

In this way a group of L binary symbols, represented by the coefficients α_{ij} $(j = 1, 2, \ldots, L)$, can be transmitted simultaneously at every signalling instant kLT $(k = 0, 1, 2, \ldots)$. The elementary pulse y(t) was assumed to be essentially time-limited to T seconds and frequency-limited to the channel bandwidth W.

The receiving filters [see Fig. 1.2(b)] were assumed to have impulse responses given by

$$h_j(t) = \sum_{\ell=0}^{N-1} b_{j\ell} y(t - \ell T) \qquad (3)$$

---

* It can always be assumed, without loss of generality, that N is even and that if $a_{jo} = 0$ then $a_{j(N-1)} \neq 0$ for any j.

($j = 1, 2, \ldots, L$). The analysis of the system under the assumption that intersymbol interference is to be avoided at the detector output has led to the following conclusions:

(a) Given $N>1$ the optimum performance is obtained for $L>1$;

(b) Very little (if any) improvement in symbol-error rate can be obtained by using $L>2$.

For this reason only the case $L = 2$ was studied in detail. The correlation between the errors obtained at the detector output may, however, be different for other values of L, particularly in the presence of long noise bursts.

Throughout this study the decision device was assumed to use just one sample per symbol ($M = 1$). The reason for this is that for $M>1$ no system could be devised which was free from intersymbol interference at the detector output, apart from some trivial examples equivalent to the case $L = M = 1$. The decision device was further assumed to consist simply of a parallel-to-serial converter followed by a zero-threshold detector.

Thus defined, the system will show no intersymbol interference at the detector output if and only if the samples delivered to the decision device exhibit no artificial intersymbol interference. A criterion was derived in Chapter IV for choosing the elementary pulse y(t) and the coefficients $a_{j\ell}$ and $b_{j\ell}$ in Equations (2) and (3) in such a way as to satisfy the above necessary and sufficient conditions and furthermore to avoid any interchannel interference in a frequency-division multiplexed (FDM) system. There are grounds for supposing that in the presence of Poisson impulse noise the optimum sequences of coefficients $\{a_{j\ell}\}$ and $\{b_{j\ell}\}$ ($\ell = 0, 1, \ldots, N-1$) are nearly uniform*. For this reason a technique was devised for generating

---

* A sequence of numbers with equal absolute values is termed uniform.

uniform sequences which can be used in the system. The intuitive reason behind the use of uniform sequences is that, for given N and y(t), the responses of the receiving filters to an isolated noise impulse will have nearly the minimum peak amplitudes obtainable, provided that y(t) is approximately time-limited to T seconds. However, this may not be the case when a burst of noise impulses is considered.

The error-rate analysis of the system designed on the basis of uniform sequences of coefficients has shown that a critical SNR exists above which the technique is beneficial and below which it can only be harmful. Furthermore, above this critical SNR the error-rate (a) decreases as N increases, and (b) is lower when the PDF of the energy (within the channel bandwidth) of the elementary disturbance has a short tail, and (c) increases with the average duration of the noise bursts*.

It can readily be concluded from Equations (1) and (2) that the combined waveform transmitted over the channel has the following form:

$$\sum_{k=0}^{\infty} A_k y(t - kT)$$

where the A_k constitute a multilevel sequence. It follows from the conclusion (c) above that a reduction in error-rate can be obtained in the presence of strongly non-Poisson types of noise by performing a scrambling operation on the A_k at the transmitter followed by the inverse operation at the receiver. In fact, after being subjected to the scrambling-descrambling operation the noise will look more like a Poisson impulse noise.

---

* It is assumed in this chapter that, as the noise characteristics change, the error probability of the conventional system (L = M = 1) remains constant.

The smearing of the responses of the receiving filters to an elementary impulsive disturbance, in the attempt to decrease their peak amplitudes, is the underlying principle in the method just described. When using this principle, other authors have always assumed that L = 1. Their results suffer from the following limitations:

(a) If pulses of the form in Equation (2) are used, as in Ref. [8-1], intersymbol interference cannot be eliminated when L = 1;

(b) If a frequency-domain approach is used, as in Ref. [8-2], the resulting "optimum" waveforms seem difficult to realize and show no advantage over the ones proposed here.

8.1.2 Rate-reduction technique

The case in which the decision device has available more than one sample per transmitted symbol (M>1) was considered in Chapter V. In this case a receiver capable of avoiding any intersymbol intefererence could only be devised under the assumption that the transmitted waveforms are essentially non-overlapping. To this effect it was assumed that

$$f_1(t) = \sum_{i=0}^{M-1} a_{1i} y(t - iT) \qquad (4)$$

In order to prevent the samples delivered to the decision device from exhibiting any intersymbol interference it was further assumed that

$$h_1(t) = b_{1o} y(t) \qquad (5)$$

The above waveform design has already been used in the literature but the associated decision device was meant for a noise governed by the same PDF at all sampling instants, and thus needing no time distribution in its characterization (continual noise) [8-3]. In the presence of impulsive noise the

decision device should be able to distinguish between the samples affected by impulsive noise and the samples affected mainly by Gaussian noise. In the proposed decision device a block termed noise detector fulfils this function and directs each sample, according to its type, to one of two branches where the accepted samples are processed nonlinearly to obtain two decision statistics. The decision about the transmitted symbol is normally based on the decision statistic resulting from the samples that are more likely to have been affected mainly by Gaussian noise. If the magnitude of this decision statistic, however, is much smaller than the magnitudes of the signal samples it must be concluded either that the noise detector has failed in some samples* or that all the M samples have been corrupted by impulsive noise. In either of these cases a second decision statistic must be employed which is computed from the samples which are most likely to have been affected by impulsive noise. By computing this second decision statistic from all M samples a simpler receiver structure can be obtained at the expense of a slight increase in error-rate (see Section 5.2.3 and Appendix 2.1).

The error-rate analysis was carried out in Chapter V under the assumption that the coefficients a_{1i} in Equation (4) have equal values. The same types of noise were used as for the smearing technique and the following main results obtained:

(a) The error-rate decreases as the number, M, of pulse repetitions increases;

(b) For a given $M>1$ the improvement obtained, with respect to the conventional system ($M = 1$), increases as the SNR decreases, owing to the higher efficiency of the noise detector at low SNR's;

(c) For given $M>1$ and SNR the error-rate increases as the average noise-burst length increases, thus suggesting the use of a scrambling-descrambling operation as in the previous section;

---

* It follows from the analysis in Chapter V that under normal conditions these samples are most likely affected by impulsive noise.

(d) If the SNR is sufficiently low then

$$P_e \simeq \tfrac{1}{2} P_x$$

where P_e is the error probability at the output of the waveform detector and P_x is the probability of both decision statistics being necessary for making a decision.

This last result suggests a means of making the receiver adaptive in the presence of a non-stationary impulsive noise. In fact, the receiver parameters can be adjusted so as to minimize the estimate of P_x and thus approximately minimize P_e.

It was shown in Chapter VII that if a powerful error-correcting code is added to the above system a higher transmission-rate is obtained for a fixed error-rate. It was further concluded that, if the fraction of signal samples strongly affected by impulsive noise is low, the maximum transmission-rate is achieved when M = 1.

8.2 SUGGESTIONS FOR FURTHER RESEARCH

Some unanswered questions which could be the starting point of further research are outlined below.

8.2.1 Smearing technique

A means of increasing the parameter M would be a useful achievement. This would possibly lead to an improved decision device and could perhaps be effected by increasing the number of receiving filters.

Bounds on the error probability in the presence of non-Poisson types of noise should be derived. These bounds would provide a means of calculating the sequences of coefficients $\{a_{j\ell}\}$ and $\{b_{j\ell}\}$ used in Equations (2) and (3). For this purpose a method of generating any set of sequences with the required autocorrelation and crosscorrelation properties would be quite useful.

After having solved the above problems the use of a scrambling-descrambling operation should be compared with the use of non-uniform sequences. To show that these two methods are not equivalent, it it sufficient to point out that, for a given average transmitted power, uniform sequences give rise to the maximum peak transmitted power*.

8.2.2 Rate-reduction technique

In this area of research the most important problem is the development of more efficient noise detectors. In the case of non-Poisson types of noise the noise detector should decide which samples are more likely to have been strongly corrupted by impulsive noise by analysing simultaneously the entire group of M samples.

Methods of implementing adaptive receivers in the presence of non-stationary impulsive noise also seem to deserve consideration.

---

* See Equation (70) in Chapter IV.

APPENDIX 1*

---

* In this appendix the references to the main text pertain to Chapter IV, unless otherwise stated.

1.1 PROOF OF THEOREMS 1 AND 2

If the pulse $g_n(t-k\delta)$ of Fourier spectrum

$$G_n(f)\,\varepsilon^{-j2\pi k\delta f} =$$

$$= \frac{G_n}{2}\left[\varepsilon^{j\alpha_n} S(f-2n\beta) + \varepsilon^{-j\alpha_n} S(f+2n\beta)\right]\varepsilon^{-j2\pi k\delta f}$$

is received and if the receiving filter has the impulse response $r_i(t - m\delta)$ where

$$r_i(t) = R_i\, x^*(-t)\cos(4\pi i\beta t - \gamma_i)$$

and thus

$$R_i(f) = \frac{R_i}{2}\left[\varepsilon^{-j\gamma_i} X^*(f-2i\beta) + \varepsilon^{j\gamma_i} X^*(f+2i\beta)\right],$$

then the signal samples at the instants $\ell\delta$ at the receiving filter output are given by

$$\int_{-\infty}^{\infty} G_n(f)R_i(f)\,\varepsilon^{j2\pi(\ell - k - m)\delta f}\,df. \qquad (A.1)$$

If $x(t) = s(t)$ these samples are zero except for $n = i$ and $\ell = k+m$ in which case their values are

$$r_n = \tfrac{1}{2}G_n R_n E_s \cos(\gamma_n - \alpha_n).$$

If $\gamma_n = \alpha_n$ then $g_n(t)$ and $r_n(t-m\delta)$ are matched impulse responses and r_n is maximum. If $\gamma_n = \alpha_n + \frac{\pi}{2}$ the two carriers are in quadrature and $r_n = 0$. This proves Theorem 1.

If now $x(t)$ and $s(t)$ are associated Nyquist pulses the integral (A.1) is zero for any values of the integers involved in it, which proves Theorem 2.

PROOF OF THEOREM 3

Since

$$A_{k\ell} = \int_{-\infty}^{\infty} s_a(t)s_a^*(t+2kT)\,\varepsilon^{j4\pi\ell\beta t}\,dt$$

$$= \frac{E_s}{N}\sum_{m,n} a_m a_n \int_{-\infty}^{\infty} y(t-mT)y^*(t-nT-2kT)\,\varepsilon^{j4\pi\ell\beta t}\,dt$$

$$= \frac{E_s}{N}\,E_y \sum_{n} a_n\, a_{n+2k}$$

and

$$B_{k\ell} = \int_{-\infty}^{\infty} s_a(t) s_b^*(t+2kT)\, \varepsilon^{j4\pi\ell\beta t}\, dt$$

$$= \frac{E_s}{N} E_y \sum_n b_n a_{n+2k}$$

where $\beta = \frac{1}{\rho T}$, the theorem follows.

PROOF OF THEOREM 4

Since $s(t)$ is time-limited to $[-T/2, T/2]$ the condition (15), with $\delta = T$, is fulfilled for any $k \neq 0$. For $k = 0$

$$A_{on} = \int_{-T/2}^{T/2} s^2(t) \cos\frac{4\pi nt}{\rho T} dt$$

$$= \begin{cases} E_s, & n = 0 \\ 0, & n \neq 0. \end{cases}$$

Therefore, if $\rho = 2$,

$$s^2(t) = \frac{E_s}{T} G_a\left(\frac{t}{T}\right)$$

$$= \begin{cases} E_s/T, & |t| < T/2 \\ 0, & |t| > T/2. \end{cases}$$

If $\rho = 1$, A_{on} can be written as follows:

$$A_{on} = 2 \int_0^{T/2} s^2(t) \cos\frac{4\pi nt}{T} dt$$

and thus, in the interval $[-T/2, T/2]$,

$$s^2(t) = \frac{E_s}{T} + \sum_{n=1}^{\infty} b_n \sin\left(\frac{4\pi n}{T}|t|\right) \qquad (A.2)$$

where

$$b_n = \frac{4}{T} \int_0^{T/2} s^2(t) \sin\frac{4\pi nt}{T} dt.$$

Equation (A.2) shows that

$$s^2(t) = \frac{E_s}{T} + \varphi(t)$$

where $\varphi(t)$ is antisymmetrical in $[0, T/2]$ with respect to the point $t = T/4$. Therefore

$$s^2\left(t - \frac{T}{2}\right) = \frac{E_s}{T} - \varphi(t), \qquad 0 \leq t \leq T/2$$

and

$$s^2(t) + s^2(t-T/2) = 2E_s/T, \qquad 0 \leqslant t \leqslant T/2.$$

PROOF OF THEOREM 5

$$A_{on} = 2 \int_0^{T/2} r^2(t) \cos\frac{4\pi nt}{T} dt$$

$$= 2 \int_0^{T/2} s^2(\frac{T}{2} - t) \cos\frac{4\pi nt}{T} dt$$

$$= 2 \int_0^{T/2} s^2(x) \cos\frac{4\pi nx}{T} dx = E_s \delta_{on}$$

where δ_{on} is the Kronecker delta.

$$B_{on} = 2 \int_0^{T/2} s(t)\, s(\frac{T}{2} - t) \sin\frac{4\pi nt}{T} dt$$

$$= 2(-1)^n \int_{-T/4}^{T/4} s(\frac{T}{4} + x)\, s(\frac{T}{4} - x) \sin\frac{4\pi nx}{T} dx$$

$$= 0, \quad \text{any } n,$$

since

$$f(x) = s(\frac{T}{4} + x)\, s(\frac{T}{4} - x)$$

is an even function.

1.2

According to the description given in the main text, the detection of the coefficient α_o of Equation (43) is based on the sample produced at $t = \ell T$ by the sampler 1 [Fig. 4.2(b)], the value of which is,

$$Z_o = \frac{\sqrt{E_s}}{N} \sum_k \alpha_{2k} \sum_i a_i\, r_{i+2k} + \frac{\sqrt{E_s}}{N} \sum_k \alpha_{2k-1} \sum_i b_i r_{i+2k}$$

Similarly, the detection of the coefficient α_{-1} is based on the sample produced at $t = \ell T$ by the sampler 2, which is given by

$$Z_{-1} = \frac{\sqrt{E_s}}{N} \sum_k \alpha_{2k-1} \sum_i b_i s_{i+2k} + \frac{\sqrt{E_s}}{N} \sum_k \alpha_{2k} \sum_i a_i s_{i+2k};$$

Therefore, if Equations (49) and (50) are valid, it follows that $Z_0 = \alpha_0 A_1$, and $Z_{-1} = \alpha_{-1} A_2$ [see Equations (56) and (57)] and no intersymbol interference arises.

If the noise n(t) in Fig. 4.2(b) is assumed to be Gaussian and to have a constant power spectral density σ_o^2, then the noise variances at the outputs of the samplers 1 and 2 are respectively

$$\sigma_1^2 = \sigma_0^2 \int_{-\infty}^{\infty} Z_r^2(t)dt = \frac{\sigma_o^2}{N} \sum_i r_i^2$$

and

$$\sigma_2^2 = \sigma_0^2 \int_{-\infty}^{\infty} Z_s^2(t)dt = \frac{\sigma_o^2}{N} \sum_i s_i^2$$

where

$$Z_r(t) = \frac{1}{\sqrt{N}} \sum_i r_i \, h(t - iT)$$

$$Z_s(t) = \frac{1}{\sqrt{N}} \sum_i s_i \, h(t - iT).$$

If the signal samples are assumed to have constant magnitudes A_1 and A_2, it is easy to show that those noise variances attain the minimum values $\sigma_1^2 = G^2\sigma_0^2$ and $\sigma_2^2 = H^2\sigma_0^2$ if and only if Equations (54) and (55) are satisfied.

Now let expression (68) be derived under the conditions specified in the main text, which imply that

$$<\alpha_n \alpha_m> = \delta_{nm} \text{ (Kronecker delta).} \qquad (A.3)$$

On defining [see Equation (47)]

$$s_L(t) = \sum_{k=-L}^{L} \left[\alpha_{2k} s_a(t-2kT) + \alpha_{2k-1} s_b(t-2kT) \right]$$

then

$$P_s = \lim_{L \to \infty} \frac{1}{4LT} \int_{-\infty}^{\infty} \langle s_L^2(t) \rangle \, dt.$$

According to Equation (A.3)

$$\langle s_L^2(t) \rangle = \sum_{k=-L}^{L} \left[s_a^2(t - 2kT) + s_b^2(t - 2kT) \right]$$

and thus, since

$$\int_{-\infty}^{\infty} s_a^2(t)dt = \frac{E_y E_s}{N} \sum_i a_i^2 \qquad (A.4)$$

$$\int_{-\infty}^{\infty} s_b^2(t)dt = \frac{E_y E_s}{N} \sum_i b_i^2, \qquad (A.5)$$

the expression (68) follows.

Whenever $s_a(t)$ and $s_b(t)$ are associated Nyquist pulses, the argument used in deriving Equations (A.4) and (A.5) can also be used to derive Equation (68) with no restrictions imposed on the data sequence $\{\alpha_i\}$.

If in Fig. 4.2(b) the noise n(t) is a white Gaussian noise of spectral density σ_0^2 then the noise autocorrelation function at the output of the receiving filter H(f) is

$$R_1(\tau) = \sigma_0^2 \int_{-\infty}^{\infty} h(t) \, h(t - \tau)dt.$$

Similarly, the autocorrelation function at the output of the delay line L_r is

$$R_a(\tau) = \sigma_0^2 \int_{-\infty}^{\infty} Z_r(t) \, Z_r(t - \tau)dt.$$

Therefore, if h(t) and $Z_r(t)$ are Nyquist pulses it follows that, for $i \neq 0$,

$$R_1(iT) = 0$$

and

$$R_a(2iT) = 0.$$

These relations mean that two noise samples iT seconds apart at

the receiving filter output or 2iT seconds apart at the delay line output are statistically independent.

1.3 PROOF OF THEOREM 6

$$X_k = \sum_i b_i\, b_{i+2k} = \sum_i a_{N-i+1}\, a_{N-i-2k+1}$$

$$= \sum_j a_j\, a_{j-2k}.$$

Thus the sequence B is self-orthogonal. Defining N as the smallest even integer (N = 2L) such that $a_i = 0$ when $i<1$ or $i>N$, then

$$Y_k = \sum_i b_i\, a_{i+2k} = \sum_i (-1)^i\, a_{2L-i+1}\, a_{i+2k}$$

$$= -\sum_{\ell=1}^{2M} (-1)^\ell\, a_\ell\, a_{2M-\ell+1}$$

where $\ell = N-i+1$ and $M = L+k \geq 1$. Therefore

$$Y_k = -\sum_{\ell=1}^{M} (-1)^\ell\, a_\ell\, a_{2M-\ell+1} - \sum_{\ell=M+1}^{2M} (-1)^\ell\, a_\ell\, a_{2M-\ell+1}$$

$$= -\sum_{\ell=1}^{M} (-1)^\ell\, a_\ell\, a_{2M-\ell+1} + \sum_{j=1}^{M} (-1)^j\, a_j\, a_{2M-j+1}$$

$$= 0, \qquad j = 2M - \ell + 1.$$

Therefore, A and B are associated sequences.

PROOF OF THEOREM 7

Defining

$$C = \{a_1, a_2, \ldots, a_N, b_1, b_2, \ldots, b_N\}$$

(all other elements being zero) it is obvious that C is self-orthogonal. Now note that, in view of Equation (59),

$$d_i = (-1)^i\, b_{N-i+1} = (-1)^{N+1} a_i = -a_i,$$

for $i \leqslant N$, and thus Theorem 6 completes the proof.

Given the self-orthogonal sequence $A = \{a_i\}$, Theorem 6 states that, for any b,

$$b_i = b(-1)^i a_{N-i+1} \tag{A.6}$$

is a solution of the linear system of equations

$$\sum_i b_i\, a_{i+2k} = 0, \qquad \text{any } k.$$

It can be proved as follows that any solution of this system satisfies Equation (A.6) for some b. In matrix notation this system takes on the following form for N = 8:

$$\begin{bmatrix} a_8 & 0 & 0 & 0 & 0 & 0 & 0 \\ a_6 & a_7 & a_8 & 0 & 0 & 0 & 0 \\ a_4 & a_5 & a_6 & a_7 & a_8 & 0 & 0 \\ a_2 & a_3 & a_4 & a_5 & a_6 & a_7 & a_8 \\ 0 & a_1 & a_2 & a_3 & a_4 & a_5 & a_6 \\ 0 & 0 & 0 & a_1 & a_2 & a_3 & a_4 \\ 0 & 0 & 0 & 0 & 0 & a_1 & a_2 \end{bmatrix} \begin{bmatrix} b_2 \\ b_3 \\ b_4 \\ b_5 \\ b_6 \\ b_7 \\ b_8 \end{bmatrix} = -b_1 \begin{bmatrix} a_7 \\ a_5 \\ a_3 \\ a_1 \\ 0 \\ 0 \\ 0 \end{bmatrix} \tag{A.7}$$

It can be assumed without any loss of generality that $a_8 \neq 0$. The first equation of the system then gives

$$b_2 = -\frac{b_1}{a_8} a_7$$

which implies that $b_1 \neq 0$ (otherwise $b_1 = b_2 = 0$). The determinant of the system (A.7) is given by

$$D = a_8 \cdot \begin{vmatrix} a_7 & a_8 & 0 & 0 & 0 & 0 \\ a_5 & a_6 & a_7 & a_8 & 0 & 0 \\ a_3 & a_4 & a_5 & a_6 & a_7 & a_8 \\ a_1 & a_2 & a_3 & a_4 & a_5 & a_6 \\ 0 & 0 & a_1 & a_2 & a_3 & a_4 \\ 0 & 0 & 0 & 0 & a_1 & a_2 \end{vmatrix}$$

Since $a_1 \neq 0$ and/or $a_2 \neq 0$ it is obvious that the last three rows of D, as well as its first three, are linearly independent. Moreover, since $A = \{a_i\}$ is a self-orthogonal sequence, any of the first three rows is orthogonal to any of the last three. Therefore $D \neq 0$ and the system (A.7) has a unique solution, which is

$$b_i = -\frac{b_1}{a_N}(-1)^i a_{N-i+1}.$$

The previous proof can be easily extended to any (even) value of N.

The group of permutation operations referred to in the main text can be described as follows. Consider a vector W and divide it into L pairs of components:

$$W = \{P_1, P_2, \ldots, P_L\}, \qquad N = 2L = 2^n.$$

The basic operation T_1 consists in writing the odd pairs first and the even ones next:

$$T_1 W = \{P_1, P_3, \ldots, P_{L-1}, P_2, P_4, \ldots, P_L\}.$$

If now W is divided into $M = 2^{m-1}$ parts (m = 2, 3, ..., n-2), that is

$$W = \{W_1, W_2, \ldots, W_M\},$$

the relation

$$T_m W = \{T_1 W_1, T_1 W_2, \ldots, T_1 W_M\}$$

defines a new operation T_m. In all cases where $n \leqslant 5$ the following properties were proved to exist by direct verification:

(a) All different products of the operations $T_1, T_2, \ldots, T_{n-2}$ form a group of (n-1)! operations, the identity operation being one of them.

(b) Any operation of this group gives rise to an orthogonal set of self-orthogonal sequences when applied to the uniform self-orthogonal sequences of the basic set generated by Equation (60).

No general proofs could be found for these properties which are conjectured to be valid for any value of N.

The previous operations were also applied to many non-uniform sequences generated by Equations (60) and (61) and the resulting sequences were self-orthogonal when and only when the starting sequences had symmetrical envelopes*.

1.4

Given the N-long binary sequence $A = \{a_i\}$, $a_i = \pm 1$, it is sometimes more convenient to use instead a sequence $X = \{x_i\}$ of zeros and ones obtained as follows

$$X_i = \begin{cases} 0 & \text{if } a_i = +1 \\ 1 & \text{if } a_i = -1 \end{cases}$$

It is easy to see that if A is self-orthogonal then its length N must be even and the elements of X must satisfy the following relations**:

$$(\text{mod } 2) \sum_{i=1}^{2r} (x_i \oplus x_{N-2r+i}) = \begin{cases} 1, & r \text{ odd} \\ 0, & r \text{ even} \end{cases}$$

provided that $2 \leqslant 2r < N$. However, the sequence

$$X = \{1 \quad 0 \quad 1 \quad 0 \quad 1 \quad 1 \quad 1 \quad 1\}$$

satisfies the previous relations but does not correspond to a self-orthogonal sequence.

PROOF OF THEOREM 8

For r = 1 the above relations give

$$x_1 \oplus x_2 \oplus x_{N-1} \oplus x_N \equiv 1$$

For r = 2:

$$x_1 \oplus x_2 \oplus x_3 \oplus x_4 \oplus x_{N-3} \oplus x_{N-2} \oplus x_{N-1} \oplus x_N \equiv 0$$

---

* The sequence $\{|a_i|\}$ is called the envelope of $\{a_i\}$.

** The sign $\oplus$ denotes modulo 2 addition.

By adding the two previous relations it can be concluded that

$$x_3 \oplus x_4 \oplus x_{N-3} \oplus x_{N-2} \equiv 1.$$

This process may be continued to show that, for any k such that $2 \leqslant 2k < N$,

$$x_{2k-1} \oplus x_{2k} \oplus x_{N-2k+1} \oplus x_{N-2k+2} \equiv 1 \qquad (A.8)$$

This relation shows that in a self-orthogonal sequence A the vectors

$$(a_{2k-1}, a_{2k}) \quad \text{and} \quad (a_{N-2k+1}, a_{N-2k+2})$$

must be orthogonal. Let it now be proved that if $N = 2n > 2$ then n cannot be odd. In fact, if

$$N = 2(2M - 1), \qquad M \geqslant 2$$

then Equation (A.8) above will give for k = M

$$x_{2M-1} \oplus x_{2M} \oplus x_{2M-1} \oplus x_{2M} \equiv 1$$

which cannot be true. It thus follows that n = 2M and that N = 4M, q.e.d.

The relationship between associated self-orthogonal sequences and complementary sequences can be expressed by the following theorem.

Theorem: If two binary self-orthogonal sequences are associated with each other then they are complementary*.

Proof: Due to Equation (51) in the main text, the autocorrelation functions of $A = \{a_i\}$ and $B = \{b_i\}$ are related as follows:

$$h_b(j) = \sum_{i=1}^{N-j} b_i \, b_{i+j}$$

$$= \sum_{i=1}^{N-j} (-1)^i \, a_{N-i+1} \, (-1)^{i+j} \, a_{N-i-j+1}.$$

---

* See definition (64) in the main text.

On making N-i-j+1 = r it follows that

$$h_b(j) = (-1)^j \sum_{i=1}^{N-j} a_r \, a_{r+j}$$

$$= (-1)^j \, h_a(j), \qquad 0 \leqslant j < N.$$

Since A is self-orthogonal it is possible to write

$$h_a(2k) = 0, \qquad 0 < 2k < N.$$

It thus follows that

$$h_a(j) + h_b(j) = 0, \qquad 0 < j < N$$

and thus A and B are complementary sequences, q.e.d.

By considering the complementary sequences of length 10 given in Ref. [4-4] it can be concluded that the converse of the previous theorem is not true.

The following table gives the basic self-orthogonal sequences of length 20 beginning with two +1's.

TABLE 4.5*: Self-orthogonal sequences of length 20.

```
+ + - - - - + - - - + - - - - + - + + -
+ + - - - - - + - - - + - - + - + - - +
+ + - - - - - - + - - - + - - + - + + -
+ + - - - - - - - + - - - + + - + - - +
+ + + + - - - + - - - + - - + - - + - +
+ + + + - - + - - - + - - - - + + - + -
+ + + + - - + + + - + + + - + - - + - +
+ + + + - - + + - + + + - + - + + - + -
+ + - + + + - + + - + + + + + + - - - + -
+ + + - + + + - - + + + + + - + - - + -
+ + - - - + + - + + - + + + + + + - + -
+ + - - + - - + + + + - + + + + - + - +
+ + + - + + + - + - - - + + - + - - + -
+ + - + + + - + - + - - + + + - - - - +
+ + + + - + - + + + + - + + - - + - - +
+ + + + + - + - + + - + + + - - - + + -
```

---

* The listed sequences together with those associated with them can be reversed to produce a total of 64 sequences. If then these sequences are multiplied by -1, the 128 possible binary self-orthogonal sequences of length 20 are obtained.

1.5

Given the CHF F(u) corresponding to the PDF f(x), it is possible to calculate the exceedence probability function (EPF)

$$Q_f(x) = \int_x^\infty f(y)dy$$

without first calculating f(x). For reasons explained in Ref. [4-8], the best way is to take an appropriate reference CHF G(u), whose EPF $Q_g(x)$ is known, and to calculate

$$s(x) = \int_x^\infty [f(y) - g(y)]\, dy = Q_f(x) - Q_g(x)$$

instead of $Q_f(x)$. It is easy to show that

$$S(u) = \int_{-\infty}^{\infty} s(x)\, \varepsilon^{jux}\, dx$$

$$= \frac{F(u) - G(u)}{ju}$$

and that, for real F(u) and G(u), S(0) = 0. A computer program has been written to find s(x) by applying the Fast Fourier Transform algorithm to the samples of S(u). A symmetrical Laplace PDF was taken as g(x).

Now let $s_1(x)$ be either $s_{a1}(x)$ or $s_{b1}(x)$ and $F_1(u)$ be either $F_{a1}(u)$ or $F_{b1}(u)$ [see Equations (96) and (97)]. On defining

$$D_i(u) = \int_{-\frac{1}{2}}^{\frac{1}{2}} F_{r_1}\left(\frac{u}{\sqrt{\nu_1}}\, s_1(x+i)\right)dx$$

and

$$F_{1L}(u) = \exp\left\{\nu_1 \sum_{i=-L}^{N+L-1} [D_i(u) - 1]\right\}$$

it can be shown that

$$F_1(u) = \lim_{L \to \infty} F_{1L}(u).$$

If instead of using $F_{1L}(u)$, for which $F_{1L}(\infty) = \exp[-\nu_1(2L+N)] = h_L$, one uses the CHF

$$R_L(u) = \frac{F_{1L}(u) - h_L}{1 - h_L},$$

for which $R_L(\infty) = 0$, the accuracy of the numerical results is improved. Defining $Q_{rL}(x)$ as the EPF of $R_L(u)$, then the EPF of $F_1(u)$, for $x>0$, is given by

$$Q_{f_1}(x) = \lim_{L\to\infty}(1 - h_L)Q_{rL}(x).$$

Under the assumed conditions the numerical results were found sufficiently accurate for L = 2.

If the elementary pulse y(x) is time-limited to T sec then

$$D_i(u) = \int_{-\frac{1}{2}}^{\frac{1}{2}} F_{r_1}\left(\frac{ua_i y_1(x)}{\sqrt{\nu_1 N}}\right)dx = H\left(\frac{a_i u}{\sqrt{N}}\right), \qquad (A.9)$$

and thus Equations (101), (102) and (103) follow. The non-zero semi-invariants corresponding to Equations (101) and (102) are respectively [4-10]

$$A_{2k} = \lambda_{2k}\sum_i a_i^{2k}$$

and $$B_{2k} = \lambda_{2k}\sum_i b_i^{2k}, \qquad k\geq 1,$$

where the λ_{2k} are semi-invariants of the CHF $\phi_1(u)$:

$$\lambda_{2k} = \frac{\nu_1}{(\nu_1 N)^k}\,\mu_{2k}\int_{-\infty}^{\infty} y_1^{2k}(x)dx,$$

the μ_{2k} being the even-order moments of $p_{r_1}(x)$. It can be shown that A_{2k} and B_{2k}, $k>1$, attain their minimum value under the conditions (24) when $a_i = b_i = 1$, i = 1, 2, ..., N, which means that the noise PDF is closest to the Gaussian PDF when uniform sequences are used. As the error probability computations have shown, the fact that the noise tends to become Gaussian is beneficial when the SNR exceeds a certain threshold and thus it appears that uniform or nearly uniform sequences should yield the minimum error probability for SNR's above this threshold. Moreover, it can be shown that the fraction of errors due to a single noise impulse is minimized if uniform sequences are used

and the SNR is sufficiently high. In fact, if one and only one noise pulse is observed, the noise CHF is given by* [see Equation (A.9)]

$$H_1(u) = \frac{1}{N}\sum_{i=1}^{N} H\left(\frac{a_i u}{\sqrt{N}}\right)$$

and the corresponding PDF and EPF are respectively

$$h_1(x) = \frac{1}{\sqrt{N}}\sum_{i=1}^{N} \frac{1}{a_i} h\left(\frac{x\sqrt{N}}{a_i}\right)$$

$$Q_1(x) = \frac{1}{N}\sum_{i=1}^{N} Q\left(\frac{x\sqrt{N}}{a_i}\right)$$

where h(x) and Q(x) are the PDF and EPF of H(u). It can be shown that if

$$\frac{d}{dy}\left[y^3 h(y)\right] < 0 \quad \text{for} \quad y > A$$

then $Q_1(B)$ is minimum if $a_i = 1$, $i = 1, 2, \ldots, N$, and $B > A/\sqrt{N}$.

It may seem advisable to minimize the error probability, as a function of the parameters a_i, by using some numerical optimization technique. Yet, the enormous computation time it would take renders this method impractical.

Up to now the noise pulses were assumed to occur in a purely random way. To conclude this appendix a case of non-Poisson noise, where the minimization of the error probability may lead to strongly non-uniform transmitted sequences $A = \{a_i\}$ and $B = \{b_i\}$, is considered. It is assumed that the impulse response of the receiving filter in Fig. 4.2(b) is time-limited to $[-T/2, T/2]$. Thus, each noise pulse affects only one signal sample. Moreover, the following time structure is assumed for the noise:

(a) The noise pulses occur in bursts in such a way that each burst affects L consecutive signal samples.

---

* This CHF corresponds to a noise obtained by normalizing to unit variance the noise observed at the point a in Fig. 4.2(b) under the assumed conditions.

(b) Each noise-free interval contains at least N-1 signal samples.

Therefore, each N-long received sequence is either noise-free or affected by one and only one noise burst.

The noise samples at the input of the delay lines in Fig. 4.2(b) are assumed to obey a Gaussian distribution with variance σ_z^2. Since each noise burst can have M = N+L-1 different positions with respect to the referred delay lines, the noise samples obtained at the point a in Fig. 4.2(b) can have any of the variances σ_i^2, i = 1, 2,..., M, given by

$$\sigma_i^2 = \frac{\sigma_z^2}{N} \sum_{j=1}^{N} \alpha_{ij} \, r_j^2$$

where $[\alpha_{ij}]$ is a M x N matrix of zeros and ones. Therefore, the average error probability is given by

$$P_{eL} = \frac{1}{2M} \sum_{i=1}^{M} \operatorname{erfc}\left(\frac{A_s}{\sqrt{2}\,\sigma_i}\right)$$

On making

$$x_j = r_j^2$$
$$S_i^2 = \frac{1}{N} \sum_{j=1}^{N} \alpha_{ij} \, x_j \qquad \text{(A.10)}$$

and

$$\mu = \frac{A_s}{\sigma_z}$$

it follows that

$$P_{eL} = \frac{1}{2M} \sum_{i=1}^{M} \operatorname{erfc}\left(\frac{\mu}{\sqrt{2}\,S_i}\right).$$

The problem is thus to minimize P_{eL} assuming that the variables x_j are constrained by Equation (74), that is

$$\sum_{j=1}^{N} x_j = N. \qquad \text{(A.11)}$$

It is thus possible to write, according to the method of the Lagrange multipliers,

$$X = P_{eL} - \lambda \frac{\mu}{2MN} \sum_{j=1}^{N} x_j$$

$$\frac{\partial X}{\partial x_j} = \frac{\mu}{2MN} \left[\sum_{i=1}^{M} X_i \alpha_{ij} - \lambda \right] = 0 \qquad \text{(A.12)}$$

and

$$\frac{\partial^2 X}{\partial x_j \partial x_k} = \frac{\mu}{4MN^2} \sum_{i=1}^{M} \frac{\partial X_i}{\partial S_i} \frac{\alpha_{ij}}{S_i} \alpha_{ik} \qquad \text{(A.13)}$$

where

$$X_i = \frac{1}{\sqrt{2\pi}} \frac{1}{S_i^3} \exp\left(-\frac{\mu^2}{2S_i^2}\right)$$

and

$$\frac{\partial X_i}{\partial S_i} = \frac{X_i}{S_i}\left(\frac{\mu^2}{S_i^2} - 3\right).$$

In matrix notation Equation (A.12) takes on the following form:

$$[X_i][\alpha_{ij}] = \lambda [V_j] \qquad \text{(A.14)}$$

where $V_j = 1, \quad j = 1, 2, \ldots, N.$

If L = 1 then $[\alpha_{ij}]$ is the N x N identity matrix and thus

$$X_j = \lambda, \qquad i \leq j \leq N.$$

Therefore the variables S_j have the same value which, according to Equations (A.10) and (A.11), is given by

$$S_i^2 = \frac{x_i}{N} = \frac{1}{N}.$$

It can finally be concluded from Equation (A.13) that, if L = 1 and $\mu > \sqrt{3/N}$, the uniform self-orthogonal sequences minimize the error probability P_{eL}.

Now consider the following particular case:

$$N = 4, \; L = 2 \quad \therefore \quad M = 5.$$

The matrix $[\alpha_{ij}]$ is in this case

$$[\alpha_{ij}] = \begin{bmatrix} 1 & 0 & 0 & 0 \\ 1 & 1 & 0 & 0 \\ 0 & 1 & 1 & 0 \\ 0 & 0 & 1 & 1 \\ 0 & 0 & 1 & 1 \end{bmatrix}$$

and the system (A.14) can be written as follows:

$$\begin{cases} X_1 + X_2 = \lambda \\ X_2 + X_3 = \lambda \\ X_3 + X_4 = \lambda \\ X_4 + X_5 = \lambda \end{cases} \quad \therefore \quad \begin{cases} X_1 = X_3 = X_5 \\ X_2 = X_4 \\ X_1 + X_2 = \lambda . \end{cases}$$

Therefore:

$$\begin{cases} S_1^2 = S_3^2 \\ S_3^2 = S_5^2 \\ S_2^2 = S_4^2 \end{cases} \quad \therefore \quad \begin{cases} x_1 = x_2 + x_3 \\ x_2 + x_3 = x_4 \\ x_1 + x_2 = x_3 + x_4 . \end{cases}$$

On taking into account Equation (A.11) it finally follows that*

$$\begin{cases} x_1 = x_4 = 4/3 \\ x_2 = x_3 = \frac{2}{3} \\ S_1^2 = S_3^2 = S_5^2 = \frac{1}{3} \\ S_2^2 = S_4^2 = \frac{1}{2} . \end{cases}$$

In view of Equation (A.13), the previous values correspond to a minimum of P_{eL} provided that $\mu > \sqrt{3/2} = 1.225$. According to Equations (77), a pair of optimum associated self-orthogonal sequences that can be transmitted is thus

$$A = \left\{ \frac{2}{\sqrt{3}}, \sqrt{\frac{2}{3}}, -\sqrt{\frac{2}{3}}, \frac{2}{\sqrt{3}} \right\}$$

$$B = \left\{ \frac{2}{\sqrt{3}}, \sqrt{\frac{2}{3}}, \sqrt{\frac{2}{3}}, -\frac{2}{\sqrt{3}} \right\} .$$

The above method can be used for other values of L and N. The

---

* Note that the values x_i correspond to sequences with symmetrical envelopes.

optimum envelope $\{|r_i|\}$ obtained will always be symmetrical but in some cases no self-orthogonal sequence exists with this envelope. This means that in general the constraints of self-orthogonality must be included in the formulation of the optimization problem.

APPENDIX 2*

---

* In this appendix, the references to the main text pertain to Chapter V, unless otherwise stated.

2.1

In order to calculate the probabilities P_{eu} and P_x by means of Equations (68) and (69) in the main text, a method is needed for calculating the coefficients in the expansion of $(a + b + c)^M$. In order to find this method it is first noted that

$$(a+b+c)^2 = (a+b+c)(a+b+c) = a.a + a.b + a.c + b.a + b.b + b.c + c.a + c.b + c.c.$$

For M = 3, the above expression is simply multiplied by (a+b+c), and so on. If every time combining factors or terms are avoided then a sum of 3^M terms, which are all the possible permutations of the elements a, b and c in M positions, is obtained. In order to obtain these 3^M permutations, the simplest way is to generate, one after the other, the integers from zero to 3^M-1, written in base 3. In Equation (67), ℓ_i, m_i and n_i can thus be interpreted as the number of 0's, 1's and 2's, respectively, in the M-digit integer under consideration; the coefficient N_i is the total number of integers corresponding to the same set (ℓ_i, m_i, n_i).

The relation (70) can be justified as follows. If

$$\alpha \ll 1 \quad \text{and} \quad p\beta \ll q \tag{A.1}$$

then, according to Equations (64) to (66),

$$P_+ \simeq q, \quad P_- \simeq p\beta_- \quad \text{and} \quad P_0 \simeq p(1 - \beta). \tag{A.2}$$

Assuming that $\emptyset_i = +1$, in the case of an outcome of probability

$$G_i P_-^{d_i} P_0^{e_i} P_+^{f_i}, \qquad d_i = f_i,$$

the following samples are obtained at the sampler output in Fig. 5.4 : d_i samples of values $-A + \alpha_j$, f_i samples of values $A + \beta_k$ and e_i samples of values $A + \gamma_n$, where $-\varepsilon_2 < \alpha_j < \varepsilon_1$, $-\varepsilon_1 < \beta_k < \varepsilon_2$ and $A + \varepsilon_2 < |A+\gamma_n| < A-\varepsilon_1$. In view of relations (A.2) it may be concluded that the f_i samples $A+\beta_k$ are most likely affected by Gaussian noise alone, and that all the other samples

are most likely affected by impulsive noise. Because $\rho_{dB} > 12$ dB, most of the errors occur when impulsive noise is present and thus the f_i noise samples β_k may be neglected. The e_i noise samples γ_n will be replaced by e_i independent random variables with PDF $p_z(x)$. The random variables α_j can either be neglected or replaced by d_i independent random variables with PDF $p_z(x)$. In the first case the relation (70) is obtained. In the second case the contribution from the α_j is overestimated and the following approximation is obtained

$$P_x P_{ex} \simeq \sum_{i=1}^{G} G_i P_-^{d_i} P_o^{e_i} P_+^{f_i} E_{k_i}(e_i A) \qquad (A.3)$$

where $k_i = d_i + e_i$. In the numerical examples discussed in Section 5.3, the values given by relations (70) and (A.3) were found to be nearly equal. This is due to the fact that in these examples $P_- \ll P_0$ and thus the cases in which $d_i > 0$ have a much lower probability than those in which $d_i = f_i = 0$. This is in agreement with the comments made about the relation (58) in the main text.

It is important to note that the conditions (A.1) are, from a practical viewpoint, equivalent to the conditions (83) and (84) since usually $q \simeq 1$.

2.2

In this section, Equation (77) in the main text is proven. If $\varepsilon_1 = \varepsilon_2 = \varepsilon_0$ and $\sigma_w = 0$ then, according to Equations (33), (34), (40) and (41),

$$\alpha_+ = 1 \qquad \alpha_- = 0$$

$$\beta_+ = 1 - 2Q_z(\varepsilon_o/k_z)$$

and

$$\beta_- = Q_z\left(\frac{2A - \varepsilon_0}{k_z}\right) - Q_z\left(\frac{2A + \varepsilon_0}{k_z}\right)$$

Equations (75) and (76) then follow. Now note that

$$\lim_{\varepsilon_0 \to 0} \beta = 0$$

and thus

$$P\left[\hat{\theta}_i = 1 \,\middle|\, \theta_i = 1\right] = 1 - \beta \underset{\varepsilon_0 \to 0}{\longrightarrow} 1.$$

Therefore, if $\varepsilon_0 \simeq 0$ the upper branch of the receiver will only fail to reach a correct decision when all samples are affected by impulsive noise, that is, when

$$\lim_{\varepsilon_0 \to 0} P_{eu} = 0$$

and

$$\lim_{\varepsilon_0 \to 0} P_x = p^M.$$

In view of the above-mentioned Equations (75) and (76) it follows that, for $\sigma_w = 0$,

$$P_+\big|_{\varepsilon_0 \to 0} = q \qquad P_-\big|_{\varepsilon_o \to 0} = 0$$

$$P_0\big|_{\varepsilon_0 \to 0} = p$$

$$\left.\frac{dP_+}{d\varepsilon_0}\right|_{\varepsilon_0 \to 0} = 2p\, p_z(0)$$

$$\left.\frac{dP_-}{d\varepsilon_0}\right|_{\varepsilon_0 \to 0} = 2p\, p_z(2A)$$

$$\left.\frac{dP_0}{d\varepsilon_0}\right|_{\varepsilon_0 \to 0} = -2p\, p_z(0) - 2p\, p_z(2A).$$

On using Equation (69) the result

$$\frac{dP_x}{d\varepsilon_0} = \sum_{i=1}^{G} d_i G_i P_-^{d_i - 1} P_0^{e_i} P_+^{f_i} \frac{dP_-}{d\varepsilon_0} +$$

$$\sum_{i=1}^{G} e_i G_i P_-^{d_i} P_0^{e_i - 1} P_+^{f_i} \frac{dP_0}{d\varepsilon_0} +$$

$$\sum_{i=1}^{G} f_i G_i P_-^{d_i} P_0^{e_i} P_+^{f_i - 1} \frac{dP_+}{d\varepsilon_0}.$$

is obtained. On defining

$$\xi(n) = \begin{cases} 1 & \text{if } n = 0 \\ 0 & \text{if } n \neq 0, \end{cases}$$

it follows that

$$\left.\frac{dP_x}{d\varepsilon_0}\right|_{\varepsilon_0 \to 0} = 2\, X_{10}\, p^{M-1}\, q\, p_z(2A) - 2\, M\, X_{00}\, p^M [p_z(0) + p_z(2A)]$$

where

$$X_{k0} = \sum_{i=1}^{G} \xi(d_i - k) G_i, \qquad k = 0, 1.$$

Since

$$\left.\frac{dP_x}{d\varepsilon_0}\right|_{\varepsilon_0 \to 0} = 0 \qquad \text{for} \quad \mu = \mu_0$$

it is easy to derive Equation (77) for $j = 0$. The expressions resulting from the minimization of P_e are labelled by $j = 1$ and are easily derived by noting that, in Equation (68), $a_i \geq 1$, which entails that

$$\left.\frac{dP_{eu}}{d\varepsilon_0}\right|_{\varepsilon_0 \to 0} = 2\, p^M\, Y\, p_z(2A)$$

where

$$Y = \sum_{i=1}^{F} \xi(a_i - 1) F_i.$$

Due to the similarity between Equations (69) and (70)

$$\left.\frac{d}{d\varepsilon_0}(P_x\, P_{ex})\right|_{\varepsilon_0 \to 0}$$

can be found simply by replacing G_i by $G_i E_{e_i}(e_i A_1)$ in $dP_x/d\varepsilon_0|_{\varepsilon_0 \to 0}$. Equation (77) will then follow.

2.3

In this section, the method of calculating the error probability $P_{e\ell}$, defined by Equation (57), is explained.

If in Fig. 5.4 the block T is assumed linear, the CHF $F_n(\omega)$ of the noise samples at the input of the threshold detector is, according to Equation (7), given by

$$F_n(\omega) = (q\, F_w(\omega) + p\, F_z(\omega))^M$$

$$= \sum_{i=0}^{M} p_M(i)\, F_w^{M-i}(\omega)\, F_z^i(\omega)$$

where $p_M(i)$ is given by Equation (8) and

$$F_w(\omega) = \exp(-\frac{\sigma_w^2}{2}\omega^2)$$

In Case 1

$$F_z(\omega) = \exp(-\frac{\sigma_z^2}{2}\omega^2)$$

and thus

$$F_n(\omega) = \sum_{i=0}^{M} p_M(i)\, \exp(-\frac{\zeta_i^2\sigma_w^2}{2}\omega^2)$$

where

$$\zeta_i^2 = M + i(\zeta^2 - 1), \qquad \zeta = \frac{\sigma_z}{\sigma_w}.$$

Therefore, in Case 1

$$P_{e\ell} = \frac{1}{2}\sum_{i=0}^{M} p_M(i)\, \operatorname{erfc}(\frac{M\rho}{\zeta_i\sqrt{2}}),$$

where $\rho = A/\sigma_w$. If $p = 1$, all the $p_M(i)$ are zero except for $i = M$ and thus

$$P_{ez} = \frac{1}{2}\operatorname{erfc}(\frac{\rho}{\zeta}\sqrt{\frac{M}{2}}).$$

In Case 2

$$F_z(\omega) = \exp(-\beta|\omega|)$$

and thus in order to calculate $P_{e\ell}$ the method developed in Chapter IV can be used or those noise samples due to the Gaussian noise component alone can be neglected, provided that $\rho_{dB} > 12$ dB and $\zeta \gg 1$. The latter method gives

$$F_n(\omega) \simeq \sum_{i=0}^{M} p_M(i)\, F_z^i(\omega)$$

$$\simeq \sum_{i=0}^{M} p_M(i)\, \exp(-\beta i|\omega|)$$

and thus

$$P_{e\ell} \simeq \sum_{i=1}^{M} p_M(i) \left(\frac{1}{2} - \frac{1}{\pi} \operatorname{tg}^{-1} \frac{M\rho}{i\zeta}\right),$$

where $\rho = A/\beta$. If $\zeta_{dB} \geqslant 20$ dB and $\rho_{dB} > 12$ dB, the previous method of computing $P_{e\ell}$ is accurate enough. If, however, $\rho_{dB} \ll 12$ dB, it is not possible to neglect the noise samples of variance σ_w^2 and $P_{e\ell}$ will have to be calculated directly from $F_n(w)$, as explained in Chapter IV. It is easy to see that in Case 2

$$P_{ez} = \frac{1}{2} - \frac{1}{\pi} \operatorname{tg}^{-1} \frac{\rho}{\zeta}.$$

Finally, it is important to point out that, in both cases studied, if the noise samples of variance σ_w^2 are neglected, the expression obtained for $P_{e\ell}$ depends on ρ and ζ, only through the ratio $\mu = \rho/\zeta$.

APPENDIX 3*

* In this appendix the references to the main text pertain to Chapter VI, unless otherwise stated.

3.1

If h(t) is time-limited to the interval $[T/2, T/2]$ then

$$f_1(t) = \sqrt{T}\, h(tT)$$

According to Theorem 4 in Chapter IV, h(t) will be a Nyquist pulse if and only if $f_1^2(t)-1$ is an odd function with respect to the point $t = \frac{1}{4}$ in the interval $[0,\frac{1}{2}]$. From Equations (35), (36) and (40) it follows that

$$v = \frac{z^2}{B^2} = \frac{f_1^2(t)}{B^2}$$

and

$$t = r(B\sqrt{v}) = s(v).$$

Therefore, h(t) will be a Nyquist pulse if and only if $s(v)-\frac{1}{4}$ is an odd function with respect to the point $v = \frac{1}{2}$ in the interval $[0,1]$. From Equation (42) it follows that

$$p(v) = -2\frac{ds}{dv}$$

and thus it can be concluded that h(t) is a Nyquist pulse if and only if p(v) is an even function with respect to $v = \frac{1}{2}$ in the interval $[0,1]$.

3.2 COMPUTER PROGRAM FOR MONTE CARLO SIMULATION

The computer program used to calculate the results of Section 6.3 will now be described. The program is based on the following assumptions:

(i) The impulsive noise at the receiver input is modelled as a sequence of Dirac impulses with statistically independent intensities (see Section 2.3);

(ii) The impulse response of the receiving filter is time-limited to an interval of T seconds duration.

Under these conditions the noise samples delivered to the decision device are statistically independent and can be generated within a reasonable time of computation.

The listing of the program is included at the end of this appendix. The program structure is as follows:

(a) Main routine: PROGRAM MONTE

Control parameters: ICASE, LCASE, MODE.

ICASE controls the use of the subroutines RANGE and RANGE1 (see below) which generate the sequence of noise samples. If ICASE = 1 or 2 the samples of a Poisson impulse noise are generated. In these cases the random variables u_{1i} in Equation (55) are assumed to have unit variance, that is

$$\sigma_{u1}^2 = \nu_1 \sigma_r^2 / p = 1 \qquad \therefore \quad \sigma_r = \sqrt{p/\nu_1}.$$

When ICASE = 3 or 4 the random variables u_{1i} are drawn directly from a prescribed distribution. For ICASE = 3 the time distribution defined by Equations (63) and (64) is used whereas for ICASE = 4 the time structure is given by Equations (69) and (70).

If LCASE = 1 the background noise is assumed absent. If LCASE = 2 a background Gaussian noise is considered but its contribution to the noise samples that include impulsive noise is neglected.

The parameter MODE controls the subroutines DCSN and ZNL (see below).

Other parameters:

PU = p, QU = q.

When ICASE $<$ 4, p can take any value between 0 and 1. When ICASE = 4 an easy generation of the random integers k and n defined by Equations (69) and (70) imposes that p be given by the reciprocal of an integer denoted by LU in the program. The parameter r in Equation (70) is denoted by LR.

RNU1 = ν_1, see Equation (27).

SIGMA = σ_r if ICASE = 1 or 2;

= 1 if ICASE = 3 or 4.

When ICASE = 3 or 4 the parameter SIGMA denotes a dispersion parameter of the random variables u_{1i}, which is chosen as the parameter k_z in Chapter V (see footnote on page 115).

A: magnitude of the signal samples.

ADB expresses A in dB:

$$ADB = 20 \log_{10} A.$$

$B = A/\sqrt{p}$.

BDB expresses B in dB and thus gives the ratio between the average signal power and the average impulsive noise power whenever the latter is finite.

SIGMW = σ_w, standard deviation of the background Gaussian noise.

RAW = $1/\sigma_w$ and thus gives the impulsive-to-Gaussian noise ratio as defined in Chapter V, Equation (44).

RAWDB expresses RAW in dB.

EPSI is the receiver parameter ε_0 (see experiments 1 to 4).

$Z = \varepsilon_0/\sigma_w$; ZDB expresses Z in dB.

The subroutines RANGE and RANGE1 generate JK noise samples each time they are called. By calling them NTOTAL times, a total of NTOTAL*JK samples can be generated.

When the system described in Chapter IV is being simulated the parameters M1, M2 and N are given the following values:

$$M1 = M2 = 1, \quad N = 2^{L-1}.$$

The parameter N is the length of the self-orthogonal sequences. All the values of L from L1 to L2 are considered. When the system described in Chapter V is being studied the following values are used:

L1 = L2 = 1 $\quad\therefore\quad$ N = 1.

The parameter M is the number of pulse repetitions. All the values of M from M1 to M2 are considered.

(b) SUBROUTINE RANGE (KS, R, ICASE, LCASE, FFX).

This subroutine generates KS noise samples which are stored in the array R. If ICASE = 1 or 2 the method described by Equations (51) and (53) is used to generate samples of Poisson impulse noise. If ICASE = 1, the subroutine RANDI (see below) generates values which are distributed according to $p_{s_1}(x)$. If ICASE = 2, RANDI generates values which obey the PDF $p_r(x)$. LCASE has the same meaning as above.

The argument FFX represents the function

$$FFX(U) = |f_1(U/2)|/B$$

[see Equation (49)]. In all the simulation experiments studied in Section 6.3 the following case was considered:

$$FFX(U) = \cos(\pi U/2).$$

This case corresponds to the pulse given by Equation (35), Section 4.2. FUNCTION FFX(X) is only used when ICASE = 2.

RNU1, QU, SIGMA and SIGMW are input parameters to this subroutine through a COMMON statement.

(c) SUBROUTINE RANGE1 (KS, LCASE, R)

When ICASE = 4 this subroutine is called to generate KS noise samples which are stored in the array R. The burst and gap lengths are selected according to the probability distributions (69) and (70). It is assumed that the parameter r is an integer and that p is the reciprocal of some integer $\ell > 1$. Therefore $v = 1 + (\ell - 1)(r-1)$ is an integer. Under these conditions both the gap and the burst lengths obey a Pascal distribution.

SIGMA, SIGMW, LR and LU are input parameters to this subroutine through a COMMON statement.

(d) SUBROUTINE CARLO (NTYPE, MODE, N, M, SS, ADB, NT, R, JK, NX, NE)

This subroutine is intended to add the noise to the signal, simulate the decision procedure and count the number of errors, NE, observed in NT data bits. The arguments MODE, N, M and ADB have the meaning explained in (a). The array R contains JK noise samples. When N>1 the array SS contains a self-orthogonal sequence of length N which represents the received signal samples associated with each one of the data bits. This array SS is generated by subroutines SOFGEN and SIGNAL (see below). If NTYPE = 1 all the components of SS have the same absolute value. This value of NTYPE was assumed in experiment 5 (see Subsection 6.3.5).

When N = 1 also NX = 1. When N>1 the argument NX is the number of signalling intervals between two consecutive transmitted self-orthogonal sequences. In experiment 5 the value NX = 2 was taken.

(e) SUBROUTINE SOFGEN (KM, NR, IND, N)

This subroutine generates an integer array N containing a self-orthogonal sequence whose elements have unit absolute value. The method of generation is that used in Section 4.2.3 to construct Table 4.1. The dimension of the array N must be a power of 2, the exponent of which is KM. If KM>2 the array IND (of dimension KM-2) must be given before calling this subroutine. In order to obtain the sequences of Table 4.1 all the components of IND must be set equal to unity. By choosing a different array, subjected to the conditions

$$1 < IND(L) \leqslant L+1$$

(L = 1, 2, ..., KM-2), the sequences of the other orthogonal

sets (see Appendix 1.3) can be generated. The integer NR is the order of the generated sequence N within the orthogonal set specified by the array IND. Before this subroutine is called, the input arguments KM, NR and IND must thus be specified. If sequences of length greater than 64 are required, the dimension of the array NB (see listing) must be increased.

(f) SUBROUTINE SIGNAL (NTYPE, KM, IS, DIR, S)

Before calling this subroutine the subroutine SOFGEN must be called to generate a self-orthogonal sequence IS. The argument KM has the same meaning as above.

If NTYPE = 1 the output array S is simply set equal to IS. If NTYPE >1 the array S also depends on the array DIR. In this case the array S is generated according to Equations (60) and (61) in Chapter IV and the array DIR is related to the parameters μ_i (i = 1, 2, ..., KM) in these equations in the following way:

$$\mu_k = (1 - \text{DIR}(k))\pi/4.$$

The output vector S has a length equal to the number of its components.

(g) FUNCTION FFX(X)

See section (b) above.

(h) SUBROUTINE DCSN (MODE, M, A, RX, IE)

The input arguments MODE, M and A have already been defined in (a). The input array RX contains the M noise samples delivered to the decision device for a given data element. These noise samples are calculated by subroutine CARLO which calls DCSN to make the decision. The output argument IE is equal to unity when an error occurs and to zero otherwise.

If MODE = 1 a linear decision device is simulated, which is optimum against Gaussian noise. If MODE = 2 the receiver shown in Fig. 3.5 is simulated. If MODE = 3 the receiver shown in Fig. 5.4 is simulated.

EPSI (see (a) for definition) is an input parameter to this subroutine through a COMMON statement.

(i) FUNCTION ZNL (X, Y, MODE)

This subroutine is called by DCSN to simulate the blocks ZNL and T shown in Figs. 3.5 and 5.4 respectively. The argument X represents the magnitude of the signal samples which was denoted by A above. The argument MODE has the same meaning as above.

(j) Random-number generators

SUBROUTINE RANDI (NN, SIGMA, A, B)

This subroutine generates NN (1 or 2) values of a random variable with dispersion parameter SIGMA, as explained in (a). If NN = 1, only A is generated and if NN = 2, both A and B are generated. This subroutine calls another random-number generator in accordance with the distribution required.

FUNCTION RANF(X) and
FUNCTION UNIF(X)

The values given by these two functions are uniformly distributed in the interval (0,1). RANF is included in the system library of the computer CDC 6400 on which this program was run. The program was tested in situations for which an exact solution is known. It was found out that the agreement between the results of the simulation and the exact solution improved when RANF was replaced by UNIF in some program statements. It is believed that this improvement stems from the more accurate behaviour of UNIF near the limits of the interval (0,1).

SUBROUTINE NORMAL (NN, SIGMA, A, B)

This subroutine generates NN values of a Gaussian variate with zero mean and standard deviation SIGMA. If NN =1, only A is generated and if NN = 2, both A and B are generated.

SUBROUTINE LAPLAC (X)

In this case, the value X of a Laplace variate with zero mean and unit variance is generated.

SUBROUTINE PASCAL (P, L, K)

The integer K obeys a Pascal distribution, that is,

$$\text{Prob}\,[K] = \binom{-L}{K}(-P)^K(1-P)^L$$

(K = 0, 1, 2, ...) .

SUBROUTINE POISSN (P,K)

The integer K obeys a Poisson distribution, that is,

$$\text{Prob}\,[K] = \exp(-P)(P^K/K!)$$

(K = 0, 1, 2, ...).

SUBROUTINE CAUCHY (X)

The random number X obeys a symmetrical Cauchy PDF such that the absolute value of X has unit median.

A detailed description of the simulation techniques underlying the previous five subroutines can be found in Refs. [6-3,4].

PROGRAM LISTING (FORTRAN IV)

```
      PROGRAM MONTE (INPUT,OUTPUT,TAPE5=INPUT,TAPE6=OUTPUT)
      DIMENSION R(4000)
      DIMENSION IND(4),IR(64),DIR(6),SS(64),LE(40,6,6),KT(6,6)
      COMMON RNU1,QU,SIGMA,SIGMW,EPSI,LR,LU
      EXTERNAL FFX
      ICASE=3
      LCASE=2
      MODE=3
C     NOW SET VALUES OF PU, QU, RNU1
      IF(ICASE.EQ.4) GO TO 201
      RNU1=1.0/8.0
      QU=EXP(-RNU1)
      PU=1.0-QU
      GO TO 202
201   CONTINUE
      LU=8
      PU=1.0/FLOAT(LU)
      QU=1.0-PU
      RNU1=-ALOG(QU)
202   PUL=-10.*ALOG10(PU)
      WRITE(6,152) PU,PUL,QU,RNU1
152   FORMAT (1X,8E15.5)
      JK=2000
      LR=4
      L1=1
      L2=1
      M1=1
      M2=3
      RAWDB=32.0
      ZDB=9.0
      IL=40
      MTOTAL=25
      NTYPE=1
      YK=112111716655168.0
C     XK=2.0**48
      XK=281474976710656.0
      NR=1
      IND(1)=IND(2)=IND(3)=1
      WRITE(6,420)
      WRITE(6,200) ICASE,LCASE,MODE
200   FORMAT (1X,8I15)
      WRITE (6,420)
      IF(ICASE.EQ.4) WRITE (6,200) LU,LR
      ADB1=12.0-RAWDB
      ADB2=26.0-PUL
      CF=0.115129254649702
      IF(LCASE.EQ.1) GO TO 510
      RAW=EXP(RAWDB*CF)
      SIGMW=1.0/RAW
      Z=EXP(ZDB*CF)
```

```
      EPSI=Z*SIGMW
      WRITE(6,710)
      WRITE(6,152) RAW,EPSI
510   DO 151 L=L1,L2
      DO 151 M=M1,M2
      DO 151 I=1,IL
151   LE (I,M,L)=0
      ZK=RANF(YK)
      SIGMA=1.0
      IF(ICASE.LT.3) SIGMA=SQRT(PU/RNU1)
      DO 160 K=1,MTOTAL
      IF (ICASE.LT.4) CALL RANGE(JK,R,ICASE,LCASE,FFX)
      IF(ICASE.EQ.4)  CALL RANGE1(JK,LCASE,R)
      DO 140 L=L1,L2
      KM=L-1
      N=2**KM
      CALL SOFGEN(KM,NR,IND,IR)
      CALL SIGNAL(NTYPE,KM,IR,DIR,SS)
      NX=1
      IF(N.GT.1) NX=2
      DO 161 M=M1,M2
      KT(M,L)=INT(FLOAT(JK+NX-N)/FLOAT(NX*M))
      DO 162 I=1,IL
      ADB=ADB1+FLOAT(I+I-2)
      IF(ADB.GT.ADB2) GO TO 161
      CALL CARLO(NTYPE,MODE,N,M,SS,ADB,KT(M,L),R,JK,NX,NE)
162   LE(I,M,L)=LE(I,M,L)+NE
161   CONTINUE
140   CONTINUE
160   CONTINUE
      DO 141 L=L1,L2
      N=2**(L-1)
      DO 192 M=M1,M2
      WRITE(6,420)
420   FORMAT(1X//////)
      WRITE(6,142) N,M
142   FORMAT(12X,4H N=,I4,11X,4H M=,I4)
      WRITE (6,143)
143   FORMAT(1X//)
      FAT=1.0/FLOAT(MTOTAL*KT(M,L))
      DO 100 I=1,IL
      ADB=ADB1+FLOAT(I+I-2)
      IF(ADB.GT.ADB2) GO TO 192
      A=EXP(ADB*CF)
      BDB=ADB+PUL
      B=EXP(BDB*CF)
      PE=FAT*FLOAT(LE(I,M,L))
      WRITE(6,190) A,ADB,B,BDB,PE
190   FORMAT(1X,2(2E15.5,5X),E15.5)
100   WRITE(6,710)
```

```
710   FORMAT(1X)
192   CONTINUE
141   CONTINUE
      WRITE(6,420)
      YK=AINT(RANF(-1.)*XK)
      WRITE(6,998)YK
998   FORMAT(1X,F22.1)
      STOP
      END



      SUBROUTINE RANDI(NN,SIGMA,A,B)
      CALL CAUCHY(A)
      A=A*SIGMA
      IF(NN.EQ.1) RETURN
      CALL CAUCHY(B)
      B=B*SIGMA
      RETURN
      END



      FUNCTION FFX(X)
      FFX = COS(1.5707963267948966*X)
      RETURN
      END



      FUNCTION ZNL(X,Y,MODE)
      COMMON RNU1,QU,SIGMA,SIGMW,EPSI
      GO TO (100,100,200),MODE
100   CONTINUE
      ZNL=X
      RETURN
200   CONTINUE
      ZNL=X
      RETURN
      END



      SUBROUTINE RANGE(KS,R,ICASE,LCASE,FFX)
      DIMENSION R(KS)
      COMMON RNU1,QU,SIGMA,SIGMW,EPSI
      IF(ICASE.EQ.2) SIGMA=SIGMA*1.414213562373095
      KR=KRX=0
      DO 800 L=1,KS
      R(I)=0.0
```

```
      IF(ICASE.EQ.3) GO TO 730
      CALL POISSN(RNU1,LX)
      IF(LX.EQ.0) GO TO 750
      IF(KR.EQ.0) GO TO 700
      R(I)=BB
      KR=0
      LX = LX - 1
      IF(LX.EQ.0) GO TO 800
  700 KR=MOD(LX,2)
      JL=(LX-KR)/2
      IF(JL.EQ.0) TO GO 600
      DO 500 J=1,JL
      CALL RANDI(2,SIGMA,AA,BB)
      IF(ICASE.EQ.1) GO TO 510
      AA=AA*FFX(RANF(0.0))
      BB=BB*FFX(RANF(0.0))
  510 R(I)=R(I)+AA+BB
  500 CONTINUE
      IF(KR.EQ.0) GO TO 800
  600 CALL RANDI(2,SIGMA,AA,BB)
      IF(ICASE.EQ.1) GO TO 520
      AA=AA*FFX(RANF(0.0))
      BB=BB*FFX(RANF(0.0))
  520 R(I)=R(I)+AA
      GO TO 800
  730 XX+UNIF(0.0)
      IF(XX.LT.QU) GO TO 750
      IF(KR.EQ.0) GO TO 740
      R(I)=BB
      KR=0
      GO TO 800
  740 CALL RANDI(2,SIGMA,AA,BB)
      R(I)=AA
      KR=1
      GO TO 800
  750 IF(LCASE.EQ.1) GO TO 800
      IF(KRX.EQ.0) GO TO 720
      R(I)=DD
      KRX=0
      GO TO 800
  720 CALL NORMAL(2,SIGMW,CC,DD)
      R(I)=CC
      KRX=1
  800 CONTINUE
      RETURN
      END
```

```
      SUBROUTINE RANGE1(KS,LCASE,R)
      DIMENSION R(KS),KR(2),PX(2),LX(2),BB(2)
      COMMON RNU1, QU,SIGMA,SIGMW,EPSI,LR,LU
      NC=0
      PX(2)=1.0/FLOAT(LU)
      PX(1)=1.0-PX(2)
      KR(1)=KR(2)=0
      LX(1)=LR
      LX(2)=1+(LU-1)*(LR-1)
100   CONTINUE
      DO 800 I=1,2
      CALL PASCAL(PX(I),LX(I),KK)
      KK=KK+1
      IF(I.EQ.1. AND.LCASE.EQ.1) GO TO 710
      IF(KR(I).EQ.0) GO TO 700
      NC=NC+1
      R(NC)=BB(I)
      IF(NC.EQ.KS) RETURN
      KR(I)=0
      KK=KK-1
      IF(KK.EQ.0) GO TO 800
700   KR(I)=MOD(KK,2)
      JL=(KK-KR(I))/2
      IF(JL.EQ.0) GO TO 600
      DO 500 J=1,JL
      IF(I.EQ.1) CALL NORMAL(2,SIGMW,AA,BB(1))
      IF(I.EQ.2) CALL RANDI(2,SIGMA,AA,BB(2))
      NC=NC+1
      R(NC)=AA
      IF(NC.EQ.KS) RETURN
      NC=NC+1
      R(NC)=BB(I)
      IF(NC.EQ.KS) RETURN
500   CONTINUE
      IF(KR(I).EQ.0) GO TO 800
600   IF(I.EQ.1) CALL NORMAL(2,SIGMW,AA,BB(1))
      IF(I.EQ.2) CALL RANDI(2,SIGMA,AA,BB(2))
      NC=NC+1
      R(NC)=AA
      IF(NC.EQ.KS) RETURN
      GO TO 800
710   DO 720 J=1,KK
      NC=NC+1
      R(NC)=0.0
720   IF(NC.EQ.KS) RETURN
800   CONTINUE
      GO TO 100
      END
```

```
      SUBROUTINE CARLO (NTYPE,MODE,N,M,SS,ADB,NT,R,JK,NX,NE)
      DIMENSION SS(N),R(JK)
C     DIMENSION RX(M)
      DIMENSION RX(20)
      M1=M*NX
      NE=ID=0
      CF=0.115129254649702
      B=EXP(ADB*CF)*SQRT(FLOAT(N))
      DO 500 K=1,NT
      IP=ID
      DO 160 I=1,M
      SUM=0.0
      DO 190 J=1,N
      TERM=R (IP+J)
      IF (NTYPE.EQ.2) TERM=TERM*SS(J)
190   SUM=SUM+TERM
      RX(I)=SUM
160   IP=IP+NX
      CALL DCSN(MODE,M,B,RX,IE)
      NE=NE+IE
500   ID=ID+M1
      RETURN
      END
```

```
      SUBROUTINE SOFGEN(KM,NR,IND,N)
C     IF(KM.LE.2) ARRAY IND IS NOT USED
C     DIMENSION IND(KM-2),N(ND),NB(ND) WHERE ND=2**KM
C     MAKE SURE THAT KM.GE.0 AND 1.LE.NR.LE.ND
C                    1.LE.IND(L).LE.(L+1)
      DIMENSION IND(1),N(1)
      DIMENSION NB(64)
      IF(KM.GT.0) GO TO 600
      N(1)=1
      RETURN
600   DO 100 J=1,KM
100   NB(J)=-1
      DO 410 L=1,NR
      DO 200 J=1,KM
      NB(J)=-NB(J)
      IF (NB(J).EQ.1) GO TO 200
      GO TO 410
200   CONTINUE
410   CONTINUE
      N(1)=N2=1
      DO 420 I=1,KM
      N1=N2+N2+1
      DO 400 J=1,N2
      NX=N1-J
      N(NX)=N(J)
      IF(NB(I).EQ.-1) N(NX)=-N(NX)
400   NB(I)=-NB(I)
420   N2=N2+N2
      IF(KM.LT.3) RETURN
      ND=2**KM
      NL=KM-2
      KT=KM-1
      DO 530 L=1,NL
      NG=IND(L)-1
      IF(NG.EQ.0) GO TO 530
      NV=2**(KT-L)
      IL=2**(L-NG)
      KL=2**NG
      NX=KL*NV
      NY=NX+NX
      NS=0
      DO 560 L=1,IL
      N1=N2=NS
      DO 550 K=1,KL
      DO 520 J=1,NV
      NB(N1+J)=N(N2+J)
520   NB(N1+NX+J)=N(N2+NV+J)
      N1=N1+NV
550   N2=N1+NV
```

```
560   NS=NS+NY
      DO 540 J=1,ND
540   N(J)=NB(J)
530   CONTINUE
      RETURN
      END


      SUBROUTINE SIGNAL(NTYPE,KM,IS,DIR,S)
C     IF (NTYPE.EQ.1) S IS SET EQUAL TO IS
C     IF (NTYPE.GT.1) S DEPENDS ALSO ON DIR
C     DIMENSION IS(ND),DIR(KM),S(ND)
      DIMENSION IS(1),DIR(1),S(1)
      ND=2**KM
      IF (NTYPE.GT.1) GO TO 600
      DO 500 I=1,ND
500   S(I)=FLOAT(IS(I))
      RETURN
600   SN=SQRT(FLOAT(ND))
C     HI=PI/4.0
      HI=0.7853981633974483
      LJ=1
      S(1)=1.0
      DO 200 I=1,KM
      DIR(I)=1.0-DIR(I)
      KJ=LJ+LJ+1
      X=HI*AMOD(DIR(I),4.0)
      A=COS(X)
      B=SIN(X)
      DO 300 J=1,LJ
      S(KJ-J)=S(J)*B
300   S(J)=S(J)*A
200   LJ=LJ+LJ
      DO 400 L=1,ND
400   S(I)=SIGN(S(I),FLOAT(IS(I)))*SN
      RETURN
      END


      SUBROUTINE DCSN(MODE,M,A,RX,IE)
      DIMENSION RX(M)
      COMMON RNU1,QU,SIGMA,SIGMW,EPSI
      IE=0
      SUM=0.0
      GO TO (100,200,300),MODE
100   TEST=-A*FLOAT(M)
      DO 400 L=1,M
```

```
400   SUM=SUM+RX(I)
      GO TO 600
200   TEST=0.0
      DO 500 I=1,M
      XX=A+RX(I)
500   SUM=SUM+ZNL(XX,A,MODE)
      GO TO 600
300   TEST=0.0
      BB=A+A
      IT=0
      DO 700 I=1,M
      AA=RX(I)+BB
      IF(ABS(RX(I)).LT.EPSI) IT=IT+1
700   IF(ABS(AA).LT.EPSI) IT=IT-1
      IF(IT.EQ.0) GO TO 810
      IF(IT.LT.0) IE=1
      RETURN
810   DO 800 I=1,M
      XX=A+RX(I)
800   SUM=SUM+ZNL(XX,A,MODE)
600   IF(SUM.LT.TEST) IE=1
      RETURN
      END



      FUNCTION UNIF(X)
      UNIF=RANF(0.0)
      UNIF=UNIF+RANF(0.0)
      IF(UNIF.GT.1.0) UNIF=UNIF-1.0
      RETURN
      END



      SUBROUTINE NORMAL(NN,SIGMA,A,B)
C     DISTRIBUTION N(0,SIGMA**2)
C     IF(NN.EQ.1) ONLY A IS GENERATED
C     IF(NN.EQ.2) BOTH A AND B ARE GENERATED
C     A AND B ARE INDEPENDENT VARIATES
      Y=RANF(0.)
      Z=RANF(0.)
      X=6.28318530717958*Z
      AA=SQRT(-2.*ALOG(Y))
      AA=AA*SIGMA
      A=AA*COS(X)
      IF(NN.EQ.1) RETURN
      B=AA*SIN(X)
      RETURN
      END
```

```
      SUBROUTINE LAPLAC(X)
C     LAPLACE DISTRIBUTION
C     UNIT VARIANCE
      R=RANF(0.0)
      R=0.7071067811865 48*ALOG(R)
      X=RANF(0.0)-0.5
      X=SIGN(R,X)
      RETURN
      END


      SUBROUTINE PASCAL(P,L,K)
      PX=1.0/ALOG(P)
      K=0
      DO 100 I=1,L
      RX=ALOG(UNIF(0.0))
100   K=K+INT(RX*PX)
      RETURN
      END


      SUBROUTINE POISSN(P,K)
      K=0
      B=EXP(-P)
      TR=1.0
300   TR=TR*UNIF(0.0)
      IF(TR-B) 100,200,200
200   K=K+1
      GO TO 300
100   RETURN
      END


      SUBROUTINE CAUCHY(X)
C     X.....CAUCHY VARIATE
C     ABS(X) HAS UNIT MEDIAN
      PI=3.141592653589793
      R=RANF(0.0)-0.5
      X=TAN(PI*R)
      RETURN
      END
```

N.B. The previous listing corresponds to the first run of Experiment 1 (see Subsection 6.3.1). In the second run the constant YK (see statement 34 of the main routine) should be given the value written out in the first run so as to ensure that the basic random-number generator RANF will start where it stopped in the first run, as stated in Section 6.3.

For the other experiments the following modifications should be introduced and in some cases the basic parameters should be reset:

Experiment 2:

```
      SUBROUTINE RANDI (NN,SIGMA,A,B)
      CALL NORMAL (NN,SIGMA,A,B)
      RETURN
      END
```

Experiment 3:

```
      FUNCTION ZNL(X,Y,MODE)
      COMMON RNU1,QU,SIGMA,SIGMW,EPSI
      GO TO (100,100,200),MODE
100   CONTINUE
      ZNL=X
      RETURN
200   CONTINUE
      AA=1.0+(X+Y)**2
      BB=1.0+(X-Y)**2
      RETURN
      END
```

Experiment 4:

The same program structure as in Experiment 1.

Experiment 5:

```
      SUBROUTINE RANDI (NN,SIGMA,A,B)
      CALL LAPLAC(A)
      A=A*SIGMA
      IF(NN.EQ.1) RETURN
      CALL LAPLAC(B)
      B=B*SIGMA
      RETURN
      END
```

GLOSSARY OF SYMBOLS AND TERMS

$[a_i]$	vector
$[a_{ij}]$	matrix
$\|a_{ij}\|$	determinant
δ_{ij}	Kronecker delta (if i=j then $\delta_{ij}=1$; if $i\neq j$ then $\delta_{ij}=0$)
$\delta(t-t_o)$	Dirac delta function with spike at $t=t_o$
erf	error function [See Ref. [2-36], p. 336]
erfc	complementary error function
E_s	energy of the signal s(t)
$E[x]$	expected value of the random variable x
$\varepsilon^y=\exp(y)$	exponential function where ε is the natural base of logarithms
f	frequency
$g^r(t)$	$=[g(t)]^r$
$g^*(t)$	complex conjugate of g(t)
$G_a(t)$	rectangular pulse (=1 if $\|t\|<0.5$; =0 if $\|t\|>0.5$)
$\mathrm{Im}[z]$	imaginary part of the complex number z (if $z=a+jb$ then $\mathrm{Im}[z]=b$)
j	imaginary unit
$\hat{k}_i$	estimate of k_i
log	natural logarithm
$\log_b$	logarithm to the base b
$\Lambda(x)$	likelihood ratio
$\binom{n}{i}$	number of combinations of i out of n
n(t)	sample waveform of a noise process
(n,k,t)	a linear code capable of correcting t random errors (n = code length, k = number of information digits)

$\omega = 2\pi f$	angular frequency (radians per second)
P_e	probability of error
P_M	peak transmitted power
P_S	average transmitted power
$P[E] = \text{Prob}[E]$	probability of the event E
$P[E\|C]$	probability of the event E conditioned on the occurrence of the event C
$P[E_1,\ldots,E_n\|C_1,\ldots,C_m]$	probability of the simultaneous occurrence of the events $E_1,\ldots,E_n$ conditioned on the simultaneous occurrence of the events $C_1,\ldots,C_m$.
$\text{Re}[z]$	real part of z
$S(f)$	Fourier transform of s(t)
sinc x	$= \frac{\sin \pi x}{\pi x}$
sgn x	signum function (=1 if $x>0$; =0 if $x<0$)
t	continuous time
$t_n = t_o + nT$	discrete time (n=...,-2,-1,0,1,2,...)
$\bar{x} = \langle x \rangle$	mean value of the random variable x
$\|z\|$	modulus of the complex number z
$\simeq$	approximately equal
$\gtrsim$	greater than or approximately equal
$\lesssim$	less than or approximately equal
$\gg$	much greater than
$\ll$	much less than
$\therefore$	therefore
$\oplus$ (mod 2)	modulo 2 addition
* (on line)	convolution
* (superscript)	complex conjugate of a number (i.e. z^*)

A/D converter	analog-to-digital converter
CHF	characteristic function
EPF	exceedence probability function [See page 27, Eq. (2)]
FDM	frequency-division multiplex
HF	high frequency
IGNR	impulsive-to-Gaussian-noise ratio
OFC	orthonormal function coding
PDF	probability density function
PSC	parallel-to-serial converter
r.m.s value	root-mean-square value
SGNR	signal-to-Gaussian-noise ratio
SINR	signal-to-impulsive-noise ratio
SNR	signal-to-noise ratio
SPC	serial-to-parallel converter
VLF	very low frequency

Baud - signalling rate of one pulse per second.

Hertz (Hz) - frequency of one cycle per second.

Analog signal - continuous-time waveform with continuous amplitude.

Baseband waveform - analog waveform essentially frequency-limited to an interval (0,F) for a given F.

Discrete-time signal - any signal that is defined only at the instants $t_n=t_o+nT$ (n=1...,-2,-1,0,1,2,...) for some T.

Non-continual noise - a noise defined in terms of a given time distribution and exhibiting different properties in adjacent intervals of time.

Threshold detector - any device that makes a binary decision by comparing the input voltage with a threshold value.

Null-zone detector - any device that only makes a binary decision when the input voltage is outside the interval defined by two threshold values. For an input voltage inside this interval (null-zone) no decision is made and an erasure (or null) symbol is produced.

Decision device - that part of a receiver which decides on each transmitted symbol on the basis of a set of decision statistics obtained from the received signal.

REFERENCES

References to Chapter I

1-1 W.W. Peterson and E.J. Weldon, Jr.,
"Error-Correcting Codes", The M.I.T. Press, 1972, 2nd Edn.

1-2 R.W. Lucky, J. Salz, E.J. Weldon, Jr.,
"Principles of Data Communication", 1968, McGraw-Hill.

1-3 J.M. Wozencraft, I.M. Jacobs,
"Principles of Communication Engineering", J. Wiley, 1965.

1-4 R.M. Lerner,
"Design of Signals", in Chapter 11 of "Lectures on Communication System Theory", Ed. E.J. Baghdady, McGraw-Hill, 1961.

1-5 R.H. Richard, W.C. Gore,
"A Nonlinear Filter for Non-Gaussian Interference",
IEEE Trans. Commun. Systems, CS-11, No. 4, pp. 436-443,
Dec. 1963.

References to Chapter II

2-1 R.M. Lerner, "Modulation and Signal Selection for Digital Data Systems", AIEE Comm. & Elect., 58, p. 661, Jan. 1962.

2-2 R.G. Enticknap, "Errors in Data Transmission Systems", IRE Trans. Commun. Syst., March 1961, pp. 15-20.

2-3 M.M. Buchner, "Some Experimental Results on Impulse Noise Classification", IEEE Trans. Comm. Tech., pp. 659-663, Dec. 1969.

2-4 A.B. Bodonyi, "Effects of Impulse Noise on Digital Data Transmission", IRE Trans. Comm. Syst., pp. 355-361, Dec. 1961.

2-5 J. Kelly, J. Mercurio, D. Willard, "Two Measuring Techniques for the Investigation of Impulsive Noise and Dropouts on Telephone Lines", AIEE Comm. & Elect., Jan. 1962, Pt. 1, p. 585.

2-6 F. Horner, J. Harwood, "An Investigation of Atmospheric Radio Noise at very low Frequencies", Proc. IEE (London), Vol. B-103, p. 743, Nov. 1956.

2-7 W.Q. Crichlow", Noise Investigation at VLF by the National Bureau of Standards", Proc. IRE, Vol. 45, June 1957, p. 778.

2-8 A.G. Frantsuz, "The Amplitude Statistical Distributions for Radio Impulsive Noise produced by Electrical Machinery", Elektrosvyaz', 9, 1958.

2-9 H.L. Yudkin, "Some Results in the Measurement of Impulse Noise on several Telephone Circuits", Proc. NEC, Vol. 16, pp. 222-231, 1960.

2-10 P. Mertz, "Model of Error Burst Structure in Data Transmission", Proc. NEC., Vol. 16, p. 232, Oct. 1960.

2-11 P. Mertz, "Model of Impulsive Noise for Data Transmission", IRE Trans. Comm. Syst., June 1961, pp. 130-137.

2-12 K. Furutsu, T. Ishida, "On the Theory of Amplitude Distribution of Impulsive Random Noise", Journal of Applied Physics, Vol. 32, July 1961, p. 1206.

2-13 P. Mertz, "Statistics of Hyperbolic Error Distributions in Data Transmission", IRE Trans. Comm. Syst., Dec. 1961, pp. 377-382.

2-14 P. Mertz, "Error Burst Chains in Data Transmission", IRE Conv. Record, Pt. 8, p. 47, March 1962.

2-15 J.M. Berger, B. Maldelbrot, "A new Model for Error Clustering in Telephone Circuits", IBM J. Res. & Dev., Vol. 7, p. 224, 1963.

2-16 S.M. Sussman, "Analysis of the Pareto Model for Error Statistics on Telephone Circuits", IEEE Trans. Comm. Syst., pp. 213-221, June 1963.

2-17 P. Beckmann, "Amplitude Probability Distribution of Atmospheric Radio Noise", J. Res. NBS, Vol. 68D, No. 6, p. 723, June 1964.

2-18 J.H. Fennick, "A Report on Some Characteristics of Impulse Noise in Telephone Communication", AIEE Comm. & Elect., Nov. 1964, pp. 700-705.

2-19 R.L. Townsend, R.N. Watts, "Effectiveness of Error Control in Data Communication over the Switched Telephone Network", The Bell System Technical Journal, pp. 2611-2638, Nov. 1964.

2-20 P. Mertz, "Impulse Noise and Error Performance in Data Transmission", AD614416, U.S. Department of Commerce, National Technical Information Service, April o965.

2-21 K. Brayer, O. Cardinale, "Evaluation of Error Correction Block Encoding for High-Speed HF Data", IEEE Trans. Comm. Tech., Vol. COM-15, pp. 371-382, June 1967.

2-22 K. Brayer, "Error Patterns measured on Transequatorial HF Communication Links", IEEE Trans. Comm. Tech., Vol. COM-16, pp. 215-221, April 1968.

2-23 J.H. Fennick, "Amplitude Distributions of Telephone Channel Noise and a Model for Impulse Noise", BSTJ, Vol. 48, pp. 3243-63, Dec. 1969.

2-24 S.Y. Tong, "A Survey of Error Control Techniques on Telephone Channels", Proc. NEC., Vol. 26, pp. 462-467, 1970.

2-25 J.H. Fennick, "Understanding Impulse Noise Measurements", IEEE Trans. Comm. Tech., pp. 247-251, April 1972.

2-26 R.L. Brewster, S.B. Patel, "Noise in the Telephone Network and its Effect on Data Transmission", Proc. 1974 Int. Zurich Seminar on Digital Comm., March 1974.

2-27 R.M. Lerner, "Design of Signals", in Chapter 11 of "Lectures on Communication System Theory", E.J. Baghdady (Ed.), McGraw-Hill, 1961.

2-28 B. Shepelavey, "Non-Gaussian Atmospheric Noise in Binary-Data, Phase-coherent Communication Systems", IEEE Trans. Comm. Syst., p. 280, Sept. 1963.

2-29 See Refs. [2-9, 18].

2-30 B.P. Kalinichev, "One-dimensional Probability Density of the Sum of Impulsive and Fluctuation Noise", Telecomm. Radio Eng., Pt. 1 (USA), No. 5, 42-6, May 1967.

2-31 See Refs. [2-10, 21, 24].

2-32 See Refs. [2-10, 11, 13, 14, 15, 16, 18, 19, 20, 21, 22, 24,25]

2-33 A.R.K. Sastry, "Estimation of Bit-Error Rates for Narrowband Digital Communication in the Presence of Atmospheric Radio Noise Bursts", IEEE Trans. Comm. Tech., p. 733, Oct. 1971.

2-34 S. Goldman, "Information Theory", Constable & Co. Ltd., 1953.

2-35 S.O. Rice, "Mathematical Theory of Random Noise", BSTJ., Vol. 23, June 1944, Vol. 44, Jan. 1945.

2-36 D. Middleton, "An Introduction to Statistical Communication Theory", McGraw-Hill, 1960, Secs. 11.2, 11.3.

2-37 A. Papoulis, "Probability, Random Variables and Stochastic Processes", McGraw-Hill, 1965, Ch. 16.

2-38 E.N. Gilbert, H.O. Pollack, "Amplitude Distribution of Shot Noise", BSTJ, pp. 333-350, March 1960.

2-39 C.W. Helstrom, "Statistical Theory of Signal Detection", Pergamon Press, 1968.

2-40 R.W. Lucky, J. Salz and E.J. Weldon, Jr., "Principles of Data Communication", McGraw-Hill, 1968.

References to Chapter III

3-1 L.R. Halsted, "On Binary Data Transmission Error Rates due to Combinations of Gaussian and Impulse Noise", IRE Trans. on Commun. Systems, Vol. CS-11, No. 4, Dec. 1963, pp. 428-435.

3-2 J.M. Wozencraft, I.M. Jacobs, "Principles of Communication Engineering", John Wiley, 1965, Chapter IV.

3-3 R.E. Ziemer, "Character Error Probabilities for M-ary Signalling in Impulsive Environments", IEEE Trans. Commun. Tech., Vol. COM-15, No. 1, Feb. 1967, pp. 32-44.

3-4 R.E. Ziemer, "Error Probabilities due to Additive Combinations of Gaussian and Impulsive Noise", IEEE Trans. on Comm. Tech., pp. 471-474, June 1967.

3-5 R.M. Lerner, "Design of Signals", in Chapter 11 of "Lectures on Communication System Theory", Ed. E.J. Baghdady, McGraw-Hill, 1961.

3-6 R.A. Wainwright, "On the Potential Advantage of a Smear-Desmearing Filter Technique in Overcoming Impulse Noise Problems in Data Systems", IRE Trans. on Comm. Syst., CS-9, No. 4, Dec. 1961, pp. 362-366.

3-7 W.R. Bennett, J.R. Davey, "Data Transmission", 1965, New York, McGraw-Hill.

3-8 J.S. Engel, "Digital Transmission in the Presence of Impulse Noise", Bell System Technical Journal, Vol. 44, No. 8, pp. 1699-1743, Oct. 1965.

3-9 W.J. Richter, T.I. Smits, "Signal Design and Error Rate of an Impulse Noise Channel", IEEE Trans. Comm. Tech., Vol. COM-19, No. 4, pp. 446-458, Aug. 1971.

3-10 E.J. Baghdady, "Linear Cancellation Technique for Suppressing Impulse Noise", IRE Wescon Conv. Record, Vol. 4, Pt. 7, pp. 27-35, 1960.

3-11 R.H. Richard, W.C. Gore, "A Nonlinear Filter for Non-Gaussian Interference", IEEE Trans. Commun. Syst., CS-11, No. 4, pp. 436-443, Dec. 1963.

3-12 H.F. Hartley, "Wideband Technique for Improving FSK Reception in Atmospheric Noise", Proc. NEC., Vol. 44, pp. 528-532, 1968.

3-13 P.A. Bello, R. Esposito, "A New Method for calculating Probabilities of Errors due to Impulsive Noise", IEEE Trans. Commun. Tech., pp. 368-379, June 1969.

3-14 J. Kapp, L. Kurz, "Performance of Two Suboptimum Detectors and Signal Selection in Gaussian and Impulsive Noise", Proc. 7th Allerton Conf. Circuit and Syst. Theory, Monticello, Ill., USA., 8-10 Oct. 1969 (New York,IEEE).

3-15 P.A. Bello, R. Esposito, "Error Probabilities due to Impulsive Noise in Linear and Hard-Limited DPSK Systems", IEEE Trans. on Commun. Tech., Vol. COM-19, No. 1, pp. 14-20, February 1971.

3-16 J.K. Omura, P.D. Shaft, "Modern Performance in VLF Atmospheric Noise", IEEE Trans. on Commun. Tech., Vol. COM-19, No. 5, pp. 659-668, Oct. 1971.

3-17 L. Kurz, "A Method of Digital Signalling in the Presence of Additive Gaussian and Impulsive Noise", IRE Int. Conv. Record, Pt. 4, pp. 161-173, 1962.

3-18 S.S. Rappaport and L. Kurz, "Optimal Decision Thresholds for Digital Signalling in Non-Gaussian Noise", IEEE Int. Conv. Record, Pt. 2, pp. 198-212, 1965.

3-19 M.K. Simon, L. Kurz, "Optimal Processing and Design of Digital Signals perturbed by Gaussian and Non-Gaussian Noise", IEEE Int. Conv. Record, Vol. 14, Pt. 7, pp. 72-84, 1966

3-20 S.S. Rappaport and L. Kurz, "An Optimal Nonlinear Detector for Digital Data Transmission through Non-Gaussian Channels", IEEE Trans. Common. Tech., Vol. COM-14, No. 3, pp. 266-274, June 1966.

3-21 R.L. Spooner, "On the Detection of a Known Signal in a Non-Gaussian Noise Process", The Journal of the Acoustical Soc. of America, Vol. 44, No. 1, pp. 141-147, July 1968.

3-22 D.L. Snyder, "Optimal Binary Detection of Known Signals in a Non-Gaussian Noise Resembling VLF Atmospheric Noise", Wescon Technical Papers, Vol. 12, Pt. 4, pp. 1-8, 1968.

3-23 J.H. Miller, J.B. Thomas, "Detectors for Discrete-Time Signals in Non-Gaussian Noise", IEEE Trans. on Inf. Theory, Vol. IT-18, No. 2, pp. 241-250, March 1972.

3-24 A. Bodharamik, J.B. Moore and R.W. Newcomb, "Optimum Detection and Signal Design for Channels with Non-but-Near-Gaussian Additive Noise", IEEE Trans. on Communications, Vol. COM-20, No. 6, pp. 1087-1096, Dec. 1972.

3-25 W.L. Black, "An Impulse Noise Cancellor", IEEE Trans. on Commun. Syst., p. 506, Dec. 1963.

3-26 M. Brilliant, "An Impulse Noise Cancellor", IEEE Trans. Commun. Systems, pp. 104-105, Sept. 1964.

References to Chapter IV

4-1 R.W. Lucky, J. Salz and E.J. Weldon, Jr., "Principles of Data Communication", McGraw-Hill, 1968, Sec. 5.1.2.

4-2 R.M. Lerner, "Design of Signals", In "Lectures on Communication System Theory", Ed. E. Baghdady, McGraw-Hill, 1961, p. 263.

4-3 M.J. Di Toro, "Communication in Time-Frequency Spread Media using Adaptive Equalization", Proc. IEEE, Vol. 56, Oct. 1968, pp. 1653-1679.

4-4 M.J.E. Golay, "Complementary Series", Trans. IRE, Vol. IT-7, No. 2, April 1961, pp. 82-87.

4-5 K. Brayer and O. Cardinale, "Evaluation of Error Correction Block Encoding for High-Speed HF Data", IEEE Trans. Comm. Tech., Vol. COM-15, pp. 370-382, June 1967.

4-6 K. Brayer, "The Improvement of Digital HF Communication through Coding, Pts. I and II", IEEE Trans. Comm. Tech., Vol. COM-16, pp. 771-786, December 1968.

4-7 A.W. Pierce, B.B. Barrow, B. Goldberg and J.R. Tucker, "Effective Application of Forward-Acting Error-Control Coding to Multichannel HF Moderns", IEEE Trans. Comm. Tech., Vol. COM-18, August 1970, pp. 281-294.

4-8 A.F. dos Santos, "Direct Computation of the Distribution Function from the Characteristic Function", Proc. IEEE, Vol. 62, No. 4, pp. 533-534, April 1974.

4-9 W.J. Richter, Jr., and T.I. Smits, "Signal Design and Error Rate of an Impulse Noise Channel", IEEE Trans. on Comm. Tech., Vol. COM-19, No. 4, pp. 446-458, August 1971.

4-10 S.O. Rice, "Mathematical Analysis of Random Noise", in "Selected Papers on Noise and Stochastic Processes", N. Wax Ed., New York: Dover, 1954, p. 133.

4-11 J.S. Engel, "Digital Transmission in the Presence of Impulsive Noise", The Bell Syst. Tech. Journal, Oct. 1965, pp. 1699-1743.

References to Chapter V

5-1 J.C. Hancock and P.A. Wintz, "Signal Detection Theory", McGraw-Hill, 1966, Section 3-2.

5-2 W. Feller, "An Introduction to Probability Theory and Its Applications", Vol. II, Chapter VI, John Wiley, 1971.

References to Chapter VI

6-1 M. Fisz, "Probability Theory and Mathematical Statistics", 3rd Edition, John Wiley, 1963.

6-2 See Ref. [4-9].

6-3 T.H. Naylor et al., "Computer Simulation Techniques", J. Wiley, 1966.

6-4 K.D. Tocher, "The Art of Simulation", The English Universities Press, Ltd., 1972.

References to Chapter VII

7-1 K. Brayer and O. Cardinale, "Evaluation of Error Correction Block Encoding for High-Speed HF Data", IEEE Trans. Commun. Tech., Vol. COM-15, pp. 370-382, June 1967.

7-2 K. Brayer, "The Improvement of Digital HF Communication through Coding, Pts. I and II", IEEE Trans. Commun. Tech., Vol. COM-16, pp. 771-786, December 1968.

7-3 A.A. Hashim and A.G. Constantinides, "Some New Results on Binary Linear Block Codes", Electronic Letters, Vol. 10, No. 3, February 1974, pp. 31-33.

7-4 A.A. Hashim and A.G. Constantinides, "A Class of Linear Binary Codes", Proc. IEE, Vol. 121, No. 7, pp. 555-558, July 1974.

7-5 A.A. Hashim, "New Families of Error Correcting Codes generated by Modification of other Linear Binary Block Codes", to appear in Proc. IEE.

7-6 A.A. Hashim, "Methods for Constructing and Decoding Block Error-Correcting Codes", Ph.D. Thesis, University of London, July 1974.

7-7 H.J. Helgert and R.D. Stinaff, "Minimum-Distance Bounds for Binary Linear Codes", IEEE Trans. Inform., Vol. IT-19, pp. 344-356, May 1973.

7-8 A.W. Pierce, B.B. Barrow, B. Goldberg and J.R. Tucker, "Effective Application of Forward-Acting Error-Control Coding to Multichannel HF Modems", IEEE Trans. Comm. Tech., Vol. COM-18, August 1970, pp. 281-294.

7-9 J.L. Ramsey, "Realization of Optimum Interleavers", IEEE Trans. Inform. Theory, Vol. IT-16, May 1970, pp. 338-345.

7-10 J.J. Stiffler, "Theory of Synchronous Communications", Prentice-Hall, 1971, Sec. 13.10, p. 432.

7-11 See Ref. [7-10], Sec. 13.9.2, p. 426.

7-12 See Ref. [7-10], Sec. 13.9.1, p. 424.

7-13 W.W. Peterson and E.J. Weldon, Jr., "Error-Correcting Codes", The M.I.T. Press, 1972, Section 3.4.

7-14 See Ref. [7-13], p. 17.

References to Chapter VIII

8-1 R.M. Lerner, "Design of Signals", in "Lectures on Communication System Theory", McGraw-Hill, 1961, pp. 274-275.

8-2 W.J. Richter and T.I. Smits, "Signal Design and Error Rate of an Impulse Noise Channel", IEEE Trans. Comm. Tech., Vol. COM-19, August 1971, pp. 446-458.

8-3 S.S. Rappaport and L. Kurz, "An Optimal Nonlinear Detector for Digital Data Transmission through Non-Gaussian Channels", IEEE Trans. Comm. Tech., Vol. COM-14, June 1966, pp. 266-274.